NORTH ATLANTIC TREATY ORGANIZATION

Science & Technology Organization (STO)

AC/323(AVT-299)TP/1159

STO TECHNICAL REPORT **TR-AVT-299**

Assessment of Anti-Icing and De-Icing Technologies for Air and Sea Vehicles

(Évaluation des technologies anti-givrage et de dégivrage destinées aux véhicules aériens et maritimes)

This report documents the findings and recommendations of the Research Task Group AVT-299.

Published January 2026

Distribution and Availability on Back Cover

NORTH ATLANTIC TREATY ORGANIZATION

AC/323(AVT-299)TP/1159

STO TECHNICAL REPORT **TR-AVT-299**

Assessment of Anti-Icing and De-Icing Technologies for Air and Sea Vehicles

(Évaluation des technologies anti-givrage et de dégivrage destinées aux véhicules aériens et maritimes)

This report documents the findings and recommendations

of the Research Task Group AVT-299.

The NATO Science and Technology Organization

Science & Technology (S&T) in the NATO context is defined as the selective and rigorous generation and application of state-of-the-art, validated knowledge for defence and security purposes. S&T activities embrace scientific research, technology development, transition, application and field-testing, experimentation and a range of related scientific activities that include systems engineering, operational research and analysis, synthesis, integration and validation of knowledge derived through the scientific method.

In NATO, S&T is addressed using different business models, namely a collaborative business model where NATO provides a forum where NATO Nations and partner Nations elect to use their national resources to define, conduct and promote cooperative research and information exchange, and secondly an in-house delivery business model where S&T activities are conducted in a NATO dedicated executive body, having its own personnel, capabilities and infrastructure.

The mission of the NATO Science & Technology Organization (STO) is to help position the Nations' and NATO's S&T investments as a strategic enabler of the knowledge and technology advantage for the defence and security posture of NATO Nations and partner Nations, by conducting and promoting S&T activities that augment and leverage the capabilities and programmes of the Alliance, of the NATO Nations and the partner Nations, in support of NATO's objectives, and contributing to NATO's ability to enable and influence security and defence related capability development and threat mitigation in NATO Nations and partner Nations, in accordance with NATO policies.

The total spectrum of this collaborative effort is addressed by seven Technical Panels who manage a wide range of scientific research activities, a Group specialising in modelling and simulation, plus a Committee dedicated to supporting the information management needs of the organization.

- AVT Applied Vehicle Technology Panel
- HFM Human Factors and Medicine Panel
- IST Information Systems Technology Panel
- NMSG NATO Modelling and Simulation Group
- SAS System Analysis and Studies Panel
- SCI Systems Concepts and Integration Panel
- SET Sensing Technology Panel
- TSI Technology and Science Incubation Panel

These Panels and Group are the power-house of the collaborative model and are made up of national representatives as well as recognised world-class scientists, engineers and information specialists. In addition to providing critical technical oversight, they also provide a communication link to military users and other NATO bodies.

The scientific and technological work is carried out by Technical Teams, created under one or more of these eight bodies, for specific research activities which have a defined duration. These research activities can take a variety of forms, including Task Groups, Workshops, Symposia, Specialists' Meetings, Lecture Series and Technical Courses.

The content of this publication has been reproduced directly from material supplied by STO or the authors.

Published January 2026

ISBN 978-92-837-2471-1

Table of Contents

List of Figures

List of Tables

List of Acronyms

AC	Advisory Circular
AI	Artificial Intelligence
AMC	Acceptable Means of Compliance
ARES	Airborne Reflective Emissive Spectrometer
ATR	Avions de Transport Régional
BCP	Backscattering Cloud Probe
CASP	Canadian Atlantic Storms Program
CBCPW	Conductor-Backed Coplanar Waveguide
CDP	Cloud Droplet Probe
CFD	Computational Fluid Dynamics
CFR	Code of Federal Regulations
CHE	Cloud Horizontal Extent
CPC	Condensation Particle Counter
CPI	Cloud Particle Image
CPW	Coplanar Waveguide
CS	Certification Specifications
DAIS	Digital Airborne Imaging Spectrometer
DCU	De-icing Control Unit
DFT	Density Functional Theory
DGA	Direction Générale de l'Armement
DGPS	Differential Global Positioning System
DLR	Deutsches Zentrum für Luft- und Raumfahrt (German Aerospace Centre)
DMT	Droplet Measurement Technologies
EASA	European Union Aviation Safety Agency
EIDI	Electro-Impulse De-Icing
EMEDS	Electro-Mechanical Expulsion De-icing System
EPIPS	Electric Pulse Ice Protection System
E-SAR	Experimental Synthetic Aperture Radar system
ETIPS	Electro-Thermal Ice Protection Systems
FAA	Federal Aviation Administration
FBG	Fiber Bragg Grating (optical fiber sensor)
FEM/BEM	Finite Element/Boundary Element Method
FIRE.ACE	First ISCCP (International Satellite Cloud Climatology Project) Regional Experiment Arctic Cloud Experiment
FOSA	Fiber Optic Sensor Array
FSSP	Forward Scattering Spectrometer Probe
FZDZ	Freezing Drizzle
FZRA	Freezing Rain
GALE	Genesis of Atlantic Lows Experiment
HRSC	High Resolution Stereo Camera
HVPS	High Volume Precipitation Spectrometer
HVSP	High Volume Spectrometer Probe

HYMAP	Hyperspectral Scanner
ICE	Ice Crystal Engineering
ICEFTD	Ice Contamination Effects Flight Training Device
ICI	Ice Crystal Icing
IDS	Ice Detection Systems
IFR	Instrument Flight Rules
IGS	Ice Crystal Generation System
INTA	Instituto Nacional de Tecnica Aeroespacial (National Institute for Aerospace Technology, Spain)
IPHWG	Ice Protection Harmonization Working Group
IPS	Ice Protection System
IR	Infrared
IRT	Icing Research Tunnel
ISCCP	International Satellite Cloud Climatology Project
IWC	Ice Water Content [g/m3]
IWT	Icing Wind Tunnel
KIAS	Knots-Indicated Air Speed [knots]
LBA	Luftfahrt-Bundesamt (German Aviation Authority)
LEA	Leading Edge Assembly
LIDAR	Laser Imaging Detection and Ranging
LIRL	LeClerc Icing Research Laboratory
LIT	Low-Interfacial Toughness
LPED	Low Power Electrothermal De-icing
LTE	Low Temperature Environment
LWC	Liquid Water Content [g/m3]
LWCP	Liquid Water Content Probe
MD	Molecular Dynamics
MED	Mean Effective Drop Diameter [µm]
MEMS	Micro Electro-Mechanical Systems
MMD	Median Mass Diameter [µm]
MOSFET	Metal Oxide Semiconductor Field Effect Transistor
MVD	Mean Volume Diameter [µm]
NACA	National Advisory Committee for Aeronautics
NCAR	National Centre for Atmospheric Research
NLR	Nationaal Lucht- en Ruimtevaart Laboratorium (Netherlands Aerospace Centre)
OAP	Optical Array Probe
OICD	Optical Icing Conditions Detector
OID	Optical Ice Detector
PCASP	Passive Cavity Spectrometer Probe
RANS	Reynolds-Averaged Navier-Stokes
ROSIS	Reflective Optics System Imaging Spectrometer
SAE	Society of Automotive Engineers
SAR	Synthetic Aperture Radar
SAT	Static Air Temperature [°C]
SLD	Supercooled Large Droplets
SLIPS	Slippery, Liquid-Infused Porous Surfaces

SMA	Shape Memory Alloy
TAMDAR	Tropospheric Airborne Meteorological Data Reporting
TDL	Tunable Diode Laser
TDR	Time Domain Reflectometry
TRL	Technology Readiness Level
TWC	Total Water Content
UAM	Urban Air Mobility
UAV	Unmanned Aerial Vehicle
UTC	Universal Time Coordinated
V&V	Verification and Validation
VFR	Visual Flight Rules
VOF	Volume of Fluid
WCRP	World Climate Research Program
WMI	Weather Modification Incorporated

AVT-299 Membership List

CO-CHAIRS

Dr. Ali BENMEDDOUR
National Research Council
CANADA
Email: ali.benmeddour@nrc-cnrc.gc.ca

Dr. Ki-Han KIM
Office of Naval Research
UNITED STATES
Email: kihan.kim@navy.mil

MEMBERS

Dr. Ghislain BLANCHARD
ONERA
FRANCE
Email: Ghislain.Blanchard@onera.fr

Dr. Alina AGÜERO BRUNA
INTA (Instituto Nacional de Técnica Aeroespacial)
SPAIN
Email: agueroba@inta.es

Dr.-Ing. Christoph DEILER
German Aerospace Center (DLR)
GERMANY
Email: christoph.deiler@dlr.de

Dr. Malte FRÖVEL
Instituto Nacional de Técnica Aeroespacial (INTA)
SPAIN
Email: frovelm@inta.es

Dr. Robert GAGNON
OCRE/NRC
CANADA
Email: robert.gagnon@nrc-cnrc.gc.ca

Ms. Paloma GARCÍA-GALLEGO
Instituto Nacional de Técnica Aeroespacial (INTA)
SPAIN
Email: garciagp@inta.es

Mr. Verner HÅKONSEN
NTNU
NORWAY
Email: verner.hakonsen@ntnu.no

Mr. Christopher James HAWKINS
Dstl
UNITED KINGDOM
Email: cjhawkins@dstl.gov.uk

Dr. Brent MARTIN
Defence Technology Agency
NEW ZEALAND
Email: b.martin@dta.mil.nz

Dr. Giuseppe MINGIONE
Centro Italiano Ricerche Aerospaziali (CIRA)
ITALY
Email: g.mingione@cira.it

Mr. Julio MORA-NOGUÉS
Instituto Nacional de Tecnica Aeroespacial (INTA)
SPAIN
Email: modsurf4.pers_externo@inta.es

Capt. Riku NIEMENMAA
Joint Systems Center
FINLAND
Email: riku.niemenmaa@mil.fi

Mr. Eric R. KREEGER
NASA
UNITED STATES
Email: richard.e.kreeger@nasa.gov

Dr. Mariarosa RAIMONDO
Institute of Science and Technology for Ceramics (ISTEC CNR)
ITALY
Email: mariarosa.raimondo@istec.cnr.it

Dr. Bayindir SARACOGLU
von Karman Institute for Fluid Dynamics
BELGIUM
Email: saracog@vki.ac.be

Dr. Thomas UIHLEIN
MTU Aero Engines GmbH
GERMANY
Email: thomas.uihlein@mtu.de

Prof. Dr. Jeroen VAN BEECK
von Karman Institute for Fluid Dynamics
BELGIUM
Email: vanbeeck@vki.ac.be

Mr. Federico VERONESI
National Research Council – Institute of Science and Technology for Ceramics (CNR-ISTEC)
ITALY
Email: federico.veronesi@istec.cnr.it

ADDITIONAL CONTRIBUTORS

Dr. Lokman BENNANI
National Aerospace Research Centre (ONERA)
FRANCE
Email: Lokman.Bennani@onera.fr

Mr. Biagio ESPOSITO
Italian Aerospace Research Centre (CIRA)
ITALY
Email: b.esposito@cira.it

Dr. Thomas BROWNE
National Research Council Canada (NRC)
CANADA
Email: thomas.browne@nrc-cnrc.gc.ca

Mr. Francisco REDONDO-CARRACEDO
Airbus Military
SPAIN
Email: francisco.r.redondo@airbus.com

Dr. Richard HANN
Norwegian University of Science and Technology (NTNU)
NORWAY
Email: richard.hann@ntnu.no

Dr. Olivier ROUZAUD
National Aerospace Research Centre (ONERA)
FRANCE
Email: Olivier.Rouzaud@onera.fr

PANEL/GROUP MENTOR

Prof. Bjørnar PETTERSEN
Norwegian University of Science and Technology (NTNU)
NORWAY
Email: bjornar.pettersen@ntnu.no

p

Assessment of Anti-Icing and De-Icing Technologies for Air and Sea Vehicles

(STO-TR-AVT-299)

Executive Summary

The objectives of the Research Task Group (RTG) activity, AVT-299, were:

1) To assess current and emerging ice detection and ice protection technologies for applications to military aircraft and ships operating in cold and humid environments; and
2) To develop a strategy for technology demonstration of ice protection concepts, through experimental testing and computational modelling and simulation.

This report presents the study conducted from January 2017 through December 2020 by the AVT-299 technical team members under the guidance of the Panel Mentor, Prof. Bjørnar Pettersen (NOR). Drs. Ali Benmeddour (CAN) and Ki-Han Kim (USA) were the Co-Chairs of AVT-299. Due to the COVID-19 pandemic that started in the spring of 2020, however, the progress of the study and the final report had been delayed. The report consists of four chapters:

1) Ice Detection Technologies;
2) Ice Protection Systems;
3) Computational Modelling and Simulation Methods; and
4) Experimental Icing Facilities.

In Chapter 1, we evaluated the maturity of various existing ice detection approaches and technologies. Despite active research and development, only a few are commercially available at present that can reliably and accurately measure atmospheric icing conditions and accretion of ice on exposed surfaces. For a safe and efficient operation in all-weather environments, sea and air vehicles must be equipped with new sensor technologies capable of detecting and discriminating the various environmental conditions. There is a strong need to further develop ice detection technologies for direct ice detection, both for current and future requirements for safe aircraft and ships operations. Furthermore, safe operations require a fast, accurate and reliable weather forecast, including nowcasting of icing conditions. With the current lack of commercially available technology and equipment that can be used by aircraft and/or sea vessel operators with little scientific background, additional research and development is necessary. Two areas are identified where improved technologies are required:

a) Detection and thickness measurement of ice accretion on surfaces; and
b) Detection of atmospheric icing conditions for reliable and robust fore- and nowcasting.

In Chapter 2, the current state of ice protection technologies and systems was reviewed, and their advantages and shortcomings highlighted. At present, only active Ice Protection Systems (IPSs) are applied on aircraft and sea vessels. Some of them (pneumatic boots, electromechanical, thermal and chemical systems) are reliable, and widely used. Innovative active technologies like piezoelectric and microwave IPS need improved efficiency and reduced weights and power consumption, particularly for Unmanned Aerial Vehicles (UAVs), most of which do not have enough available power to effectively deal with icing problems. The increasing need for low-weight and energy-efficient and environmentally friendly solutions

fosters the interest in passive technologies such as icephobic coatings. At present, no commercially available icephobic coatings would satisfy the needs of the aviation and marine industry, especially in terms of durability and adhesion to various aircraft and ships' materials (e.g., aluminum, carbon fiber- and glass fiber-reinforced polymers, metal-composite laminates). Active research and development are being conducted in academia, industry and government laboratories to mature these passive technologies and systems for practical applications. For aircraft operating in extremely severe icing environments, hybrid systems combining both active and passive technologies would be required to reduce the energy needed to operate the active systems.

In Chapter 3, a review of the current state of modelling and simulation (M&S) of IPS is presented. A significant progress has been made over the last thirty years in the development of models and numerical tools for the simulation of active IPS (mechanical and thermal). The Commercial Off-The-Shelf (COTS) icing simulation tools based on Computational Fluid Dynamics (CFD), for fluid media, and Finite-Element Methods (FEM), for solid media (crack propagation in ice, substrate deformation), are increasingly used for the design, calibration and optimization of IPS in the aeronautical industry. These tools are based on numerical methods that are well known and relatively mature, in which the models are mainly based on a macroscopic continuum description. The M&S of passive IPS (e.g., icephobic coatings) have only been studied more recently, mainly based on microscopic scales using the Molecular Dynamic (MD) theory. Although these methods yield promising results for the design of new icephobic surfaces, they are mainly used to study the properties and behavior of a coating or textured surface in simplified academic configurations because they are very computationally intensive and are limited to very small spatial and temporal scales. The M&S of a hybrid active and passive IPS presents a new challenge because of complex multi-scale physics. Emerging methodologies such as multi-scale bridging and machine learning showed a great potential for new opportunities. Nevertheless, additional research needs to be conducted in this area to realize the full potential of these promising emerging digital technologies.

In Chapter 4, we reviewed:

a) Intrinsic functions of icing test facilities, including Icing Wind Tunnels (IWTs) and flying facilities and their capabilities; and

b) Icing certification process and protocols for ice protection systems and aircraft development, which have a strong influence on the requirements for icing tests and facilities.

The U.S. Federal Aviation Administration (FAA) and the European Aviation Safety Agency (EASA) recently developed more stringent requirements for safe operating envelopes as part of the certification process. Consequently, the testing facilities must improve their capabilities to properly simulate more hazardous environment, including ice crystals and supercooled large droplet environments of freezing rain and freezing drizzle. Although the testing capabilities of IWTs and flight testing have been continuously improved, there are still challenges remaining in accurate measurements of droplets and ice shapes in IWTs and in finding desired icing conditions for flight testing in natural icing conditions. Finally, we reviewed major IWTs in the Western world in three categories: large industrial facilities, engine test cells and small-scale facilities. We described unique capabilities of each facility and testing parameter ranges. For flying test facilities, we briefly reviewed major icing aerial platforms including spray tankers, together with instrumentations and equipment used by these platforms.

Évaluation des technologies anti-givrage et de dégivrage destinées aux véhicules aériens et maritimes

(STO-TR-AVT-299)

Synthèse

Les objectifs de l'activité du groupe de recherche (RTG) AVT-299 étaient les suivants :

1) Evaluer les technologies actuelles et émergentes de détection et de protection contre le givrage pour les appliquer aux aéronefs militaires et aux navires se déplaçant dans des environnements froids et humides ; et

2) Développer une stratégie de démonstration technologique des concepts de protection contre le givrage, par le biais d'essais expérimentaux et de modélisations et simulations computationnelles.

Le présent rapport expose l'étude menée de janvier 2017 à décembre 2020 par les membres de l'équipe technique de l'AVT-299 sous la direction du parrain de la Commission, le professeur Bjørnar Pettersen (Norvège). Les Drs Ali Benmeddour (Canada) et Ki-Han Kim (États-Unis) co-présidaient l'AVT-299. L'avancement de l'étude et le rapport final ont été retardés en raison de la pandémie de COVID-19 qui a débuté au printemps 2020. Le rapport comprend quatre chapitres :

1) Technologies de détection du givrage ;

2) Systèmes de protection contre le givrage ;

3) Méthodes de modélisation et de simulation computationnelles ; et

4) Installations expérimentales de givrage.

Au chapitre 1, nous avons évalué la maturité des différentes approches et technologies existantes de détection du givrage. Malgré une recherche et développement active, il n'existe actuellement que quelques technologies commerciales capables de mesurer de manière fiable et précise les conditions de givrage atmosphérique et l'accumulation de glace sur les surfaces exposées. Pour un fonctionnement sûr et efficace, quelle que soit la météorologie, les véhicules marins et aériens doivent être équipés de nouvelles technologies capables de détecter et de distinguer les différentes conditions environnementales. Il est grandement nécessaire de développer encore les technologies de détection directe du givrage, tant pour les besoins actuels que futurs en matière de sécurité des opérations navales et aéronautiques. De plus, la sécurité des opérations exige des prévisions météorologiques rapides, précises et fiables, notamment la prévision immédiate (« nowcasting ») des conditions de givrage. Étant donné le manque actuel de technologies et d'équipements commerciaux utilisables par les exploitants d'aéronefs et/ou de navires maritimes ayant peu d'expérience scientifique, une recherche et développement supplémentaire est nécessaire. On identifie deux domaines qui nécessitent une amélioration des technologies :

a) La détection et la mesure de l'épaisseur de glace accumulée sur les surfaces et

b) La détection des conditions de givrage atmosphérique, pour une prévision et une prévision immédiate fiables.

Le chapitre 2 examine l'état actuel des technologies et systèmes de protection contre le givrage et met en lumière leurs avantages et leurs lacunes. Actuellement, les aéronefs et navires maritimes n'utilisent que des systèmes actifs de protection contre le givrage (IPS). Certains d'entre eux (protections pneumatiques, systèmes électromécaniques, thermiques et chimiques) sont fiables et largement employés. Il convient d'augmenter l'efficacité des technologies actives innovantes telles que l'IPS piézoélectrique et à micro-ondes et de réduire leur poids et leur consommation d'énergie, en particulier dans les véhicules aériens sans pilote (UAV), dont la plupart ne disposent pas d'une puissance suffisante pour régler efficacement les problèmes de givrage. Le besoin croissant de solutions légères, économes en énergie et respectueuses de l'environnement nourrit l'intérêt pour les technologies passives telles que les revêtements non givrables. Actuellement, aucun revêtement non givrable du commerce ne répondrait aux besoins de l'industrie aéronautique et navale, en particulier en termes de durabilité et d'adhérence à divers matériaux d'aéronefs et de navires (par ex., aluminium, polymères renforcés de fibre de carbone et de fibre de verre, stratifiés composites métalliques). Des travaux de recherche et développement sont en cours dans le monde universitaire, l'industrie et les laboratoires publics pour affiner ces technologies et systèmes passifs en vue d'applications pratiques. Pour les aéronefs fonctionnant dans des environnements de givrage extrêmement hostiles, des systèmes hybrides combinant des technologies actives et passives réduiraient la consommation d'énergie.

Le chapitre 3 passe en revue l'état actuel de la modélisation et simulation (M&S) des IPS. Ces trente dernières années, la mise au point de modèles et d'outils numériques simulant des IPS actifs (mécaniques et thermiques) a enregistré des progrès importants. Les outils commerciaux (COTS) de simulation du givrage basés sur la dynamique des fluides computationnelle (CFD), pour les fluides, et les méthodes par éléments finis (FEM), pour les solides (propagation des fissures dans la glace, déformation des substrats), sont de plus en plus utilisés pour concevoir, étalonner et optimiser les IPS dans l'industrie aéronautique. Ces outils reposent sur des méthodes numériques bien connues et relativement matures, dans lesquelles les modèles reposent principalement sur une description macroscopique du continuum. La M&S des IPS passifs (par ex., les revêtements non givrables) n'a été étudiée que récemment, principalement à l'échelle microscopique, à l'aide de la théorie de la dynamique moléculaire (MD). Bien que ces méthodes donnent des résultats prometteurs pour la conception de nouvelles surfaces non givrables, elles servent principalement à étudier les propriétés et le comportement d'un revêtement ou d'une surface texturée dans des configurations théoriques simplifiées, car elles nécessitent énormément de calculs et se limitent à de très petites échelles spatiales et temporelles. La M&S d'un IPS hybride, actif et passif, présente un nouveau défi, en raison de la physique complexe à de multiples échelles. Les méthodologies émergentes, telles que le rapprochement de multiples échelles et l'apprentissage automatique, ouvrent potentiellement de grandes opportunités. Néanmoins, d'autres recherches doivent être menées dans ce domaine pour tirer pleinement parti de ces technologies numériques émergentes et prometteuses.

Au chapitre 4, nous avons examiné :

a) Les fonctions intrinsèques des installations d'essais de givrage, y compris les souffleries de givrage (IWT) et les installations de vol et leurs capacités ; et

b) Le processus de certification du givrage et les protocoles des systèmes de protection contre le givrage et de mise au point d'aéronefs, qui ont une forte influence sur les exigences des essais et des installations de givrage.

La Federal Aviation Administration (FAA) des États-Unis et l'Agence européenne pour la sécurité aérienne (AESA) ont récemment établi des exigences plus strictes concernant les domaines de fonctionnement sûrs dans le cadre du processus de certification. Par conséquent, les installations d'essai doivent améliorer leurs capacités à simuler correctement un environnement plus dangereux, y compris les cristaux de glace et les environnements de grosses gouttelettes surfondues favorables à une pluie ou une bruine verglaçante. Bien que les capacités d'essai des IWT et des essais en vol aient été continuellement améliorées, il reste difficile de mesurer avec précision les gouttelettes et la forme du givrage dans les IWT et de trouver les conditions souhaitées pour les essais en vol en conditions de givrage naturelles. Enfin, nous avons

examiné les grandes IWT d'Occident appartenant à trois catégories : grandes installations industrielles, bancs d'essai de moteurs et petites installations. Nous avons décrit les capacités uniques de chaque installation et les plages des paramètres d'essai. Pour les installations d'essai en vol, nous avons brièvement passé en revue les grandes plateformes aériennes sujettes au givrage, incluant les bombardiers d'eau, ainsi que l'instrumentation et l'équipement utilisés par ces plateformes.

Chapter 1 – ICE DETECTION TECHNOLOGIES

Christoph Deiler
German Aerospace Center
GERMANY

Federico Veronesi and Mariarosa Raimondo
Institute of Science and Technology for Ceramics
ITALY

Julio Mora, Paloma García and Malte Frovel
Instituto Nacional de Técnica Aeroespacial (INTA)
SPAIN

Bob Gagnon, Thomas Browne
National Research Council
CANADA

Richard Hann
Norwegian University of Science and Technology
NORWAY

1.1 INTRODUCTION

One of the earliest accounts of in-flight icing on aircraft parts was given by Alcock and Brown following their historic first non-stop transatlantic aircraft flight in June 1919. The flight was in a modified World War One Vickers Vimy bomber aircraft that had an open cockpit that exposed the heroic pilot (Alcock) and navigator (Brown) to all of the weather conditions such a journey over the North Atlantic has to offer. The flight initiated on June 14 in a farmer's field in St. John's, Newfoundland and finished approximately 16 hours later with a non-injurious crash-landing in a bog near Clifden in County Galway, Ireland. Icing was observed on the wings at times during the flight, and also snow/ice build-up on a critical petrol-overflow gauge. Brown had to kneel on his seat and raise himself up into the ferocious cold airstream (~ 110 mph) so that he could reach the gauge and scrape the snow/ice off. This dangerous and painful task was required multiple times and may, according to an alleged statement by Alcock, have involved Brown using a knife to remove the snow/ice.

This early report of aircraft icing and "mitigation" (based on the information in Ref. [1]) shows that monitoring the accretion of ice on exposed surfaces of aircraft and marine vessels is essential for the safe and effective decision making of crews operating these vehicles. Ice accretion on air and sea vehicles is by no means a new phenomenon with the earliest means of detection being visual observation. Once ice was observed to be building up on a surface, depending on the severity and location of ice build-up, crews would relocate the vehicles to a region where the atmospheric conditions were less prone to icing and would potentially allow the ice to melt due to higher temperatures. More recently, sensor technologies have been developed to detect icing. The ability of a sensor to detect and alert crews of accreted ice alleviates the task load of already overworked crews and it can also provide the ability to detect ice much earlier than visual detection (with a limited field of view for the observation) would allow. Nevertheless, monitoring of visual cues for ice detection is a common practice especially in aviation and basis for ice detection on most of today's modern transport aircraft. With future developments of air and sea vehicles, however, this simple method for ice detection will not be sufficient anymore. Furthermore, despite the inherent advantages that ice detection sensors provide it has only been in recent years that new aviation regulations have been developed to address the need for ice detection, and in the marine sector there are still no regulations that govern the detection of accreted ice.

A historical review on the evolution of ice detection technologies for aircraft is provided by Jackson and Goldberg [2]. The first commercial ice detection sensor was developed in 1956 and installed on the engine inlet of a Lockheed C-130 Hercules aircraft. It was a pneumatic probe designed to monitor the differential dynamic pressure across the probe, which would change in the presence of accreted ice. Ice detection technology has evolved and grown significantly since this initial design, and the technologies that exist today vary widely in their design, what they detect, and their intended field of use.

Ice detection systems also have applications in the marine industry; however, their use is not as commonplace as they are in aviation. Marine icing, on both ships and offshore platforms, results from not only meteorological conditions similar to aircraft icing but also freezing sea spray. Ice accretion on the decks of ships can negatively impact stability and lead to the capsizing and loss of vessels. Unlike the aviation industry, there are currently no regulations in place that address the use of ice detection systems on marine vessels.

Technologies exist that, for example, detect ice accretion on exposed surfaces, detect the corresponding type of ice, provide an estimate of the rate of accretion, or a combination of these. There are also technologies, which do not directly monitor ice accretion but rather monitor atmospheric conditions in the vicinity of the vehicle to identify when icing is likely to occur, or monitor the performance of the vehicle to infer when ice accretion has likely occurred. Technologies have been developed for a wide range of applications including airplanes, Unmanned Aerial Vehicles (UAVs), helicopters, and marine vessels. They are also being used extensively in field and laboratory research.

The objective of this chapter is to introduce the concept of ice detection technologies and provide a review of existing types of technologies. While it isn't practical to document every existing technology, the intent is to detail the primary operating principles and provide specific examples for each.

For this report, NRC conducted a literature and patent survey in addition to the already available literature and knowledge available to the authors to obtain a wide overview on the field of ice detection. The NRC survey resulted in additional 349 patents and 249 publications since 1993, which could have been relevant for this report. After analysis and evaluation, the information obtained from these patents and publications was included in the following sections.

1.2 NEED FOR ICE DETECTION TECHNOLOGIES

The majority of ice detection technologies are designed with the intent to improve the safe operation of air and sea vehicles. The United States Federal Aviation Administration (FAA) and the European Aviation Safety Agency (EASA) regulations for the certification of ice protection and detection systems were introduced for large transport aircraft in Appendix C and recently Appendix O to Part 25 (14 CFR Part 25 [3] respectively CS-25 [4]) in response to several high profile aviation accidents that resulted from icing events. The regulations are focused on aircraft-level ice protection certification. They do not explicitly prescribe the means of ice detection but do imply the need for ice detection systems to detect and differentiate between different meteorological icing conditions. The main driver for the need of this differentiation is that an aircraft might only be certified for flight in certain icing conditions and must avoid others. A detailed overview of the FAA and EASA regulations is provided by Jackson [5]. The need to improve the safe operation of aircraft, along with the new FAA and EASA regulations, has driven the development of ice detection technologies.

Also, new additions to the airspace like UAVs and urban air mobility (UAM) aircraft face the hazards of icing. These emerging technologies have specials needs for ice detection since they tend to be more sensitive to icing compared to larger manned aircraft [6]. Consequently, improved ice detection technologies are required for UAVs and UAM, which need to be developed.

Ice accretion on ships and offshore platforms also poses significant safety hazards in the marine industry. Large accumulations of ice build-up on the decks of ships create hazardous working environments for the crew and reduce stability of ships, which can cause capsizing. Ice detection technologies have been developed for the marine sector but not to the same extent as for the aviation industry.

The use of ice detection systems for research and development represents another significant area of application. Sensors measuring icing conditions and ice detectors are used extensively in field and laboratory research to provide a means of monitoring ice accretion and validating Ice Protection Systems (IPSs) and numerical icing models.

As an example, a selection of recent and ongoing research projects related to ice detection technologies for aircraft and sea vessels is given in Table 1-1.

Table 1-1: Example Selection of National and International Research Projects Related to Ice Detection.

Acronym	Title	Application	Type of Activity	Objective
PFIDS	Primary In-Flight Icing Detection System (Ice and Icing Conditions)	Aircraft	EU Project, Clean Sky 1 2008 – 2016	Design robust and reliable ice detection systems.
EXTICE	EXtreme ICing Environment	Aircraft	EU Project, FP7 2008 – 2012	Study preliminary icing wind tunnel upgrades for simulating SLD conditions.
SuLaDI	Supercooled Large Droplet Icing	Aircraft	National German project 2011 – 2016	Investigation of SLD-icing conditions including development of reliable ice detection technologies (direct detection of ice accretion and indirect detection monitoring aircraft characteristics).
HAIC	High Altitude Ice Crystals	Aircraft	EU Project, FP7 2012 – 2017	Development and testing (wind tunnel and flight) of icing conditions detectors. Development of acceptable means of compliance.
PHOBIC2ICE	Super Ice Phobic Surfaces to Prevent Ice Formation on Aircraft	Aircraft	Horizon 2020 + Canada 2016 – 2019	Development of the IWT and performance of ice formation and accretion tests. Ice detector tests.
ICASSIO	Icing Conditions Interrogation, Detection and Discrimination Systems Contributing to Flight Safety and Ice Protection Optimization	Aircraft	EU Project, Clean Sky 2 2017 – 2021	Provide the ice accretion rate indication.
Flagship ICE	Flagship Program ICE founded by PRORA (Italian Aerospace Research Program)	Aircraft	National Italian Project 2018 – 2020	Technologies and methodologies for the design of IPSs and sensors.
SENS4ICE	SENSors and Certifiable Hybrid Architectures for Safer Aviation in ICing Environment	Aircraft	EU Project, Horizon 2020 2019 – 2023	Development of sensor technologies for robust hybrid ice detection as a combination of different approaches to cover detection of the full icing envelope.

1.2.1 Aircraft Icing (FAA and EASA Regulations)

Aircraft icing normally occurs during flight through certain atmospheric conditions containing supercooled liquid water and manifests in ice accretions on the airframe. Also, ice accretions can form on-ground from e.g., freezing rain or snow.

Figure 1-1 shows an example for ice accretion on different parts of the airframe during flight which is still present after landing.

Figure 1-1: Ice Accretion on Different Part of an Airplane; Left: Nose; Mid: Engine Inlet; Right: Sensor Probe. Courtesy of NRC Canada, Flight Research Laboratory.

For certification purposes the FAA and EASA (14 CFR Part 25 [3] respectively CS-25 [4]) recognize three types of ice detection systems for use on aircraft: Advisory Ice Detection Systems (AIDS), Primary Manual Ice Detection Systems (PMIDS) and Primary Automatic Ice Detection Systems (PAIDS). AIDS are used only to provide back-up indication that icing conditions have been encountered and flight crews must still activate IPS based on their standard flight manual criteria. PMIDS provide the primary indication that icing conditions have been encountered. The system provides a signal to the flight crew who must then manually activate the IPS. PAIDS also provide the primary indication that icing conditions have been encountered but the IPS is activated automatically.

Jackson and Goldberg [2] have identified several advantages and disadvantages of the different types of ice detection systems. There is an increased initial cost associated with primary ice detection systems. In order for primary systems to meet reliability requirements there must be at least two ice detectors installed, and additional costs may be incurred due to the level of integration associated with primary systems. Despite high initial costs, primary systems offer potential fuel savings and reduced pilot workload. When pilots activate IPSs based on manual criteria (typically total temperature reading and visible moisture sighting) actual accreted ice will only be present for a very short period of time. These false activations of the IPS have a significant draw down on fuel as modern ice protections systems (mainly thermal) require a significant amount of power from the engines or generators. When relying on a primary system, pilots are no longer required to monitor temperature, visible moisture, or ice accretion thus reducing their workload. Furthermore, a more dedicated activation of the countermeasures to icing would be a huge step in the direction of a more environmentally friendly air transport.

1.2.1.1 Primary Ice Detection Certification Requirements

Flight crews have a critical reliance on primary ice detection systems, and as such, the FAA and EASA have developed certification requirements for primary ice detectors. In addition to the overarching requirements that apply to all equipment installed on aircraft, it must be demonstrated that an ice detector can effectively detect ice when an aircraft is operating within a defined set of atmospheric icing conditions. There are three

defined sets of atmospheric icing conditions, each with an associated certification. A brief overview of these certifying requirements is presented below. Once certified, operation outside the boundaries of the associated icing condition(s) is prohibited and recognized as an operating limitation. For a complete understanding of primary ice detection certification, it is necessary to refer to the corresponding FAA and EASA regulations. A thorough overview and discussion of primary ice detection certification is provided by Jackson [5].

1.2.1.1.1 14 CFR Part 25 – Appendix C

Appendix C to the regulations 14 CFR Part 25 [3] respectively CS-25 [4] addresses a set of atmospheric conditions that an aircraft must be able to safely operate in to be certified for flight in icing. Since 1964, this definition is used to design aircraft ice detection and protection systems for modern aircraft, and cover the major parts of the most likely icing conditions [7]. Icing conditions are defined through envelopes of different atmospheric parameters. In detail, Appendix C provides the boundaries for the "probable maximum" (99%) value of cloud water concentration (liquid water content "LWC"), the actual droplet size distribution (droplet median volumetric diameter (MVD)), ambient temperature and pressure altitude. Although Appendix C is only defined up to 22,000ft, icing conditions above this altitude should also be considered. Appendix C identifies two types of icing conditions, which aircraft should withstand and ice detectors should detect:

- Continuous Maximum conditions (i.e., stratiform clouds), which are lower in Max LWC but longer in horizontal extent.
- Intermittent Maximum conditions (i.e., cumuliform clouds), which are higher in Max LWC but shorter in horizontal extent.

With regard to ice detection technologies, not only could the atmospheric conditions respectively corresponding to characteristic parameters be used for ice detection but also the resulting ice formations on detector probes or aircraft surfaces.

1.2.1.1.2 14 CFR Part 25 – Appendix O

Appendix O to 14 CFR Part 25 or CS-25 was developed following the 1994 crash of the American Eagle ATR-72 aircraft near Roselawn, Indiana, USA [8]. The cause of this tragic accident was the presence of Supercooled Large Droplets (SLD) in the clouds, which led to the formation of an ice ridge on the aircraft's wings where the de-icing boots were not effective. The subsequent loss of control of the aircraft could not be prevented by the pilots as the aircraft was neither designed nor certified to withstand ice formations caused by these SLD conditions [7].

The probability for the occurrence of SLD-icing conditions in the atmosphere is quite low. The definition of Appendix C to 14 CFR Part 25 in the 1960s, which led to a huge increase in aviation safety, did not consider these conditions and until the Roselawn accident and several others in the 1990s, flight in icing conditions did not result in a significant number of fatal aircraft accidents. With the increase of air traffic during the last decades, however, the encounter of the even rare SLD-icing conditions becomes more likely. Consequently, the regulation authorities decided to also cover the SLD conditions with a dedicated appendix to the certification regulations. Introduced in 2014, the definition of the icing envelopes for SLD conditions is new to aircraft manufactures and aviation suppliers but will become important for today's and future aircraft developments and certifications. Appendix O addresses the set of environmental conditions that an aircraft must be able to safely operate in to be certified for flight into SLD (freezing rain and/or freezing drizzle).

1.2.1.1.3 14 CFR Part 33 – Appendix D

Appendix D to 14 CFR Part 33 [9] provides the definition of ice crystal and mixed phase (both liquid water and ice crystals) conditions, for which an engine must be capable to operate safely within its normal

parameters. In consequence, the Appendix D addresses an additional set of environmental conditions that an aircraft must be able to safely operate in to be certified, even if the crystals themselves pose only a minor threat to the airframe. Nevertheless, as the engines are essential for aircraft operations, these certification requirements are not less important for certification and operation. Hence, the mixed phase and ice crystal conditions pose another challenge to ice detection technologies because the conditions must be discriminated from the (pure) liquid water icing conditions, adding further definition as to whether the aircraft is still operated within its certified limits.

1.2.2 Marine Icing

Regarding ice detection and ships, we note that there are two contexts where detection of ice is important. One concerns marine icing that accumulates directly on vessels. The other context regards detection of ice conditions (e.g., level ice sheets, ice floes, glacial ice masses) on the sea surface that ships may have to contend with or avoid. In this report the AVT-299 committee deals specifically with marine icing. Information on the detection of sea surface ice conditions can be found in the report by the AVT-300 committee.

The current authors are not aware of any ice detection regulations for marine icing (see Figure 1-2). The progress on detection and mitigation of marine icing has been slow, compared to that for icing on aerial vehicles. We think this is mostly due to the relatively large extents and thicknesses of marine icing accumulations on sea-going vessels, and the greatly varying array of object shapes and sizes involved (e.g., decks, walkways and stairs, antennas, lifeboats, wire/cables, and so on). There are very few existing options for detecting/measuring/forecasting the accumulations. Hence, regulating such options may be premature at this stage. Nevertheless, in this section some guidance is provided on how marine icing may be predicted using numerical modeling or by using some very approximate expressions and nomograms. Additionally, there is mention of one technology for marine icing detection and thickness measurement.

Figure 1-2: Typical Ice Accretion on Sea Vehicles; Left: HMNZS WELLINGTON in the Ross Sea (Feb/Mar 2011), Courtesy of Chris Howard, Chief Naval Architect, RNZN; Right: Sailors Battle Ice on USS McCampbell (https://navaltoday.com/2017/02/08/uss-mccampbell-sailors-battle-ice-ahead-of-japan-port-call/).

Note: The text in quotations below is taken directly from the document "International Standard ISO 35104:2018(E), Petroleum and natural gas industries – Arctic operations – Ice management" [10].

Atmospheric icing occurs when environmental conditions exist that cause water in the atmosphere, in the form of rain, fog, or wet snow, to freeze onto exposed surfaces, antennas, and cables; it is generally of little consequence.

Sea spray icing is the result of spray from vessel interaction with waves, and also due to wind-driven spume droplets from wave crests, freezing onto the vessel's superstructure. This is more severe than atmospheric icing and can lead to a thick layer of ice forming on the vessel's structure, which can make decks dangerous, prevent doors and hatches from being opened, and if allowed to continue, can possibly result in stability issues for the vessel. This type of icing can be reduced by prudent operation of a transiting vessel or stationary platform, but if it occurs, it might require physical removal of the ice before it becomes too serious.

Sea spray icing can affect the IM [ice management] vessels and sheltering can be effective. If severe icing occurs, ice management vessels can be pulled from duty, which can affect the safety of the facility or operation [11].

A number of approaches can be considered to calculate icing build-up, like the ones presented by Kulyakhtin (MARICE) [12] and Overland et al. [13]. Further references are listed in the review paper by Sultana et al. [14]. The approach of Kulyakhtin is considered to be the most advanced detailed physics-based time-dependent model. It requires more inputs than other models, including specific geometrical aspects of the ships or structures, and so it is not as simple to use as the other models.

RIGICE is an icing model developed for various offshore platforms [15]. RIGICE is more appropriate for the large fixed/floating structures whereas Overland's expression (associated with fishing vessels) might be appropriate for IM vessels.

These methods do not always lead to the same end result. For instance, results from Overland's expression differ from the other models at low sea surface temperatures; at higher sea surface temperatures, the models roughly agree [16]. *Alternatively, simple nomograms can be used* [17]. *A survey of icing data and guidelines was performed when developing the Arctic Operations Handbook* [18].

There is a lack of good quality field data that can be used to validate icing models. The uncertainty in the estimates obtained from the models should be considered.

In reference to the statement above, concerning the lack of good data on marine icing events, it is noted that very few time-series records of quantifiable ice accumulations during icing events have been documented. The data from Gagnon et al. [19] and the associated time-lapse record of an actual icing event on an offshore supply vessel (Marine_Icing_Event.avi, available on Science Connect) are rare.

With respect to laboratory research related to marine icing, at this time there are only two indoor marine icing wind tunnel facilities. One is at the University of Alberta, Canada [20] and the other one is a smaller facility, located at Hokkaido University, Japan [21].

1.3 TYPES AND CLASSIFICATIONS OF EXISTING TECHNOLOGIES

This section presents an overview of different ice detection principles and technologies. In order to make an assessment on the different principles a list of advantages and disadvantages together with an estimation of the technology availability is given at the end of each subsection. Table 1-2 provides the metric for the technology availability assessment in three different categories. The individual assessments are given in Table 1-3 for the "Detection of Ice Accretion on Surfaces" (Section 1.3.1.9), in Table 1-4 for the "Detection of Atmospheric Icing Conditions: Fore- and Nowcasting" (Section 1.3.2.5) and in Table 1-5 for "Detection of Altered Air Vehicle Performance Characteristics" (Section 1.3.3.3).

It is to be noted that the following assessment is based on the information gathered for this report and therefore might not reflect the actual status of all developments based on the physical principles presented.

Table 1-2: Metric for General Classification of Technology Readiness, Based on NASA TRL Classification [22].

Low	Low TRL (1-3)	Basic concept or principle evaluation in experimental phase
Med	Medium TRL (4-6)	Technologies under development or testing of sensors
High	High TRL (7-9)	Sensors or products fully exploited and commercially available

1.3.1 Detection of Ice Accretion on Surfaces

To reduce unnecessary de-icing actions and increase airplane availability, development of in situ ice thickness monitoring capability is strongly desired. Several techniques have been reported to monitor ice layer build-up [2].

1.3.1.1 Wave Frequency (Acoustic, Ultrasonic, Microwave, Coplanar)

Wave frequency methods are widely used in many different fields of technology, science or medicine, among others. In past decades, their principles have inspired many different sensing technologies, and non-destructive evaluation methods.

1.3.1.1.1 Acoustic

The ice accretion on a lifting surface modifies the flow: when the surface gets rougher due to ice accretion, the smooth flow along the upper surface of the airfoil tends to separate sooner, generating local small-scale turbulence aft of the leading edge. Sensitive microphones can receive this signal, and by analyzing the noise spectrum the ice-induced turbulence can be detected [2].

These techniques have been mostly explored for helicopter applications. There are some relevant studies in literature that show different degrees of technology development:

- **Modeling:** Chen et al. [23] used Helicopter Multi-Block Computational Fluid Dynamics (HMB CFD) solver, to approximate the acoustics-based signals to iced shapes in helicopter rotors. Several candidate monitoring positions were assessed for acoustic sensors to be placed on the helicopter fuselage. The influence of ice on the aero-acoustic characteristics of a rotor was calculated, and parameters such as the ice amount and the icing position on the blade were quantified. Chen et al. [24] further established the acoustic characteristics of iced AH-1G/OLS rotor by using a CFD model as well as sophisticated numerical and mathematical approximations. Those data were compared with experimental data of an SRB rotor model, and predicted that a tiny ice amount on the rotor can make the aero-acoustic characteristics change a lot, for instance, the ice with only 1.2% of blade volume makes the sound pressure decrease by 15% at the 255° azimuthal angle.
- **Experimental:** The Adverse Environment Rotor Test Stand (AERTS) facility at The Pennsylvania State University facility is highlighted in many studies in literature. For instance, it was used in the two following cases: Cheng [25] studied the change of the discrete frequency noise (thickness noise and steady loading noise) due to ice accretion, which was calculated by using PSU-WOPWOP, and proposed an acoustic prediction code. Cheng et al. [26] quantified the surface roughness at the early stage of helicopter rotor ice accretion by acoustic measurements, in the frequency bandwidth region ranging from 10 kHz to 24 kHz.

1.3.1.1.2 Ultrasonic

Each time a sound wave finds an interface with a different sound speed, a fraction of the energy of that sound wave is reflected back to its source. This is a principle similar to radar. Narrow sonic pulses are used, and the differences in the reflected signals are monitored. This type of ice detector requires a sophisticated algorithm to determine the presence of ice [2].

There are some proposed technologies in the literature in different degrees of development:

- **Modeling:** ultrasonic waves have been simulated to predict the runback ice accretion on aerodynamic surfaces of composites [27] using a finite element model approximation. Computational studies of finite element/boundary element method (FEM/BEM) were used by Rose [28] to predict the behavior of ultrasonic guided waves for inspection and structural health monitoring, as well as ice detection. Gao and Rose [29] were able to discriminate different types of ice (mixed, rime and glaze) with thicknesses from 0.5 to 2 mm using an ultrasonic guided wave simulation method.
- **Experimentation:** Zhao and Rose [30] also studied the Probability-based Reconstruction Algorithm (PRA) based on ultrasonic guided wave tomography methods applied to ice detection on plate-like structures, and on rotary and fixed-wing aircraft. Liu et al. [31] investigated the frequency dependent attenuation of acoustic waves that is related to the ice micro-structure and density. In this way it may be possible to distinguish different types of ice.
- **In-flight:** Goodrich Company [32] published the in-flight results of an ultrasonic guided waves method, with two capabilities: to detect the accumulation of ice on the surface of the aircraft wing leading edge, and to determine when such ice is shed and/or sublimated. The detection sensors were installed on the aircraft wing leading edge, and results were compared with commercial probe-style ice detectors mounted on the fuselage. The proposed sensors detected the ice accretion in the same way as other commercial systems do and also detected the ice release, which is a valuable signal in case of ice protection failure. Liu et al. [33] were able to detect ice layers less than 1 mm in thickness on the control surface (stabilizer) of an aircraft wing structure utilizing integrated Ultrasonic Transducers (UTs). These were based on piezoelectric film sensors fabricated by a sol-gel spray technique for aircraft environments, and that were suitable for temperatures ranging from -80 to 100°C.
- Le Pimpec and Plaisir [34] presented a method to detect ice accretion on-ground and in-flight, and to detect the presence of anti-icing fluids in order to assess their effectiveness. The sensor is based on the measurement of the acoustic impedance of ultrasonic waves.

Rose [35] gave a summary of practical recommendations for the utilization of guided wave systems that are used for non-destructive evaluation. It includes theoretical and experimental aspects such as phase velocity, group velocity, attenuation dispersion curves, and solutions to problems in tubing, piping, hidden corrosion detection in aging aircraft, adhesive and diffusion bonding, and ice detection.

1.3.1.1.3 Coplanar

Bassey and Simpson [36] proposed the use of compatible coplanar transmission lines as Time Domain Reflectometry (TDR) sensors for ice thickness measurements. The results showed that the propagation characteristics of electromagnetic waves in a loaded coplanar line depend on the permittivity and thickness of the test material. In a further work by Bassey and Simpson [37], they carried out a numerical comparison of the Coplanar Waveguide (CPW) and the Conductor-Backed Coplanar Waveguide (CBCPW). Results showed that the CBCPW is more sensitive, particularly at small thicknesses of the test material.

1.3.1.1.4 Microwave

A typical system was described by Jackson and Goldberg [2]:

> *microwave source is used to radiate from a slotted antenna located behind the surface to be monitored for ice. The surface above the antenna must be relatively transparent to the microwave frequency selected. When ice accumulates on the monitored surface it prevents the efficient radiation of the microwaves. By sensing the loss of radiation efficiency of the antenna, ice can be inferred.*

In 2004, NASA published a NASA Tech Brief [38], describing a system that can measure the thickness of ice from around 0.0254 mm to about 6 mm and can distinguish between ice, water (or de-icing fluid), and a mixture of ice and water (or de-icing fluid), based on microwave measurements. Bianchi et al. [39] presented theoretical calculations and experimental evaluations of the performance of microstrip sensors to evaluate the ice presence and ice thickness monitoring, based on measurements of the amplitude of the reflection coefficient at microwave frequencies.

1.3.1.1.5 Eigenfrequency

Atmospheric icing is also a challenge for wind turbines installed in cold climate conditions. One popular ice detection method on wind turbines is by monitoring the change in eigenfrequency of the turbine blade due to the added ice mass. The vibrations that are generated during normal operations are sufficient to excite the natural frequencies of the turbine blades using operational modal analysis [40]. Several commercial systems use this approach, which has the added advantage to also detect structural damage to the turbine blades early on. This detection method has not been implemented in aviation yet, but may be particularly suited to ice detection on rotors and propellers.

1.3.1.2 Optical (Infrared, Lasers, Birefringence, Refractometry, Photography)

All current remote sensing ice detection approaches operate in some part of the electromagnetic spectrum between the millimeter wave region and the visible optical region. Several physical properties can be exploited by an electro-optic approach including: optical interference effects, internal reflection, surface scattering, polarization, or spectral reflectance [41].

Many of the reported studies and patents found in the literature are based on the optical polarization shift. Jackson and Goldberg [2] described these birefringence methods as follows:

> *When polarized light (visible or infrared) is projected on a reflective surface there is retro-reflection or "back scatter" that can be detected by a properly configured sensor. When ice is present on a surface, the properties of frozen water rotate the polarization of the reflected light beam. This polarization shift is detected by the back scatter sensor and reported as detected "ice".*

Some other examples of optical methods for ice detection are summarized below.

1.3.1.2.1 Infrared (IR)

IR radiation has been widely used in recent decades for temperature monitoring. Typical sensors of this type detect the ambient IR emission from a surface due to its temperature. IR radiation can also be used to determine the chemical composition, or the physical state of a surface. Zhuge et al. [42] studied the different variation trends of near infrared images of partially covered with ice and water on Carbon Fiber Composite surfaces. By using 4 different detection wavelengths they were able to determine the presence of water and/or ice.

One of the greatest advantages of optical techniques is their non-contact characteristic. This makes these techniques very suitable for aeronautical applications, and especially for moving components such as

helicopter rotors, or aircraft blades. Some studies are based on the infrared reflection energy of the surface, before and after freezing. Zhang et al. [43] described a non-contact infrared helicopter rotor icing detection system, and through numerous static and dynamic experiments proposed some modifications in the processing algorithm to decrease the influence of the flapping and pitching motion of the rotor blade.

Gregoris et al. [41] used a Spectral Camera system developed by MD Robotics based on infrared reflectance spectroscopy, which represents a viable approach to efficient remote sensing of ice contamination on diverse surfaces. It demonstrated the ability to detect <0.5 mm thick layers of frost, ice and snow on a variety of different surfaces- even when the ice is beneath water or de-icing fluids. The Spectral Camera could be applied to aircraft ice contamination inspection, road condition monitoring and the Space Shuttle (or similar vehicle) icing assessment. IR techniques have also been used in marine sector. Rashid et al. [44] proposed an IR system for marine operations, where saline ice detection can be important for automated de-icing systems.

An important limitation for icing sensors is the operation in severe ambient conditions. This was considered in Jedi-Ace project [45], proposing a novel type of mid-infrared waveguide sensors, which exploit vibrational resonance-driven directional coupling effects besides absorption, with optical sensing elements that can be buried (1 – 10 μm) and resist systematic exposure to industrial environments without failure [46].

In order to detect ice on aircraft wings, a method based on near infrared image processing is proposed by Gao et al. [47]. According to the variety of near infrared reflectivity, four images of one object are obtained under different detection wavelengths. Water and ice can be distinguished by the different variation trends of the images. It is proved that the different reflectance spectra of water and ice in a certain wavelength band can be used to detect and measure the ice on aircraft wings made of carbon fiber composite materials. A commercial application is unknown. The TRL in this development stage is estimated to be medium.

An advantage of these camera-based IR technologies is that cameras are well-known in the aeronautical field and have a high TRL. A drawback can be found in the difficulty to calibrate these cameras, because different lighting conditions and changing surface conditions alter the reflected IR spectrum.

1.3.1.2.2 Laser

Zhang et al. [48] observed great differences between the absorption rate (infrared laser with the wavelength of 1450 nm) on the ice and the detected surface. The energy reflected using the photoelectric detector was enough to detect the ice accretion on a helicopter rotor. Zhang et al. [49] used neural networks, and measurements of the infrared laser reflection coefficient from the underlying surface, to determine the thickness of different ice types on the surface of a helicopter rotor blade.

Lin et al. [50] studied IR laser back-reflection and energy-absorption for different incident and observation angles to determine the reflection coefficient of the surface under the ice on aircraft airfoils.

Gagnon et al. [51] presented results of a patented technology to measure the thickness of ice layers on surfaces. It incorporates two optically-based methods, involving a laser and a camera that give it capability to measure the thickness of clear or foggy layers of solid or liquid on surfaces. The device is capable of measurements on moving surfaces such as wind turbines, and aircraft propellers and rotors. Details of a prototype are presented along with thickness data (in the range 1 mm to 10 mm) acquired during two test programs. One study was on clear ice layers where measurements were obtained from a distance of around 15 m, with a measurement accuracy of ±0.1 mm, and the other was on foggy ice layers at a distance of around 13 m, with an accuracy of ±0.4 mm. Within 2020/2021 (possible limitations due to the COVID-19 pandemic permitting), this technology will be used in conjunction with a novel icing mitigation technology in lab tests. The intention is to demonstrate the controlled removal (at a distance) of icing accumulations from surfaces of aircraft components.

1.3.1.2.3 Others

Zhuge et al. [52] used an improved Harris feature point detection algorithm to extract feature optical points of interest in ice detection. In the process of aircraft residual ice detection based on near infrared spectrum method, the qualities of the images, such as brightness and contrast, are easily influenced by sunlight, weather and other factors. This method helps to automatize this process. Shajiee et al. [53] developed a novel ice sensing and active de-icing method for wind turbines, based on Optical Frequency-Domain Reflectometry (OFDR) to yield a) Ice thickness measurement within micron accuracy; as well as b) An identification of the type of ice present. Ikiades et al. [54] proposed an optical technique to measure the scattered and reflected light from the ice surface and volume. By measuring the intensity and polarization properties of the backscattered, reflected and transmitted light, the technique could determine the thickness and type of ice on an airfoil in icing wind tunnel tests.

Gagnon et al. [19] have described a visual-based Marine Icing Monitoring System (MIMS) for monitoring marine icing accumulation on offshore rigs and vessels. The system consists of a CPU connected to two high-resolution digital cameras that are positioned to view expansive areas, or smaller areas depending on requirements, where icing could occur. The system is standalone, needing only a standard 110 VAC power source. The computer controls each camera so that pictures are taken at regular intervals (every 12 minutes). The system has a satellite phone so that it can be checked and controlled remotely. Images from the cameras are analyzed manually or automatically using image-analysis software, to yield ice accumulation thickness time series for multiple locations within the field of view.

1.3.1.3 Fiber Optics

In the last two decades the use of optical fibers has been significantly increased. Optical fibers permit transmission over longer distances and at higher bandwidths (data rates) than electrical cables. In addition, fibers are immune to electromagnetic interference, a problem from which metal wires suffer. Optical fibers typically include a core surrounded by a transparent cladding material with a lower index of refraction. Light is kept in the core by the phenomenon of total internal reflection, which causes the fiber to act as a waveguide. Very sensitive sensors can be imbedded in the sensor core such as Fiber Bragg Gratings (FBG) for measuring strain and temperature changes. These sensors are widely used in the development of sensors, including ice detection.

1.3.1.3.1 Light Scattering Sensors

Measuring the scattering and reflection of light using fiber optic sensors is one of the most frequent applications for fiber optic ice sensing in aeronautical applications. The principle of this direct ice detecting sensor system is based on the light scattering due to the presence of ice. As shown in Figure 1-3, in one optical fiber (1) a light of certain wavelength is emitted by a laser source or equivalent light source. This light exits the fiber in the surface to be monitored. Next to the emitting fiber is another optical fiber that receives scattered light (2) and is connected to a photodiode. Both fibers are in parallel or in a certain angle, so that the emitted light from fiber (1) does not reach directly the fiber (2). In the case that ice accretes on the surface, the light from fiber (1) is scattered and enters fiber (2) and as a consequence an electric signal is produced by the photo diode. The intensity of the scattered light depends on the thickness of the ice and the ice type (see Figure 1-3).

First activities with this type of sensor system were performed by Armstrong et al. [55] in 2003 for the application in aircraft and rotorcraft. Individual optical fibers were used in this case. Ikiades et al. [56] performed experiments on a wing profile, which has an “L” shape window with source (1) and signal fiber (2), Figure 1-3 (left). Changing the displacement of the source and signal fiber, he obtained the typical intensity distribution as a function of ice thickness. Putting the source fiber parallel to the signal fiber was done by the same group [56] to investigate the effect of glazed and rime ice on polarized light. On the basis of the above design, a set of fibers was arranged in a linear array equidistantly at a pitch of 1 mm [57], which

are capable of measuring the thickness of ice and its accretion rate. The final signal obtained in these experiments is light intensity. Ikiades et al. [57], [58] have published some other interesting optic detection studies based on this technique, which showed good results after validation in an IWT.

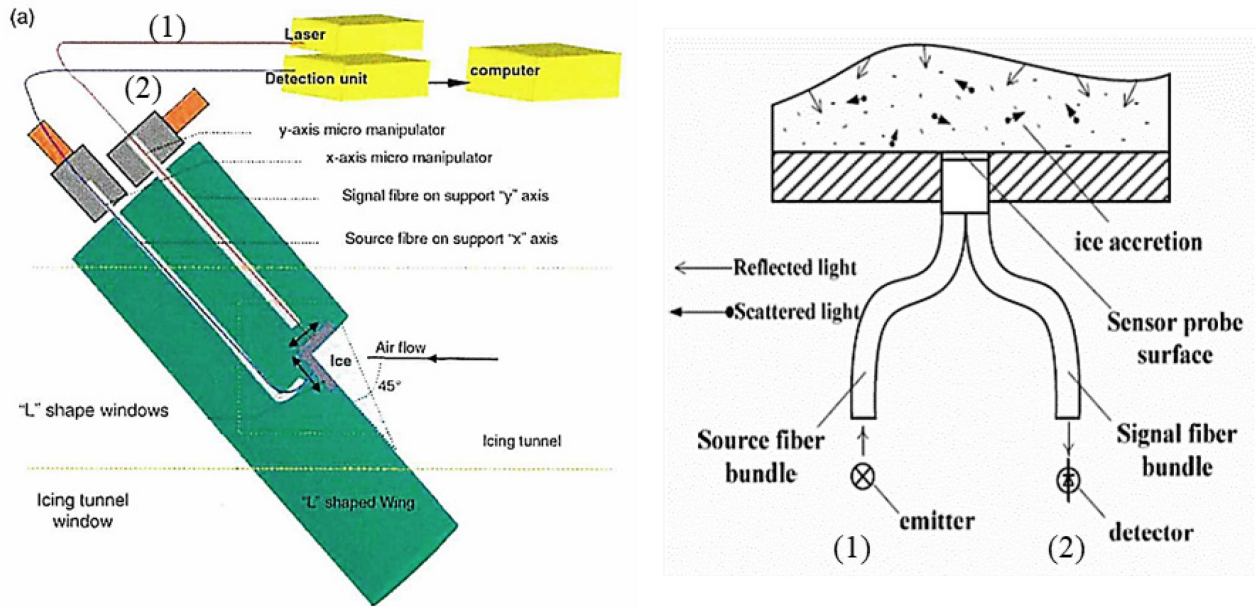

Figure 1-3: Left: "L" Shaped Sensor Window from Ref. [56]. Right: Configuration of the Sensor Head from Ref. [58].

Li et al. [59] worked on the same fiber optic technology. The design of the sensor probe was optimized to increment the performance. The fiber optic ice sensor was fabricated as a bifurcated fiber bundle, consisting of a source fiber bundle and a signal fiber bundle, forming the shape "Y", which is shown in Figure 1-3, right. The results obtained from the calibration experiments demonstrated the feasibility of the fiber optic ice detection system. The use of Artificial Neural Networks (ANN) improved the evaluation of ice type and ice thickness [60]. Glaze and rime ice from 1 mm to 10 mm have been detected and the different ice types have been differentiated.

Armstrong et al. [61] at Cambridge Optical Sciences in the UK developed another fiber optic device that uses the reflection of light to detect ice layers with thicknesses that range from several millimeters down to as little as 100 μm. Furthermore, the optical ice sensor can distinguish air, water and even different types of ice. The device is compact and prepared to be attached to the leading edge of an aircraft wing or to the rotors on a helicopter, and it weighs less than 200 g, which is considerably lighter than existing electro-mechanical sensors.

Ge et al. [62] optimized the sensor head by implementing fiber bundles instead of individual optical fibers. The fiber bundles were grouped together and the ends were polished with two different angles, 30º and 50º. The part of the fibers from the 30º fiber bundle emitted the light whilst the 50º polished fiber bundles received the scattered light. This configuration incremented the sensitivity of the sensor and enabled it to differentiate between ice types and ice thickness, see Figure 1-4. Zou et al. [63], [64], presented similar results using a compound fiber optic ice sensor consisting of two source fiber bundles and two signal ones. All the bundles had oblique fiber end-faces that were not perpendicular to the fiber axis. The IWT results showed that this sensor is able to detect different types of ice: glaze, and rime, and its thickness.

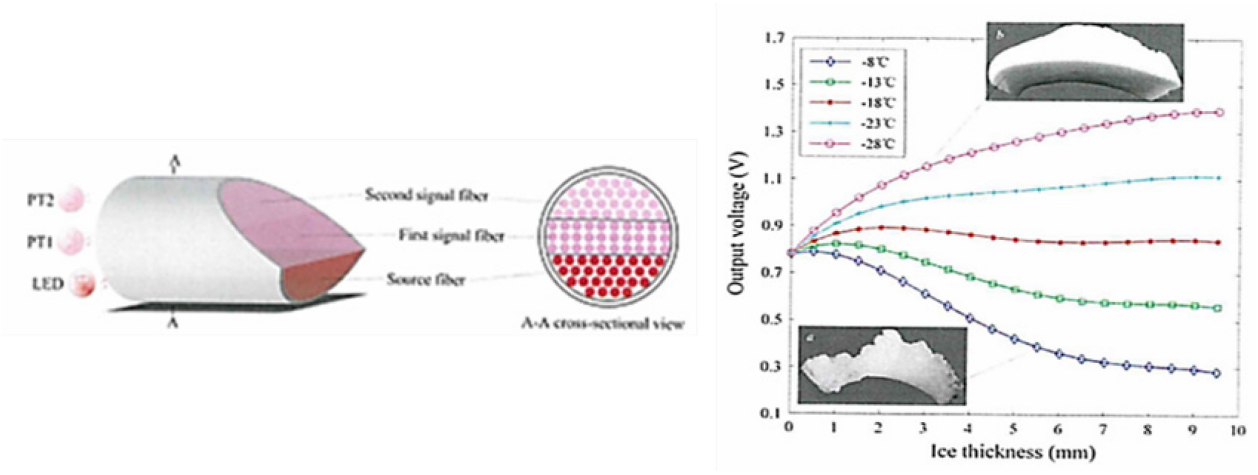

Figure 1-4: Left: Sensor Head Composed of One Fiber Bundle and Two Signal Bundles. Right: Output Voltage as Function of Ice Thickness [62]. Glaze ice accreted (down) at -8ºC and rime ice at -28ºC (up).

Zou et al. [63] added a robust packaging of the sensor fiber bundles in a metallic flexible tube and polished the fiber head only in one angle, Figure 1-5. This sensor system from Zou et al. [63] is a relatively simple and robust construction that can be integrated in aircraft structures. Flush integration is possible as well as integration in separate sensor probes. An automated evaluation of the surface icing can be achieved with adequate sensing algorithms. The commercial availability of such a system is unknown. The TRL is medium but it seems that higher TRL can be reached.

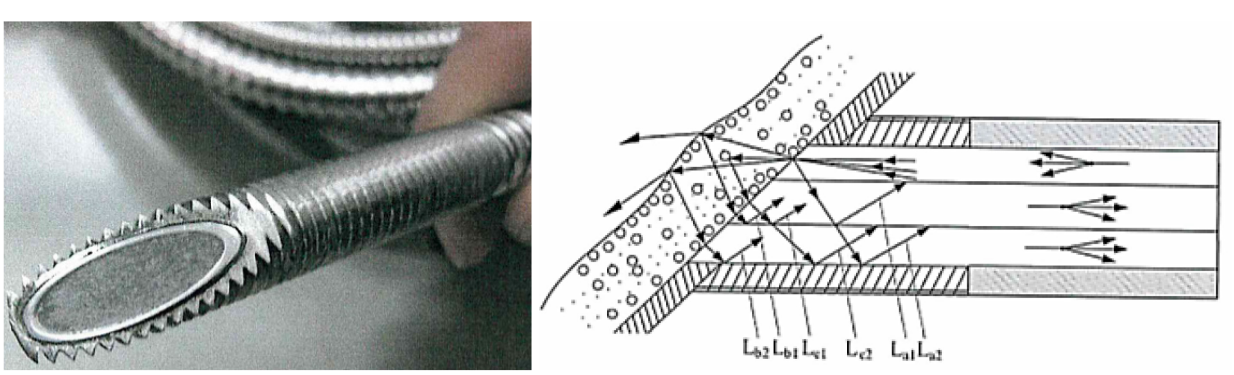

Figure 1-5: Left: Picture of the Fiber Optic Sensor Integrated in a Flexible Metal Tube [63]. Right: Optical Transmission in the Fiber Bundles for Rime Ice.

Recent publications by Amiropoulos et al. [66] and by Ikiades [57] reported an improvement for determining the thickness and type of ice in real time using a linear Fiber Optic Sensor Array (FOSA), see Figure 1-6. This new development applies a linear FOSA using high Numerical Aperture, Multi-Mode Plastic Optic Fibers and compared their detection characteristics with the polished fiber-tip sensor array used in the earlier work. The results obtained gave much improved intensity characteristics, which enhanced the detection efficiency of the sensor.

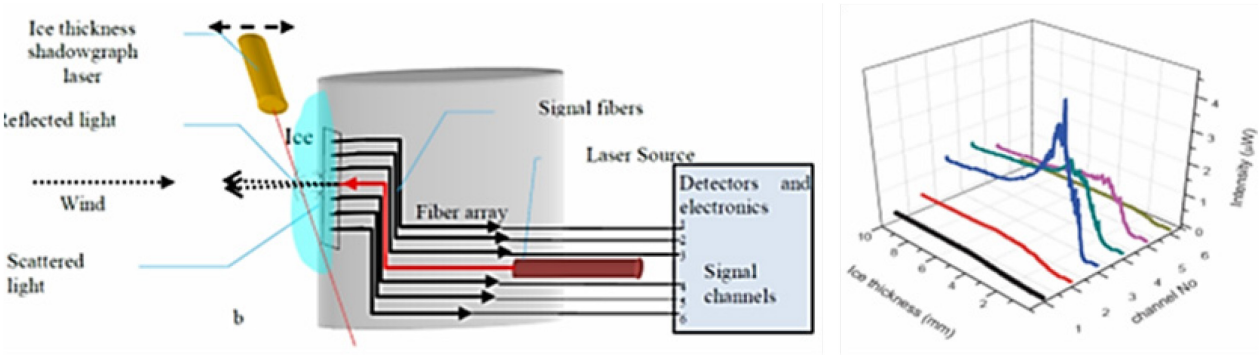

Figure 1-6: Left: Optical setup for the Fiber Optic Sensor Array (FOSA) Reported in Ref. [57] and Ref. [66]. Right: Sensor output from IWT tests with glace ice at -5ºC from Ref. [66].

A general drawback of all fiber optic sensor designs using the light scattering in the accreted ice is the need for optically clean sensor surfaces. Any dirt or contamination of the surface such as oil or insects can significantly influence the measurements. These sensors could be used to differentiate between Appendix C and Appendix O conditions, when at least two of them would be installed in locations where for one only droplets of small size (Appendix C) impinge and for the other only big-sized drops (Appendix O) impinge on the aerodynamic surface (which mainly occurs far behind the leading edge).

1.3.1.3.2 Photonic Sensors

The light that passes through photonic sensors, such as evanescent-field waveguides, can interact with the surrounding medium and sense the presence of ice that is deposited on top of the sensor head. These sensors are normally quite fragile glass designs that cannot be installed in harsh aeronautical environment where the pressure of the airstream, erosion, contamination, vibrations and elevated temperature changes can damage the sensors and make them inoperative. However, Martinez et al. [46] recently presented a nanophotonic sensor for ice detection that can stand the harsh aeronautical environment. The sensor is packaged in an optical chip where the sensing element is buried inside, protected by some microns of glass on top. It resists systematic exposure to industrial environments without failure. The surface sensor chip is fiber-coupled and can monitor the structural phase of water (liquid-supercooled-solid), as well as the type of ice micro-structure (clear or rime). It has been demonstrated in IWT tests that the sensor can detect ice layers with nanometric (~100 nm) to microscopic (~30 μm or higher) thicknesses, see Figure 1-7.

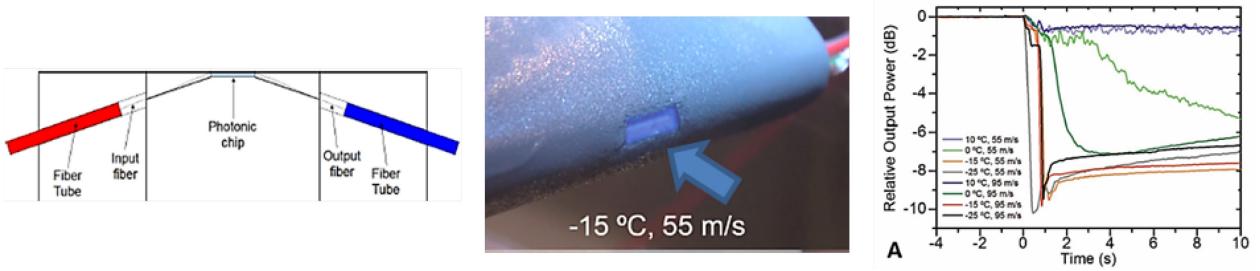

Figure 1-7: Left: Side View of the Installed Photonic Chip in the Wing Surface. Mid: Image of the NACA0012 Airfoil with the Integrated Photonic Chip in the Leading Edge During IWT Test (LWC: 0.2g/m^3, MVD: 40 microns). Right: Sensor Output During IWT Tests [45].

The sensor can be integrated in flat parts of aeronautical profiles without interfering significantly in the airstream or can be integrated in separate sensor probes. The sensor shows very early ice detection within fractions of a second. A drawback of photonic sensors in general is the fact that only the first microns of ice

thickness are detected, but the following ice accretion cannot be evaluated. This fact would require a frequent de-icing of the sensor. The TRL of the photonic sensor is medium, having demonstrated its performance in a simulated aeronautical environment inside an IWT. A commercialization of these sensors is not known.

1.3.1.3.3 Fiber Optic Switch

The optical fiber itself can be used as an icing sensor, as it has been claimed by Klainer and Milanovich [67] (Figure 1-8). The Fiber Optic Sensor (FOS) is designed so that no light is transmitted when water is present but as soon as ice begins to form, light is relayed. In addition, limited quantitative information can be made available on the rate of ice formation. Alternatively, the sensor can be formed from another type of optical waveguide instead of an optical fiber. The ice sensor is formed by placing spaced stripes of a cladding material on a fiber optic core, or other waveguide structure, where the cladding has a refractive index close to ice and the core has an index greater than the cladding but less than water. The advantages of the ice sensor include: small, lightweight, inexpensive and flexible. The instrumentation needed to operate the ice FOS is simple, small, lightweight, inexpensive and easy to operate.

A drawback is, as mentioned also in the light scattering sensors, that contamination on the sensor can make it inoperative. A commercial application is unknown. The TRL level in this development stage is low.

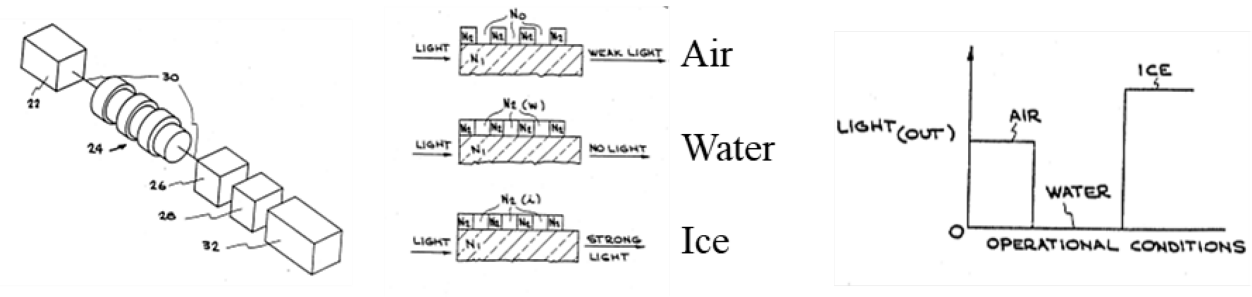

Figure 1-8: Left: Principle Sketch of the Fiber Optic Switch with the Optical Fiber Structured with Strips of Cladding (Part No. 24). Mid: Principle Performance. Right: Light Output from the Optical Sensor Fiber from Klainer and Milanowich [67].

1.3.1.4 Heat Transfer

The phase change from supercooled water to ice causes the liberation of latent heat. Energy is liberated and the water, which is converted to ice, heats up towards 0ºC. The end temperature by this effect depends on the quantity of water that participates in the phase change, the ambient temperature, the heat flux of the ice by radiation, convection and conduction that reduces the liberated latent heat energy. Different techniques have been developed that use the latent heat liberation as a measure of the ice accretion.

1.3.1.4.1 Fiber Bragg Grating Sensors (FBGS)

The measurement of the latent heat liberation can be made by fiber Bragg grating sensors. These sensors have a very low mass, fast response and very low heat conduction. The sensors can be embedded in a capillary and be protected by this from the harsh aeronautical environment. They can be surface embedded or directly embedded in structural composite material used in the aeronautical industry.

A lightweight fiber optic detector (FOD) able to detect early ice formation has been developed by Frovel et al. [68]. It is a double sensor design where one sensor is integrated directly in the aerodynamic surface with close contact to the air stream and a second sensor integrated behind the first one but inside the structure, see Figure 1-9. The difference between both sensor outputs is used to evaluate the icing condition. Fast ambient

air temperature changes can be differentiated from ice formation. The position of this sensor couple in the aerodynamic surface enables to distinguish between Appendix C and Appendix O conditions. The sensor has been tested in the INTA IWT for standard icing conditions of Appendix C and Appendix O. A TRL of 4 to 5 has been estimated based on these IWT tests in representative conditions. The early ice formation and accretion was detected immediately in all the tested conditions of temperature (-5 to -20ºC), liquid water content (0.2 to 2 g/m^3) and droplet size (20 to 100 microns). Depending on the condition, the ice accretion was still detected with even more than 10 mm of ice thickness over the sensor. Metallic sensor probe designs are equipped with electrical heating to melt the accreted ice when needed. The fiber optic technology provides a sensor that is immune to electromagnetic interferences and that is operative even in heavy thunderstorms and lightning conditions. A commercial ice sensor based on FBGS is not available.

A drawback of this sensor is that quite expensive fiber optic interrogators are still needed for the FBGS. An advantage is that this sensor technology is not affected by surface contamination such as dirt, insects, oil, etc. Appendix C and Appendix O conditions can be discriminated by applying several individual FBGSs along the chord of the profile.

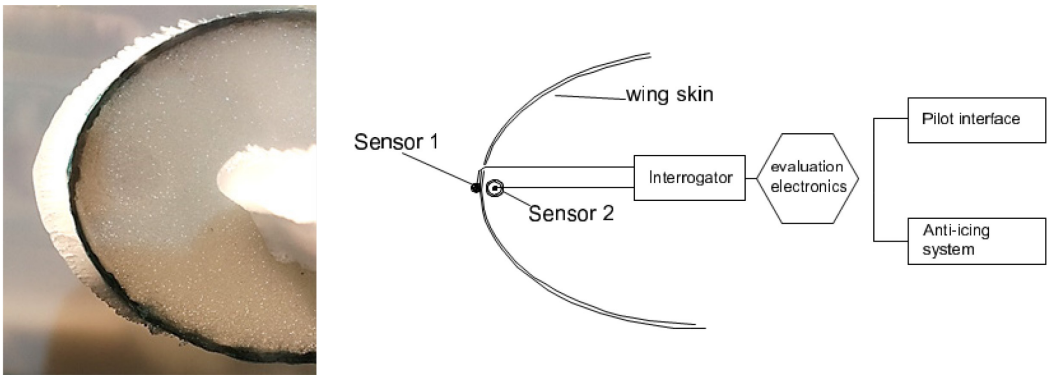

Figure 1-9: Left: FOD Installed in the Leading Edge of an Airfoil Made of Carbon Fiber Reinforced Plastic in Sandwich Structure with a Several Millimeter Thick Ice Layer. Right: Principle Sketch of the Sensor System [68].

1.3.1.4.2 Electrical Temperature Sensors

Electric temperature sensors such as thermocouples, thermistors and resistant temperature detectors can also be used to measure the latent heat of the water/ice phase change. Designs of these kinds of ice detectors are quite old already and have been found first in a US patent from Tribus and Moyle [69] from 1953. In this sensor design one thermocouple (25) is in contact with the airstream and detects the liberated latent heat from the water/ice conversion, whilst the second one (20) measures only the airstream temperature, Figure 1-10 (left). If icing occurs, the difference between both temperature measurements provokes a signal in the connected Wheatstone bridge circuit.

A later design using thermocouples was patented later by Khurgin [70]. In this case, the thermocouples (16B and 16A in Figure 1-10 (right)) were installed under the face sheet (44) of the aerodynamic surface to be monitored. Again, a differential temperature measurement was made with one sensor being in close contact to the surface and another being more isolated. Commercial sensors of this type are not known. Advantages of these designs are the easy electronics needed for monitoring and the state-of-the-art sensors used for measuring the temperatures. A clear drawback of these designs from Ref. [69] and Ref. [70] is the thermal conductivity of the metallic sensors and their metal housings. The liberated latent heat can be significantly dissipated by thermal conduction when the sensors are in a relatively massive metal housing. Also, the calibration of these devices is highly specific to the location and implementation of the sensors.

Currently, a new system is being developed for unmanned aircraft [71]. The system generates thermal signals with an electro thermal icing protection system. The thermal signals are recorded with thermocouples and compared against a clean reference signal. The system is able to identify icing conditions, existing ice accretions, and non-icing conditions. This system is prone to require a significant quantity of electrical energy.

The electrical heat transfer sensors can be used also to differentiate between App C and App O conditions, when they are installed in places where only drops of a certain size impinge.

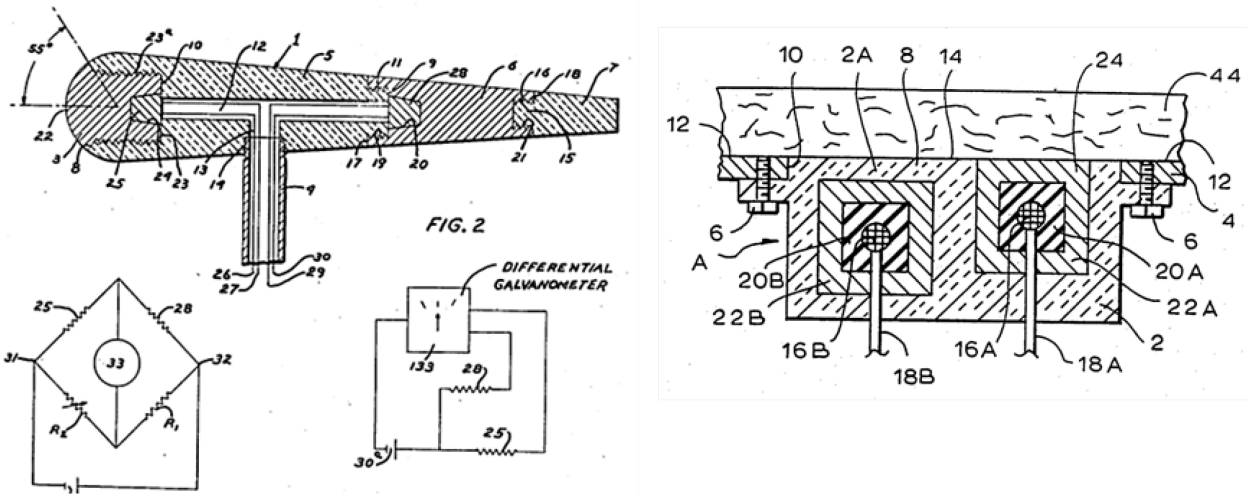

Figure 1-10: Design of Heat Transfer Sensor Using Electrical Thermocouple Measurements Left: Ref. [70], Right: Ref. [71].

1.3.1.5 Mechanical (Vibrating Probes, Diaphragm, Piezoelectric)

Mechanically resonant structures are attractive as transducing elements in sensor systems due to their inherently high sensitivities to small variations in applied loads [72] Furthermore, spurious drifts in the resonant frequency can be cancelled by monitoring differences in measured resonant frequencies of matched structures.

1.3.1.5.1 Vibrating Probes

Vibrating probes for ice detection were fabricated by Rosemount Inc.. In this device, ice accretes on an axially vibrating probe, causing the vibration frequency to decrease [73]. Their use is favored because these sensors are readily available, easy to install and simple to operate [74]. They are designed to be used as warning systems for incipient aircraft and antenna icing, and not as precisely calibrated scientific instruments. Moreover, as an ice detector ages its rest frequency decreases. As another significant limitation, variations in probe design and placement are usually restricted in order to favor ice accretion and minimize resonant frequency shifts due to accumulation of water and other fluids. Furthermore, the acceptable probe geometries and orientations may adversely affect the local airflow during aircraft operation [72].

1.3.1.5.2 Diaphragm Icing Sensor

This is a kind of safety equipment for airplane flight based on the piezoelectric resonance principle [75]. The main element of the piezoelectric resonator is the diaphragm mechanical oscillator made from piezoelectric material. The input voltage from the electrodes is transformed into mechanical stress of the mechanical

oscillator through the piezoelectric effect; conversely, the deformation of the mechanical oscillator caused by mechanical stress produces output charge on the electrodes through piezoelectric effect. Electric actuating signals can be applied to cause mechanical vibration, and also electric signals in direct proportion to vibration amplitude are output. This system can be regarded as a single-order mechanical vibration system where the corresponding relation between its resonant frequency f_0, effective mass m, and equivalent stiffness k is:

$$f_0 = C\sqrt{k/m}$$

where C is a constant. This piezoelectric device is able to work as an icing sensor because when there is no additional mass on the piezoceramic plate, it vibrates at its own resonant frequency f_0. When icing (or liquid water) occurs on the plate, which will influence the stiffness k of the system and its effective mass, the resonant frequency will also be influenced. In some configurations as the thickness of ice increases, k increases and eventually the resonant frequency f increases. Therefore, the ice thickness can be measured if we can detect f. Several geometries have been developed for these kinds of sensors [72], [76], which are mostly fabricated by micromachining of silicon wafers. Moreover, they can distinguish between ice and water films. However, due to the harsh environment of airplane flight, the sensitivity and linearity of the sensor may decline, along with severe zero drift, thus causing frequent faults of the sensor [76]. Furthermore, these sensors are effective for thin ice layers (less than 1.5 mm thick), therefore they are useful for the observation of early icing stages and lab-scale experiments. However, when the ice layer grows thicker (as in real operational conditions) the sensitivity of the piezoceramic element decreases.

1.3.1.5.3 Other Piezoelectric-Based Sensors

There are some other examples of sensors based on piezoelectric transducers and the ultrasonic waves that they can generate [75]. Compared to diaphragm sensors, these devices can be fabricated with easier techniques like sol-gel, allowing also deposition on curved (e.g., leading edges) or flexible surfaces. These sensors perform ice thickness measurements using longitudinal acoustic waves. Their sensitivity is excellent (they can detect ice layers as thin as 0.3 mm), but detection and thickness estimation are limited to the area underneath the sensor or sensor array surface, while the Plain Acoustic Waves (PAW) techniques provide information for the path length (e.g., meters) along which they propagate. Wang et al. [77] proposed a different architecture for a vibration-based sensor. The sensing element of the ice detector detects icing conditions by magnetostrictive oscillation. The magnetostrictive alloy sensing tube is mounted to the dome at midpoint, which exposes half the tube to the airstream (see Figure 1-11). A magnet that is located inside the dome causes a unidirectional magnetic bias to develop axially through the tube. A drive coil that is attached to the sensing tube drives the sensing element. A magnetic field is induced by the magnet and drive coil, which causes the magnetostrictive material to expand and contract. Together with the feedback coil and an operational amplifier, these elements form a magnetostrictive oscillator (MSO) circuit whose resonant frequency is dependent on the natural resonant frequency of the sensing element when in the no-ice condition. Similar to Rosemount vibrating detectors, ice accretion alters the resonant frequencies. However, Wang et al. did not test the sensor and only did a mathematical analysis of its characteristics.

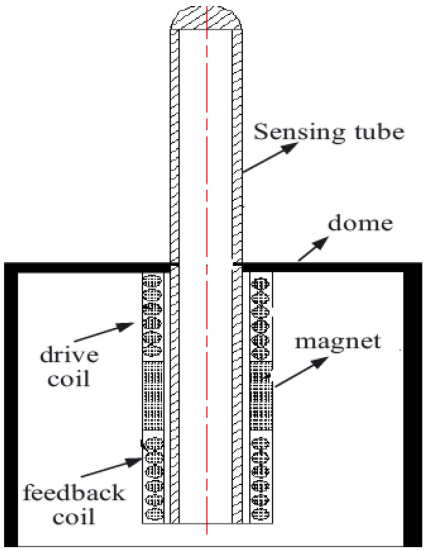

Figure 1-11. Sketch of the Magnetostrictive Sensor [77].

1.3.1.6 MEMS and Inter-Digital Transducer

Micro Electro-Mechanical Systems (MEMS) have relevant potential as sensors for a wide range of phenomena. The technology is currently being applied to the structural health monitoring of accelerometers, gyroscopes and vibration monitoring devices with signal processing electronics to provide real-time indicators of incipient failure of aircraft components with a known history of catastrophic failure due to fracture [78]. More recently, some attempts have been made to extend the application field to ice detection on aircraft, including ice growth on surfaces. One of their major advantages is that they allow wireless control [79] (e.g., via microwave systems when interfaced with an Inter-Digital Transducer [80]), a crucial aspect for application in rotating systems [81] and in aircraft in general [82]. Such microsensors are extremely small so they can be embedded into structural materials. They can also be mass-produced and are therefore potentially cheap [83]. Additionally, a range of sensor types can be integrated onto a single chip with built-in electronics, providing a low power microsystem.

1.3.1.7 Electrical-Based Sensors (Capacitance, Impedance, Time Domain Reflectometry, Piezoelectric)

Some detection systems are based on the measurement of an electrical observable (e.g., capacitance, impedance, voltage or current) by a sensor (capacitor, resistor, etc.). The values of such observable parameters change when an ice layer forms and grows.

1.3.1.7.1 Capacitance

DeAnna et al. [84] reported fabrications of a micromachined, silicon-based, flush-mounted sensor capable of distinguishing between an ice-covered and a clean surface by changes in capacitance. It employs a bulk micromachined boron-doped silicon diaphragm (size from 1 x 1 mm to 3 x 3 mm), which serves as one plate of a parallel-plate capacitor. This is bonded to a second silicon wafer, which contains the fixed electrodes – one to drive the diaphragm by application of a voltage, the other to measure the deflection by a change in capacitance. The diaphragm and the gap between parallel-plate capacitors is 2 micrometers. Current is applied and changes in capacitance are monitored to assess ice formation on the sensor. Since the sensor uses capacitive actuation, it uses very little power and is an ideal candidate for inclusion in a wireless sensing system.

1.3.1.7.2 Impedance

Some very recent papers report the embedding of commercial piezoelectric modules in curved sheet-metal compounds for ice detection [85], [86]. The modules are placed inside an aluminum sheet sandwich structure surrounded by an adhesive layer. Similar to diaphragm icing sensors, these systems are able to detect ice accumulation due to changes in resonant frequencies. However, in this case resonance shift is measured through evaluation of impedance and phase angle between voltage and current. Even though the results obtained in tests inside a cooling chamber at temperatures down to -40°C are promising, it is not clear whether these devices can provide information about ice layer thickness. Impedance measurements can also be combined with other measurements (e.g., temperature, thermal conductivity) to assess the thickness of a glaze ice layer [87]. However, this method is not suitable to rime ice due to the presence of cracks and voids in the ice layer.

1.3.1.7.3 Time Domain Reflectometry

Time Domain Reflectometry (TDR) is based on the principle that the propagation velocity of a pulse of electromagnetic wave in a transmission line surrounded with a test material is a reflection of the dielectric constant of the material [88]. The dielectric constant in turn depends on the water content of the medium. Hence, by measuring the time delay of the propagating pulse, the water content of the medium can be determined. The TDR technique is relatively cost effective and safe. TDR has high spatial and temporal resolution and is capable of providing continuous automated measurements. One great advantage of using TDR as ice detection technique is that it allows wide area detection. Coplanar TDR transmission lines can be used as TDR sensors for thickness measurements, as they allow the test material to be placed conveniently on the sensor for non-destructive measurements [36].

1.3.1.7.4 Other Electrical-Based Sensors

Quite recently, Berg et al. [89] introduced metal rubber sensors for non-destructive, normal force detection of ice accretion on aerospace structures. Metal Rubber is a piezoresistive material that exhibits a change in electrical resistance in response to physical deformation. It is produced as a freestanding sheet that is assembled at the molecular level using alternating layers of conductive metal nanoparticles and polymers. As the volume percentage of the conductive nanoparticle clusters within the material is increased from zero, the onset of electrical conduction occurs abruptly at the percolation threshold. Electrical conduction occurs due to electron hopping between the clusters. If a length of the material is strained, the clusters move apart so that the efficiency of electron hopping decreases and electrical resistance increases. The resulting change in resistance as a function of the change in strain in the material, at a specific volume percentage of conductive clusters, can be interpreted as the transduction response of the material.

1.3.1.8 Alpha-Particle / MOSFET

Quite recently, a new ice detection system for aircraft applications has been reported [90]. Unlike the most common icing detectors that are based on optics, this new system uses α particles. An α-particle source is attached to the wing of the aircraft, and a detector that mainly depends on a Metal Oxide Semiconductor Field Effect Transistor (MOSFET) is placed a few centimeters away from the source. As the α-particles strike the detector, they deposit their positive charges on the gate of the MOSFET (n-channel), and the transistor turns ON. If, however, a layer of ice builds up on the wing and prevents the α-particles from reaching the detector, the MOSFET shuts OFF. The new detector is more reliable than optics-based detectors because it is an integral part of the wing and hence cannot miss the formation of ice, especially if it is mounted on the leading edge. It is also insensitive of non-condensed phases like air moisture. Moreover, this sensor has a very low detection limit: α particles can be effectively stopped by a 0.1 mm thick water or ice layer, while mechanical systems usually have a lower detection limit of 0.5 mm. The proposed technology has been tested in an icing wind tunnel to simulate different real flight conditions and proved effective also when external disturbances like dust and lightning are present.

One of the drawbacks of this sensor is that a layer of water will also stop α particles in the sensor just described. Hence, the sensor is insensitive to the difference between water and ice. This hindrance can be partially overcome by adding a temperature sensor that provides information about the particle-blocking layer.

1.3.1.9 Assessment of Technologies

To summarize the information provided in this subsection, Table 1-3 gives individual assessments for the "Detection of Ice Accretion on Surfaces".

Table 1-3: Assessment on Principles/Technologies for Detection of Ice Accretion on Surfaces.

Technology	Assessment of Advantages (Top Row) and Disadvantages (Bottom Row)	TRL
Wave Frequency Section 1.3.1.1	The studied technologies can distinguish between water, and different types of ice. References are not available regarding the sensitivity/accuracy of the technologies esp. for small ice thickness (lower 1mm) and the potential of App. C/O discrimination.	Med
	The applicability of all technologies is dependent on the ice thickness, and for thicknesses lower than 1 mm the sensitivity is not adequate. The technologies could be good for ice thickness determination but not for very early ice detection.	
Optical Section 1.3.1.2	High-medium sensitivity, applicable to early stages of ice accretion In all but one case, references are not available regarding the sensitivity/accuracy of the technologies. The greatest advantage is that the methods are non-contact, and therefore do not require any installation on the surfaces of interest.	Med
	The technologies can distinguish between water and different types of ice, but in most cases references are not available regarding the sensitivity/accuracy.	
Fiber Optics Section 1.3.1.3	High sensitivity, applicable to early stages of ice accretion. Can be used to differentiate between App. C and App. O conditions (14 CFR Part 25).	Med
	Need for optically clean sensor surfaces. Any dirt or contamination of the surface can significantly influence the measurements. Lack of in-flight testing.	
Heat Transfer Section 1.3.1.4	High sensitivity to very early stages of ice accretion. Not effected by surface contamination such as dirt, insects, oil, etc. Can be used to differentiate between App. C and App. O conditions (14 CFR Part 25).	Med
	In the case of electrical systems elevated electrical power is needed. Need for de-icing when functioning as an isolated probe. Lack of in-flight testing.	
Mechanical Section 1.3.1.5	High sensitivity, applicable to early stages of ice accretion.	High
	Decrease in performance with time as resonant frequencies can change.	
MEMS and Inter-Digital Transducer Section 1.3.1.6	Small size, wireless control, which makes them ideal for rotating systems.	Low-Med
	Lack of testing in in-flight icing conditions.	
Electrical-based Sensors Section 1.3.1.7	Possibility to distinguish ice from water.	Med
	Often increase radar cross-section of the aircraft.	
Alpha-particle / MOSFET Section 1.3.1.8	Embedding the sensor in the wing increases reliability.	Low
	Very limited investigation, unable to distinguish ice from liquid water, or other liquids or particles.	

Among mechanically resonant devices, vibrating probes are definitely the most established sensors and they have been applied on aircrafts for many years. Further research is probably unnecessary in this field. On the other hand, MEMS and electrical-based sensors have much more potential in this perspective as they are wireless technologies that allow remote control. Moreover, TDR sensors are able to distinguish between ice and water layers, which is a feature that few other technologies have. For the same reason, alpha-particle sensors are not likely to be further investigated.

1.3.2 Detection of Atmospheric Icing Conditions: Fore- and Nowcasting

The recent improvements and research in aviation have focused on the subject of aircraft safe flight even in severe weather conditions. As one type of such weather conditions, icing has been found to have a notably negative effect on the aircraft flight performance, and has resulted in several fatal accidents [91]. Safety and cost saving are the most important issues in air transportation. Current aviation research and development has begun to focus more on creating aircraft that are safe and reliable under severe weather conditions. Aerodynamic changes of the airframe in-flight must be determined at early onset so that the pilot or auto-pilot can take the most important remedial actions to avoid a disaster.

1.3.2.1 Electromagnetic Radiation (Radar, Radiometer)

Ideally, all aircraft would be equipped with in-flight icing remote detection instrumentation that would provide detailed route-specific icing information, however budgetary constraints and technology short-falls limit the practicality of this option. Therefore, a ground-based system with the capability to provide icing information to all aircraft entering and departing a terminal area is a key element in facilitating icing detection and avoidance [92]. Radars and radiometers are ideal candidates for this purpose.

Dual-polarization radars typically transmit horizontally and vertically polarized electromagnetic waves and receive backscattered signals [93]. Due to the anisotropy of illuminated hydrometeors, their radar backscatter cross-sections are not the same for the different polarizations. Signal properties change continuously as the waves propagate yielding information that can be used to estimate particle size, shape, orientation, and thermodynamic phase [94]. Also dual-frequency radars are used for remote sensing of LWC [95], [96]. At first, it was thought that dual-wavelength radar could only be used for LWC determination for clouds that are either wholly liquid, or for which an accurate and reliable method for removal of the Mie scatterers and ice crystals from the signal is available [97]. More recently, microwave radiometers have been studied for the detection of icing conditions [98], but experimental validation of this model is still lacking.

In a recent paper, Serke et al. [92] combined a dual-polarization radiometer with Colorado State University's CHILL polarized Doppler radar to improve the detection of in-flight icing hazards to aircraft in the near airport environment. CHILL was named after the original joint developmental project by the University of Chicago and the Illinois State Water Survey [99]. The collocated instruments allowed for the liquid water path and water vapor measurements derived from the radiometer to be merged with the radar moment fields to determine microphysical and water phase characteristics aloft. The radiometer was field tested at Colorado State University's radar site near Greeley, Colorado during the summer of 2009. Case study data collected during the test period demonstrated the potential of dual-polarization radiometer to aid in in-flight icing hazard detection, as it allowed for the positive identification of spherical liquid hydrometeors.

1.3.2.2 Optical (LIDAR, Lasers)

Quite similar to the radar-based detection of icing conditions, optical-based sensors facilitate detection of liquid water drops in the atmosphere. However, as Laser Imaging Detection and Ranging (LIDAR) systems work within the optical spectrum, they have a different sensitivity to cloud parameters: LIDAR systems are more sensitive to small drops, as a result of the very short wavelength in comparison to the droplet size [100]. This is basically the reason for LIDAR systems being used for cloud base or ceiling detection as they

cannot be used to detect the vertical cloud structure, which is optically thick, and hence the light signals are extinguished. However, they can provide information about cloud parameters (such as liquid or ice water content) and are often used in combination with radar systems on ground [101] or in space [102]. The correlation between radar reflectivity and optical extinction allows the characterization of cloud drop size and cloud water content [101]. Nevertheless, Heymsfield et al. [103] showed that it is possible to develop algorithms to extract cloud parameters such as ice water content from LIDAR measurements solely (in case radar measurements cannot be used for cloud parameter retrieval).

1.3.2.3 Environmental Sensors

Liquid and frozen cloud particles can be detected with scattering spectrometers, Optical Array Probes (OAPs) and hotwire type probes. Scattering spectrometers measure the light intensity of an incident laser scattered on small droplets or ice particles in the forward or backward directions. The particles can be discriminated by size and using the backward scattered light intensity the shape of the particles can be measured. Optical array probes record the shadow of a particle produced by in incident laser beam on a photodiode. The image of the shadow is focused onto a plane containing a linear photodiode array, and illuminated and non-illuminated pixels are recorded at a rate that permits reconstruction of the image. These probes are generally used for detection of larger particles (> 50 μm). The hotwire probes use a heated wire to detect cloud droplets that evaporate on impact. The wires are heated to the same temperature, with a bridge feedback ensuring that their temperatures remain constant throughout. The difference in current needed to keep the wire at constant temperature relates to the amount of liquid water content contained in the impacted droplets. These are the main probes that are used for particle spectrum and liquid water content measurements in airborne studies.

1.3.2.4 Satellites

The remote detection of icing conditions using satellite imagery benefits from the increasing computational power during the last three decades. In additional, more satellites monitoring earth's environment and atmosphere were launched since the 1990s and provide the base data for the prediction and detection of cloud formations favoring certain icing conditions.

A direct diagnosis of icing conditions from satellite data is not possible, but the conditions can be predicted from cloud physics parameters, which can be obtained from cloud images in different channels of the light spectrum. For example, Ellrod and Nelson [104] described a way for the detection of icing conditions from satellite images relying on three infrared and one visible light channel. They show that the presence of supercooled water droplets in clouds is related to the brightness temperature difference between different infrared channels and the brightness of the clouds in visible imagery. During daylight, the shortwave channel is typically much warmer than the longwave channel for clouds consisting of supercooled water droplets, and at night vice-versa [104]. Based on this knowledge and work, Minnis et al. [105] proposed a way for the diagnosis of icing conditions from similar satellite data and named the following parameters (retrieved from the images using different methods) as indicative: cloud temperature (must be below 273 K), cloud height and thickness, phase, optical depth, effective droplet radius or effective ice crystal diameter, and liquid water path or ice water path. Given that, the challenge is to convert information about these parameters into reliable ice detection. Furthermore, the validation of the detection results is very difficult as normally in situ measurements of the real conditions in the clouds are not available. Several research projects like the Alliance Icing Research Study (AIRS II) [106], [107] allowed making direct measurements with research aircraft in the observed clouds to provide validation data.

There are several products for satellite-based icing detection and forecast available (see Ref. [107] and Ref. [105] for some examples) but these have some limitations such as the spatial and temporal resolution or they may only be applicable to certain areas or countries. The results of these tools still need to be analyzed by specialists. There is today no automated solution available, which evaluates satellite images and reports certain atmospheric icing conditions to the user.

1.3.2.5 Assessment of Technologies

To summarize the information provided in this subsection, Table 1-4 gives individual assessments for the "Detection of Atmospheric Icing Conditions: Fore- and Nowcasting".

Table 1-4: Assessment on Principles/Technologies of Atmospheric Conditions (Fore-/Nowcasting).

Technology	Assessment of Advantages (Top Row) and Disadvantages (Bottom Row)	TRL
Electromagnetic Radiation Section 1.3.2.1	Size distribution of water drops can be provided	High
	Only suitable for ground-based systems	
Optical Section 1.3.2.2	Complementary information to Radar measurement to remotely determine atmospheric icing conditions	Low
	No standalone ice detection, only for ground-based applications	
Environmental Sensors Section 1.3.2.3	High precision measurements of atmospheric icing conditions	High
	Only for scientific purposes due to size, weight and necessary data evaluation effort	
Satellites Section 1.3.2.4	Based on already existing weather satellite images, software evaluation requires no additional hardware, icing detection for large areas and forecast	Med
	Limitations on spatial and temporal resolution, no automation, individual data analysis by specialists required	

Technologies based on radars deserve further studies due to their numerous advantages: they exploit existing infrastructures therefore, they are cheap; they are on-ground systems that can monitor many aircrafts at the same time and are not subjected to harsh in-flight atmospheric conditions. The evaluation of satellite data could be very promising for detection of atmospheric conditions prone to icing around the globe, especially around areas with less infrastructure (and consequent utilization of other technologies). With computational power still increasing, big data analysis is becoming faster and more efficient with regard to near future satellite-based methods that have high potential. Even with currently low TRL the major task is to develop suitable software to reach higher TRL, which is relatively cheap compared to technology development. Nevertheless, there would also be the need to increase spatial and temporal resolution to obtain better information.

1.3.3 Detection of Altered Air Vehicle Performance Characteristics

Icing has hazardous effects on air vehicles by changing their performance characteristics. Especially for fixed-wing aircraft, ice accretion on lift-producing surfaces will likely cause a significant degradation of aircraft aerodynamics. These changes can directly cause a change in the aircraft's dynamic behavior, controllability and performance. These changes are also strongly dependent on the type, intensity and location of ice accretion on the aircraft surfaces, which are in turn a result of atmospheric conditions (in general liquid water icing conditions) encountered and flight parameters during the exposure to these conditions. Nevertheless, there are several generalities in the observable changes of aircraft characteristics. There are numerous approaches normally used to predict the aircraft characteristics from flight data measurements, commonly known as system-identification techniques, which might also allow recovering/predicting the effects of ice accretion from flight data gathered from "iced aircraft". After the well-known icing-related accidents in the 1990s different system-identification techniques were widely investigated concerning their applicability for ice detection (by detection of corresponding changes in aircraft

performance characteristics). The main goal was to develop ice detection and envelop protection functions, using only standard aircraft instrumentation and avionics. Nevertheless, all the approaches must be evaluated and assessed concerning certain criteria, such as:

- Reliability and robustness against atmospheric disturbances;
- Safe aircraft operations;
- Applicability to existing avionics systems without major modifications;
- Capabilities to be implemented in recent or near future aircraft developments;
- Usability in all parts of the operational envelope; and
- No, or at least a very low number of, false alarms.

Figure 1-12 shows the anticipated aerodynamic degradation due to the effects of airframe ice accretion: the maximum aircraft lift coefficient and maximum angle of attack (stall) are reduced whereas the drag coefficient increases significantly for any particular lift coefficient value. The basic principle of the indirect ice detection approach is to detect aspects of this degradation in terms of monitoring model parameters describing the altered aerodynamics. On the one hand, these parameters might be part of an aerodynamics model representing, for example, the total aircraft lift or drag coefficient. On the other hand, linear state-space models, which represent the degraded aircraft dynamics, are approximated and then the corresponding stability and control derivatives are compared to a nominal reference. Using the latter, the aircraft dynamics must be excited (either using dynamic maneuver command inputs or utilizing excitations from the non-steady atmosphere), which might result in passenger discomfort or might cause the aircraft to exceed the limits for safe operations.

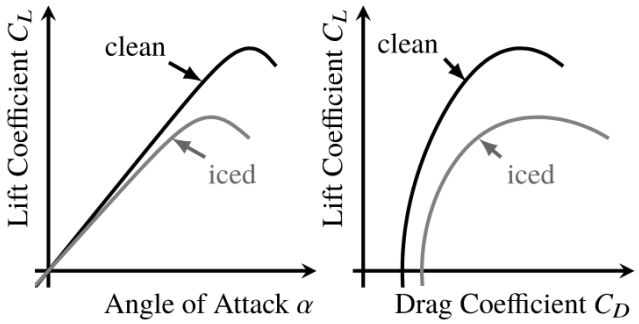

Figure 1-12: Schematic Illustration of Anticipated Aerodynamic Degradation Caused by Icing on an Airplane; Adapted from Ref. [108].

1.3.3.1 Indirect Methods

One early example for this indirect ice detection approach using the estimation of changed aircraft performance characteristics was introduced by Bragg et al. [109] in 1998. The proposed interdisciplinary approach of the “smart icing system” relies on the estimation of several derivatives of a dynamics simulation model within the system architecture. With further development of this system [110] the authors propose an icing detection technique based on a trained neural network evaluating the estimation results for changes in the dynamic aircraft characteristics. Another approach using the same idea is the “dynamic icing detection system” concept published first by Myers et al. [111], which extends the principle of the “smart icing system” by not only using the estimation of dynamic model parameters but also considering the estimated aircraft drag increase with ice accretion. Myers et al. found that the aircraft drag shows a higher sensitivity to icing than other parameters such as those in a linear state-space model (i.e., stability and control derivatives). Moreover, an estimation of the icing-induced drag increase can be obtained from steady safe flight

conditions without the necessity to excite the aircraft's dynamics. The latter is necessary to estimate the aircraft's stability and control derivatives and might bring the aircraft into a dangerous flight situation near stall. Hence, the focus on the icing-induced drag increase and consequently the aircraft flight performance will not exceed the safe operation limits under icing conditions.

Another concept for ice detection using the identification of altered aircraft characteristics is given by Gingras and colleagues [112], [113], and Ranuado et al. [114]: the "Icing Contamination Envelope Protection" (ICEPro) concept utilizes an estimation of dynamics model parameters in the frequency domain using a well-established system-identification technique involving special small amplitude excitation maneuvers. These small excitations might mitigate the risk of exceeding the limits for safe aircraft operations under icing influence. Nevertheless, they pose some risk to the aircraft and the strategy may not be acceptable for aircraft operations, civil or military.

Basically, many different approaches for indirect ice detection follow the basic idea of estimating changes in aircraft dynamics (stability and control), but use different techniques to achieve this goal: Melody et al. [115], [116] compared the H-infinity method for parameter estimation with other techniques. They also concluded from their work that a designated dynamic aircraft excitation for ice detection should be avoided during normal operations. Another approach combining an H-infinity algorithm for parameter estimation with an artificial neural network for subsequent ice detection is presented by Schuchard et al. [117] and Dong and Ai [118]. In the latter approach, the neural network is further used to identify the location of the ice accretion on the aircraft. Aykan et al. [119], [120] propose an approach for ice detection based on stability parameter change using neural networks solely.

Nevertheless, all these methods are based on the principal assumption that distinct changes of dynamic aircraft behavior are significant and unique characteristics caused only by icing. However, the change of dynamic aircraft characteristics might not serve as a fully-defined result of aircraft icing, as these changes are strongly dependent on the locations and form of ice shapes on the aircraft, the conditions that cause the ice accretion and the aircraft design itself. For example, Deiler [121] showed this by the flight dynamics evaluation of two different aircraft for different icing cases. One further result of this evaluation was that the aircraft drag increase might be a consistent indication of ice accretion during flight in ice conditions.

After the fatal accidents with ATR aircraft in the 1990s, ATR developed a system for aircraft performance monitoring that is based on monitoring the aircraft drag increase caused by icing [122]. The system is not meant to specifically detect icing, but to warn pilots about performance degradation. In icing conditions the detection itself is still the obligation of the pilots to determine. Today, the aircraft performance monitoring is standard on all ATR aircraft and has already provided a significant safety increase. Following the method of performance monitoring and/or aircraft drag estimation seems to be a more promising method than estimating the change of stability and control derivative for ice detection. Consequently, Deiler and Fezans [123] proposed a new approach for monitoring the aircraft performance for ice detection purposes throughout the entire flight without pilot interaction, which is based on the icing research results of the last two decades, together with the knowledge gained from the ATR aircraft performance monitoring system.

Besides these approaches that are mainly dedicated to detect the altered vehicle characteristics due to ice accretion on fixed-wing airplanes, some work has also been done in the field of rotary-wing aircraft. As ice accretion on the rotor blades causes a loss of rotor performance, this could be monitored and used for ice detection. For example, McKillip [124] proposed a system approach for the V-22 osprey, which relies on the monitoring of several flight parameters and a fault detection filter to draw conclusions about icing.

Given this information about the basic principle of indirect ice detection, by monitoring aircraft performance characteristics, and other developments during the last decades, it is clear that these approaches are promising but have not reached a high TRL with respect to their specific application to ice detection.

Furthermore, these approaches do not allow discrimination of icing conditions (i.e., conditions defined in Appendix C and O of the certification regulations). Nevertheless, in combination with other indicators for icing (supporting measurements of atmospheric conditions, ice accretion on surfaces, etc.) the indirect ice detection methods could significantly enhance aviation safety. Additionally, indirect ice detection might also serve as an indicator for a potential encounter of icing conditions in flight, which might be verified by some additional subsequent evaluations of suitable measurements. The big advantage of the indirect ice detection approaches presented above is the applicability to modern fully instrumented aircraft without any additional hardware installation, other than software, and some potential for full automation and acceptable reliability. However, as the indirect ice detection approaches use special references for a specific aircraft, the system must be developed for each application individually. Even with ATR using a certain system for performance monitoring on their aircraft, to date no indirect ice detection system is commercially available that provides "plug-and-play" support for an arbitrary air vehicle.

1.3.3.2 Direct Methods

A direct method to identify altered vehicle performance characteristics may be achieved with a detector technology currently under development by Marinvent [125]. The technology is called Airfoil Performance Monitor (APM) and is a stall detection system that can identify airflow anomalies at the trailing-edge of an airfoil. The detector measures a turbulence intensity ratio inside the boundary layer via pressure transducers [126]. By comparing the actual turbulence intensity to a clean reference value, the system can detect a change of the flow around the airfoil and consequently predict the presence of ice accretions on the airfoil, see Figure 1-13. The system has been tested in wind tunnel tests and flight test projects but has yet to be applied on a larger scale.

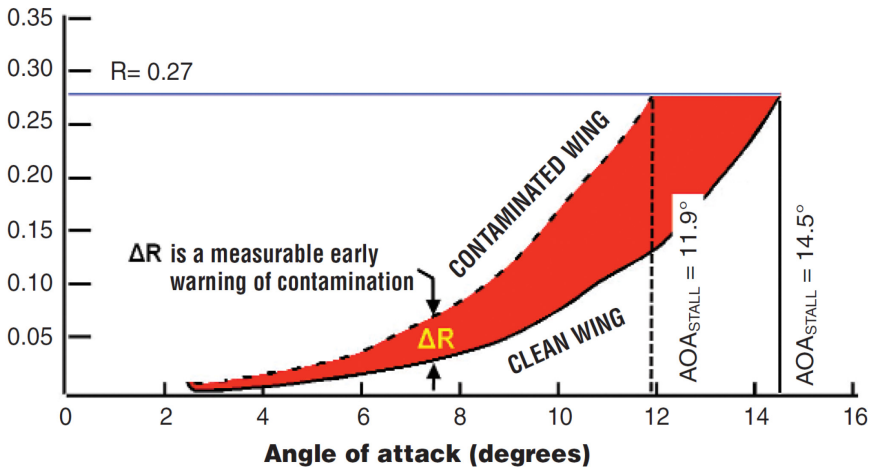

Figure 1-13: Turbulence Intensity Ratio (R) vs Angle Of Attack (AOA) for a Clean and Contaminated Wing [126].

1.3.3.3 Assessment of Technologies

To summarize the information provided in this subsection, Table 1-5 gives individual assessments for the "Detection of Altered Air Vehicle Performance Characteristics".

Table 1-5: Assessment on Principles for the Detection of Altered Vehicle Performance Characteristics.

Technology	Assessment of Advantages (Top Row) and Disadvantages (Bottom Row)	TRL
Indirect Methods Section 1.3.3.1	Utilization of existing state-of-the-art aircraft instrumentation, no additional hardware required, directly assesses the effect of icing on the vehicle.	Low
	Requires software development customized for individual aircraft, limitations on sensitivity compared to other detection principles.	
Direct Methods Section 1.3.3.2	Provides real-time information about the state of the airflow and can be used for general early stall warning.	Low-Med
	Technology not tested on a wider scale. The system might be sensitive to ice/dirt obstructing the sensor.	

Determination of altered vehicle performance characteristics allows real-time sensing of in-flight icing-related effects on the air vehicle. Hence, valuable information about the compromised vehicle capabilities is obtained – such as is necessary for highly complex flight control systems. Indirect methods are software based and mainly utilize signals from state-of-the-art aircraft avionics. Although currently at low TRL, and complementary to other detection principles, indirect methods have high potential for small aircraft or UAVs, as they do not require additional hardware increasing the air vehicles weight and complexity.

1.4 CONCLUSIONS AND RECOMMENDATIONS

The following conclusions and recommendations are based on the information presented in this chapter and the current knowledge of the authors. The technology assessment and the consequences for future research activities should be understood as moderate advice rather than technology endorsement or disapproval.

In this chapter, we evaluated various existing ice detection approaches and technologies, and generally classified the Technology Readiness Level (TRL) with Low, Medium and High in terms of their maturity in Table 1-3, Table 1-4 and Table 1-5. Despite active research and development activities in different technology areas of ice detection, only a few are commercially available at present. Depending on the field of application (airplanes or rotorcraft, sea vessels, wind turbines) as well as on requirements like the need for in situ measurements on board or a long-/short-term remote ice detection, a suitable technology must be selected. Currently only a few sensor technologies for in situ measurements are commercially available that provide a highly automated and reliable solution for direct ice detection, i.e., measuring atmospheric icing conditions or accretion on exposed surfaces. Hence, for today's civil and military applications, the existing technologies might not enable aircraft and sea vessels to operate in their full capabilities because of the limited information the systems can provide. For example, aircraft equipped with ice detectors are currently certified to operate in distinct icing conditions (App. C) but cannot operate in ice crystals or the more hazardous supercooled large droplet environment of freezing rain or drizzle. To fully operate safely in different environments aircraft must be equipped with new sensor technologies capable of detecting and discriminating the conditions. Also, the emerging applications using unmanned aircraft have special requirements that call for improved ice detection capabilities. It is clear that there is a strong need to further develop ice detection technologies for direct detection of icing conditions and accretion, both for current and future requirements for aircraft operation.

Furthermore, air and sea operations require a fast, accurate and reliable weather forecast, including nowcasting of icing conditions, for safety and efficiency. With the current lack of commercially available technology and equipment that can be used by aircraft or sea vessel operators with little scientific background, additional research and development is necessary. Although there already have been various

national and international research projects addressing these topics over the last three decades, only a limited number of technologies are fully developed and available.

Based on the study by the authors summarized in this chapter, the following recommendations for future research are offered:

- Technologies for the detection and thickness measurement of ice accretion on surfaces:
  - There is a strong demand for near-term research on technologies that distinguish between different types of icing (i.e., snow, glaze and rime ice) and other contaminants (e.g., de-icing fluid, non-ice particulate accumulations). Potential technologies include optical-based and electrical-based technologies, which can be applied to aircraft and sea vessels; for the latter especially in the form of photography.
  - With respect to aerial vehicles, we also recommend the development of technologies utilizing heat transfer. These have advantages to detect the onset of icing on the surface through sensing the initiation of freezing and can be used if it is not possible to utilize EM field and electro-mechanical sensors. Sensors using heat transfer technologies can be small and cheap to fabricate, and consequently can be easily distributed across the aircraft fuselage and wings.
- Technologies for the detection of atmospheric icing conditions for fore- and nowcasting:
  - Reliable and robust fore- and nowcasting of icing conditions will be more relevant for future aviation with increasing air traffic and a change of mission profiles with different new innovative aerial systems. Satellites can remotely detect icing conditions around the globe by sensing certain atmospheric parameters, which can be processed to yield icing-likelihood information. Future solutions should provide automated data analysis and fore-/nowcasts with high spatial and temporal resolution. To achieve this, information from local ground-based technologies (such as radar) should be included in the ice detection network. We further recommend research in this field with the caveat that some of the necessary information is already available but it needs to be analyzed properly and suitably integrated.
- Methodologies and technologies for the determination of altered vehicle flight characteristics:
  - The advantage of the indirect detection is the availability of necessary sensor information on modern aircraft. The technology is mainly complementary to other detection methods and is not foreseen to have the highest priority for research although it can deliver high benefit for low cost. Nevertheless, with regard to novel aerial systems such as UAVs of various sizes these methods might provide high potential for ice detection, whereas other technologies may be too heavy (or not deployable) on the small-size airframe. Therefore, the recommendation for future research does depend on the particular application.

1.5 REFERENCES

[1] Lynch, B., Yesterday We Were in America: Alcock and Brown – First to Fly the Atlantic Non-Stop. Haynes Publishing UK, November 2009.

[2] Jackson, D. G. and Goldberg, J.I., “Ice detection systems: A historical perspective,” SAE Technical Paper, 2007.

[3] Federal Aviation Administration (FAA), “Federal Aviation Regulations (title 14 of the Code of Federal Regulations), part 25 – airworthiness standards: transport category airplanes”, Federal Aviation Administration (FAA), Washington, DC, USA.

[4] Federal Aviation Administration (FAA), "Certification Specifications for Large Aeroplanes, CS-25 large aeroplanes", European Union Aviation Safety Agency (EASA), Cologne, Germany.

[5] Jackson, D.G., "Primary ice detection certification under the new FAA and EASA regulations," SAE 2015 International Conference on Icing of Aircraft, Engines, and Structures, paper 2015-01-2105, SAE, 2015. https://doi.org/10.4271/2015-01-2105

[6] Hann, R. and Johansen, T.A., "Unsettled topics in UAV icing", SAE EDGE Research report, 2020.

[7] Jeck, R.K., "Icing design envelopes (14 CFR Parts 25 and 29, Appendix C) converted to a distance-based format", DOT/FAA/AR-00/30, Federal Aviation Administration (FAA), Washington, DC, USA, April 2002.

[8] National Transportation Safety Board (NTSB), "In-flight Icing Encounter and Loss of Control Simmons Airlines, American Eagle Flight 4184 Avions de Transport Regional (ATR) Model 72-212, N401AM", Aircraft Accident Report (NTSB/AAR-96/02). Washington, DC, USA, 1996.

[9] Federal Aviation Administration (FAA), "Federal Aviation Regulations (title 14 of the Code of Federal Regulations), part 33 – airworthiness standards: aircraft engines", Federal Aviation Administration (FAA), Washington, DC, USA.

[10] ISO/TC 67/SC 8 – Arctic operations, "Petroleum and natural gas industries – Arctic operations – ice management", Standard ISO 35104:2018, International Organization for Standardization, October 2018.

[11] Stallabrass, J.R., "Trawler icing. A compilation of work done at NRC", Mechanical Engineering report MD-56, NRC No. 19372, National Research Council, Ottawa, Canada, 1980.

[12] Kulyakhtin, A., and Tsarau, A., "A time-dependent model of marine icing with application of computational fluid dynamics", Cold Regions Science and Technology, 104-105, pp. 33-44, August – September 2014.

[13] Overland, J.E., Pease, C.H., Preisendorfer, R.W., Comiskey, A. L., "Prediction of vessel icing". J. Climate Appl. Meteor., 25, pp. 1793-1806, 1986.

[14] Sultana K. R., Dehghani S. R., Pope K., Muzychka Y.S. A review of numerical modelling techniques for marine icing applications. Cold Regions Science and Technology, 2017. https://doi.org/10.1016/j.coldregions.2017.08.007

[15] Forest, T., Lozowski, E. and Gagnon, R., "Estimating marine icing on offshore structures using RIGICE04", International Workshop on Atmospheric Icing on Structures (IWAIS), Montreal, 2005.

[16] Makkonen, L., Brown, R.D., Mitten, P.T., "Comments on prediction of vessel icing for near-freezing sea temperatures", Weather Forecasting, 6, pp. 565-567, 1991.

[17] Pease, C.H., and Comiskey, A.L., "Vessel icing in Alaskan waters", NOAA Data report ERL PMEL-14, December 1985.

[18] Arctic Operations Handbook, 2013. Available at: https://research.wur.nl/en/publications/arctic-operations-handbook-generic-framework-for-environmental-as/

[19] Gagnon, R., Sullivan, M., Pearson, W., Bruce, W., Cluett, D., Gibling, L. and Li., L.F., "Development of a marine icing monitoring system", Proceedings of POAC 2009, Lulea, Sweden, 2009.

[20] Foy, C.E, Gates, E.M., and Lozowski, E.P., "Design, instrumentation and performance of a refrigerated marine icing wind tunnel", Proceedings International Symposium on Cold Regions Heat Transfer, Edmonton, Alberta, Canada, pp. 137-142, American Society of Mechanical Engineers (ASME), June 1987.

[21] Fukusako, S., Horibe, A., and Tago, M., "Ice Accretion characteristics along a circular cylinder immersed in a cold air stream with seawater spray", Experimental Thermal and Fluid Science, 2, Issue 1, pp. 81-90, 1989.

[22] N.N., "Technology readiness level definitions", NASA, 1988, https://www.nasa.gov/pdf/458490main_TRL_Definitions.pdf

[23] Chen, X., Zhao, Q., and Barakos, G., "Numerical analysis of rotor aero-acoustic characteristics for ice detection based on HMB solver", 74th Annual Forum and Technology Display of the American Helicopter Society, Phoenix, AZ, USA, May 15th – 17th, 2018.

[24] Chen, X., Zhao, Q.J., and Ma, Y.Y., "Mechanism analyses on aeroacoustic characteristics of iced rotor for ice detection", Proc. of the 73rd Annual American Helicopter Society Forum, pp. 9-11, May 2017.

[25] Cheng, B., Helicopter Rotor Noise Investigation During Ice Accretion, Thesis (Ph.D.) The Pennsylvania State University, Publication Number: AAT 10583700; ISBN: 9781369625424; Source: Dissertation Abstracts International, Volume: 78-08(E), Section: B, 2016.

[26] Cheng, B., Han, Y., Brentner, K.S., Palacios, J.L., and Morris, P.J., "Quantification of rotor surface roughness due to ice accretion via broadband noise measurement", In American Helicopter Society 70th Annual Forum Proceedings, 2014.

[27] Zhuge, J., Zhan, X., Wu, J., Wang, K., and Wang, Y., "Ultrasonic propagation characteristics for remnant icing detection", 9th International Conference on Modelling, Identification and Control (ICMIC), pp. 459-464, IEEE, July 2017.

[28] Rose, J.L., "Ultrasonic guided waves in structural health monitoring", Key Engineering Materials, 270, pp. 14-21, Trans Tech Publications, 2004.

[29] Gao, H., and Rose, J.L., "Ice detection and classification on an aircraft wing with ultrasonic shear horizontal guided waves", IEEE Transactions on Ultrasonics, Ferroelectrics, and Frequency Control, 56(2), pp. 334-344, 2009.

[30] Zhao, X., and Rose, J.L., "Ultrasonic guided wave tomography for ice detection", Ultrasonics, 67, pp. 212-219, 2016.

[31] Liu, Y., Chen, W., Bond, L.J., and Hu, H., "A feasibility study to identify ice types by measuring attenuation of ultrasonic waves for aircraft icing detection", ASME 2014 12th International Conference on Nanochannels, Microchannels, and Minichannels. American Society of Mechanical Engineers, V01BT22A003–V01BT22A003–10, August 2014.

[32] Hongerholt, D.D., Willms, G., and Rose, J.L., "Summary of results from an ultrasonic in-flight wing ice detection system", AIP Conference Proceedings, 615(1), pp. 1023-1028, May 2002.

[33] Liu, Q., Wu, K.T., Kobayashi, M., Jen, C.K., and Mrad, N., "In situ ice and structure thickness monitoring using integrated and flexible ultrasonic transducers", Smart Materials and Structures, 17(4), paper 045023, 2008.

[34] Le Pimpec, M., and Plaisir, F., "Ultrasonic technology: A solution for in-flight and on-ground ice detection", In ICAS, 21st Congress, Melbourne, Australia, September 1998.

[35] Rose, J.L., "Guided wave nuances for ultrasonic nondestructive evaluation", IEEE transactions on ultrasonics, ferroelectrics, and frequency control, 47(3), pp. 575-583, 2000.

[36] Bassey, C.E., and Simpson, G.R., "Aircraft ice detection using time domain reflectometry with coplanar sensors", IEEE Aerospace Conference, pp. 1-6, IEEE, March 2007.

[37] Bassey, C.E., and Simpson, G.R., "A comparison of the coplanar waveguide (CPW) and conductor-backed coplanar waveguide (CBCPW) for use as aircraft ice sensors", IEEE Antennas and Propagation Society International Symposium, pp. 821-824, IEEE, July 2006.

[38] Joseph, P.J., Glynn Jr, D.P., and Joseph, J.C., "Microwave system for detecting ice on aircraft", NASA Tech Briefs, pp. 9-10, February 2004.

[39] Bianchi, M., d'Ambrosio, G., Massa, R., and Migliore, M.D., "Microwave devices for ice detection on aircraft", Journal of Microwave Power and Electromagnetic Energy, 31(2), pp. 83-86, 1996.

[40] Gantasala, S., Luneno, J.- C., and Aidanpää, J.-O., "Identification of ice mass accumulated on wind turbine blades using its natural frequencies", Wind Engineering, 42(1), pp. 66-84, 2018. https://doi.org/10.1177/0309524X17723207

[41] Gregoris, D., Yu, S., and Teti, F., "Multispectral imaging of ice", Canadian Conference on Electrical and Computer Engineering, 4, pp. 2051-2056, IEEE Cat. No. 04CH37513, IEEE, 2004.

[42] Zhuge, J.C., Yu, Z.J., and Gao, J.S., "Ice detection based on near infrared image analysis", Applied Mechanics and Materials, 121, pp. 3960-3964. Trans Tech Publications, 2012.

[43] Zhang, J., Li, R., and Zhang, Q., "The experimental study and improvement of helicopter rotor non-contact infrared icing detection system", In 2012 IEEE 11th International Conference on Signal Processing, 1, pp. 429-433. IEEE, October 2012.

[44] Rashid, T., Khawaja, H.A., and Edvardsen, K., "Ice detection of pure and saline ice using infrared signature", Sensors and Transducers Journal, 206(11), pp. 82-87, November 2016.

[45] Rehfeld, N., Berton, B., Diaz, F., Tanaka, T., Morita, K., Kimura, S., "JediAce: Japanese-European de-icing aircraft collaborative exploration", in Aviation in Europe – Innovating for Growth. Proceedings of the Seventh European Aeronautics Days, London, 20 – 22 October 2015, Luxembourg: Publications Office of the European Union 2017. ISBN 978-92-79-59141-9; doi:10.2777/62810

[46] Martínez, J., Ródenas, A., Stake, A., Traveria, M., Aguiló, M., Solis, J., Osellame, R., Tanaka, T., Berton, B., Kimura, S. and Rehfeld, N., "Harsh-environment-resistant OH-vibrations-sensitive mid-infrared water-ice photonic sensor", Advanced Materials Technologies, 2(8), paper 1700085, August 2017.

[47] Gao, J.-S., Han, R.-Y., Qiao, W., and Yu, Z.-J., "Near infrared multispectral solution to ice detection on CF composite material wings", Guangxue Jingmi Gongcheng/Optics and Precision Engineering, 19(6), pp. 1250-1255, June 2011. http://dx.doi.org/10.3788/OPE.20111906.1250

[48] Zhang, J., Li, L., Chen, W., and Zhang, H., "Non-contact icing detection on helicopter and experiments research", International Conference in Swarm Intelligence, pp. 465-473, June 2011.

[49] Zhang, Z., Ye, L., Zhang, J., and Wu, X L., "Active infrared icing detection using neural networks", Journal of Huazhong University of Science and Technology (Natural Science Edition), 6, 2010.

[50] Lin, Y., and Chengrui, Z., "Research on active infrared icing detection for helicopter rotors", Journal of Wuhan University of Technology, 32, pp.121-125, 2010.

[51] Gagnon, R.E., Groves, J., and Pearson, W., "Remote ice detection equipment – RIDE", Cold Regions Science and Technology, 72, pp. 7-16, March 2012.

[52] Zhuge, J., Zhang, W., Zhan, X., Wang, K., Wang, Y., and Wu, J., "Image matching method based on improved Harris algorithm for aircraft residual ice detection", 4th International Conference on Information, Cybernetics and Computational Social Systems (ICCSS), pp. 273-278, IEEE, July 2017.

[53] Shajiee, S., Wagner, P., Pao, L., and McLeod, R., "Development of a novel ice sensing and active de-icing method for wind turbines", 50th AIAA Aerospace Sciences Meeting including the New Horizons Forum and Aerospace Exposition, p. 1153, 2012.

[54] Ikiades, A., Armstrong, D., and Howard, G., "Optical diffusion and polarization characteristics of ice accreting in dynamic conditions using a backscattering fibre optic technique", Sensors and Actuators A: Physical, 140(1), pp. 43-50, June 2007.

[55] Armstrong, D., Hare, G., Kloeppel, V., Lawrence, M., Dalton, T., Konstantaki, M., and Ikiades, A., "Air Conformal Ice Detection System (A.C.I.D.S) for the power optimised, ice protected aircraft / rotorcraft," SAE Technical Paper 2003-01-2103, 2003.

[56] Ikiades, A., Howard, G. and Armstrong, D.J., "Measurement of optical diffusion properties of ice for direct detection ice accretion Sensors," Sensors and Actuators A: physical, 140(1), pp. 24-31, June 2007.

[57] Ikiades, A., "Direct ice detection based on fiber optic sensor architecture", Applied Physics Letters, 91, pp.104-106, September 2007. https://doi.org/10.4271/2003-01-2103

[58] Ikiades, A., Spasopoulos, D., Amoiropoulos, K., Richards, T., Howard, G., and Pfeil, M., "Detection and rate of growth of ice on aerodynamic surfaces using its optical characteristics", Aircraft Engineering and Aerospace Technology, 85(6), pp. 443-452, 2013.

[59] Li, W., Zhang, H., Ye, L. and Zheng, Y., "Fiber-optic ice detection system for aeroplane application", International Workshop on Intelligent Systems and Applications, pp. 1-4, IEEE, 2009.

[60] Li, C., Li, W., Ye, L., and Zhang, J., "A fiber-optic aircraft icing detection system using double optical paths based on the theory of information fusion", Chinese Journal of Sensors and Actuators, 22, pp. 1352-1355, September 2009.

[61] Armstrong, D., Hare, G., Kloeppel, V., Lawrence, Dalton, T., Konstantaki, M., and Ikiades, A., "Air Conformal Ice Detection System (A.C.I.D.S) for the Power Optimised, Ice Protected Aircraft / Rotorcraft," SAE Technical Paper 2003-01-2103, 2003.

[62] Ge, J., Ye, L., and Zou, J., "A novel fiber-optic ice sensor capable of identifying ice type accurately", Sensors and Actuators A: Physical, 175, pp. 35-42, March 2012. http://dx.doi.org/10.1016/j.sna.2011.12.016

[63] Zou, J., Ye, L., and Ge, J., "Ice type detection using an oblique end-face fibre-optic technique", Measurement Science and Technology, 24(3), paper 035201, 2013.

[64] Zou, J.H., Ye, L., An, J., Ge, J.F., and Liu, Z.J., "Fiber-optic Ice Detector for Meteorological Observation", [J]. Instrument Technique and Sensor, 4, 2012.

[65] Zou, J., Ye, L., Ge, J., and Zhao, C., "Novel fiber optic sensor for ice type", Measurement, 46(2), pp. 881-886, February 2013. http://dx.doi.org/10.1016/j.measurement.2012.09.020

[66] Amiropoulos, K., Spasopoulos, D., and Ikiades, A., "Fiber optic sensor for ice detection on aerodynamic surfaces using plastic optic fiber tapers" Advanced Photonics Congress (BGPP, IPR, NP, Networks, NOMA, Sensors, SOF, SPPCom), Zurich, Switzerland, July 2nd – 5th, OSA, 2018.

[67] Klainer, Stanley M., and Milanovich, Fred P., "Optical sensor for the detection of ice formation and other chemical species", US Patent 4,913,519, August 1990.

[68] Frovel, M., Fernandez-Medina, A.B., Mora, J., Agüero, A., Sor, S., López Herredera, R., Garcia, A., and Gonzales, M., "System And Method For Detecting Ice Formation On A Body", Patent: PCT/EP2019/074091, 2019.

[69] Tribus, M., and Moyle, M. P., "Ice Detection Apparatus", US Patent 2,766,619, October 1953.

[70] Khurgin, B., "Two-resistor ice detector" US Patent 4,882,574, November 1989.

[71] Hann, R., Borup, K., Zolich, A., Sorensen, K., Vestad, H., Steinert, M., and Johansen, T.A., "Experimental investigations of an icing protection system for UAVs", International Conference on Icing of Aircraft, Engines, and Structures, paper 2019-01-2038, SAE, 2019. https://doi.org/10.4271/2019-01-2038

[72] Roy, S., Izad, A., DeAnna, R.G., and Mehregany, M., "Smart ice detection systems based on resonant piezoelectric transducers", Sensors and Actuators A: Physical, 69(3), pp. 243-250, September 1998. https://doi.org/10.1016/S0924-4247(98)00101-0

[73] Claffey, K.J., Jones, K.F., and Ryerson, C.C., "Use and calibration of Rosemount ice detectors for meteorological research," Atmospheric Research, 36(3-4), pp. 277-286, May 1995.

[74] Ramsay A.C., and Laster, M.E., "Status of the ASOS freezing rain sensor," in 6th Conference on Aviation Weather Systems, pp. 460-465, 1995.

[75] Liu, Q., Wu, K.T., Kobayashi, M., Jen, C.K., and Mrad, N., "In situ ice and structure thickness monitoring using integrated and flexible ultrasonic transducers", Smart Materials and Structures, 17(4), August 2008. https://doi.org/10.1088/0964-1726/17/4/045023

[76] Zhang, Z., Zhang, J., Ye, L., and Zhang, Y., "Research on the application of neural network in diaphragm icing sensor fault diagnosis", in Advances in Neural Networks – ISNN 2009, pp. 589-600, 2009. https://doi.org/10.1007/978-3-642-01507-6_67

[77] Wang, H., Huang, X., Hong, R., and Fang, C., "Establishment and analysis of mathematic model for ice detector", 2007 8th Int. Conf. Electron. Meas. Instruments, ICEMI, pp. 4714-4717, 2007.

[78] Kim, J.-S., Vinoy, K.J., and Varadan, V.K., "Wireless health monitoring of cracks in structures with MEMS-IDT sensors", Proc. SPIE 4700, Smart Structures and Materials 2002: Smart Electronics, MEMS, and Nanotechnology, July 2002. https://doi.org/10.1117/12.475048

[79] Varadan, V.V., Tellakula, A.R., Hollinger, R.D., Li, C.-T., and Varadan, V.K., "Wireless IDT microsensors for subsurface sensing", Proc. SPIE 4129, Subsurface Sensing Technologies and Applications II, July 2000. https://doi.org/10.1117/12.390633

[80] Varadan, V.K., and Varadan, V.V., "Wireless smart conformal MEMS-based sensors for aerospace structures", in AIAA Defense and Civil Space Programs Conference and Exhibit, 1998. https://doi.org/10.2514/6.1998-5244

[81] Varadan V.K., and Varadan, V.V., "MEMS for measuring deflection, acceleration, and ice sensing on rotorcraft", in Proc. SPIE, 1996 Symposium on Smart Materials, Structures, and MEMS, April 1998. https://doi.org/10.1117/12.305612

[82] Varadan, V.K., Varadan, V.V., and Bao, X.-Q., "IDT, SAW, and MEMS sensors for measuring deflection, acceleration, and ice detection of aircraft", in Proc. SPIE 3046, Smart Structures and Materials 1997: Smart Electronics and MEMS, June 1997. https://doi.org/10.1117/12.276610

[83] Varadan, V.K., "Wireless microsensors for health monitoring of aircraft structures", in Proc. SPIE 4981, MEMS Components and Applications for Industry, Automobiles, Aerospace, and Communication II, January 2003. https://doi.org/10.1117/12.479561

[84] DeAnna, R.G., Mehregany, M. and Roy, S., "Microfabricated ice-detection sensor", in Proc. SPIE 3046, Smart Structures and Materials 1997: Smart Electronics and MEMS, June 1997. https://doi.org/10.1117/12.276618

[85] Drossel, W.G., Nestler, M., Mäder, T., and Schönherr, J., "Piezoceramics in sheet-metal compounds for icing detection", 8th Conf. Smart Struct. Mater. SMART 2017 6th Int. Conf. Smart Mater. Nanotechnol. Eng. SMN 2017, Madrid, Spain, pp. 393-399, June 2017.

[86] Mäder, T., Nestler, M., Kranz, B., and Drossel, W.G., "Studies on sheet-metal compounds with piezoceramic modules for icing detection and de-icing," Adv. Eng. Mater., 20(12), pp. 1-9, 2018.

[87] Jarvinen, P., "Aircraft ice detection method", in 45th AIAA Aerospace Sciences Meeting and Exhibit, AIAA, January 2007. https://doi.org/10.2514/6.2007-696

[88] US Army Corps of Engineers, "Wide-area ice detection using time domain reflectometry," Cold Regions Research and Engineering Laboratory, ERDC/CREEL TR-02-15, October, p. 37, 2002.

[89] Berg, M., Lalli, J., Claus, R., and Kreeger, R.E., "Metal rubber sensor technology to enable in-flight icing measurement", in SPIE 10168, Sensors and Smart Structures Technologies for Civil, Mechanical, and Aerospace Systems, April 2017. https://doi.org/10.1117/12.2260135

[90] Bakhoum, E.G., Cheng, M.H.M., and Van Landingham, K.M., "Alpha-particle-based icing detector for aircraft," IEEE Trans. Instrum. Meas., 63(1), pp. 185-191, 2014.

[91] Caliskan, F., and Hajiyev, C., "A review of in-flight detection and identification of aircraft icing and reconfigurable control", Progress in Aerospace Sciences, 60, pp. 12-34, July 2013.

[92] Serke, D.J., Reed, K.A., Negus, J., Blanchette, L., Ware, R., and Kennedy, P.C., "A new narrow-beam, multi-frequency, scanning radiometer and its application to in-flight icing detection", Atmospheric Research, 185, pp. 84-91, March 2017. https://doi.org/10.1016/j.atmosres.2016.10.016

[93] Brandes, E., Vivekanandan, J., and Rasmussen, R., "Rain-snow discrimination with polarimetric radar," 10th Conference on Aviation, Range, and Aerospace Meteorology, paper 40653, American Meteorological Society, May 2002.

[94] Schneider, T.L., Reinking, R.F., Campbell, W.C., and Clark, K., "NOAA/ETL'S polarization radar-microwave radiometer system for detecting in-flight icing conditions-progress in the design and development of GRIDS," in 10th Conference on Aviation, Range, and Aerospace Meteorology(ARAM), Portland, OR, USA, pp. 220-223, 2002.

[95] Lefevre, R.J., Shipley, C.A., Woods, D.N., and van Daalen Wetters, R.F., "In-flight icing hazard detection radar," IEEE Natl. Radar Conf. – Proc., pp. 695-698, 2000.

[96] Ellis, S.M., Vivekanandan, J., Brandes, E.A., Stith, J.L., and Keeler, R.J., "Aircraft icing detection using S-band polarization radar measurements", in 9th Conference on Aviation, Range, and Aerospace Meteorology, paper 16467, American Meteorological Society, 2000.

[97] Vivekanandan, J., Zhang, G., and Politovich, M.K., "An Assessment of droplet size and liquid water content derived from dual-wavelength radar measurements to the application of aircraft icing detection", J. Atmos. Ocean. Technol., 18(11), pp. 1787-1798, November 2001.

[98] Adams, I.S., and Bobak, J., "The feasibility of detecting supercooled liquid with a forward-looking radiometer", IEEE J. Sel. Top. Appl. Earth Obs. Remote Sens., 11(6), pp. 1932-1938, 2018.

[99] Mueller, E.A. and Silha, E.J., "Unique features of the CHILL radar system", in 18th Conference on Radar Meteorology, Atlanta, Ga., March 28 – 31, 1978, Preprints. (A79-25626 09-47) Boston, Mass., American Meteorological Society, pp. 381-382, 1978.

[100] Löhnert, U., Crewell, S., and Simmer, C., "An integrated approach toward retrieving physically consistent profiles of temperature, humidity, and cloud liquid water", Journal of Applied Meteorology, 43, pp. 1295-1307, March 2004. doi: 10.1175/1520-0450(2004)043<1295:AIATRP> 2.0.CO;2.

[101] Krasnov, O., and Russchenberg, H., "A synergetic radar-lidar technique for the LWC retrieval in water clouds" 7th International Symposium on Tropospheric Profiling, Boulder, Colorado, USA, June 11 – 17, 2006.

[102] Thorsen, T.J., Fu, Q., and Comstock, J.M., "Cloud effects on radiative heating rate profiles over Darwin using ARM and A-train radar/lidar observations", J. Geophys. Res. Atmos., 118, 5637-5654, 2013. doi:10.1002/jgrd.50476

[103] Heymsfield, A.J., Winker, D., and van Zadelhoff, G.-J., "Extinction-ice water content-effective radius algorithms for CALIPSO", Geophys. Res. Lett., 32, L10807, 2005. doi:10.1029/2005GL022742

[104] Ellrod, G.P., and Nelson, J.P., "Detection of potential aircraft icing regions with GOES multi-spectral data", 35th Aerospace Sciences Meeting and Exhibit, Reno, NV, USA, American Institute of Aeronautics and Astronautics, Inc. (AIAA), January 1997. doi:10.2514/6.1997-412

[105] Minnis, P., Smith, W.L., Nguyen, L., Khaiyer, M.M., Spangenberg, D.A., Heck, P.W., Palikonda, R., Bernstein, B.C., and McDonough, F., "A real-time satellite-based icing detection system", Proceedings of 14th International Conference on Clouds and Precipitation (467), Bologna, Italy, July 2004.

[106] Nguyen, L., Minnis, P., Spangenberg, D.A., Nordeen, M.L., Palikonda, R., Khaiyer, M.M., Gultepe, I., and Reehorst, A.L., "Comparison of satellite and aircraft measurements of cloud microphysical properties in icing conditions during ATREC/AIRS-II", 11th Conference on Aviation, Range, and Aerospace, Hyannis, MA, USA, American Meteorological Society (AMS), October 2004.

[107] Murray, J., Nguyen, L.A., Daniels, T.S. , Minnis, P., Schaffner, P.R., Cagle, M.F., Nordeen, M.L., Wolff, C.A., Anderson, M.V., Mulally, D.J., Jensen, K.R., Grainger, C.A., and Delene, D.J., "Tropospheric Airborne Meteorological Data and Reporting (TAMDAR) Icing Sensor Performance during the 2003/2004 Alliance Icing Research Study (AIRS II) ", 43rd AIAA Aerospace Sciences Meeting and Exhibit, Reno, NV, USA, American Institute of Aeronautics and Astronautics, Inc. (AIAA), January 2005. doi: 10.2514/6.2005-258

[108] NATO RTO, "Ice Accretion Simulation", AGARD Advisory Report 344, Advisory Group for Aerospace Research and Development (AGARD) – Fluid Dynamics Panel Working Group 20, North Atlantic Treaty Organization (NATO), Neuilly-Sur-Seine, France, December 1997.

[109] Bragg, M.B., Perkins, W.R., Sarter, N.B., Basar, T., Voulgaris, P.G., Gurbacki, H.M., Melody, J.W., and McCray, S.A., "An interdisciplinary approach to inflight aircraft icing safety", 36th AIAA Aerospace Sciences Meeting and Exhibit, Reno, NV, USA, American Institute of Aeronautics and Astronautics, Inc. (AIAA), January 1998. doi:10.2514/6.1998-95.

[110] Bragg, M.B., Basar, T., Perkins, W.R., Selig, M.S., Voulgaris, P.G., Melody, J.W., and Sarter, N.B., "Smart icing systems for aircraft icing safety", 40th AIAA Aerospace Sciences Meeting and Exhibit, Reno, NV, USA, American Institute of Aeronautics and Astronautics, Inc. (AIAA), January 2002. doi:10.2514/6.2002-813

[111] Myers, T.T., Klyde, D.H., and Magdaleno, R.E., "The Dynamic Icing Detection System (DIDS) ", 38th AIAA Aerospace Science Meeting and Exhibit, Reno, NV, USA, American Institute of Aeronautics and Astronautics, Inc. (AIAA), January 1999. doi:10.2514/6.2000-364

[112] Gingras, D.R., Barnhart, B., Ranaudo, R., Ratvasky, T.P., and Morelli, E., "Envelope protection for in-flight ice contamination", 47th Aerospace Science Meeting, Orlando, FL, USA, American Institute of Aeronautics and Astronautics, Inc. (AIAA), January 2009. doi:10.2514/6.2009-1458

[113] Gingras, D.R., Barnhart, B., Ranaudo, R., Martos, B., Ratvasky, T.P., and Morelli, E., "Development and implementation of a model-driven envelope protection system for in-flight ice contamination", AIAA Guidance, Navigation and Control Conference, Toronto, ON, Canada, American Institute of Aeronautics and Astronautics, Inc. (AIAA), August 2010. doi:10.2514/6.2010-8141

[114] Ranuado, R.J., Martos, B., Norton, B., Gingras, D.R., Barnhart, B., and Ratvasky, T.P., "Piloted simulation to evaluate the utility of a real time envelope protection system for mitigating in-flight icing hazards", AIAA Atmospheric and Space Environments Conference, Toronto, ON, Canada, American Institute of Aeronautics and Astronautics, Inc. (AIAA), August 2010. doi:10.2514/6.2010-7987

[115] Melody, J.W., Basar, T., Perkins, W.R., and Voulgaris, P.G., "Parameter identification for inflight detection and characterization of aircraft icing", Control Engineering Practice, 8(9), pp. 985-1001, September 2000. doi:10.1016/S0967-0661(00)00046-0

[116] Melody, J.W., Hillbrand, T., Basar, T., and Perkins, W.R., "H∞ parameter identification for inflight detection of aircraft icing: the time-varying case", Control Engineering Practice, 9(12), pp. 1327-1335, December 2001. doi:10.1016/S0967-0661(01)00081-8

[117] Schuchard, E.A., Melody, J.W., Basar, T., Perkins, W.R., and Voulgaris, P., "Detection and classification of aircraft icing using neural networks", 38th AlAA Aerospace Sciences Meeting and Exhibit, Reno, NV, USA, American Institute of Aeronautics and Astronautics, Inc. (AIAA), January 2000. doi:10.2514/6.2000-361

[118] Dong, Y. and Ai, J., "Research on inflight parameter identification and icing location detection of the aircraft", Aerospace Science and Technology, 29(1), pp. 305-312, August 2013. doi:10.1016/j.ast. 2013.03.012

[119] Aykan, R., Hajiyev, C., and Caliskan, F., "Aircraft icing detection, identification and reconfigurable control based on Kalman filtering and neural networks", AIAA Atmospheric Flight Mechanics Conference and Exhibit, San Francisco, CA, USA, American Institute of Aeronautics and Astronautics, Inc. (AIAA), August 2005. doi:10.2514/6.2005-6220

[120] Aykan, R., Hajiyev, C., and Caliskan, F., "Kalman filter and neural network-based icing identification applied to A340 aircraft dynamics", Aircraft Engineering and Aerospace Technology, 77(1), pp. 23-33, February 2005. doi: 10.1108/00022660510576019

[121] Deiler, C., "Flight characteristics of iced aircraft", AIAA Atmospheric Flight Mechanics Conference, AIAA Scitech 2019 Forum, San Diego, CA, USA, American Institute of Aeronautics and Astronautics, Inc. (AIAA), January 2019. doi:10.2514/6.2019-0560

[122] Petit, G., "Method and device for detecting degradation of performance of an aircraft", US Patent 2005/0288895 A1, United States Patent and Trademark Office, December 2005.

[123] Deiler, C., Fezans, N., "Performance-based ice detection methodology", AIAA Atmospheric Flight Mechanics Conference, AIAA Aviation 2017 Forum, Denver, CO, USA, American Institute of Aeronautics and Astronautics, Inc. (AIAA), June 2017. doi: 10.2514/6.2017-3394

[124] McKillip, R.M., "Aircraft icing detection system", US Patent 6,304,194 B1, United States Patent and Trademark Office, 16. October 2001.

[125] Marinvent Product website, Airfoil Performance Monitor (APM). http://www.marinvent.com/solutions/apm/

[126] Van Dyke, D. "Airfoil performance monitor", Professional Pilot, 3, 2011.

Chapter 2 – ICE PROTECTION SYSTEMS

Federico Veronesi and Mariarosa Raimondo
National Research Council – Institute of Science and Technology for Ceramics
ITALY

Giuseppe Mingione
Centro Italiano Ricerche Aerospaziale
ITALY

Brent Martin
Defence Technology Agency
NEW ZEALAND

Richard Hann and Verner Håkonsen
Norwegian University of Science and Technology
NORWAY

Ki-Han Kim
Office of Naval Research
UNITED STATES

Julio Mora Nogues
Instituto Nacional de Técnica Aeroespacial INTA,
SPAIN

Bob Gagnon
National Research Council (NRC)
CANADA

2.1 INTRODUCTION

This chapter deals with the Ice Protection Systems (IPS) in air and sea vehicles operating in Low Temperature Environments (LTE). The aims of this chapter are to:

- Describe why aircraft and sea vessels need IPS;
- Assess the existing regulations concerning IPSs for different applications;
- Review the current IPS technologies, along with the most relevant challenges to be faced in the future.

In both aeronautics and marine communities, ice accretion on the air and sea vehicles causes performance degradation and safety hazard. Icing on aircraft surfaces decreases aerodynamic performance, which occasionally results in catastrophic accidents. Historically, there have been several fatal aircraft accidents caused by icing, which led to the creation of more stringent safety regulations. Ice accretion on ships operating in LTE will develop hazardous working environment on the deck as well as loss of ship stability. Unless proper mitigation measures are taken, the ship could experience listing, slow roll, or even eventual capsizing.

This chapter is organized in four main sections. In Section 2.2, the most harmful effects of icing phenomena on aircraft and sea vehicles are listed, which illustrate the needs for IPS. Section 2.3 highlights the existing regulations and operational conditions that the IPS should meet to obtain certification. In Sections 2.4 and Section 2.5, major existing IPS technologies are evaluated, highlighting their operational mechanisms, advantages and challenges. Section 2.6 includes some conclusions on the current state and suggestions for future research on IPS, based on the cited bibliography.

2.2 NEED FOR ICE PROTECTION SYSTEMS

2.2.1 Aircraft

The undesirable effects of icing phenomena on aircraft are manifold:

- Aerodynamic effects: Ice build-up on aircraft surface increases drag, reduces lift and takeoff performance, and may cause destructive vibration [1], [2];

- Maneuverability: Control surfaces become unbalanced or frozen. Fixed slots are filled, and movable ones jammed. Moreover, control surfaces (e.g., aileron) could lose effectiveness or cause unexpected aircraft attitude;
- Sensors and instrumentation: Exposed sensors can be affected providing incorrect flight information to the pilot and to the flight control systems (e.g., freezing of Pitot tubes). Icing could also impact the engine performance and radio reception;
- Release of ice blocks: Ice chunks can break off and cause engine failures and structural damage. Fuselage aft-mounted engines are particularly susceptible to Foreign Object Damage (FOD). Ice on the wing could break off during takeoff due to the flexing of the wing and go directly into the engine, leading to surge, vibration, and complete thrust loss.

All these effects make necessary the use of suitable IPS for aircraft components for a wide range of icing conditions. For aircraft, icing is usually divided in two main conditions: on-ground icing and in-flight icing. The former is caused by freezing of moisture on the aircraft surfaces (e.g., upper surfaces of the wing, tail plane and fuselage) and is usually tackled by spraying the aircraft with freezing-depressant fluid before take-off. On the other hand, in-flight icing is mainly caused by supercooled water, i.e., water at temperatures below 0°C that is in a metastable liquid state and freezes immediately when making contact with a nucleation point (in this case, an aircraft surface). Supercooled water can be found in different forms: suspended in clouds in the form of droplets, as freezing precipitation impinging on the aircraft front surfaces, and also in combination with ice crystals as in wet snow.

IPSs are used on aircraft to protect from in-flight icing on the following airplane components (Figure 2-1):

- Wing leading edge;
- Horizontal and vertical stabilizer leading edges;
- Engine cowl leading edges;
- Propellers;
- Propeller spinner;
- Air data probes;
- Flight deck windows;
- Water and waste system lines and drains;
- Antennae.

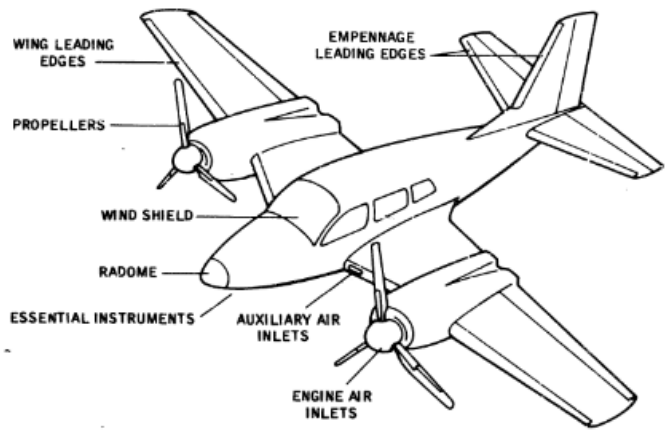

Figure 2-1: Areas of Airframe that may Require Ice Protection [3].

Icing occurs on all aircraft classes, including business and large transportation aircraft. However, regional and small aircraft are more susceptible to icing phenomena since they usually fly at lower altitude than larger aircraft where atmospheric conditions are more favorable to ice accretion. Supercooled water is most likely to be found at altitudes between 1000 and 5000 m where most small aircraft fly. Moreover, icing on smaller aircraft, including Unmanned Aerial Vehicles (UAVs), creates more serious problems than on larger aircraft because small aircraft have less available power for IPS, and are therefore more sensitive to icing hazards [4]. In the absence of an on-board human pilot who is able to identify the icing conditions, there is an even greater need for efficient and integrated ice detection and protection systems. Also, novel aircraft types used for urban air mobility applications are facing challenges with regards to icing.

The ice accretion problem is of interest not only from the safety point of view, but also in terms of fuel consumption reduction and consequent reduction of environmental impact. The need for a clean leading edge to improve aerodynamic performances and for IPS with reduced power consumption are providing new incentive for research and development in ice protection technology.

It is clear that IPSs play a crucial role in improving aircraft operational efficiency and safety. For this reason, several research projects have been devoted to the investigation of innovative aircraft IPSs with enhanced performance. Table 2-1 presents a list of the most relevant research projects related to aircraft IPS in the last decade.

Table 2-1: Example Selection of National and International Research Projects Related to Aircraft IPS.

Acronym	Title	Framework (Period of Performance)	Objective
EIROS [5]	Advanced ice and erosion resistant composite materials	EU Horizon2020 (2016 – 2019)	Development of high-performance composite materials with increased erosion resistance, anti-icing characteristics and self-healing properties for operation in extreme environments.
HELADA [6]	Coatings against ice accretion and erosion in aerodynamic components in aircraft	Spanish Framework (2013 – 2017)	Development and testing of durable anti-icing coatings for aircraft components.
GAINS [7]	Green airframe icing novel system	EU Clean Sky 2 Airframe Platform (2015 – 2022)	Address solutions for leading edge slat IPS technology, design and certification.
ICESURFER	Icephobic surfaces for components based on polymer composites	Polish national program “Leader” National Center for Research and Development (2019 – 2021)	Development of and modification of outer surface of polymer composites in order to achieve icephobic properties.
ICEMAN	Anti-icing sustainable solutions by development and application of icephobic coatings	Norway Grants, Poland-Norway bilateral cooperation (2020 – 2023)	Development and modification of polymer coatings deposited on different types of substrates.

Acronym	Title	Framework (Period of Performance)	Objective
INDUCTICE [8]	Induction technology to prevent ice build-up on aircraft during flight	EU Clean Sky 2 (2016 – 2019)	Development of an efficient, modular, and lightweight electromagnetic induction based IPS, which uniformly heats the wing leading edge surface.
INSPIRE	Innovative systems to prevent ice on regional aircraft	EU Clean Sky 2 Regional Platform (2017 – 2021)	Electrothermal IPSs for regional aircraft wing ice protection.
JEDI-ACE [9]	Japanese-European de-icing aircraft collaborative exploration	Japan + EU Horizon2020 (2012 – 2016)	Integrated IPS: an integrated approach, consisting of combined passive anti-icing coating, active de-icing devices and ice sensors.
MAI-TAI [10]	Multidisciplinary approach for the implementation of new technologies to prevent accretion of ice on aircraft	Spanish Framework (2019 – 2022)	Development and testing of durable active, passive and hybrid solutions for icing on aircraft components.
NO-ICE ROTOR [11]	No-ice rotor	EU Clean Sky 2 (2017 – 2021)	Development of ultra-high reliability heater layers which can be embedded into the rotorcraft's composite structures to provide anti-icing and de-icing capability.
PANIPLAST [12]	Industrial development of PANIPLAST process poly(aniline) conductive polymers	EU Horizon2020 (2015 – 2016)	Development of high conductivity organic polymers to be used as anti-icing and de-icing systems.
PHOBIC2ICE [13]	Super ice phobic surfaces to prevent ice formation on aircraft	EU Horizon2020 + Canada (2016 – 2019)	Development of environment-friendly, scalable, and durable anti-icing solutions.
SOUNDOFICE	Sustainable smart de-icing by surface engineering of acoustic waves	EU Horizon2020-FETOPEN-2018-2020 topic (2020 – 2024)	Development of a radically new solution for ice removal from different materials.
STORM [14]	Efficient ice protection systems and simulation techniques of ice release on propulsive systems	EU Horizon2020 (2013 – 2017)	Research in the domains of ice release mechanisms understanding and prediction, ice accretion within the engine environment and innovative IPSs.

2.2.2 Sea Vessels

Ice build-up on ocean-going vessels has several negative impacts on the vessel's performance and safe operation (seakeeping). The primary concern is from the accretion of large amounts of ice on the superstructure increasing the vessel's topside weight. The location of the ice is important as weight added to

higher areas of a vessel will have a greater impact on stability compared to ice present closer to the water line. Added weight from ice can increase the roll period of a vessel (side-to-side motion) and in extreme cases prevent the vessel from recovering from a roll.

Ice accumulation can occur rapidly in extreme weather conditions (gale force winds and air temperatures below 1.7°C) with rates of up to 2 tons per hour recorded in the Arctic [15] and similar levels observed in the Antarctic [16]. Smaller vessels are more at risk from this phenomenon.

Ice build-up also has negative impacts on other critical areas and systems including:

- Communications equipment such as dishes and antennae. These devices are often located at high points on the vessel and may be difficult for personnel to safely access in icing conditions to manually remove ice;
- Bridge windows where visibility is critical for safe operations;
- Safety equipment such as life rafts that rely on hydrostatic sensors to deploy which can be covered or blocked by ice;
- Exterior decking and walkways can become dangerous when covered in ice hindering movement of personnel.

2.3 EXISTING REGULATIONS

In this section, the existing regulations that are specifically related to IPS for large aircraft and sea vessels are briefly summarized. US and European regulations are reported as they are the most significant in the NATO framework.

2.3.1 Regulations for Aircraft

Federal Aviation Administration (FAA) and European Aviation Safety Agency (EASA) are the US and respective EU authorities with powers to regulate all aspects of civil aviation, including the construction and operation of airports, and the management of air traffic. In this report, EASA regulations are indicated as CS (Certification Specification) while FAA requirements are indicated as 14 CFR (Title 14 of Code of Federal Regulation) for brevity. EASA [17] and FAA [18] regulations have a similar structure:

- CS-23 / CFR-23: Small aircraft.
- CS-25 / CFR-25: Large aircraft.
- CS-27 / CFR-27: Normal helicopter.
- CS-29 / CFR-29: Transport helicopter.
- CS-33 / CFR-33: Engine.
- CS-P / CFR-35: Propeller.

In FAA regulations, IPSs are first invoked in CFR-25—Airworthiness Standards: Transport Category Airplanes, Subpart F – Equipment, Paragraph 1419 – Ice Protection. This paragraph states that, in order for an airplane to receive certification for flight in icing conditions, it must be able to operate safely in the icing conditions established in Appendix C to 14 CFR. The safe operability can be assessed with an analysis of IPSs for the various aircraft components. Such analysis necessarily includes in-flight tests of the IPS in all possible conditions, with optional laboratory tests and simulations.

The icing atmospheric conditions are defined as envelopes in the Appendix C to CS-25 and CFR-25, in which an aircraft to be certified must be able to fly safely. These icing envelopes are defined for two types of icing conditions: one is for *continuous maximum icing conditions* encountered in stratiform clouds or

layer-type clouds and the other for *intermittent maximum icing conditions* encountered in cumuliform clouds or convective clouds (see Figure 2-2). These envelopes are presented in terms of three variables: Liquid Water Content (LWC) vs Mean Effective Drop Diameter (MED) for a range of temperature (from 0°C to –30°C). The MED is approximately equivalent to the Median Droplet Diameter (MVD), which is more often used nowadays. The shaded areas in Figure 2-2 represent the icing conditions for which an aircraft has to be certified for safe operation. Appendix C provides additional diagrams in terms of expected temperature range for a given altitude (Figure 2-3). The aircraft manufacturers should use the temperature-altitude envelopes in Figure 2-3 to identify the ambient temperature the aircraft will fly through based on the aircraft flight envelope. In Figure 2-2, by using the LWC-MED diagram for a given temperature it is possible to evaluate the critical LWC as a function of MED.

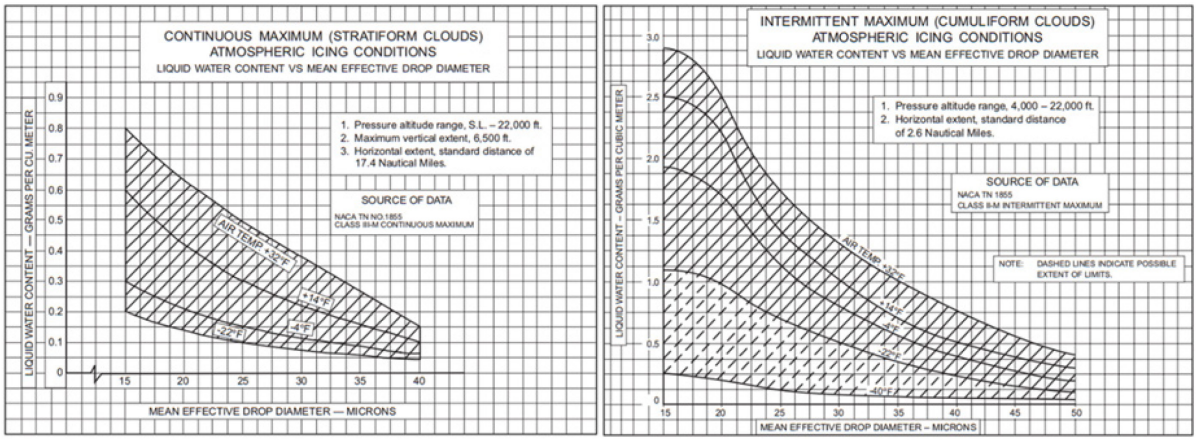

Figure 2-2: Icing Envelopes of Appendix C (LWC vs MED): (Left) Continuous Maximum (Stratiform Clouds) Icing Conditions and (Right) Intermittent Maximum (Cumuliform Clouds) Icing Conditions [19].

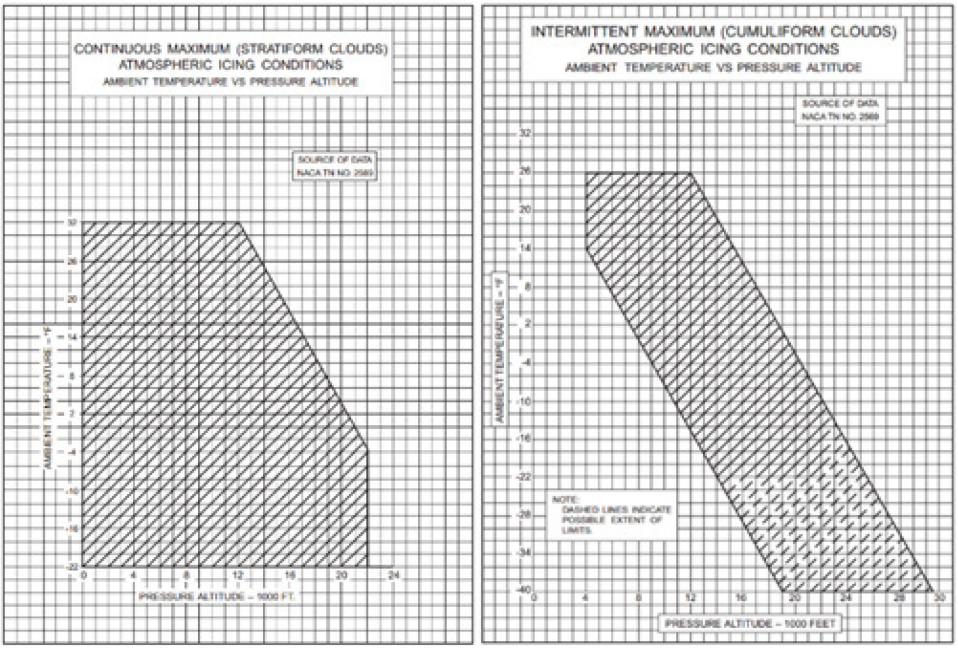

Figure 2-3: Icing Envelopes of Appendix C (Ambient Temperature vs Pressure Altitude): (Left) Continuous Maximum (Stratiform Clouds) Icing Conditions and (Right) Intermittent Maximum (Cumuliform Clouds) Icing Conditions [19].

These icing envelopes were developed for a specified reference distance of 17.7 nautical miles (nmi) for stratiform clouds and 2.6 nmi for cumuliform clouds. If for some reason the design (exposure) distance for ice protection systems is different from the reference distances of 17.7 nmi or 2.6 nmi, respectively, the originally selected LWC values may change. The correct LWC values can be obtained by corrective factors to the LWC as a function of Cloud Horizontal Extent presented in Figure 2-4. For example, to find the LWC to be expected as an average during flight through 100 nmi of stratiform icing clouds, the corrective factor of 0.46 is taken from Figure 2-4 (left). Thus, for stratiform clouds in which MED (or MVD) is 30 μm and the temperature is -10°C (+14°F), the maximum average LWC over 100 nmi is expected to be 0.46 x 1.0 g/m^3 = 0.46 g/m^3.

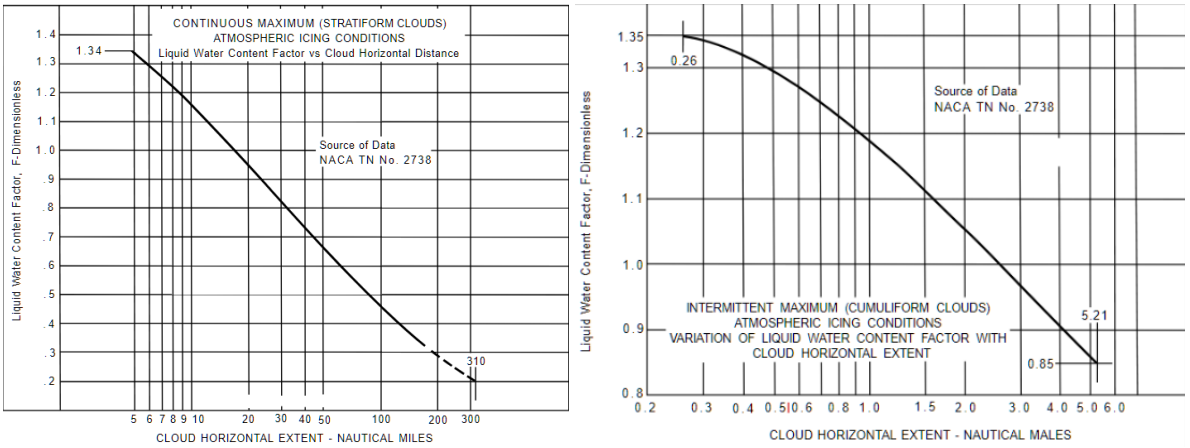

Figure 2-4: Corrective Factor to the LWC versus the Cloud Horizontal Extent for (Left) Stratiform and (Right) Cumuliform Clouds.

Severe icing conditions with Supercooled Large Droplets (SLD) were not included in the original icing envelopes of Appendix C. Therefore, a long certification process has been implemented arriving at an amendment to previous certification regulations. New envelopes for SLD were developed and introduced in Appendix O (see Figure 2-5) and for ice crystals and mixed phase in Appendix P. These new Appendices are applicable only to large aircraft (CS-25 and CFR-25) and engines (CS-33 and CFR-33).

Specifically, the following paragraphs of the regulations have been updated by including requirements for safe operations in SLD, ice crystal and mixed phase (ice crystals mixed with liquid water droplets):

- CS-25.1326: Pitot heat indication systems;
- CS-25.1419: Ice protection;

while the following have been added:

- Appendix O: SLD;
- Appendix D (EASA) and P (FAA): Ice crystal and mixed phase;
- CS-25.1420: Requirements that must be met in SLD icing conditions for large airplanes to be certified;
- CS-25.1324: Flight instrument external probes heating systems.

In the new regulation, both CS-25.1420 and CFR-25.1420 require that in addition to CS-25.1419, the aircraft must be capable of operating safely in accordance with the following three conditions:

- Operate safely after encountering the icing conditions defined in Appendix O,
- Operate safely in a selected portion of Appendix O conditions, detect when the aircraft is operating in conditions that exceed the selected portion, and then operate safely while exiting all icing conditions,
- Operate safely in all icing conditions in Appendix O.

In the new regulations [17], [18], some differences between EASA and FAA are present:

- The FAA proposed the exclusion of airplanes with certain attributes, i.e., airplanes with a Maximum Takeoff Weight (MTOW) larger than 60,000 lbs. and without reversible flight controls.
- The mixed phase and ice crystals environments are proposed by FAA for Pitot tubes and Angle of Attack sensors (CFR-25.1323 and CFR-25.1324).

The new Appendix O is the same for both EASA and FAA (Figure 2-5).

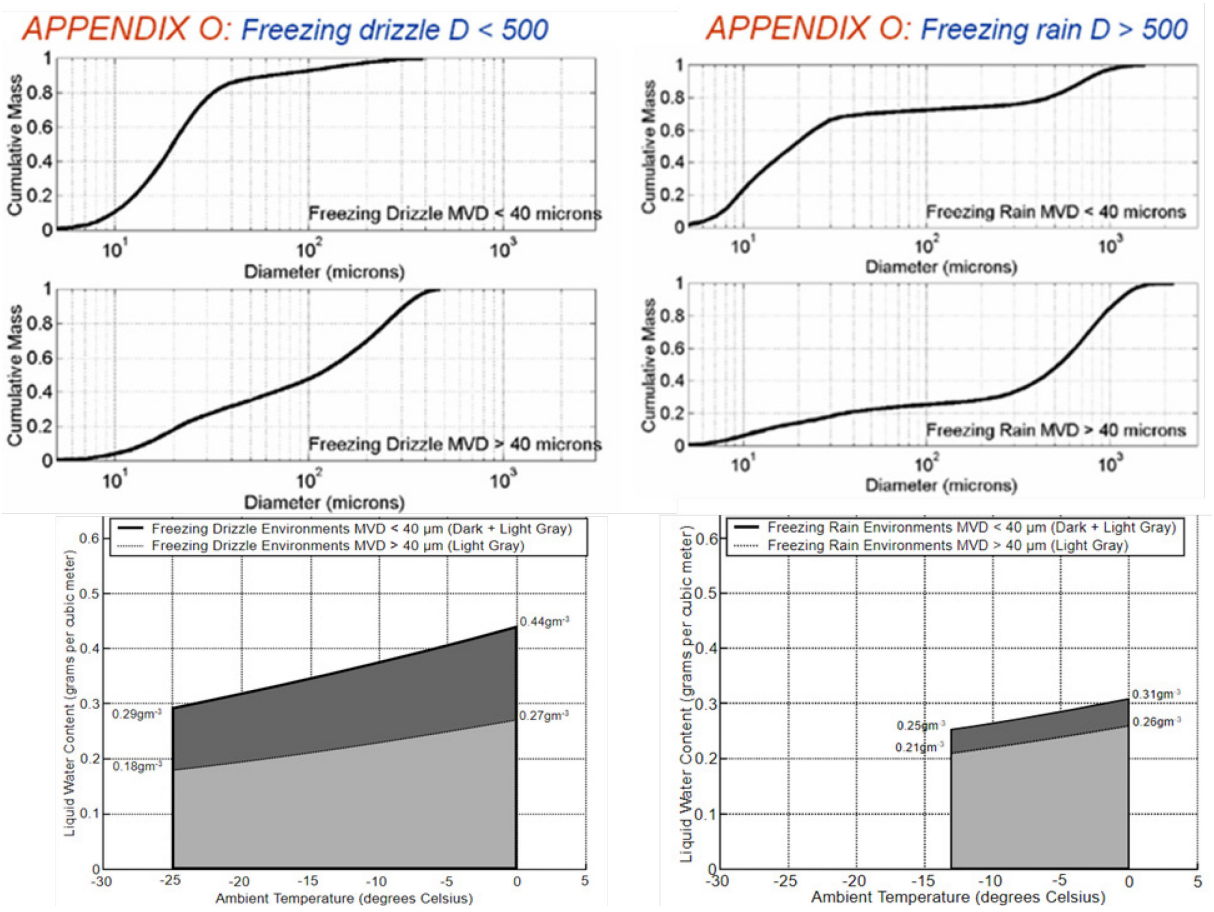

Figure 2-5: New Icing Envelopes of Appendix O: (Left) Freezing Drizzle Condition, (Right) Freezing Rain Conditions [20].

Two conditions, Freezing Drizzle and Freezing Rain, are defined:

- Freezing drizzle D < 500 μm
  - LWC up to 0.44 g/m^3
  - Droplet sizes of 100 to 500 μm
  - Temperatures 32°F to -13°F (0° C to -25°C)
  - Horizontal cloud extent with LWC factor 1 is 17.4 Nm (32.22 km).

- Freezing rain D > 500 µm
  - LWC up to 0.31 g/m^3
  - Droplet sizes of 100 to 2000 µm
  - Temperatures 32°F to -9°F (0°C to -13°C)
  - Horizontal cloud extent with LWC factor 1 is 17.4 Nm (32.22 km).

For each condition, LWC-Temperature and Temperature-Altitude diagrams are provided and two different droplet spectra defined, namely MVD < 40 µm and MVD > 40 µm.

The LWC represented in both Freezing Drizzle (FZDZ) and Freezing Rain (FZRA) is valid only for the reference distance of 32.2 km (17.7 nmi) for stratiform clouds. When the exposure distance (IWT exposure time) exceeds the reference distance of 32.2 km, a scale factor is provided to derive the LWC in both FZDZ and FZRA conditions (Figure 2-6), which is equivalent to the corrective factor to LWC vs Cloud Horizontal Extent in Appendix C (Figure 2-4).

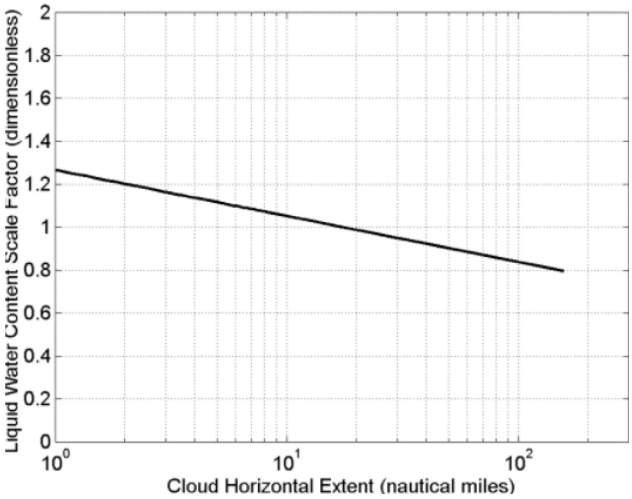

Figure 2-6: Appendix O: Distance Correction Factor.

Icing is addressed in several sections of certification requirements. The most relevant sections concerning ice protection are CS-25.1419 Ice protection (and related explicative material Acceptable Means of Compliance AMC 25.1419) and CS-25.1420 Supercooled large drop icing conditions (and related explicative material in AMC 25.1420).

Linked to previous sections is CS-25.21 (and related explicative material AMC 25.21), which provides indication on how to demonstrate compliance with icing requirements and on aircraft performances in icing conditions.

Other icing-related sections concern, for example, propellers CS-25.929 AC 25-28 Propeller de-icing (and related explicative material AMC 25.929) and power plant CS-25.1093 Powerplant Icing (and related explicative material AMC 25.1093).

While the aforementioned regulations refer to EASA requirements, similar requirements exist for FAA regulation, i.e., CFR-25.1419 (and related AC 25.1419), CFR-25.1420. FAA provides acceptable means of showing compliance with the airplane performance and handling characteristics certification requirements for flight in the icing conditions defined in Appendices C and O of Title 14, Code of Federal Regulations part 25 in the AC 25.25.

It is important here to mention that a substantial difference exists between the EASA and FAA requirements. For the EASA CS-25.21g (2) and (3), and Appendix O apply to all aircraft categories, whereas for the FAA the equivalent CFR-25.21(g) 1 and Appendix O are applicable only to aircraft with a maximum takeoff gross weight of less than 60,000 lbs, or those equipped with reversible flight controls. In practice this means, SLD certification requirements for EASA must be demonstrated for all aircraft, while for FAA it is necessary only for small aircraft, or aircraft without powered flight control.

Other parts of 14 CFR deal with ice protection for other types of air vehicles (e.g., rotorcrafts in CFR-27) or different parts of the aircraft (e.g., engines in CFR-33), but nothing more is added on IPSs.

IPSs are also mentioned in:

- CFR-121.321 (Operations in Icing) tackles the problem of small aircraft (i.e., weighing less than 60,000 lbs.) operating in conditions conducive to airframe icing, i.e., with visible moisture at temperature below 5°C. It mandates to activate IPSs when such conditions are met, which can be certified either by visual inspection or by an ice detection system. If none of the two procedures is feasible, IPSs must be activated for precaution during takeoff and landing procedures
- CFR-121.629 (Operation in Icing Conditions). In this paragraph, the on-ground de-icing/anti-icing program for aircraft showing ice accretion is discussed. A generic "de-icing /anti-icing fluid" is mentioned.

2.3.2 Regulations for Sea Vessels

Compared to the extensive regulations related to aircraft icing, there are no comparable regulations for icing on sea vessels. In 2006, the American Bureau of Shipping (ABS) published the *"Guide for Vessels Operating in Low Temperature Environments"* [15] to address various design, operation and crew requirements related to extreme cold weather conditions (-10°C or less). The preparation of a ship for safe operation in extreme cold weather conditions is defined as winterization.

Some references to IPSs can be found in the guide. In Section 3 – Hull Construction and Equipment, Paragraph 3.2 – Deckhouses, it is stated that at least half of bridge windows should be heated and equipped with cleaning systems to remove ice.

Possible IPSs are extensively listed in Appendix 4 – Notes on Vessel Systems and Machinery, Paragraph 1.1 – De-icing and Heat Tracing. It suggests installing permanent de-icing systems on vessels meant to operate in LTE (e.g., in Arctic climates) for long periods. The Appendix also indicates possible designs for IPSs, namely steam systems (including saltwater spray), thermal oil systems, electric resistance heaters, hot air generators, and manual removal. Moreover, anti-icing systems are mentioned along with possible designs, including coatings. De-icing of communication devices (i.e., antennae) must be also considered.

Moreover, Appendix 2 – Notes on Materials, Welding and Coatings, Paragraph 5.2 – Ice Release Coatings has been added in 2015. In addition to sprayable fluids with ant-icing properties, it states that icephobic coatings can be applied on the hull and other externally exposed surfaces like decks, deck houses and so forth. However, they should not be applied on walkways due to their inherent slipperiness. The Appendix also states that testing standards for these coatings are under development.

Similar class guides have been published by both Lloyd's Register (UK) and DNV-GL (Norway, Germany). The Lloyds Register *"Rules for the Winterisation of Ships"* [21] gives guidance on ice removal and prevention for vessels and equipment. The IPS aspects of this rules document are provided in Chapter 1, Sections 5 and 11. The IPS recommendations focus predominantly on heating and covers for critical systems as well as manual ice removal. The DNV-GL *"Winterization for Cold Climate Operations"* [22] Chapter 2, Section 1 gives an overview of IPSs in the anti-icing, anti-freezing and de-icing subsection indicating a general preference for passive systems. Some detail is given on expected operating temperature of thermal IPSs.

2.4 TYPES AND CLASSIFICATION OF EXISTING TECHNOLOGIES FOR AIRCRAFT APPLICATION

An IPS for large passenger aircraft typically involves ice detection components and icing mitigation techniques, including anti-icing and/or de-icing methods. Anti-icing prevents ice from accreting on the surfaces when there is an icing hazard predicted, while de-icing removes the accreted ice layer once it has been detected. Both strategies can also be divided into active and passive methods. Active methods use external systems and require an energy supply by either mechanical, thermal or chemical means, while passive methods take advantage of the physical properties of the surface to eliminate or prevent icing. Hybrid active/passive designs also exist.

Active anti-icing systems can be divided into running-wet and evaporative concepts. When applied on aircraft surface, the advantage of these IPSs is that no ice accumulates on the airfoil and no aerodynamic performance degradation due to ice occurs. In running-wet systems, the surface temperature should be higher than 3 – 4°C to prevent icing. In this condition, water solidification is inhibited, and all incoming water is kept in liquid state. A significant drawback is that the resulting water layer (i.e., runback water) flows downstream and can cause ice accumulation in non-protected area [23]. In evaporative systems, which are designed to prevent runback, temperatures around 100°C are required to evaporate all incoming water within the protected area [24], [25], [26]. These temperatures not only require a huge power availability but are close to the softening point of some epoxies and resins (although some thermosetting plastics are available for higher operating temperatures). The continuous operating temperature should be less than 50°C with the most commonly used polymeric materials.

In active de-icing systems, ice is allowed to accumulate and then is removed after a certain time with a periodic procedure. The advantage of these systems over anti-icing systems is that energy and power requirement is lower, but the drawback is that intercycle icing has to be accurately evaluated and performance degradation with intercycle icing has to be verified. Active de-icing systems can be thermal or mechanical. Thermal de-icing systems consist of heaters installed on the airfoil leading edge. Ice is allowed to build up for a period (intercycle ice) before the heater is turned on. Once the heater is on, the ice is shed off, and the heater is turned off again. The on-off cycle is controlled either by a de-icing timer or by the aircraft computer. This permits minimal use of electric power, as the requirement is for only enough heat to melt the thin layer of ice holding the mass of ice to the blade. Once the ice is loosened from the inside, the aerodynamic force removes the ice. For de-icing systems, however, ice identification must be fast to avoid aerodynamic losses. To lower energy consumption, the airfoil can be divided into separately controlled sections. Also, there can be significant performance degradations related to the intercycle ice [27]. The shed ice pieces can be a hazard for downstream aircraft components (e.g., engine inlets, propellers, antennae). For mechanical systems, a minimum ice layer thickness is required for shedding, and thin layers formed on the leading edge are harder to remove due to lower aerodynamic forces. It has been proposed [28] to combine a heated element on the leading edge with a mechanical system placed elsewhere.

In the past, several researchers have reviewed the various IPSs. Among them, in this section, active IPSs are classified into mechanical, thermal, or chemical systems, depending on the main principle used to detach or avoid ice formation. Mechanical systems can be divided into pneumatic systems, piezoelectric-based systems, and electromagnetic systems. Some non-conventional systems, e.g., based on shape memory alloys, can be considered mechanical systems as well. Thermal systems can be classified into electrothermal and hot air systems. Chemical IPSs can also be used to avoid in-flight icing. Some non-conventional methods based on microwave-sensitive materials can also be considered thermal systems. On the other hand, passive IPSs can be categorized as coatings and modified surfaces. Finally, semi-passive systems have been recently introduced.

A completely different problem is ground icing. Due to its peculiarities this subject has to be addressed in a separate section.

In summary, the existing IPS technologies for aircraft can be classified as follows:

- Active Systems
  - Mechanical – Pneumatic Boot, Electromechanical, Piezoelectric, Shape Memory Alloys
  - Thermal – Electrothermal, Hot Air, Microwave
  - Chemical
- Passive Systems
  - Coatings
  - Modified surfaces
- Semi-passive Systems
- Ground Icing

2.4.1 Active Systems

2.4.1.1 Mechanical Systems

The principle of mechanical IPS is to create surface deformation that would debond the ice from the surface. For most aircraft, mechanical IPSs can be divided into pneumatic, piezoelectric, electromagnetic, and non-conventional (e.g., Shape Memory Alloys).

For very small aircraft, the simplest mechanical system consists of manual scraping of ice while the aircraft is on the ground.

2.4.1.1.1 Pneumatic Boot Systems

Pneumatic boot systems [29] have been the standard de-icing method for piston engine aircraft since 1930s. These systems are still being used for modern propeller-driven small aircraft, in which more energy-demanding IPS (e.g., an electrothermal system) is not possible or recommendable. Moreover, pneumatic boots are largely used also for relatively large aircraft and on some specific aircraft components (e.g., air intakes, leading edge).

The boot surfaces remove ice accumulations mechanically by alternately inflating and deflating tubes within a boot that covers the surface to be protected. Inflation of the tubes under the accreted ice breaks the ice into particles and destroys the ice bonded to the surface. Aerodynamic forces and centrifugal forces on rotating airfoils then remove the ice.

This de-icing method is designed to remove ice after it has accumulated rather than to prevent its accretion on the surface, i.e., it cannot be used as an anti-icing device. Conventional pneumatic boots are constructed of fabric-reinforced synthetic rubber or other flexible material. The material is wrapped around and bonded to the leading edge surfaces to be de-iced on wings or empennage. Pneumatic boots are easily retrofitted, require little power, and are a lightweight system of reasonable cost.

The tubes in the pneumatic boot are usually oriented spanwise but may be oriented chordwise if dictated by a particular design (Figure 2-7).

In addition to the boots, the primary components of a pneumatic system are a regulated pressure source, a vacuum source, and an air distribution system. Miscellaneous components may include check and relief valves, air filters, control switches and timer, and electrical interfaces including fuses and circuit breakers. A regulated pressure source is required to ensure expansion of all tubes in the system to design limits and

within design rise times. If tube expansion is too slow, de-icing effectiveness is lessened. The vacuum source is essential to ensure positive deflation and keep the tubes collapsed during non-icing flight conditions to minimize the aerodynamic penalty.

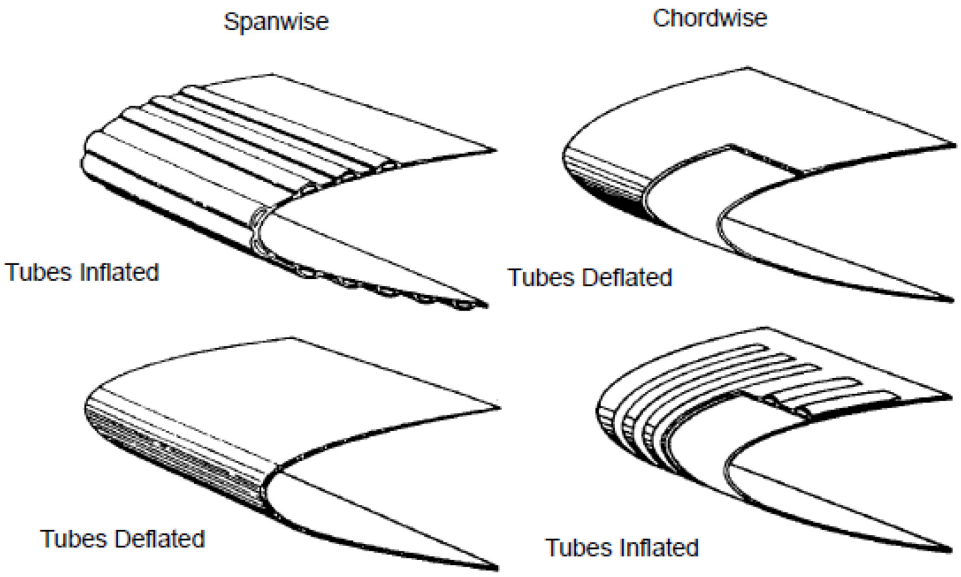

Figure 2-7: Examples of Pneumatic IPSs [30].

It is to be noted that this technology is not always effective, as accreted ice layers sometimes stay attached to the surface. Another drawback is that the leading edge is not smooth due to the pneumatic boots, thus increasing aerodynamic friction drag. The pneumatic IPS is not compatible with the laminar flow concept to improve aerodynamic performance.

2.4.1.1.2 Electromechanical Systems

Electromechanical de-icing systems use a mechanical force to accelerate the skin of a structure such that ice adhered to that structure is removed [31]. Accelerations are of a high rate with small amplitudes. This is called an impulse. The initial impulse results in a shock wave of sinusoidal decay giving several cyclical displacements of the surface.

Typically, actuators are installed underneath the skin of the structure (Figure 2-8). An electric current is applied to the actuator which is either of a solenoid type or a deformed coil type. These actuators will deform the surface at known amplitude in a known time and if correctly designed, will overcome the force of adhesion and expel ice from the surface.

One of the first reported electromechanical IPS is the Electro-Impulse De-icing (EIDI) system by NASA [32], [33]. It was tested in the laboratory, in the NASA Icing Research Tunnel, and in flight. EIDI was demonstrated to be an effective and practical IPS for small aircraft, turbojet engine inlets, elements of transport aircraft, and helicopter rotor blades. It could also be applied to nonmetallic surface materials.

The instantaneous power requirements for operating this type of system are typically too high to provide from the aircraft power distribution network directly to the actuator. However, the average power required is much lower considering the short solenoid operating time versus the relatively long cycle time between activation, i.e., milliseconds versus minutes. These two design constraints result in: a) the need to provide an energy storage bank to provide the peak power and b) the need to provide low average power to charge the

storage bank. The energy storage bank consists of an array of capacitors, each of which is capable of storing enough charge to power one actuator. The actuator operating sequence and regime is controlled by discharging the capacitor bank.

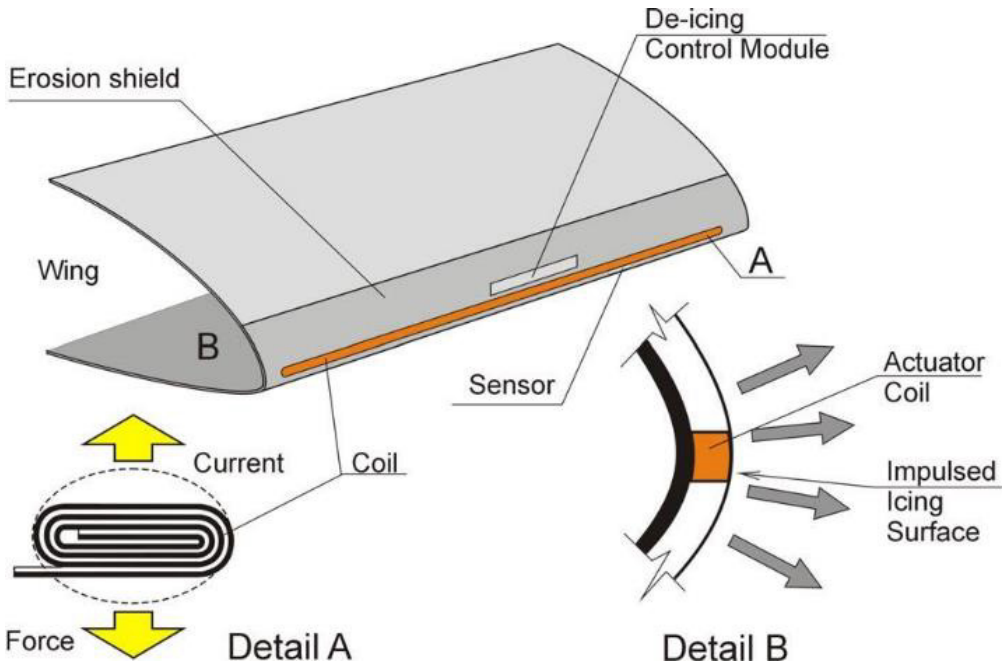

Figure 2-8: Typical Electromechanical Ice Protection System Configuration [31].

Several factors are critical to the effectiveness of a mechanical de-icing system:

- Surface structure skin mass.
- Surface structure skin stiffness.
- Ice type (rime, glaze, mixed) which is related to temperature.
- Ice thickness to be removed.

This system does have some limitations, however. When de-icing impulses are required a low current is supplied to the energy storage bank on light gauge wires and high currents from capacitors are fed to the actuators on larger gauge wires. The energy storage bank must be located close to the actuation system, otherwise the feed wire weight penalty is too high. The energy storage bank is also a very heavy item due to the weight of capacitors required to store the energy for the actuators. Moreover, electromagnetic and acoustic waves generated by these IPSs may interfere with other on-board instruments. Finally, aerodynamic skin stiffness requirements for large aircraft can be at odds with the lack of stiffness required to make electromechanical expulsive or impulsive de-icing practical.

There are several patents and commercial products based on this concept. For example, Innovative Dynamics Inc. (Ithaca, NY, USA) produced the Electric Pulse Ice Protection System (EPIPS) [34], which is an acceleration-based de-icer for ice protection on ships and aircraft (Figure 2-9).

This system provides an efficient low voltage and low power solution for both metal and composites where sufficient electrical power is not available. The de-icer features a series of eddy current actuator coils and electronics packaged into an integrated actuator assembly. Actuator coils are strategically placed behind the leading edge to apply impulsive loads directly to the outer surface material. The rapid acceleration de-bonds

and sheds ice into the airstream in a very efficient manner, removing ice layers as thin as 0.050". The system has a modular architecture whose main components are the de-icing control unit, the actuator electronic modules, and the leading edge assembly modules.

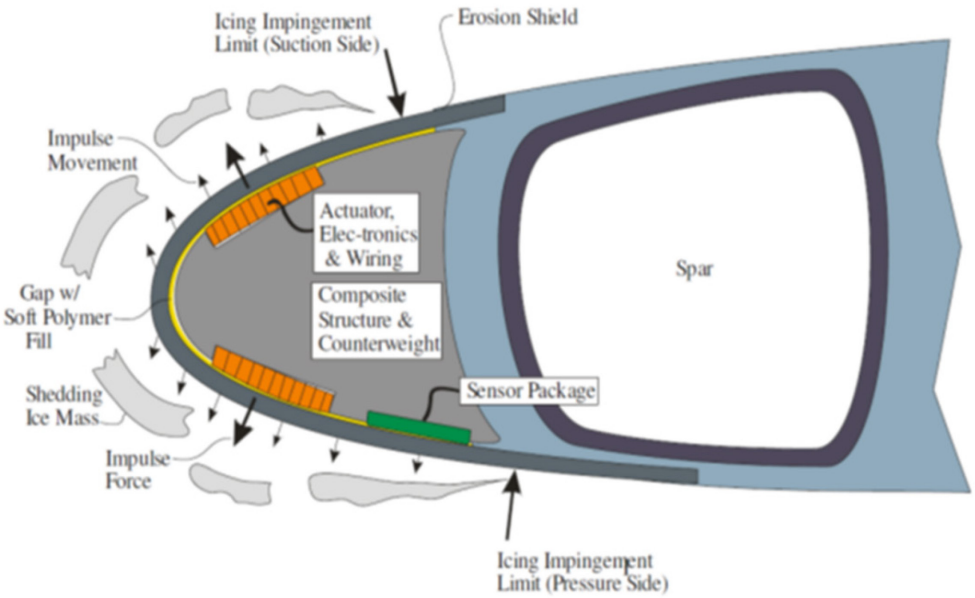

Figure 2-9: Schematic principle of the EPIPS by Innovative Dynamics Inc. [34].

Another type of electromechanical IPS is the electro-expulsive de-icing system as proposed by the US patent no. 6102333 – "Electromagnetic expulsion de-icing system" [35]. The described invention (Figure 2-10) uses electromagnetic actuators mounted within the airfoil, having low voltage and current requirements. Each actuator is made by conductive strips fabricated on a flexible dielectric sheet which is then rolled into a flattened elongated tube, thus creating coils.

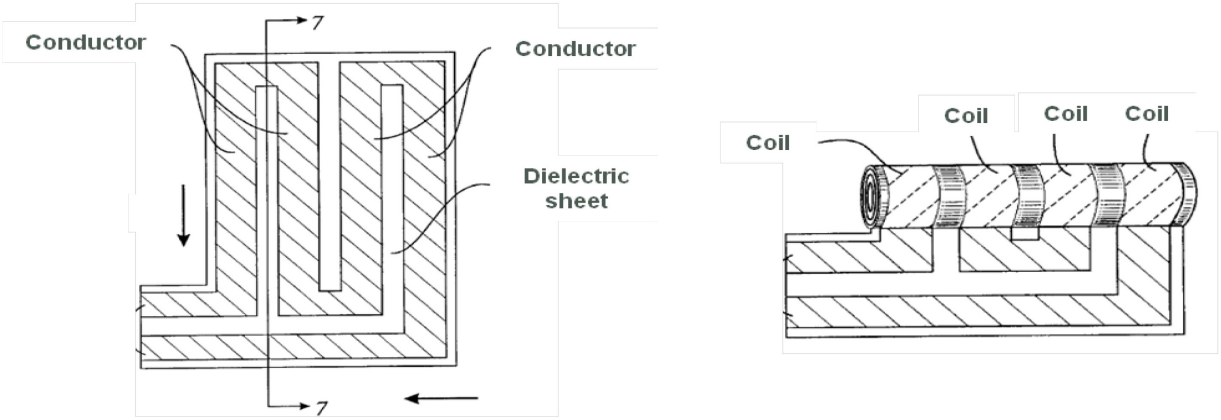

(a) (b)

Figure 2-10: (a) Pattern of Conductive Strips on a Dielectric Sheet Used to Fabricate the Electromagnetic Actuator; (b) Patterned Dielectric Sheet Rolled into a Flattened Elongated Tube [35].

The elongated tubes are then bonded within channels along the airfoil, beneath the ice-prone surface. When the system is actuated, current is discharged through the coils which results in a rapid expansion of it, changing from a flat shape to a more oval shape (Figure 2-11). This expansion exerts an impulsive force on the surface of the airfoil, thereby expelling ice accretions as thick as 12 mm.

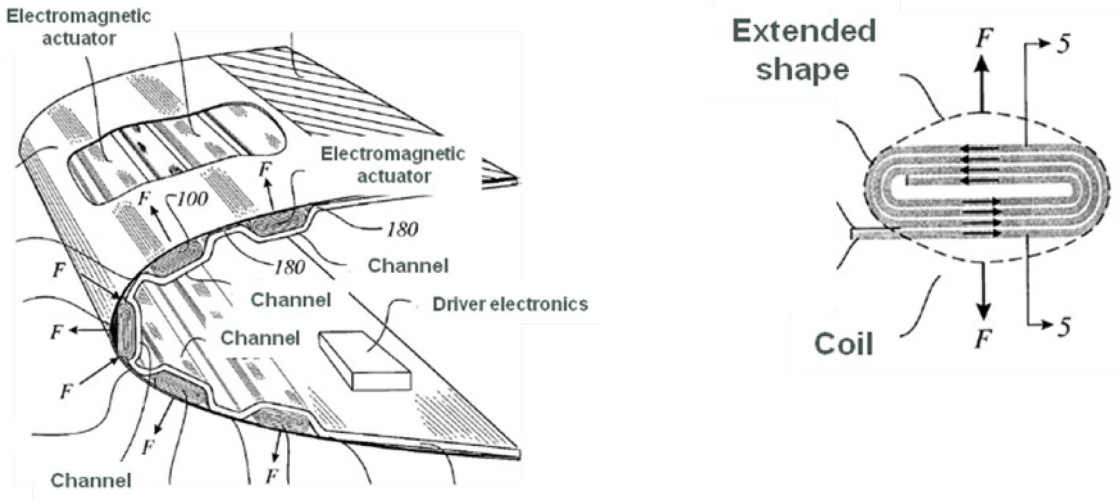

(a) (b)

Figure 2-11: (a) Perspective View Through a Cross Section of a Typical Airfoil Having an Electromagnetic Expulsion De-Icing System (b) Cross Sectional View of an Electromagnetic Actuator Showing the Extended Shape of the Coil [35].

A system based on this concept is the Electro-Mechanical Expulsion De-icing System (EMEDS) and is available on the market, produced by Cox & Company (Plainview, NY, USA). The EMEDS is the first ice protection technology to receive FAA certification in 50 years and is currently in-service on multiple commercial aircraft (FAA Part 23 and Part 25) and military aircraft. It is based on the US patent no. 6102333 described above. EMEDS comprises three main units: an electronic de-icing control unit for timing and system control, an energy storage bank to deliver high current electrical pulses, and a leading edge assembly, consisting of actuators mounted in an airfoil-shaped structure with a metal or composite erosion shield (Figure 2-12).

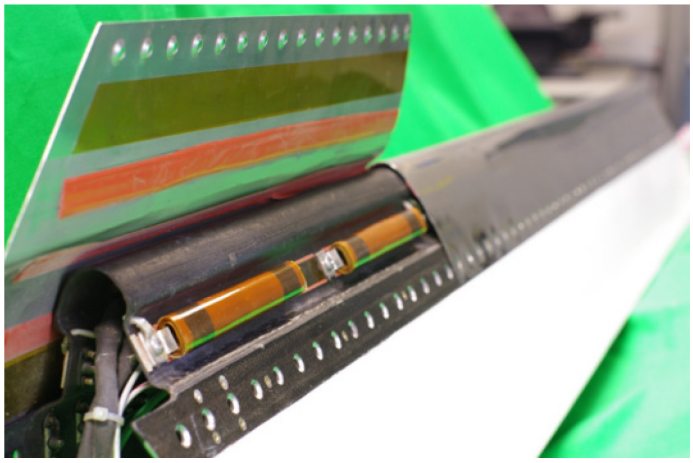

Figure 2-12: EMEDS Leading Edge Assembly Mounted on the Airfoil [36].

As reported in the patent, the system works by delivering a microsecond-duration, high current electrical pulse to the actuators which in turn generate opposing electromagnetic fields that cause the actuators to change shape rapidly. This change of the actuator shape is transmitted to the erosion shield of the leading edge assembly causing it to flex and vibrate at high frequencies. This rapid motion results in acceleration-based de-bonding of accumulated ice on the erosion shield. The system is available for both civil and military aircraft including Raytheon Premier I, Raytheon Hawker Horizon, HondaJet HA-420 and Boeing P-8A.

2.4.1.1.3 Piezoelectric Systems

Piezoelectricity is the physical phenomenon for which certain materials can convert mechanical energy to electrical energy and vice versa.

Active ice protection and detection systems for aircraft based on piezoelectric effect have been actively developed over the past few decades [37]. The main idea behind such de-icing systems is the use of piezoelectric actuator or transducer for creating mechanical vibrations in a structure (e.g., aircraft wing or engine nacelle) that has a risk of ice formation, creating a stress field in this structure. If such stress field is large enough at the interface of two materials (e.g., outer shell of the wing and layer of ice) it leads to a de-bonding of these two materials. In the example (Figure 2-13) the device is activated by applying a fast voltage pulse from the power supply to the terminals, which increases the strain of the piezoelectric layer. The strain causes the device to push forward away from the leading edge, thus detaching the accreted ice. The use of multiple thin layers allows decreasing the voltage needed to activate the active elements, thus reducing the size and weight of the power supply unit.

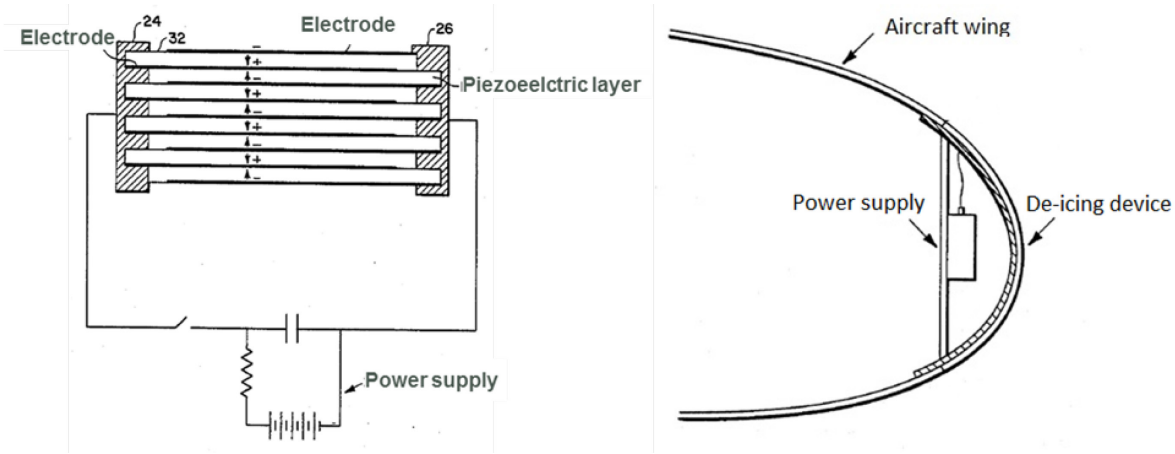

Figure 2-13: Schematic View of a Piezoelectric Device According to the US Patent 4545553 [38].

Piezoelectric IPSs can be classified based on:

- Principles of operation: Generation of either localized vibrations (repulsive) or ultrasonic shear waves (e.g., lamb waves) in the structure to be de-iced.
- Placement of active elements: Piezoelectric elements can be placed either inside or outside of aircraft structure or integrated into the structure. An example of piezoelectric IPS placed inside the aircraft structure has been reported by Endres et al. [30], who assessed the de-icing behavior of an IPS based on piezoceramic actuators beneath the leading edge.
- Type of active piezoelectric elements: Different types of piezoelectric elements can be used, including bulk piezoelectric materials, continue structure on the basis of active coatings, or thin laminates (e.g., tape cast materials).

Schulz et al. [39] reported an application of piezoelectric IPS on rotor blades. They used integrated piezoelectric actuators to twist the blade and achieve de-icing. This system was tested in the Adverse Environment Rotor Test Stand at the Pennsylvania State University and proved the capability to remove accreted ice with thickness ranging from 3 mm to 8 mm. Based on finite element simulations of the de-icing mechanism, the authors also proposed a new design for an active twist blade for the removal of even thinner ice layers (i.e., down to less than 2 mm thick).

The advantages of piezoelectric IPS over other electromechanical IPS include [30]:

- Less energy consumption.
- Smaller amplitude of generated vibrations, resulting in reduced electromagnetic and acoustic interference.
- Less structural fatigue.
- Reduced weight.

However, piezoelectric-based technologies are still not mature enough to be applied on large scale aircraft and require further research and optimization.

2.4.1.1.4 Shape Memory Alloys

Shape Memory Alloys (SMA) are materials with the unique property to change their shape and generate forces through a phase transformation when an appropriate amount of energy is provided to the material. This energy is typically applied by heating the SMA material. Transformation temperature between 100°C and -100°C are possible depending on SMA composition.

An IPS using SMA technology with a US patent (US patent no. 5686003 – Shape memory alloy de-icing technology [40]) was developed by Innovative Dynamics Inc. (Ithaca, NY, USA). This concept employs SMA materials to mechanically deform a surface and thereby removing ice [41]. In the reported invention, a thin sheet of SMA is mounted over the leading edge, with an electric heating layer and a pre-loaded polymer interposed in between (Figure 2-14). When actuated, the electric heating layer heats up the SMA so it returns to its stored shape. In particular, the SMA contracts and moves towards the airfoil, further compressing the polymer layer. Upon cooling, the pre-loaded polymer expands the SMA away from the airfoil to the initial shape. A pre-loaded polymer layer is needed since SMA cannot both expand and contract, so a way to re-strain the SMA material is required.

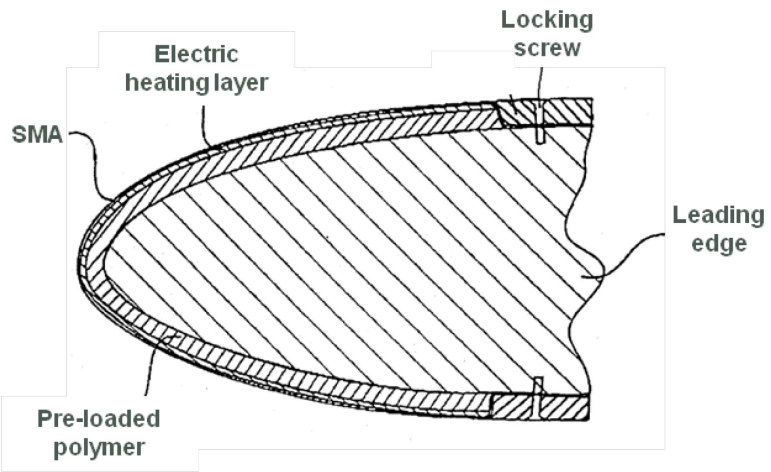

Figure 2-14: (Cross Section of the Leading Edge of an SMA-Based IPS [40].

As SMA is heated up it contracts, thus developing a shearing action between SMA layer and the ice, which is then peeled off (Figure 2-15).

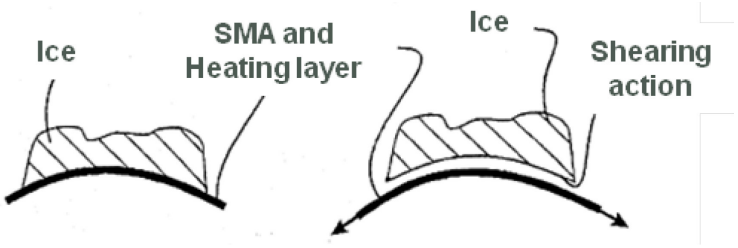

Figure 2-15: De-Icing Mechanism Performed Through the Shearing Action of the SMA when Heated Up.

2.4.1.2 Thermal Systems

Thermal systems are some of the most mature IPS, currently being applied in aircraft [31] and ships. Usually, they are divided into electrothermal and hot air systems. Electrothermal IPSs use thermal pads that are heated by using the Joule effect, while hot air systems use hot air, usually spilled from the engine. Moreover, it is also worth mentioning non-conventional thermal systems based on microwaves.

2.4.1.2.1 Electrothermal Systems

Electrothermal systems use resistive circuits buried in the airframe structure to generate heat when a current is applied [37]. Three configurations are possible:

- De-icing systems: periodically shed small ice build-ups by melting surface-ice interface with a high rate of heat input. When the adhesion at the interface becomes low enough, the aerodynamic forces (on wings and stabilizers) and/or the centrifugal forces (on propeller blades) remove the ice; sometimes, continuously heated parting strips are used to separate the ice accretion in several segments that can shed easier.
- Anti-icing systems: these systems prevent the ice from building up. There are two categories of anti-icing systems:
  - Running-wet systems: provide only enough heat (typically surface temperature ≥ 5°C) to prevent freezing on the heated surface. Beyond the heated surface of a running-wet system, water can freeze resulting in runback ice. Running-wet systems must be designed carefully so as not to permit build-up of runback ice in critical locations.
  - Evaporative anti-icing systems: supply sufficient heat (typically surface temperature ≥ 20°C) to evaporate all water droplets impinging upon the heated surface.

Anti-icing systems require more power than de-icing systems. Hence, anti-icing systems can achieve de-icing as well with less energy consumption. Different manufacturers have worked on developing anti-icing and de-icing systems by improving the materials and the layout of the systems developed in the first half of the 20th century.

Modern electrothermal IPS architectures are usually based on multilayered materials, with layer composition and thickness depending on the specific design. Their common operational principle in de-icing mode is shown in Figure 2-16. A parting strip (heater C) is always activated to break the continuity of the ice layer, while other heaters are activated periodically. These heating elements melt the ice layer and create a liquid water film, hence reducing ice adhesion to the surface. Once the adhesion force is lower than aerodynamic forces, the ice block is shed.

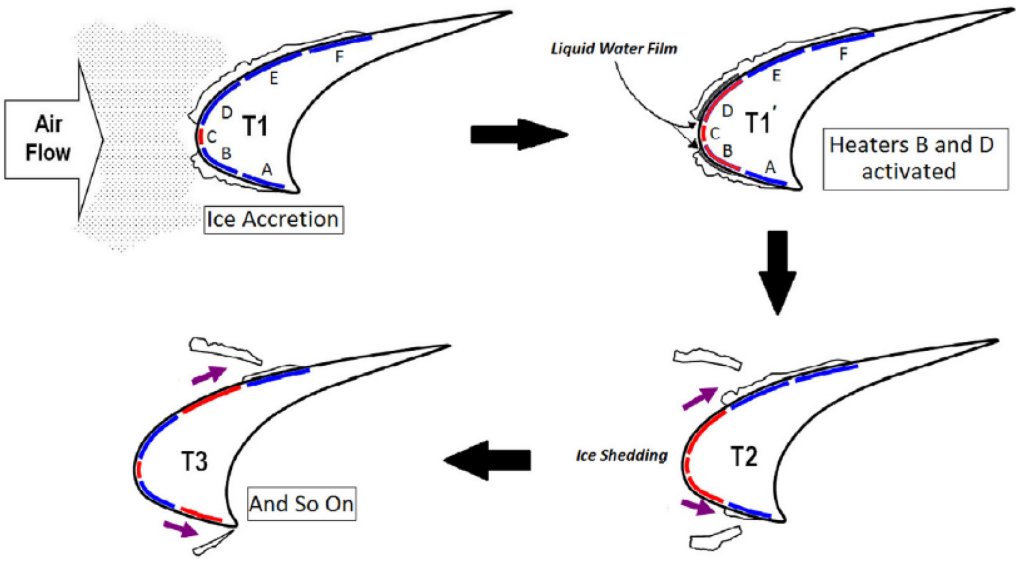

Figure 2-16: Illustration of an Electrothermal IPS Operating in De-Icing Mode [42].

ThermaWing™ developed by Kelly Aerospace Thermal Systems [43], [44] and Spraymat™ by GKN Aerospace [45] are examples of technologies using electrothermal elements for either de-icing or anti-icing mode. The ThermaWing™ is a heating layer attached to the leading edge of aerodynamic elements of small planes such as Cessna 350 and 400. Spraymat™ is a more complex technology using sprayed metals embedded inside airfoils. It has been used on helicopter blades and on the Boeing 787 Dreamliner wings with an integrated heating element that incorporates a sprayed metal conductive layer within the laminate stack at the leading edge.

The increasing use of polymeric composites instead of metals to reduce aircraft weight is not compatible with traditional electrothermal IPS due to the high temperatures that would induce melting. To address this problem, Mohseni and Amirfazli [46] developed an innovative electrothermal IPS that is compatible with fiberglass/epoxy composites. A manufacturing technique was developed to implement the electrothermal anti-icing system in the form of discrete constantan thermal elements with a specific pattern inside the composite airfoil. However, the reported IPS has not been applied yet to any known aircraft.

Recently, promising studies have focused on the development of more efficient electrothermal IPS, i.e., lighter systems with lower energy consumption and enhanced repairability. The replacement of traditional metallic resistive elements by lighter polymeric layers doped with resistive particles, or by graphite and carbon nanotube layers is currently investigated. These resistive materials can induce homogeneous surface heating through the Joule effect, leading to lower fuel consumption compared to ordinary electrothermal IPS. In this regard, different approaches to this type of materials are being developed by research institutions and enterprises. NASA spin-off Northcoast Technologies Ltd. (US) [47] developed a flexible and electrically conductive graphite foil as de-icing system. A research group at the Embry-Riddle Aeronautical University [48] implemented a flexible thermoelectric de-icing material based on conductive carbon fiber mesh embedded in glass fibers. Buschhorn et al. [49] from the Massachusetts Institute of Technology developed an array of piled-up carbon nanotubes films with a heat dissipation larger than 1kW/m^2 at -25°C, with potential application to IPS. Within the PANIPLAST project [12], [50], the French company, STILZ Chimie, started the development of highly conductive organic polymer *(poly)aniline*, with enhanced stability, flexibility, and safety. These polymers could be dispersed in different matrix like resins, paints, inks, or plastics to make these materials conductive. Deeper investigation in this field could help improve the efficiency of this type of IPS.

2.4.1.2.2 Hot Air Systems

Thermal systems used for the purpose of preventing the formation of ice or for de-icing airfoil leading edges usually use heated air ducted spanwise along the inside of the leading edge of the airfoil and distributed around its inner surface [51].

These thermal pneumatic anti-icing systems are used for wings, leading edge slats, horizontal and vertical stabilizers, engine inlets, and more. There are several sources of heated air, including hot air bled from the turbine compressor, engine exhaust heat exchangers, and ram air heated by a combustion heater.

Thermal wing anti-icing systems for business jet and large-transport category aircraft typically use hot air bled from the engine compressor. Relatively large amounts of hot air can be bled off the compressor, providing a satisfactory source of anti-icing heat. The hot air is routed through ducting, manifolds, and valves to components that need to be anti-iced.

The bleed air is routed to each wing leading edge by an ejector in each wing inboard area (Figure 2-17). The ejector discharges the bleed air into Piccolo tubes for distribution along the leading edge. Fresh ambient air is introduced into the wing leading edge by two flush-mounted ram air scoops in each wing leading edge, one at the wing root and one near the wingtip. The ejectors entrain ambient air, reduce the temperature of the bleed air, and increase the mass airflow in the Piccolo tubes. The wing leading edge is constructed of two skin layers separated by a narrow passageway. The air directed against the leading edge can only escape through the passageway, after which it is vented overboard through a vent in the bottom of the wingtip.

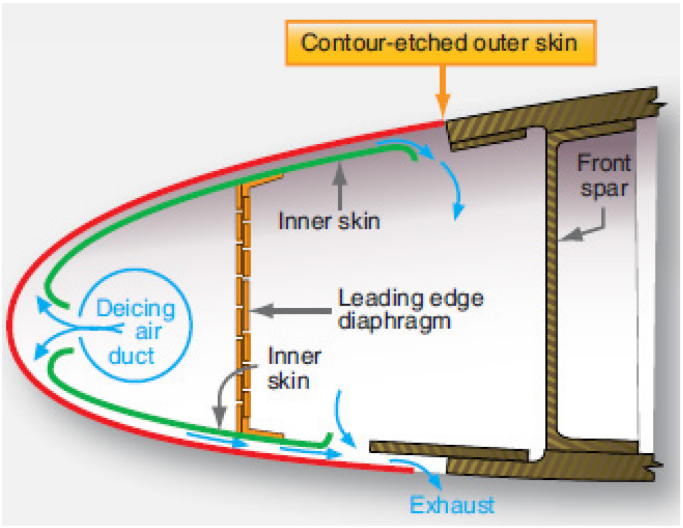

Figure 2-17: Typical Hot Air System [52].

2.4.1.2.3 Microwave Systems

The aforementioned thermal IPSs are characterized by a high energy consumption during the flight and slow ice melting due to the thermal diffusion of the heat in the wing material. Moreover, composites are increasingly used in aircraft to reduce the weight and, hence, the fuel consumption. However, these composite materials have a far worse thermal conductivity than metals, undergoing delamination in the case of using hot air systems. Microwaves can be a viable method to transmit thermal energy to the airfoil that has to be de-iced [53] and are compatible with fiber-reinforced composites, as described in a few US patents [54], [55], [56].

This family of IPS generally comprises microwave generators which transmit energy to the airfoil. If the airfoil is conductive, or it is covered with a microwave-absorbent material, the microwaves are absorbed and converted into thermal energy which thereby heats up the structure and performs de-icing.

2.4.1.3 Chemical Systems

Chemical systems can also be used for in-flight icing protection. In the so-called weeping wings system [31], antifreeze fluid is pumped from panels mounted on the leading edges of wings, horizontal and vertical stabilizers. The solution mixes with the supercooled water in the cloud, depresses its freezing point, and allows the mixture to flow off the aircraft without freezing.

The disadvantage of this system is that a reservoir containing the antifreeze fluid must be carried, and therefore usually these systems are applicable only for small general aviation aircraft.

2.4.2 Passive Systems

Recently, the search for passive IPSs has led to the fabrication of several icephobic surfaces. Attending to the different approaches and the expected properties of the new designed materials, icephobic materials could be defined as:

- Low-wetting materials: superhydrophobic materials exhibiting high water contact angles (above 150°) lead to smaller contact area and shorter contact time between impinging water droplets and the solid surface, thus maintaining a dry surface and reducing the probability of ice accretion [57].
- Materials delaying ice nucleation: if water droplets settle on the surface, the process of ice nucleation (especially heterogeneous nucleation) should be delayed as much as possible, at as low temperature as possible, to prevent ice formation [58].
- Materials with low ice adhesion: if ice accretes on the surface, the ice should be removed as easily as possible. Some authors [59] defined icephobic materials by an ice adhesion strength $\tau_{ice} < 100$ kPa (more than one order of magnitude smaller than that observed for metals like aluminum and steel), while others defined them by shear strength between 150 kPa and 500 kPa [60].

Ideally, icephobic surfaces should be designed to simultaneously meet these three design criteria in order to mitigate ice accretion most effectively and to promote ice shedding. In addition, for most practical purposes, the icephobic materials should exhibit a certain level of durability.

Compared to active IPSs, icephobic materials are appealing as they require neither input of energy to be effective nor activation from the crew. Thus, their application on aircraft would lead to reduced energy consumption, smaller environmental impact (related to reduced fuel consumption and use of chemicals) and simplification of aircraft design (in case heating elements become unnecessary) and flight operation.

2.4.2.1 Coatings

Several papers in the literature deal with the fabrication of icephobic coatings. Most of them demonstrate the icephobic properties of superhydrophobic surfaces, however, it is important to state that superhydrophobic surfaces are not necessarily icephobic [58], [59], [61].

Most of the icephobic coatings debated in the literature or found in the US Patent Collection Database follow two main design principles [37]: surface texturing at the micrometer and nanometer scale followed by a chemical functionalization and infusing low surface energy polymeric matrices with functional lubricants.

- **Textured and functionalized coatings.** Most of the coatings in this category are polymer-based. Compared to hard materials like ceramics and metals, they are cheaper and require milder processing conditions (e.g., low annealing temperatures). They also allow to adopt simple wet deposition techniques like spraying, dipping, or casting. Most of these coatings fall under two categories:
  - Fluoropolymers like polytetrafluoroethylene (PTFE) either in bulk or film form [62], fluorinated silicone rubber/polyurethane coatings [63], perfluoropolyether (PFPE), polyvinylidene fluoride (PVDF) [64]. They display the best superhydrophobicity and can reduce ice adhesion compared to bare aluminum if surface features are small enough (i.e., preventing mechanical interlocking of ice). One of their main drawbacks is the lack of durability, which can be partially enhanced by addition of dispersed nanoparticles [65]. Moreover, fluorinated polymers are potentially harmful to the environment and to human health [63], [66];
  - Viscoelastic polysiloxanes (i.e., silicones). These materials are interesting due to their ability to hinder hydrogen bonds between water and surface, which are one of the most relevant forces that regulate ice adhesion [67], [68]. In addition, their chemistry allows for the introduction of a wide range of functional groups, and the facile introduction of substructures in these coatings could have a tremendous impact on lowering the ice adhesion (i.e., ice adhesion strength down to 1 kPa for such "dry" chemically unmodified silicone-based coatings) [69]. However, these coatings have limitations related to their adhesion to the substrates (i.e., need for primers) and their resistance to abrasion and erosion. Again, the latter can be improved through addition of oxide nanoparticles [69], in addition to functional chemical groups that allow for autonomous self-healing [70], [71].

  Many other polymers have been textured to impart anti-icing properties, e.g., epoxy resins bearing silica nanoparticles [72].

  Textured coatings often suffer from a common problem: they can lose their repellency in humid environments due to condensation and frosting occurring between surface features, which also drastically increases ice adhesion. However, recent studies have made progress in mitigating condensation freezing by introducing local humidity sinks through sacrificial ice stripes on chemically functionalized microstructures [73], [74] and even bare macrotexture [75]. This has been reported to provide ice-free regions up to 96% of the surface, where potential ice build-up can fold over these regions without contact, significantly reducing the ice adhesion compared to the full-contact case. However, surface texturing (i.e., preferably high aspect ratio features) is required, which may limit use in applications like aircraft.

- **Liquid-infused materials.** This approach is more recent, as these materials were introduced in 2011 [76]. Since then, they have drawn huge interest due to their many potential applications, one of which is the fabrication of icephobic surfaces. More precisely, different infused materials have been suggested to achieve icephobicity:
  - Slippery Liquid-Infused Porous Surfaces (SLIPS), in which a nano-porous polymeric material is infiltrated with a low-freezing-point, fluorinated liquid/oil (Figure 2-18). The liquid is retained on the surface by the nanoscale structure, giving the surface a "slippery" nature that strongly hinders frost formation [77]. However, oil depletion is unavoidable and limits SLIPS durability;
  - Chemically modified polyurethane coatings that can induce the formation of a liquid water layer when their surface is covered by ice, due to the presence of hygroscopic groups [78], [79]. This liquid layer acting as lubricant causes great reduction in ice adhesion, as reported both in lab tests and in icing wind tunnel tests. However, the freezing suppression ceases once the polymer is over-saturated with water, which could occur rapidly during atmospheric precipitation of water, or when temperature is too low;

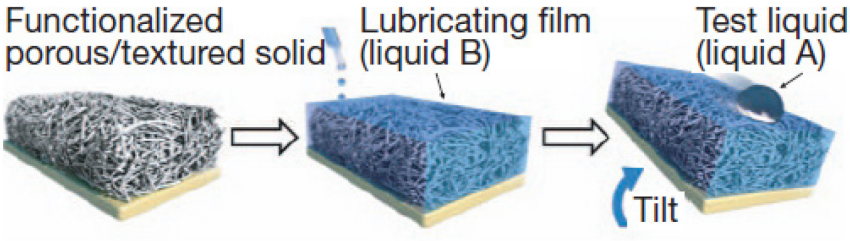

Figure 2-18: Schematics of the Fabrication of a SLIPS by Infiltrating a Functionalized Porous/Textured Solid with a Lubricant (Liquid B) to Form a Physically Smooth and Chemically Homogeneous Film on the Surface of the Substrate and Make it Repellent Towards the Test Liquid (Liquid A) [76].

- Liquid layer generator coatings which self-release lubricants whenever ice accretes on the surface, to form an interfacial liquid layer that dramatically reduces ice adhesion [80]. Recently, infusion of ethanol into a porous silicone framework has demonstrated excellent and durable icephobic properties at extremely low temperatures [81], i.e., down to -60°C, which is very appealing for operations in Arctic climates. Despite the improved longevity of liquid layer generators, compared with SLIPS for example, the liquid lubricant will eventually deplete and needs to be replenished to maintain the icephobic character of the coating;
- Coatings with controlled cross-linking density and interfacial lubricant. This very recent and promising approach is based on the synergistic anti-adhesion effects of low cross-link density polymers and lubricants that are miscible with the polymer network and allow the so-called interfacial slippage [82]. Tests have shown that these materials possess remarkable icephobic properties (i.e., ice adhesion smaller than 1 kPa) coupled with excellent durability under mechanical, thermal and chemical stresses. More recently, the same approach has been extended to a wide range of commonly used thermosets (e.g., polyurethane) and thermoplastics (e.g., polyvinylchloride, polystyrene) [83].

In addition to the aforementioned approaches to icephobic surfaces (i.e., textured coatings and liquid-infused materials), a new family of materials has been recently proposed by Golovin et al. [84]. The so-called Low-Interfacial Toughness (LIT) materials have been developed to overcome the intrinsic limitations of regular icephobic surfaces, which are based on the concept of lowering ice adhesion, defined as $\tau = F/A$ (F is the adhesion force and A is the interfacial area between the ice layer and the solid surface). This implies that, to overcome ice adhesion and shed ice from a large surface like an aircraft wing or a hull, prohibitively high forces are necessary. On the other hand, LIT materials are designed to possess low toughness ($\Gamma < 1$ J/m^2) and to require constant low-force values to shed ice, irrespective of the surface area. Thus, when LIT-coated large surfaces are covered by an ice layer, small forces can shed ice, like weak mechanical stresses or even simple gravity. Moreover, LIT coatings are obtained from cheap materials, like common polymers (e.g., polyvinylchloride, polystyrene, silicone) with plasticizers. For these reasons, LIT coatings seem to be promising candidates for application on aircraft and ship surfaces. The aforementioned paper reports exciting de-icing properties for LIT-coated surfaces on which ice was accreted statically (e.g., in a freezer, on a Peltier plate, outdoor). Further tests need to confirm whether this technology can also be useful in the icing conditions encountered by an airplane or a ship.

2.4.2.2 Modified Surfaces

In order to avoid the problem of coating adhesion, direct modification of surface topography, followed by surface chemistry functionalization, is a viable option.

For aluminum surfaces, which are extremely common in aircraft and sea vessels, anodization is a common process to hinder corrosion. When finely tuned, the same processes can be used to obtain peculiar surface morphologies with superhydrophobic and potential icephobic behavior [85]. However, little to no evidence of such properties has been demonstrated.

Laser texturing is much more versatile as it can be applied to virtually any material to create microscale features with excellent precision and repeatability. Some papers [86] report the texturing of different metals, some of which bearing additional diamond-like carbon coatings, with potential icephobic properties [87]. However, actual testing of such properties is still lacking. Moreover, application of these texturing techniques to large scale surfaces seems difficult due to their low throughput.

2.4.3 Semi-Passive Systems

Recently, researchers have been looking into semi-passive solutions for improved icephobicity to overcome some of the challenges associated with fully passive systems. Semi-passive systems are coatings with an embedded active component that requires some sort of energy input to function, which is crucial to maintain anti-icing performance. This active component is an intrinsic part of the coating, and is thus not connected to any external system, as opposed to hybrid active-passive systems (e.g., electrothermal elements embedded in a passive coating). There are several different kinds of semi-passive coatings reported in the literature; the main ones involve:

- Antifreeze-release coatings, e.g., in which a porous superhydrophobic layer with wicking channels is filled with antifreeze agent to be released in response to surface icing [88]. These coatings demonstrated excellent icephobic performance in different icing conditions (freezing fog, freezing rain, condensation frosting). This approach has led to the development of NuSil® coatings, as of today the most effective commercial icephobic treatments. Ionogels, i.e., hydrophilic gels infused with self-releasable ionic liquids, are other kinds of antifreeze coatings which have proven useful for anti-icing by effectively inhibiting both ice nucleation (both heterogeneous and homogeneous) and growth in cold humid environments [89]. However, these materials suffer from antifreeze liquid losses that limits their effectiveness in time;
- Magnetically active coatings where magnetic nanoparticles are embedded into a polymer matrix [90]. Upon application of an alternating magnetic field, the nanoparticles dissipate heat which can be used to prevent ice nucleation and promote de-icing by the generation of an interfacial liquid layer. Moreover, the incorporation of nanoparticles into the polymer can also create the surface topography required for superhydrophobicity. However, this magnetothermal effect will always require application of an alternating magnetic field which may limit the use in some applications;
- Magnetic slippery surfaces, in which an oil-based ferrofluid, applied to any substrate without any need for pre-structuring, responds to a magnetic field by excluding water droplets from the underlying substrate [91]. Such systems showed a significant delay in ice nucleation rate (down to -34°C), and enhanced droplet mobility leading to an immense reduction in ice adhesion down to 2 Pa (i.e., 2 – 3 orders of magnitude smaller than that of other state-of-the-art surfaces). Despite the fact that these ferrofluid surfaces were proven to be very stable under external shear gas flow, the constant need for a gradient magnetic field to maintain icephobic function, and to keep the ferrofluid in place on the substrate, renders their use impractical in most applications;
- Polymeric coatings with incorporated hydrophilic salts, in which dissolved ions inhibits ice nucleation upon contact with water and promotes the formation of a liquid water layer at the interface between the polymer and accreted ice [92]. Although these coatings show a great potential in anti-icing, durability is also here a major concern as the salt will deplete with time;

- Photothermal traps, which are coatings that utilize heat converted from solar illumination to mitigate ice [93]. Effective thermal traps consist of a selective light absorber, a thermal spreader, and an insulating bottom layer to assure effective lateral heat transfer from illuminated regions to the accreted ice Figure 2-19. A rapid temperature increase as high as 33°C upon illumination was reported. However, these coatings are dependent on sunlight in order to function optimally.

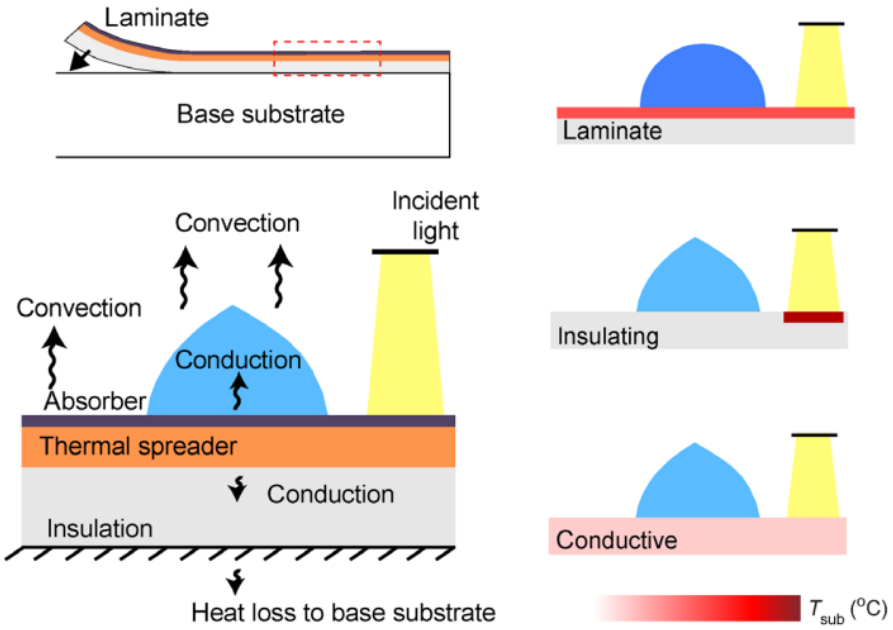

Figure 2-19: Working Principle of Photothermal Traps. A three-layer laminate coating effectively absorbs the light and directs the generated heat towards the accreted ice with minimal heat loss to the surroundings, thus causing rapid melting. Adapted from [93].

2.4.4 Ground Icing

Ice can accumulate even when the aircraft is on the ground. In this case, ice will accumulate not on the leading edge, but on all the aircraft upper surface, due to snow precipitation, or water freezing caused by low temperature.

In that case the strategy is to spray fluids on the aircraft (Figure 2-20. Fluids used to de-ice aircraft on the ground will melt the ice (freezing-depressant fluids mixed with hot water are often used) and/or protect the surface from further ice accumulation.

These fluids must remain on the aircraft surface when the aircraft is not moving, but they have to flow off the surface to maintain the wing clean during takeoff. For this reason, usually non-Newtonian fluids are used so that once shear stress caused by air flow acceleration over the wing surface increases, the fluid viscosity decreases, and the fluids fly off the surface. The most relevant characteristics of these fluids are their viscosity (which affects their capability to fly off the surface before takeoff) and duration on the surface (defined as hold-over time, which is the time for which the fluid is effective to protect the aircraft) [94].

The primary ice protection fluids currently in use consist of ethylene glycol, propylene glycol, or diethylene glycol as the freezing point depressant (approximately 88%), water (10 – 11 %), and numerous proprietary additives (1 – 2 %). De-icers designed to remove ice and snow from aircraft surfaces are referred to as Type I fluids. These fluids are typically diluted with water and heated prior to application. Anti-icers, referred to as Type II and Type IV fluids, are more viscous formulations designed to provide initial de-icing and residual

anti-icing protection on aircraft during pre-flight activities and takeoff. Type II and IV fluids are applied directly without dilution. Dispersion of ice protection fluids in the environment has been proven and causes concern for the toxicity to humans and nature [95], [96].

Figure 2-20: Application of De-Icers on an Aircraft [96].

2.5 TYPES AND CLASSIFICATION OF EXISTING TECHNOLOGIES FOR SEA VESSELS

Many of the IPS listed in Section 2.4 can also be considered for use on marine vessels. There is commonality in many systems such as those protecting sensors and windscreens/windows. For marine vessels, the prevention of excessive ice accretion, which may impact the safety of the work environment and the stability of the vessel, is the focus rather than the impact on aerodynamics. As the weight of IPSs is less of a concern for marine vessels, different techniques can be considered for use. Passive IPSs like covers and coatings are preferred as their effectiveness is not dependent on power or other services from the vessel [22].

2.5.1 Covers

The use of covers on external equipment or fittings is a passive ice protection technique that is used extensively on marine vessels [21], [22]. These can either be hard or flexible covers (generally water-resistant materials) that provide a barrier to ice formation which can easily be removed when access is required.

2.5.2 Coatings

Icephobic coatings developed for marine applications follow an almost identical approach to those used in aviation. The LIT coatings described in Section 2.4.2.1 are of particular interest to marine vessels as ice is often removed manually by crew members using mallets or other impact tools. Reducing the amount of force required to remove ice from a surface has an appreciable benefit to the vessel's crew allowing for faster ice removal and a reduction in fatigue.

Liquid-infused materials could be beneficial for marine vessels if the ice inhibiting liquid remains active for any expected period of operation in icing conditions, and the ice inhibiting liquid can be easily replenished, or the coating easily reapplied.

2.5.3 Thermal Systems

Ice prevention for critical systems and areas of operation on the external portions of a vessel can be achieved by the piped distribution of heated fluids (water) or gases (air or steam). Care must be taken in the case of fluids to ensure that the heat input is sufficient to maintain the fluid in a liquid state throughout the piping network in order to prevent blockages [22].

2.5.4 Electrothermal Systems

Electrothermal de-icing systems are required to be incorporated into critical viewing windows on a marine vessel such as those located on the bridge [21]. These heating systems are used in conjunction with wiper blades to ensure the window surface remains free of ice.

2.6 CONCLUSIONS AND PERSPECTIVES

In this chapter the current state of ice protection technologies has been reviewed. The most common technologies have been described and their advantages and shortcomings highlighted.

At present, only active IPSs are applied on aircraft and sea vessels. Some of them (pneumatic boots, electromechanical, thermal and chemical systems) are mature, reliable, and widely used. Innovative active technologies like piezoelectric [46] and microwave [53] IPS aim to improve efficiency and reduce weights, which is particularly relevant for UAVs. Even though UAVs do not have passengers, and therefore safety issues are less important than for manned aircraft, often to be effective in all-weather conditions flight clearance is required. Most UAVs may not have enough available power to effectively deal with icing problems, but it is still desirable to have some automatic procedures or systems (e.g., ice detectors) that can identify critical icing conditions and activate IPS to reduce or prevent the risk. Further research is needed, however, to develop commercial products that can be used for UAVs with available power.

The increasing need for energy-efficient and environmentally friendly solutions fosters the interest towards passive technologies. Today, no commercially available icephobic coating seems to satisfy the needs of the aviation industry, especially in terms of duration of the icephobic effect and adhesion to aircraft materials (e.g., aluminum, carbon fiber- and glass fiber-reinforced polymers, metal-composite laminates). Nevertheless, the scientific community continues investigating these passive systems, as in the recent Horizon2020 European project PHOBIC2ICE [13]. Under the NATO AVT-332 – In-Flight Demonstration of Icephobic Coating and Ice Detection Sensor Technologies activities, a flight testing is planned during 2020 – 2021 wintertime to comparatively evaluate the effectiveness of 27 icephobic coating materials developed in six NATO countries (CAN, DEU, ESP, FIN, ITA, USA). These materials will be provided by the 10 developers, which include research institutes and private enterprises. The C-212 test plane will be provided by the Instituto Nacional de Técnica Aeroespacial (INTA, Spain) and will carry the samples in natural icing conditions. Embedded cameras will record the icing events on the specimens, while different probes will determine the actual metereological conditions. A separate NATO Unclassified report will be published after the completion of flight testing and data collection by the end of 2021.

However, presumably passive IPS alone cannot solve all icing-related problems, especially for aircraft in extremely severe operational conditions [97] causing ice to accrete irrespective of surface properties. Therefore, hybrid systems combining different technologies (i.e., incorporating both active and passive IPSs) have been increasingly investigated as complete ice protection solutions. Hopefully thermal or mechanical systems may be combined with icephobic coatings to provide the desired de-icing operation [98]. This way, the energy needed to operate the active system would be greatly reduced due to the presence of the coating [99]. For example, Antonini et al. [100] demonstrated that, by depositing a coating on the leading edge, the energy consumption of an electrothermal IPS can be reduced by as much as 80%. However, testing conditions were not representative of the real icing conditions encountered by airplanes, therefore further

testing is necessary. Additional research is also needed on hybrid IPS combining piezoelectric actuators and icephobic coatings, which have shown promising results as reported by Strobl et al. [101] and Pommier-Budinger et al. [102].

2.7 REFERENCES

[1] Federal Aviation Administration, "Airplane and engine certification requirements in supercooled large drop, mixed phase, and ice crystal icing conditions," 79(213), pp. 65508-65540, 2014.

[2] European Aviation Safety Agency, "Explanatory note to decision 2014 / 001 / R amendment 12 to AMC-20," 1, pp. 1-9, October 2004.

[3] Bowden, D.T., Gensemer, A.E., and Skeen, C.A., "Engineering summary of airframe icing technical data", General Dynamics San Diego CA Convair Div., 1963.

[4] Hann, R., and Johansen, T.A., "Unsettled topics in UAV icing", SAE EDGE Research report, 2020.

[5] European Commission, Cordis Research Results, "Erosion and Ice Resistant cOmposite for Severe operating conditions," https://cordis.europa.eu/project/id/685842 (accessed 12 Dec 20205).

[6] Aimplas, "Completion of the project HELADA", 07 February 2018. https://www.aimplas.net/blog/completion-of-the-project-helada/

[7] University of Nottingham, "GAINS – Green Airframe Icing Novel Systems", https://www.nottingham.ac.uk/aerospace/projects/cleansky/gains-project.aspx (accessed 12 Dec 20205).

[8] European Commission, Cordis Research Results, "IEfficient, Modular and LigthWeight Electromagnetic Induction Based Ice Protection System https://cordis.europa.eu/project/id/717175/reporting (accessed 12 Dec 20205).

[9] European Commission, Cordis Research Results, "JEDI ACE Project – Japanese-European de-icing aircraft collaborative exploration", 30 April 2016. https://cordis.europa.eu/project/id/314335

[10] Universidat Publica de Navarra, "Primeros pasos del proyecto de investigación MAI-TAI", 20 February 2020. http://www.unavarra.es/en/sites/actualidad/contents/noticias/2020/02/20-02-20/primeros-pasos-del-proyecto-de-i.html

[11] Horizon 2020 European Union Funding for Research and Innovation, "NO-ICE ROTOR – A greener way to protect aircraft from icing", Clean Sky 2, 2018. https://www.cleansky.eu/no-ice-rotor-a-greener-way-to-protect-aircraft-from-icing

[12] European Commission, Cordis Research Results, "Industrial Development of PANIPLAST Process Poly(aniline) Conductive Polymers – PANIPLAST Project", 1 August 2014 – 31 January 2016. https://cordis.europa.eu/project/id/683373

[13] European Commission, Cordis Research Results, "Super-IcePhobic Surfaces to Prevent Ice Formation on Aircraft", https://cordis.europa.eu/project/id/690819 (accessed 12 Dec 20205).

[14] European Commission, "STORM – Efficient ice protection Systems and simulation techniques of ice release on propulsive systems", October 2013 – March 2017. https://trimis.ec.europa.eu/project/efficient-ice-protection-systems-and-simulation-techniques-ice-release-propulsive-systems

[15] American Bureau of Shipping, “Guide for vessels operating in low temperature environments”, Houston, TX, USA, 2015.

[16] Martin, B.J., Howard, C.J., and Hollis, M.J., “Evaluation of icephobic coatings”, Defence Technology Agency, 2011.

[17] European Aviation Safety Agency, EASA Regulations, https://www.easa.europa.eu/regulations (accessed 12 Dec 20205).

[18] Federal Aviation Administration, eCFR — Code of Federal Regulations, https://www.ecfr.gov/cgi-bin/text-idx?tpl=/ecfrbrowse/Title14/14tab_02.tpl (accessed 12 Dec 20205).

[19] Jeck, R.K., “Icing design envelopes (14 CFR Parts 25 and 29, Appendix C) converted to a distance-based format”, DOT/FAA/AR-00/30, Federal Aviation Administration, Washington, DC, USA, April 2002.

[20] Federal Aviation Administration, “CFR-25 appendix O supercooled large drop icing conditions”, https://www.ecfr.gov/cgi-bin/text-idx?SID=e5539cde6b5841dfadd44ccfcb39806f&mc=true&node=ap14.1.25.0000_0nbspnbspnbsp.o&rgn=div9 (accessed 12 Dec 20205).

[21] Lloyd’s Register, “Rules for the winterisation of ships”, 2020.

[22] DNV-GL, “Offshore guidelines: winterization for cold climate operations (DNVGL-OS-A201)”, 2019.

[23] Mangini, D., Antonini, C., Marengo, M., and Amirfazli, A., “Runback ice formation mechanism on hydrophilic and superhydrophobic surfaces”, Cold Regions Science and Technology, vol. 109, pp. 53-60, 2015. doi: 10.1016/j.coldregions.2014.09.012

[24] de Rosa, F. and Esposito, A., “Electrically heated composite leading edges for aircraft anti-icing applications”, Fluid Dynamics & Materials Processing, 8(1), pp. 107-128, 2011. doi: 10.3970/fdmp.2011.008.107

[25] Bendarkar, M.V., Chakraborty, I., Garcia, E., and Mavris, D.N., “Rapid assessment of power requirements and optimization of thermal ice protection systems”, in 2018 Aviation Technology, Integration, and Operations Conference, Atlanta, GA, USA, 2018, p. 4136. doi: 10.2514/6.2018-4136

[26] Meier, O. and Scholz, D., “A Handbook method for the estimation of power requirements for electrical de-icing systems”, in Deutscher Luft- und Raumfahrtkongress DLRK, Hamburg, Germany, 2010, p. 31.

[27] Broeren, A.P., Bragg, M.B., and Addy Jr, H.E., “Effect of intercycle ice accretions on airfoil performance,” Journal of Aircraft, 41(1), pp. 165-174, 2004. doi: 10.2514/1.1683

[28] Al-Khalil, K.M., Ferguson, T.F.W., and Phillips, D.M., “Hybrid ice-protection system for use on roughness-sensitive airfoils”, US Patent 5,921,502, 1999.

[29] Heinrich, A., Ross, R., Zumwalt, G., Provorse, J., Padmanabhan, V., Thompson, J., and Riley, J., Aircraft Icing Handbook, Volume 1 of 3, Federal Aviation Administration, 1991.

[30] Endres, M., Sommerwerk, H., Mendig, C., Sinapius, M., and Horst, P., “Experimental study of two electro-mechanical de-icing systems applied on a wing section tested in an icing wind tunnel”, CEAS Aeronautical Journal, 8(3), pp. 429-439, 2017. doi: 10.1007/s13272-017-0249-0

[31] Goraj, Z., "An overview of the deicing and antiicing technologies with prospects for the future", in 24th International Congress of the Aeronautical Sciences, Yokohama, Japan, 2004, pp. 1-11.

[32] Zumwalt, G.W., Schrag, R.L., Bernhart, W.D., and Friedberg, R.A., "Analysis and tests for design of an electro-impulse de-icing system", NASA Contract Report 174919, 1985.

[33] Zumwalt, G.W., Schrag, R.L., Bernhart, W.D., and Friedberg, R.A., "Electro-impulse de-icing testing analysis and design", NASA Contract Report 4175, 1988.

[34] Icesight.com, "Electric Pulse Ice Protection System EPIPS", https://www.icesight.com/electric-pulse-ice-protection-system.php (accessed 12 Dec 20205).

[35] Gerardi, J.J. and Ingram, R.B., "Electro-magnetic expulsion de-icing system", US Patent 6,102,333, 2000.

[36] Cox & Company, "Electro-Mechanical Expulsion Deicing System (EMEDS)", https://www.coxandco.com/low_power_ips.html (accessed 12 Dec 20205).

[37] Huang, X., Tepylo, N., Pommier-Budinger, V., Budinger, M., Bonaccurso, E., Villedieu, P., Bennani, L., "A survey of icephobic coatings and their potential use in a hybrid coating/active ice protection system for aerospace applications", Progress in Aerospace Sciences, vol. 105, pp. 74-97, 2019. doi: 10.1016/j.paerosci.2019.01.002

[38] Finke, R.C. and Banks, B.A., "Piezoelectric deicing device", US Patent 4,545,553 A, 1984.

[39] Schulz, M., Riemenschneider, J., and Palacios, J., "Investigation of active twist rotor for blade de-icing", in Annual Forum Proceedings – AHS International, Phoenix, AZ, USA, 3, pp. 1195-2005, 2013.

[40] Ingram, R.B. and Gerardi, J.J., "Shape memory alloy de-icing technology", US Patent 5,686,003 A, 1994.

[41] Gerardi, J.J., Ingram, R.B., and Catarella, R.A., "A Shape memory alloy based de-icing system for aircraft", in 33rd Aerospace Sciences Meeting and Exhibit, 1995, pp. 1-8. doi: 10.2514/6.1995-454

[42] Federal Aviation Administration, "Ice and rain protection", Aviation Maintenance Technician Handbook – Airframe, pp. 1-32, 2012.

[43] "Thermawing", 24 September 2020. https://en.wikipedia.org/wiki/Thermawing

[44] AviationPros, "ThermaWing aircraft deicing system from Kelly aerospace thermal systems", 20 January 2012. https://www.aviationpros.com/engines-components/aircraft-airframe-accessories/ice-protection/product/10616772/kelly-aerospace-thermal-systems-thermawing-aircraft-deicing-system

[45] GKN Aerospace Services Ltd., "SPRAYMAT trademark", 16 April 2016. https://trademarks.justia.com/721/98/spraymat-72198761.html (accessed 12 Dec 20205).

[46] Mohseni, M. and Amirfazli, A., "A novel electro-thermal anti-icing system for fiber-reinforced polymer composite airfoils", Cold Regions Science and Technology, 87, pp. 47-58, 2013. doi: 10.1016/j.coldregions.2012.12.003

[47] Rutherford, R.B. and Dudman, R.L., "Aircraft de-icing system", US Patent 6,330,986 B1, 2001.

[48] Park, M.S., Aircraft De-Icing System Using Thermal Conductive Fibers, M.Sc. Thesis, Embry-Riddle Aeronautic University, Daytona Beach, FL, USA, 2015.

[49] Buschhorn, S.T., Lachman, N., Gavin, J., Wardle, B.L., Kessler, S.S., and Thomas, G., "Electrothermal icing protection of aerosurfaces using conductive polymer nanocomposites", in 54th AIAA/ASME /ASCE/AHS/ASC Structures, Structural Dynamics, and Materials Conference, Boston, MA, USA, 2013. doi: 10.2514/6.2013-1729

[50] European Commission, "From wings to walls: EU funded project turns on a new era in heating", 16 Feb 20212. https://ec.europa.eu/newsroom/horizon2020/items/54842/en (accessed 12 Dec 20205).

[51] Papadakis, M., Wong, S.H., Yeong, H.W., Wong, S.C., and Vu, G.T., "Icing tests of a wing model with a hot-air ice protection system", in AIAA Atmospheric and Space Environments Conference, Toronto, ON, Canada, 2010, p. 7833. doi: 10.2514/6.2010-7833

[52] Stull, R., ATSC 113 – Weather for Sailing, Flying & Snow Sports, "Aircraft icing", University of British Columbia, May 2020. https://www.eoas.ubc.ca/courses/atsc113/flying/met_concepts/03-met_concepts/03g-Icing/index.html

[53] Feher, L. and Thumm, M., "Design of avionic microwave de-/anti-icing systems", in Advances in Microwave and Radio Frequency Processing, Berlin, Heidelberg: Springer Berlin Heidelberg, 2006, pp. 695-702.

[54] Feher, L. and Schnack, M., "Microwave de-icing system for aircraft", US Patent 6,207,940, 2001.

[55] Feher, L., "Compact microwave system for de-icing and for preventing icing of the outer surfaces of hollow or shell structures which are exposed to meteorological influences", US Patent 6,610,969 B2, 2003.

[56] McCollough, J. M. and Aubert, R., "Rotor blade de-icing system", US Patent 9,056,684 B2, 2015.

[57] Farhadi, S., Farzaneh, M., and Kulinich, S.A., "Anti-icing performance of superhydrophobic surfaces", Applied Surface Science, 257(14), pp. 6264-6269, 2011. doi: 10.1016/j.apsusc.2011.02.057

[58] Jung, S., Dorrestijn, M., Raps, D., Das, A., Megaridis, C.M., and Poulikakos, D., "Are superhydrophobic surfaces best for icephobicity?", Langmuir, 27(6), pp. 3059-3066, 2011.

[59] Hejazi, V., Sobolev, K., and Nosonovsky, M., "From superhydrophobicity to icephobicity: forces and interaction analysis", Scientific Reports, 3, p. 2194, 2013. doi: 10.1038/srep02194

[60] Menini, R. and Farzaneh, M., "Elaboration of Al2O3/PTFE Icephobic coatings for protecting aluminum surfaces", Surface and Coatings Technology, 203(14), pp. 1941-1946, 2009. doi: 10.1016/j.surfcoat.2009.01.030

[61] Nosonovsky, M. and Hejazi, V., "Why superhydrophobic surfaces are not always icephobic", ACS Nano, 6(10), pp. 8488-8491, 2012. doi: 10.1021/nn302138r

[62] Yang, S., Xia, Q., Zhu, L., Xue, J., Wang, Q., and Chen, Q.M., "Research on the icephobic properties of fluoropolymer-based materials", Applied Surface Science, 257(11), pp. 4956-4962, 2011. doi: 10.1016/j.apsusc.2011.01.003

[63] Susoff, M., Siegmann, K., Pfaffenroth, C., and Hirayama, M., "Evaluation of Icephobic Coatings – Screening of Different Coatings and Influence of Roughness", Applied Surface Science, vol. 282, pp. 870-879, 2013. doi: 10.1016/j.apsusc.2013.06.073

[64] Peng, C., Xing, S., Yuan, Z., Xiao, J., Wang, C., and Zeng, J., "Preparation and anti-icing of superhydrophobic PVDF coating on a wind turbine blade", Applied Surface Science, 259, 764-768. 2012. doi: 10.1016/j.apsusc.2012.07.118

[65] Wu, X., Zhao, X., Ho, J.W.C., and Chen, Z., "Design and durability study of environmental-friendly room-temperature processable icephobic coatings", Chemical Engineering Journal, 355, pp. 901-909, 2019. doi: 10.1016/j.cej.2018.07.204

[66] Dotan, A., Dodiuk, H., Laforte, C., and Kenig, S., "The relationship between water wetting and ice adhesion", Journal of Adhesion Science and Technology, 23(15), pp. 1907-1915, 2009. doi: 10.1163/016942409X12510925843078

[67] He, Z., Xiao, S., Gao, H., He, J., and Zhang, Z., "Multiscale crack initiator promoted super-low ice adhesion surfaces", Soft Matter, 13(37), pp. 6562-6568, 2017. doi: 10.1039/c7sm01511a

[68] He, Z., Zhuo, Y., He, J., and Zhang, Z., "Design and preparation of sandwich-like Polydimethylsiloxane (PDMS) sponges with super-low ice adhesion", Soft Matter, 14(23), pp. 4846-4851, 2018. doi: 10.1039/c8sm00820e

[69] Li, J., Zhao, Y., Hu, J., Shu, L., and Shi, X., "Anti-icing performance of a superhydrophobic PDMS/modified nano-silica hybrid coating for insulators", Journal of Adhesion Science and Technology, 26(4-5), pp. 665-679, 2012. doi: 10.1163/016942411X574826

[70] Zhuo, Y., Håkonsen, V., He, Z., Xiao, S., He, J., and Zhang, Z., "Enhancing the mechanical durability of icephobic surfaces by introducing autonomous self-healing function", ACS Applied Materials and Interfaces, 10(14), pp. 11972-11978, 2018. doi: 10.1021/acsami.8b01866

[71] Zhuo, Y., Xiao, S., Håkonsen, V., Li, T., Wang, F., He, J., and Zhang, Z., "Ultrafast self-healing and highly transparent coating with mechanically durable icephobicity", Applied Materials Today, 19, p. 100542, 2020. doi: 10.1016/j.apmt.2019.100542

[72] Xie, Q., Hao, T., Zhang, J., Wang, C., Zhang, R., and Qi, V, "Anti-icing performance of a coating based on nano/microsilica particle-filled amino-terminated PDMS-modified poxy", Coatings, 9, (12), p. 771, 2019. doi: 10.3390/coatings9120771

[73] Ahmadi, S. F., Nath, S., Iliff, G. J., Srijanto, B.R., Collier, C.P., Yue, P., and Boreyko, J.B., "Passive antifrosting surfaces using microscopic ice patterns", ACS Applied Materials and Interfaces, 10(38), pp. 32874-32884, 2018. doi: 10.1021/acsami.8b11285

[74] Jin, Y., Wu, C., Yang, Y., Wu, J., He, Z., and Wang, J., "Inhibiting condensation freezing on patterned polyelectrolyte coatings", ACS Nano, 14(4), pp. 5000-5007, 2020. doi: 10.1021/acsnano.0c01304

[75] Yao, Y., Zhao, T.Y., Machado, C., Feldman, E., Patankar, N.A., and Park, K.C., "Frost-free zone on macrotextured surfaces", Proceedings of the National Academy of Sciences of the United States of America, 117(12), pp. 6323-6329, 2020. doi: 10.1073/pnas.1915959117

[76] Wong, T., Kang, S. H., Tang, S.K.Y., Smythe, E.J., Hatton, B.D., Grinthal, A., and Aizenberg, J., "Bioinspired self-repairing slippery surfaces with pressure-stable omniphobicity", Nature, 477(7365), pp. 443-447, 2011. doi: 10.1038/nature10447

[77] Kim, P., Wong, T., Alvarenga, J., Kreder, M.J., and Adorno-Martinez, W.E., "Liquid-infused nanostructured surfaces with extreme anti-ice and anti-frost performance", ACS Nano, 6(8), pp. 6569-6577, 2012. doi: 10.1021/Nn302310q

[78] Chen, J., Dou, R., Cui, D., Zhang, Q., Zhang, Y., Xu, F., Zhou, X., Wang, J., Song, Y., and Jiang, L., "Robust prototypical anti-icing coatings with a self-lubricating liquid water layer between ice and substrate", ACS Applied Materials and Interfaces, 5(10), pp. 4026-4030, 2013. doi: 10.1021/am401004t

[79] Dou, R., Chen, J., Zhang, Y., Wang, X., Cui, D., Song, Y., Jiang, L., and Wang, J., "Anti-icing coating with an aqueous lubricating layer", ACS Applied Materials and Interfaces, 6(10), pp. 6998-7003, 2014. doi: 10.1021/am501252u

[80] Urata, C., Dunderdale, G.J., England, M.W., and Hozumi, A., "Self-lubricating organogels (SLUGs) with exceptional syneresis-induced anti-sticking properties against viscous emulsions and ices", Journal of Materials Chemistry A, 3(24), pp. 12626-12630, 2015. doi: 10.1039/c5ta02690c

[81] Wang, F., Xiao, S., Zhuo, Y., Ding, W., He, J., and Zhang, Z., "Liquid layer generators for excellent icephobicity at extremely low temperatures", Materials Horizons, 6(10), pp. 2063-2072, 2019. doi: 10.1039/c9mh00859d

[82] Golovin, K., Kobaku, S.P.R., Lee, D.H., DiLoreto, E.T., Mabry, J.M., and Tuteja, A., "Designing durable icephobic surfaces", Science Advances, 2(3), pp. 1-12, 2016. doi: 10.1126/sciadv.1501496

[83] Golovin, K. and Tuteja, A., "A Predictive Framework for the Design and Fabrication of Icephobic Polymers," Science Advances, 3(9), p. e1701617, 2017. doi: 10.1126/sciadv.1701617

[84] Golovin, K., Dhyani, A., Thouless, M.D., and Tuteja, A., "Low-interfacial toughness materials for effective large-scale deicing", Science, 364(6438), pp. 371-375, 2019. doi: 10.1126/science.aav1266

[85] Ganne, A., Lebed, V.O., and Gavrilov, A.I., "Combined wet chemical etching and anodic oxidation for obtaining the superhydrophobic meshes with anti-icing performance", Colloids and Surfaces A: Physicochemical and Engineering Aspects, 499, pp. 150-155, 2016. doi: 10.1016/j.colsurfa.2016.04.019

[86] Vercillo, V., Tonnicchia, S., Romano, J.-M., García-Girón, A., Aguilar-Morales, A.I., Alamri, S., Dimov, S.S., Kunze, T., Lasagni, A.F., and Bonaccurso, E., "Design rules for laser-treated icephobic metallic surfaces for aeronautic applications", Advanced Functional Materials, 30(16), p. 1910268, 2020. doi: 10.1002/adfm.201910268

[87] del Cerro, D.A., Römer, G.R.B.E., and Huis In't Veld, A.J., "Erosion resistant anti-ice surfaces generated by ultra short laser pulses", Physics Procedia, 5, pp. 231-235, 2010. doi: 10.1016/j.phpro.2010.08.141

[88] Sun, X., Damle, V.G., Liu, S., and Rykaczewski, K., "Bioinspired stimuli-responsive and antifreeze-secreting anti-icing coatings", Advanced Materials Interfaces, 2(5), pp. 25-27, 2015. doi: 10.1002/admi.201400479

[89] Zhuo, Y., Xiao, S., Håkonsen, V., He, J., and Zhang, Z., "Anti-icing ionogel surfaces: inhibiting ice nucleation, growth, and adhesion", ACS Materials Letters, 2(6), pp. 616-623, 2020. doi: 10.1021/acsmaterialslett.0c00094

[90] Cheng, T., He, R., Zhang, Q., Zhan, X., and Chen, F., "Magnetic particle-based super-hydrophobic coatings with excellent anti-icing and thermoresponsive deicing performance", Journal of Materials Chemistry A, 3(43), pp. 21637-21646, 2015. doi: 10.1039/c5ta05277g

[91] Irajizad, P., Hasnain, M., Farokhnia, N., Sajadi, S.M., and Ghasemi, H., "Magnetic slippery extreme icephobic surfaces", Nature Communications, 7(1), pp. 1-7, 2016. doi: 10.1038/ncomms13395

[92] Aydin, D., Akolpoglu, M.B., Kizilel, R., and Kizilel, S., "Anti-icing properties on surfaces through a functional composite: effect of ionic salts", ACS Omega, 3(7), pp. 7934-7943, 2018. doi: 10.1021/acsomega.8b00816

[93] Dash, S., de Ruiter, J., and Varanasi, K.K., "Photothermal trap utilizing solar illumination for ice mitigation", Science Advances, 4(8), p. eaat0127, 2018. doi: 10.1126/sciadv.aat0127

[94] Louchez, P.R., Bernardin, S., and Laforte, J.L., "Physical properties of aircraft de-icing and anti-icing fluids", in 36th AIAA Aerospace Sciences Meeting and Exhibit, Reno, NV, USA, 1998, p. 575. doi: 10.2514/6.1998-575

[95] Corsi, S.R., Geis, S.W., Loyo-Rosales, J.E., Rice, C.P., Sheesley, R.J., Failey, G.G., and Cancilla, D.A., "Characterization of aircraft deicer and anti-icer components and toxicity in airport snowbanks and snowmelt runoff", Environmental Science and Technology, 40(10), pp. 3195-3202, 2006. doi: 10.1021/es052028m

[96] Freeman, A.I., Surridge, B.W.J., Matthews, M., Stewart, M., and Haygarth, P.M., "Understanding and managing de-icer contamination of airport surface waters: a synthesis and future perspectives", Environmental Technology and Innovation, 3, pp. 46-62, 2015. doi: 10.1016/j.eti.2015.01.001

[97] Marbœuf, A., Bennani, L., Budinger, M., and Pommier-Budinger, V., "Electromechanical resonant ice protection systems: numerical investigation through a phase-field mixed adhesive/brittle fracture model", Engineering Fracture Mechanics, 230, 2020. doi: 10.1016/j.engfracmech.2020.106926

[98] Kraj, A.G. and Bibeau, E.L., "Measurement method and results of ice adhesion force on the curved surface of a wind turbine blade", Renewable Energy, 35(4), pp. 741-746, 2010. doi: 10.1016/j.renene.2009.08.030

[99] Strobl, T., Storm, S., Thompson, D., Hornung, M., and Thielecke, F., "Feasibility study of a hybrid ice protection system", Journal of Aircraft, 52(6), pp. 2064-2076, 2015. doi: 10.2514/1.C033161

[100] Antonini, C., Innocenti, M., Horn, T., Marengo, M., and Amirfazli, A., "Understanding the effect of superhydrophobic coatings on energy reduction in anti-icing systems", Cold Regions Science and Technology, 67(1-2), pp. 58-67, 2011. doi: 10.1016/j.coldregions.2011.02.006

[101] Strobl, T., Storm, S., Kolb, M., Haag, J., and Hornung, M., "Development of a hybrid ice protection system based on nanostructured hydrophobic surfaces", in 29th Congress of the International Council of the Aeronautical Sciences (ICAS), St. Petersburg, Russia, 2014.

[102] Pommier-Budinger, V., Budinger, M., Tepylo, N., and Huang, X., "Analysis of piezoelectric ice protection systems combined with ice-phobic coatings", in 8th AIAA Atmospheric and Space Environments Conference, Washington, DC, USA, 2016, p. 3442.

Chapter 3 – COMPUTATIONAL MODELLING AND SIMULATION METHODS

Ghislain Blanchard, Lokman Bennani and Olivier Rouzaud
Université de Toulouse
FRANCE

Richard Hann and Verner Håkonsen
Norwegian University of Science and Technology (NTNU)
NORWAY

Ali Benmeddour
National Research Council Canada
CANADA

3.1 INTRODUCTION

Ice Protection Systems (IPS) are systems that protect aircraft and sea vessels from the adverse effects of icing. These systems operate in complex environments involving several coupled physical phenomena. Therefore, the design, evaluation and analysis of IPS are complex tasks. In order to design efficient architectures, ice accretion rate, water droplet trajectories and heat transfer with the ambient atmosphere must be estimated. Numerical simulation is a powerful tool to tackle these problems and is complementary to experimental investigations. For the last four decades, various computer codes have been developed to design efficient IPS. This is nevertheless an arduous and challenging task which is still an active field of research.

This chapter aims at providing an overview of existing and emerging models and numerical tools for designing and evaluating IPS for air and sea vehicles. A brief review of the state-of-the-art modelling of ice accretion is presented first. Then, a review of the existing numerical models in the literature to simulate the main IPS technologies is presented. The Verification and Validation (V&V) of numerical codes, which is a major concern for certification in aeronautics, are also discussed. Finally, remaining gaps and challenges are presented.

3.2 STATE-OF-THE-ART OF NUMERICAL MODELLING OF ICE ACCRETION ON UNPROTECTED SURFACES

The formation of ice on a surface is a complex phenomenon that involves several coupled physical processes. Numerical icing tools to simulate aircraft ice accretion have been continuously developed since 1980s using Computational Fluid Dynamics (CFD) methods [1].

Typically, CFD simulations are conducted via four iterative steps (see Figure 3-1):

1) **Calculation of the flow field**. Most modern codes achieve this by solving the Reynolds-Averaged Navier-Stokes (RANS) equations [2]. The aerodynamic flow can also be obtained by coupling the inviscid equations (Euler equations) for the external flow field with the boundary layer equations (Prandtl equations) near the wall to reduce computation time, but it has several limitations [3]. Older codes use panel-methods for this step, often enhanced with empirical functions [4]. The calculation of the aerodynamic flow field is used to evaluate the heat transfer coefficient at the surfaces and to compute droplet trajectories.
2) **Droplet impingement on surfaces**. The information on how much water impinges on a surface can be calculated with either a Lagrangian or a Eulerian approach. Droplet trajectory computation enables the evaluation of the water droplet impingement limits and the collection efficiency.

3) **Solution of the mass and energy balance**. This step calculates how much of the impinging water actually turns into ice on surfaces. One of the first models devised to estimate the ice accretion was Messinger's model [5]. It has served as the basis for many ensuing aircraft icing simulation tools [4], [6], [7], [8], [9], [10] and is still in wide use to this day. This model describes the steady state ice build-up process on a surface, which is affected by a large number of terms such as aerodynamic heat transfer coefficients, evaporation, latent heat release, aerodynamic heating, IPS loads, etc. [2].

4) **Calculation of the new ice shape**. The new iced surface is calculated based on the amount of water turning into ice and the ice density at each calculation point. For CFD tools, this step can include the remeshing of the modified geometry due to ice build-up.

The exact implementation of each step varies from code to code, but the basics remain the same.

The total ice accretion can be obtained in a single time-step, multiple timesteps or with a predictor-corrector approach [3]. In a single time-step approach, the flow field is calculated once for the dry surface (no ice) and assumed unchanged during the whole duration of ice accumulation (exposure time). However, in the multiple time-step approach, the flow field is updated as ice builds up. The total duration of icing is divided into a reasonable number of time increments and after each time increment the new ice shape is extracted and used to modify the geometry of the surface. A new mesh is then generated and the flow field recalculated to take into account the change in the geometry because of ice accretion. The new mesh can either be generated by remeshing the whole computational domain or through deformation and/or local remeshing of the existing mesh while updating the ice shape. The multi-step approach is more realistic and provides more accurate ice shapes predictions but it is computationally demanding. For simple configurations, the predictor-corrector approach is a good alternative as it can provide good results, close to multi-step approach, with reduced computational cost.

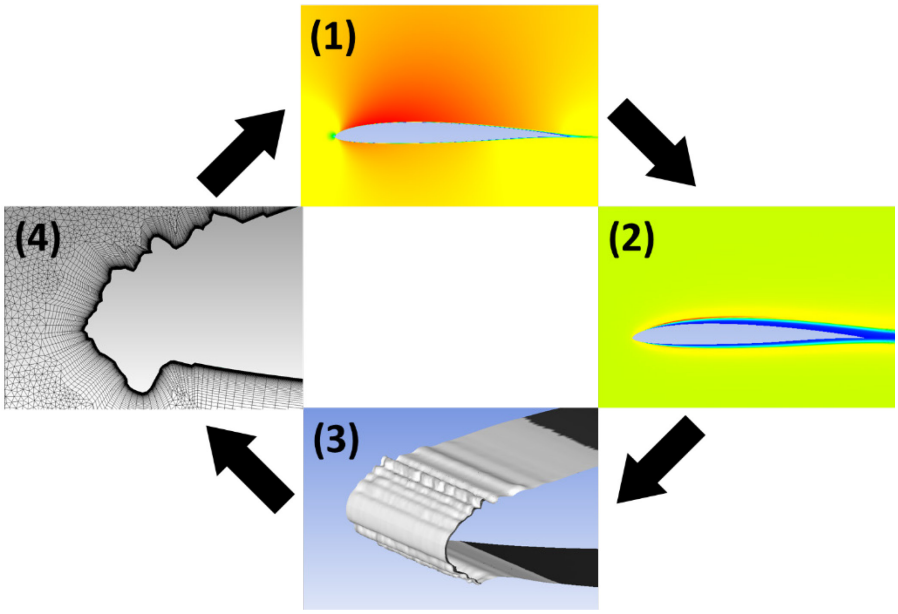

Figure 3-1: Simulation of Ice Accretion in Four Steps [11].

The development and the use of CFD tools for marine icing, e.g., MARICE [12], are more recent efforts compared to icing on aircraft. Previous icing models, e.g., ICEMOD [13] and RIGICE04 [14], were mainly based on empirical correlations and analytical equations derived for cylindrical and flat geometries [13], [15]. Unlike empirical icing models, CFD can calculate the turbulent airflow, heat transfer, and trajectories

of the droplets around the complex geometry of a vessel. Nevertheless, as the modelling of wave-generated spray is complicated and challenging, CFD models are still relying on empirical relations for the spray formation (Figure 3-2 and Figure 3-3). A review of the physics of marine icing and existing empirical models can be found in Refs. [16], [17].

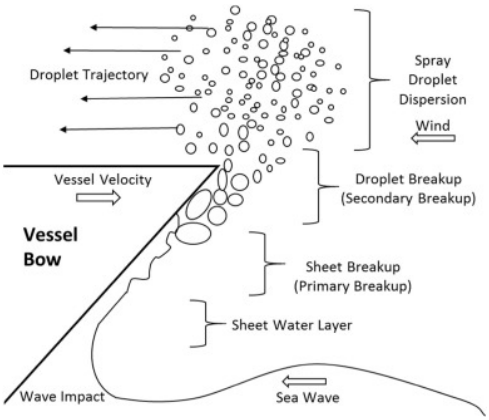

Figure 3-2: Illustration of the Wave Impact, Water Sheet Creation, and Breakup Stages [18].

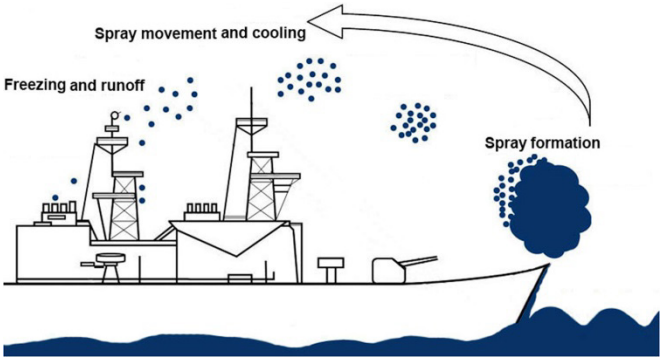

Figure 3-3: Schematic of the Spray Formation and its Movement on a Ship [16]

3.3 NUMERICAL MODELLING OF ICE PROTECTION SYSTEMS

3.3.1 Mechanical IPS

The idea of mechanical IPS is to use surface deformation to debond the ice from the surface. This process is often accompanied by a fracture in the bulk of the ice. The deformation can be generated by several means, such as inflatable boots or piezoelectric actuators. The modelling of these systems, therefore, requires a model for the actuation device, a model for the mechanical response of the protected surface and a model for the debonding and fracture of ice.

3.3.1.1 Electro-Expulse/Impulse

The basic strategy behind electro-mechanical systems is to feed a skin deforming device with high current pulses. The idea of Electro-Impulse De-Icing (EIDI) is to place coils beneath the protected surface. These coils are fixed and fed through a capacitor discharge. This creates, for an extremely short time lapse, a repulsive force between the surface and the coil. The small amplitude and high acceleration deformation of the surface then act to shed the ice. A first modelling approach for these systems was performed by researchers at Wichita State University in the U.S. during the 1980s [19], [20], [21].

Several simplified models of the actuator have been developed based on Maxwell's equations [22], [23], [24], [25]. The main output of these models is the separation force between the coil and the target surface. When compared to experimental data, these approaches yield good predictions.

Concerning the dynamic behavior of the skin, the simplest approach is to consider the skin alone and analyze its vibrational modes. This can be done using shell theory or finite element approaches [21], [26]. Knowledge of this dynamic response is important as it conditions the location of the coils and the duration of the impulse [20].

The ice shedding capabilities of an EIDI can be evaluated with several finite element methodologies. One approach is to determine the interfacial stresses between the surface and an ice layer. Using this computed value and experimental data, a failure criterion can be formulated to determine if ice shedding can occur or not [27], [28]. The effect of the impulse coil can be modelled by using a prescribed displacement extracted from experiments or by incorporating a model of force generated by the coils [29]. Recent studies show that modern multiphysics finite element software (such as Ansys) can be used to eliminate as much assumptions as possible for the space and time distributions of the magnetic forces [29]. The most recent modelling efforts concerning EIDIs use cohesive zone models to evaluate the cracking behavior of ice [29], [30]. An example of the results obtained with this kind of method is shown in Figure 3-4.

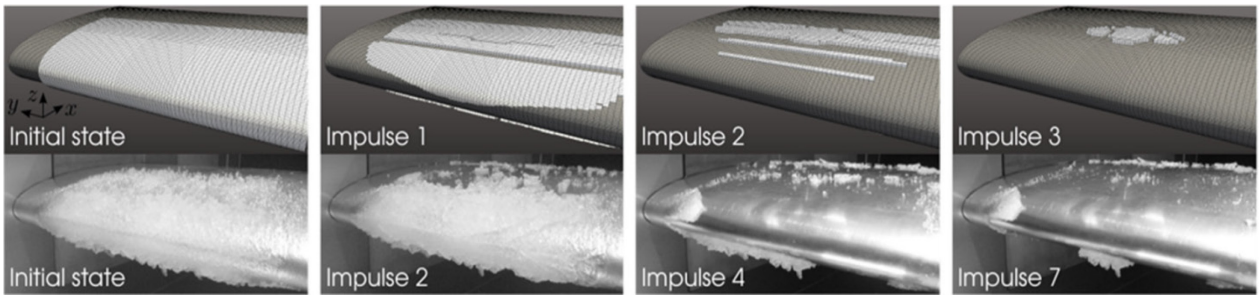

Figure 3-4: Example of Simulation (Top Row) Performed with Finite Elements and Cohesive Zone Elements and Comparison to Experiments (Bottom Row) of the De-Icing of a Leading Edge with an EIDI [31].

3.3.1.2 Vibratory IPS

The idea of vibratory de-icing systems is to generate vibrations in the protected surface. These vibrations need to generate sufficient stress at the interface with the ice (or within the ice) so as to debond/fracture the ice. Some of the first designs using this idea were based on shakers [32]. However, since 2000 the focus has mainly turned to piezoelectric actuators as the source of vibrations [33], [34], [35] .

Analytical methods have been developed to estimate the shear stress at the ice/substrate interface. The idea is to determine natural frequencies and mode shapes of the considered substrate [32]. Some authors have studied shear wave solutions [33], [36]. This can provide insight on which type of excitation will be most prone to ice shedding. For example, using such methods, Palacios et al. [36] found that ultrasonic shear waves could generate sufficient stress at the ice/metal interface to remove the ice.

Another approach is to perform finite element simulations. To do so, some authors use the capabilities of commercial software such as ABAQUS [37] or ATILA (a finite element analysis software for piezoelectric and magnetostrictive structures) [34], [38], [39], [40], [41]. Specific finite elements are available to model piezoelectric materials. For example, Figure 3-5 shows a finite element discretization of a leading edge protected by a piezoelectric actuator [42]. On the one hand, this type of simulation enables the evaluation and comparison of several design patterns in terms of efficiency. On the other hand, these tools can also be used to study ways of overcoming technological limitations. For example, it was observed in some experiments that the actuator could debond from the structure due to the failure of the bondline. This led Overmeyer et al. [40] to perform a parametric study with these tools so as to design a robust bondline configuration.

It is also interesting to note that analytical developments and finite element simulations can be combined so as to evaluate which type of excitations could be most favorable [43]. Reduced order models have also been developed and can help evaluate various design architectures [43].

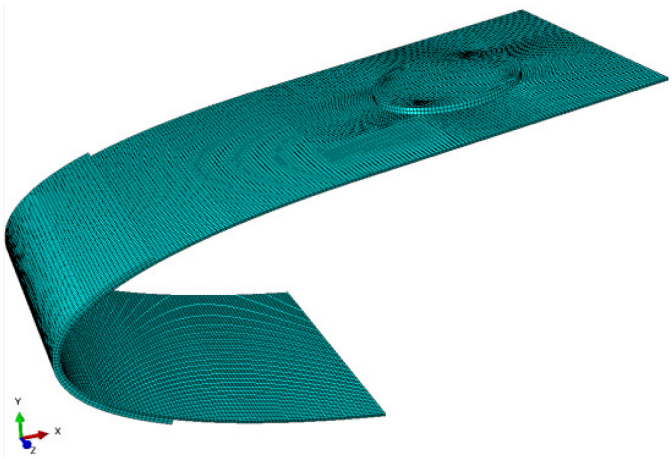

Figure 3-5: Finite Element Discretization of a Leading Edge with an Ice Layer and Protected by a Disk Piezoelectric Actuator [42].

Mechanisms by which the ice fractures and debonds from the structure have also been proposed. For example, Budinger et al. [43] assume the fracture path for several mechanisms as shown in Figure 3-6. To do so, the energy release rate is estimated using finite element computations. Griffith's theory is then used to determine the conditions for which such a process is possible.

Finally, to further assess the mechanisms proposed by Budinger et al. [43], a model based on the variational approach to fracture was proposed by Marboeuf et al. [44]. The model introduces a cohesive damage variable (d – see Figure 3-7). This variable varies between 0 (unfractured state) and 1 (fractured state). An adhesive damage variable (β – see Figure 3-7) is also introduced in the same way. No particular crack paths are assumed. As shown in Figure 3-7, simulations were performed on a flat plate geometry with an ice layer of uniform thickness on top. The simulation predicts a cohesive crack that cuts through the ice layer. The process is then followed by delamination at the ice/plate interface. The simulations tended to confirm one of the mechanisms introduced by Budinger et al. [43].

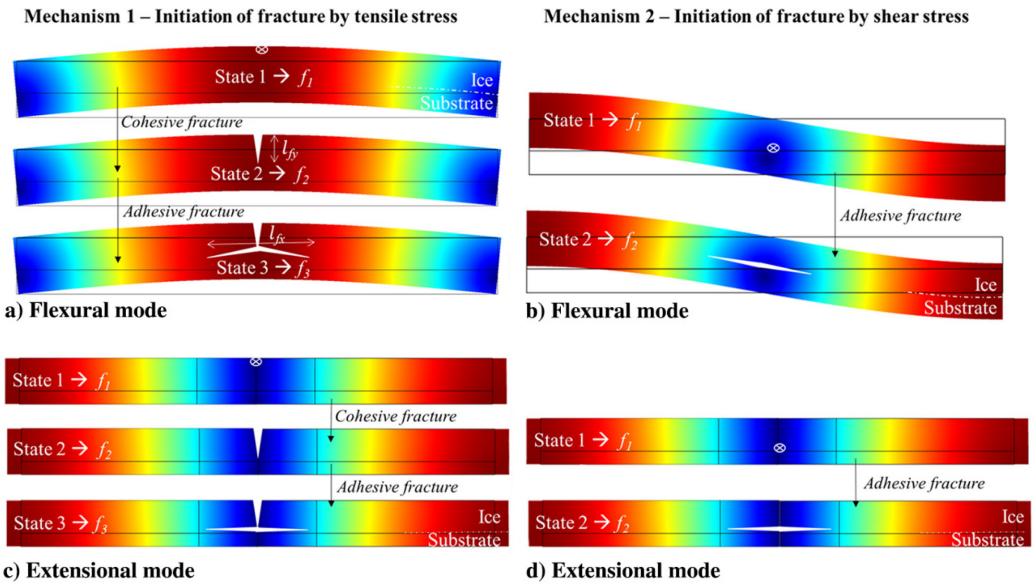

Figure 3-6: De-Icing Mechanisms Proposed by Budinger et al. [43].

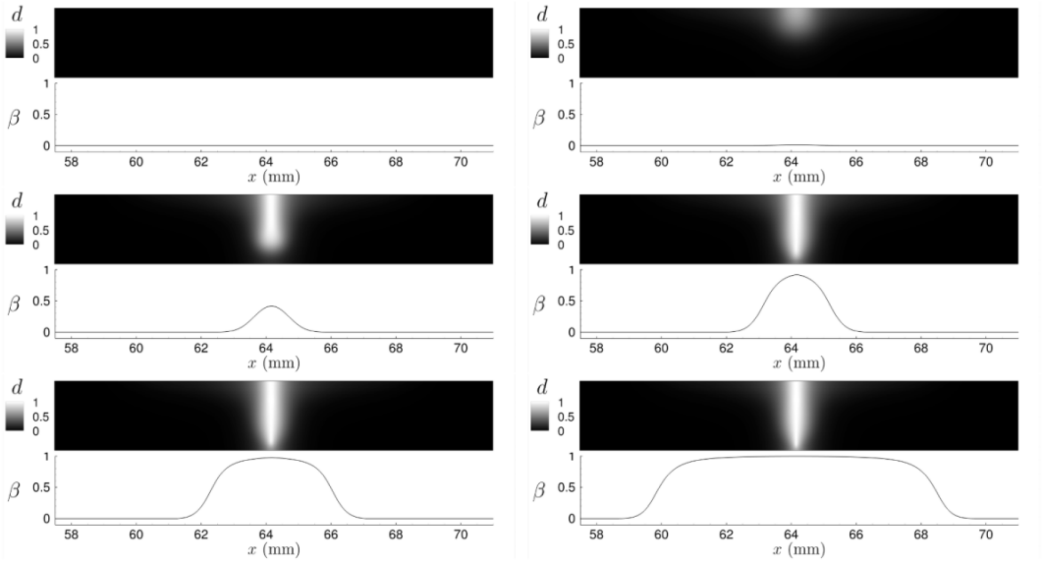

Figure 3-7: Example of a Simulation of the Fracture and Debonding Process of a Plate Under Flexural Loading. The simulation uses the variational approach to fracture [44].

3.3.2 Thermal IPS

The idea of thermal IPS is to provide heat to critical surfaces. This has the effect of either preventing ice formation by rendering the surface evaporative or running wet. Or, if ice accretion is allowed by the system, the heat then serves to melt some of the ice at the ice/critical surface interface. This will reduce the ability of ice to adhere to the surface and it will subsequently be detached by the aerodynamic forces.

The modelling of thermal IPS can be performed by combining a heat conduction solver with an accretion solver. Different methodologies for accretion are presented in Section 3.2. However, in some cases the system may also be studied in dry air conditions. In the following, the way specific systems are modelled will be presented. This will be followed by a review of possible coupling procedures.

For thermal systems, there is one common modelling aspect which is the conduction of heat in the protected surface. Several approaches have been used to model and simulate heat conduction in the skin. Simplified one-dimensional models have been formulated by some authors [45], [46]. For example, Donatti et al. [46] proposed two types of approximations. One is to consider heat conduction only in the normal direction and the other is to consider heat conduction in the tangential direction only. However, a complete model based on the heat equation and finite difference, finite volume or finite element discretization seems to also be very well established and widely used [47], [48], [49], [50], [51].

The specifics of each thermal system are presented in the following subsections.

3.3.2.1 Hot Air

Hot air ice protection is widely used in aeronautics in the form of the so-called bleed-air anti-icing system. Hot air is extracted from a compressor stage and distributed to the critical surfaces by a piccolo tube. It equips most of the large aircraft for wing and nacelle anti-icing.

In the case of the hot air system, the complicated part is to predict how much heat is transmitted to the protected surface from the hot air jets. Usually, this information is fed to the heat conduction solver by means of a Fourier-Robin boundary condition at the inner boundary. It requires the knowledge of the heat transfer coefficient with the impinging hot air jets.

A possible method is to use empirical correlations such as those reviewed by Martin [52] or Jambunathan et al. [53]. An important aspect for ice protection is to integrate design variables of the piccolo tube into the correlation which ultimately yields the heat transfer coefficient [54]. Piccolo design variables can typically be the diameter of the holes or the spacing between them. Brown et al. [55] have studied the effect of some of these variables on the heat transfer coefficient and proposed a correlation that is stated to be of reasonable accuracy. Wright [54] performed a review of possible correlations applicable to piccolo tube anti-icing. In particular, these correlations were used to perform numerical simulations which were compared to experimental data. The study showed that, with the tested correlations, the simulations overpredicted the surface temperature.

Another method to evaluate the heat transfer characteristics of the piccolo tube system is to perform numerical simulations of the internal flow [56], [57], [58], [59], [60]. These simulations are used either to study optimal designs [58], [59], for comparison with existing correlations [57] or to perform fully coupled computations of the ice protection system [60], see Figure 3-8.

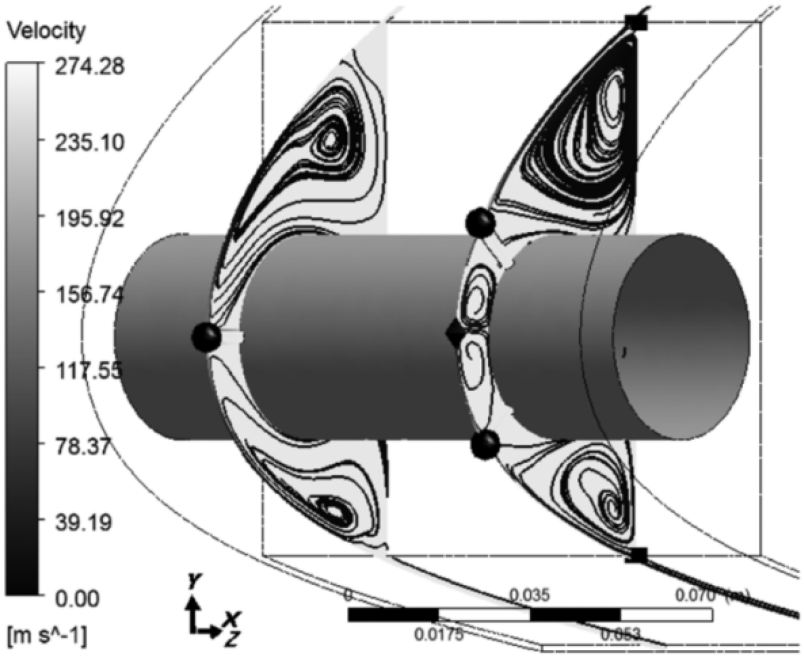

Figure 3-8: Example of a CFD Simulation of the Piccolo Tube Hot Air Internal Flow [60]

3.3.2.2 Electro-Thermal IPS

The idea is to integrate electrical heating elements into or onto the surface that one wishes to protect. These heating elements then provide the energy to either operate in anti-icing or de-icing mode. The operation of a modern electro-thermal IPS in de-icing mode is illustrated in Figure 3-9. A parting strip (here heater C) is held active during the whole cycle. The remaining heaters are activated according to a defined cycle. This acts to create a liquid water film at the interface between ice and the protected surface, hence reducing the ice ability to adhere to the surface. Once a critical amount of water film is formed the ice block is shed under the effect of aerodynamic forces.

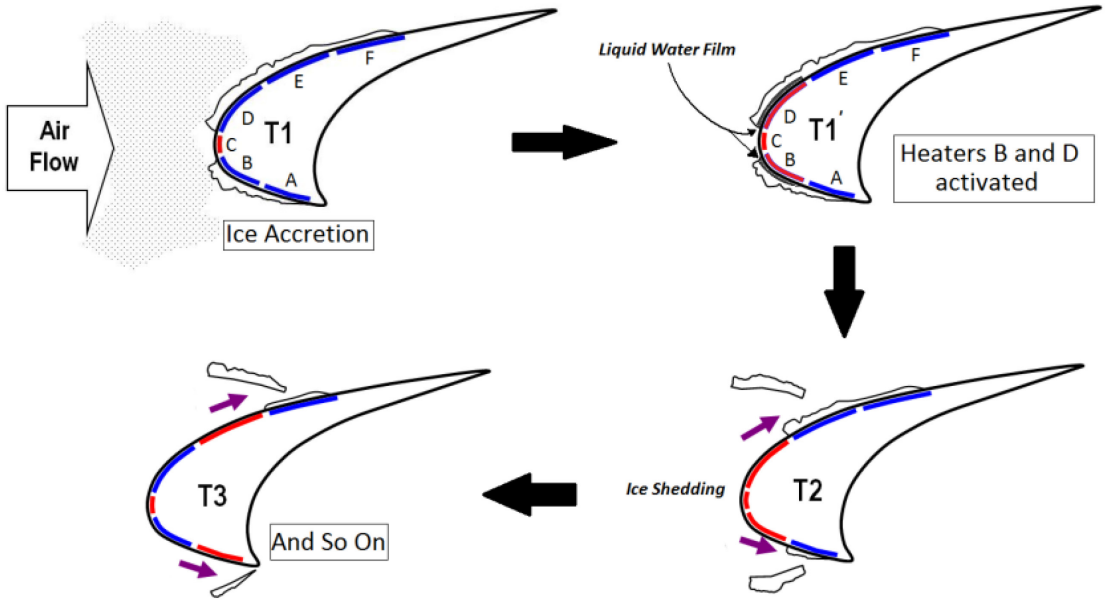

Figure 3-9: Operation of an Electro-Thermal System [61].

In electro-thermal IPS, the heater mats are usually integrated into a multi-layered material. Moreover, the materials can have anisotropic conductivities and therefore this is an essential feature that is added to the heat conduction solvers. The numerical tools also enable description of the heater activation cycle as an input. The heat provided by the heater mats is modelled as a source term. The heat equation may be solved using classical finite element or finite volume methods. Such numerical simulation tools have been developed since the 1990s by a large number of research organizations [47], [48], [51], [62], [63].

One of the difficulties in simulating electro-thermal IPS is the prediction of ice shedding in de-icing mode. However, as this is also an issue in other situations involving icing, it is discussed in a separate section (see Section 3.3.2.4).

The full unsteady simulation of an Electro-Thermal Ice Protection Systems (ETIPS) can become computationally costly. Therefore, Pourbagian and Habashi [64], [65], [66] proposed to use reduced order models based on proper orthogonal decomposition to build an optimization methodology. They introduced five design criteria: total electrical energy consumption, maximum ice thickness, final ice volume, ice shape irregularity and the ice-pressure distance (the location of the maximum ice thickness and the location of the minimum pressure coefficient).

3.3.2.3 Coupling with Ice Accretion Solver

As stated earlier, in order to perform a simulation of a thermal IPS, a coupling with an ice accretion solver is required. One approach is to directly integrate ice accretion into the general thermal model. This means that ice accretion and heat conduction in the protected surface are strongly coupled in a monolithic solver [48], [62], [63].

Another approach is to consider the heat conduction and the ice accretion solver as separate (weak coupling). For this case, Chauvin et al. [67] proposed an iterative coupling algorithm based on a Schwarz method. The idea is to use Fourier-Robin boundary conditions to transmit information from one solver to another. In that context they derived an optimized set of coupling coefficients.

3.3.2.4 Ice Shedding

Ice shedding is a mechanism in which ice is removed from the surface when the external forces (aerodynamic, centrifugal, gravity) become larger than the adhesive forces. In particular, ice shedding is an important mechanism for thermal or mechanical IPS and has been studied by many authors.

In the first generation of electro-thermal ice protection simulation codes, ice shedding was treated using empirical models. Henry [48] introduced two criteria based on the amount of melted water at the ice/airfoil interface. The first one is based on the ratio of melted water thickness to total thickness. The second is based on the ratio of melted water length to total water (solid and liquid) length. When they exceed a fixed value the ice layer is assumed to shed. Another approach is to compute the aerodynamic forces on the ice block. If the adhesion force is lower than the aerodynamic forces then the ice block is assumed to shed [62].

Scavuzzo et al. [68] performed a finite element analysis of the stresses in a fixed shape ice block under aerodynamic loading. The study was conducted in the context of electro-impulse systems. The authors concluded from their analysis that at Mach numbers lower than 0.45 the aerodynamic loading is not expected to contribute to ice shedding. However, at higher Mach numbers and high angles of attack, they consider the addition of the aerodynamic loading necessary to study ice shedding.

More recently, Zhang et al. [69] performed the computation of in-flight ice breakup. To do so, the authors used a remeshing crack propagation method to simulate the fracture of a fixed predetermined ice shape. Bennani et al. [70], [71], proposed a variational approach to model the fracture process. They also proposed possible ice shedding mechanisms which could be at play when an electro-thermal IPS is activated.

Chen et al. [72] proposed a combination of Extended-FEM (XFEM) and cohesive zone models to study ice shedding from a spinner.

Another important aspect of ice shedding is the simulation of the trajectories of the shed-ice fragments. Ice that was removed from the aircraft surface is at risk of hitting downstream components of the aircraft [73]. Ice fragments can cause substantial damage, especially if ingested into the engine or if hitting tail rotors. Several models exist that can predict the trajectory of ice fragments, e.g., Refs. [74], [75].

3.3.3 Passive IPS – Coatings and Modified Surfaces

The general idea of passive IPS is to use coatings and texturing to create superhydrophobic or icephobic surfaces (see Section 2.5.2 for more details). As these methods aim to modify the properties of the material, numerical modelling is mostly based on small-scale approaches. We present in the following the main emerging approaches in the literature.

3.3.3.1 Molecular Dynamics (MD) Approach

Molecular Dynamics (MD) simulation is the most widely used small-scale approach in the field of icing/anti-icing and relies on solving Newton's equations of motion for a system of interacting particles. In-conjunction with atomistic modelling or more coarse-grained models, MD simulations can more accurately capture the nanoscale phenomena present in ice-substrate interactions than continuum methods, such as size-effects which become evident when features are miniaturized below 100 nm. In the context of icing, the sum of these small-scale interactions constitutes the observed macroscopic behavior of ice on a given surface and are thus important to understand from a mechanistic point of view, which is the main purpose of MD simulations. With this approach, any surface with any given surface chemistry and topography can be created to simulate the interaction with both water and ice. This can provide useful information such as surface/interfacial energy, contact angle, thermal conductivity, and (nanoscale) ice adhesion strength. It can also provide, at the same time, dynamic (i.e., time-dependent) insights into icing/anti-icing processes such as ice accretion/crystallization, ice melting and ice shedding. The time

simulated for a given process is usually in the order of 10^{-9} to 10^{-6} s. The MD approach is usually limited to the nanoscale, because it will not be able to fully capture atomistic effects (such as quantum effects) at even smaller scales and becomes increasingly expensive computationally when approaching the microscale. Another limitation of the simulations is chemical modification, i.e., chemical reactions, which cannot be accounted for in MD.

There exist several open source software packages for MD simulations. The most commonly used MD codes in the literature for icing-related simulations are LAMMPS [76] and GROMACS [77]. Common for all MD approaches is that they rely on force fields as input to be able to accurately calculate interactions between atoms or coarse-grained units. The force fields are usually obtained by Density Functional Theory (DFT) calculations. Xiao et al. [78] used MD simulations for studying ice adhesion at small scale. In this particular study, the ice adhesion of a nanoscale ice cube was investigated on two different atomically rough surfaces of different hydrophilicity, namely silicon and graphene. The purpose of the study was to obtain a fundamental understanding of small-scale de-icing from a mechanistic point of view, and at the same time investigate the importance of an interfacial liquid water layer sandwiched between the ice and the substrate. The appropriate physical models for water/ice and the substrate needed to be chosen to properly reflect the molecular and atomic structure employed in the MD simulations, and in defining the interaction model between the substrate and water/ice. By utilizing the GROMACS software package, the TIP4p/ice water model and a model based on the Optimized Potentials for Liquid Simulations (OPLS) force field were chosen to build an all-atom model based on Lennard-Jones potentials (i.e., where the attractions were based on van der Waals interactions). The nanoscale I_h ice cube was given the size 7.6 × 7.1 × 2.0 nm^3 (Figure 3-10), while the substrates, fixed during the simulation, had a square shape (silicon surface area: 22.27 × 22.54 nm^2; graphene surface area: 19.81 × 19.80 nm^2) with necessary in-plane periodic boundary conditions to simulate an infinite extension. The liquid water layer, whenever accounted for, had a thickness of 1 nm.

By simulating ice detachment due to both pulling and shearing forces of the pre-equilibrated systems, the authors gained valuable insight into the small-scale ice detachment mechanics, as well as obtaining a numerical comparison for different substrate conditions (Figure 3-10).

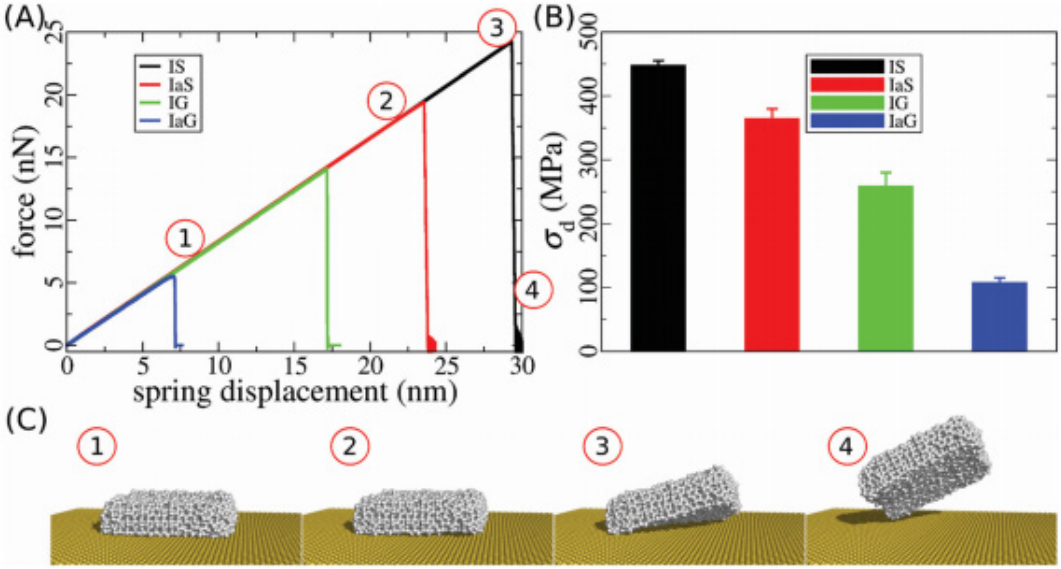

Figure 3-10: Ice Detachment Mechanics by MD Simulations. (a) Force-displacement profiles, (b) Obtained ice detachment stress, (c) Snapshots during the simulation of ice on a silicon substrate. Adapted from Ref. [78].

Ice adhesion was investigated on silicon, with and without an interfacial water layer (IS and IaS, respectively), and on graphene, with and without an interfacial water layer (IG and IaG, respectively). The ice cube was found to always detach at one of the edges in the initial stage of the process, yielding a linear force-displacement profile before a rapid decrease to no force upon detachment. In summary, this study confirmed that the higher surface energy of an atomically-smooth silicon surface resulted in greater ice adhesion strength than the lower surface energy substrate (graphene). In both cases the introduction of an interfacial liquid water lubrication layer reduced the ice adhesion by up to ~60%, as is consistent with experimental observations. It should be noted that the nanoscale ice adhesion strength obtained in these simulations cannot quantitatively be compared with those obtained in experiments, because of the higher loading rate (by 6 – 7 orders of magnitude) used in the simulations, as well as the nanoscale size of the ice cube allowing for defect-free adhesion, which will inherently lead to higher values than those obtained in experimental studies. However, the mechanisms of ice detachment should reflect those on real surfaces at microscale locations that are essentially defect-free.

Furthermore, in a more recent study, the same group demonstrated with MD simulations how sequential rupture of ice-substrate bonds (Figure 3-11) could significantly lower the ice adhesion on a fish scale-inspired surface based on graphene sheets [79]. This study showed how smart surface design by MD modelling could lower the ice adhesion, as would be expected from experiments of similar surfaces. Moreover, it demonstrated the vast capability of MD modelling to accurately replicate surfaces of any material and surface energy landscape, which exhibits a microscopic topography.

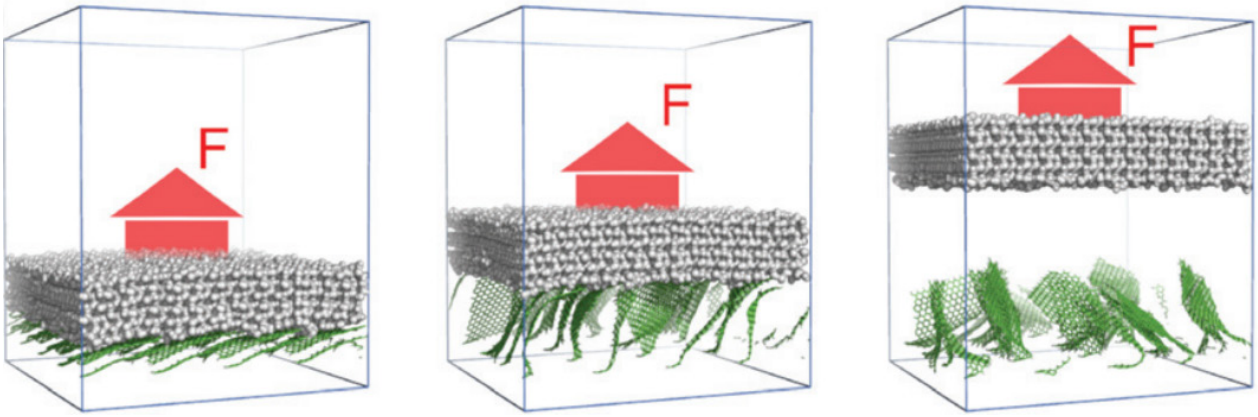

Figure 3-11: Simulation of Smart Surface Design by the MD Method. Adapted from Ref. [79].

MD simulation has further been proven as a powerful tool to gain deeper insight into other processes such as water droplet wetting mechanics [80], the effect of different lubricants on shear ice adhesion strength [81], ice nucleation and growth on surfaces of different topography (Figure 3-12) [82], [83], [84], as well as simulated melting of ice and resulting enhanced ice-substrate mobility upon contact with a surface infused with an anti-freeze agent [85]. Moreover, based on previous MD studies on water wetting characteristics, such as the determination of surface free energy [86], [87], and the study of adhesion [88] and water contact angles [89], a recent MD study demonstrated the correlation of nanoscale water contact angle and ice adhesion [90]. This represents a critical step towards reduced computational time and resources by determining ice adhesion solely through less expensive contact angle calculations.

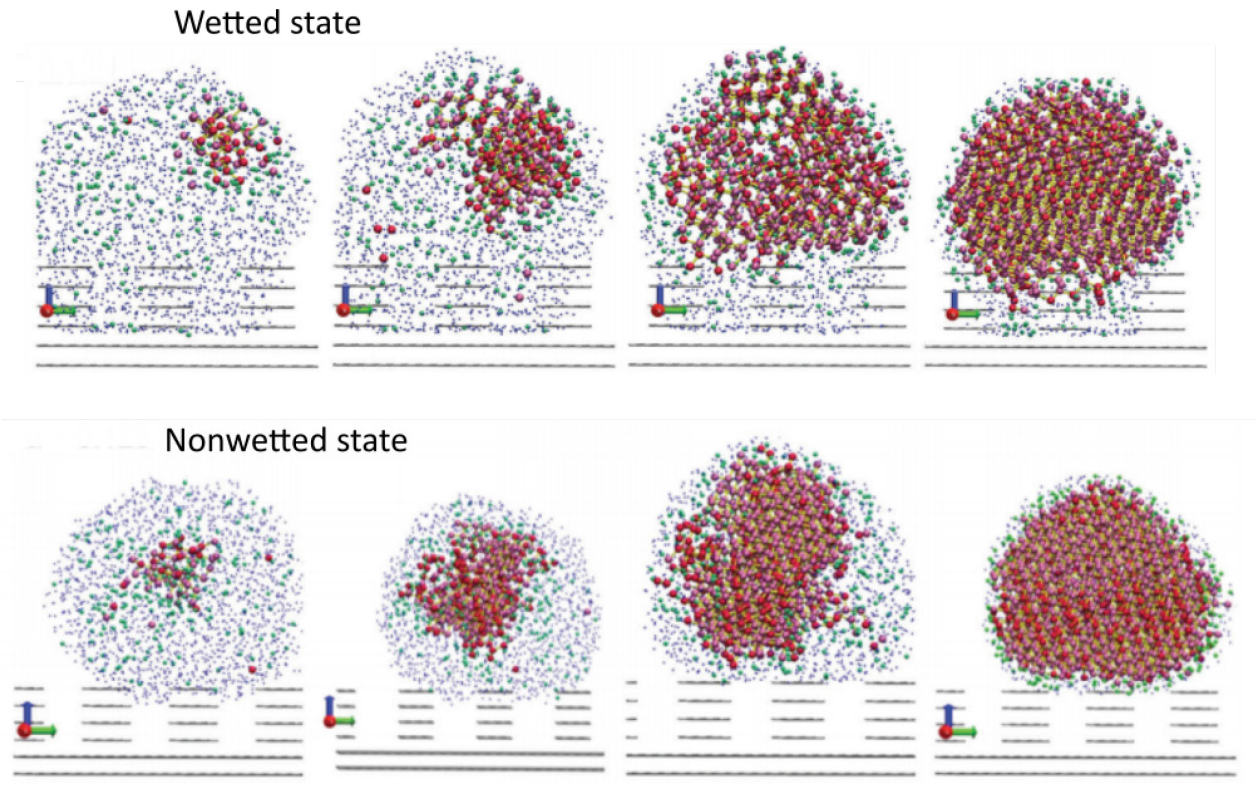

Figure 3-12: MD Simulation Snapshots of Ice Nucleation and Growth of Both Wetted and Non-Wetted Supercooled Water Droplets on Nanostructured Surfaces [83].

3.3.3.2 Atomistic Approach

To capture atomistic effects important in sub-nanoscale systems, such as quantum effects, *ab initio* (first principle) calculations need to be performed. These are important to be able to accurately obtain inter-atomic potentials to be used in less expensive larger scale simulations, such as in MD. The Density Functional Theory (DFT), which is an *ab initio* method based on quantum mechanics, is the most commonly used method for such purposes. First and foremost, DFT is restricted to very small mechanically static systems (i.e., a large system typically comprises 200 atoms), always situated at 0 K in the ground state, meaning that mechanics is not straightforward to simulate and entropic effects present at finite temperatures will not be accounted for. Therefore, for all intents and purposes, DFT cannot be used to accurately simulate icing phenomena, which is why there are only a few reports in the literature in this regard [91], [92]. The DFT could in principle be used to very accurately calculate energy/binding potentials between water molecules and the underlying material. However, these potentials are not the same as surface/binding (free) energy, which is the energy observed in experiments, since entropy is not taken into consideration. The DFT calculations are, however, important for establishing force fields, (i.e., potentials) which describe the inter-atomic interaction in solids and molecules. This will be important in MD simulations to account for physical and chemical bonding, something which cannot be intrinsically obtained in MD simulations (for which a combination, *ab initio*-MD [91], may be used in the case of chemical reactions during simulation).

There are several DFT packages available, both commercially and as open source. The most commonly used ones include Quantum Expresso [93] (open source), CP2K [94] (open source), VASP [95] (commercial) and CRYSTAL [96] (commercial).

3.3.3.3 Continuum Approach

Apart from the MD approach, another possibility is to consider the icing problem at the continuum level. In that case, current numerical methods like the Volume-of-Fluid (VOF) method are applicable as long as macroscopic models are available describing some nanoscale effects or the ice behavior as a whole, especially contact-line effects. Attarzadeh and Dolatabadi [97] proposed such an approach to investigate the impact of micro-droplets on superhydrophobic coating. Since heat transfer between the fluid (liquid or gas) and the solid is a key process, their method provides a coupling between a fluid solver and a heat conduction solver. The fluid solver relies on the VOF method with the usual conservation equations including the continuity, the momentum, the energy and the liquid fraction equations. Some specific peculiarities are introduced into the previous equations to account for the ice porosity and the liquid-solid presence (model of Tembely et al. [98]).

With this approach, the authors were able to simulate the impact of micro-droplets at ambient temperature on cold coated micro-structured surfaces for different material substrates (aluminum and TiO2). Simulations show that the behavior of the droplet during the impact is completely different since it bounces off on the TiO2 surface while it is pinned on the aluminum surface (Figure 3-13 and Figure 3-14). The authors point out that the release of the latent heat inside the aluminum substrate is more important than inside the TiO2 one, leading to the pinning of the triple point line. The calculations exhibit several important features like the freezing delay and the ice nucleation during the whole process depending on surface characteristics.

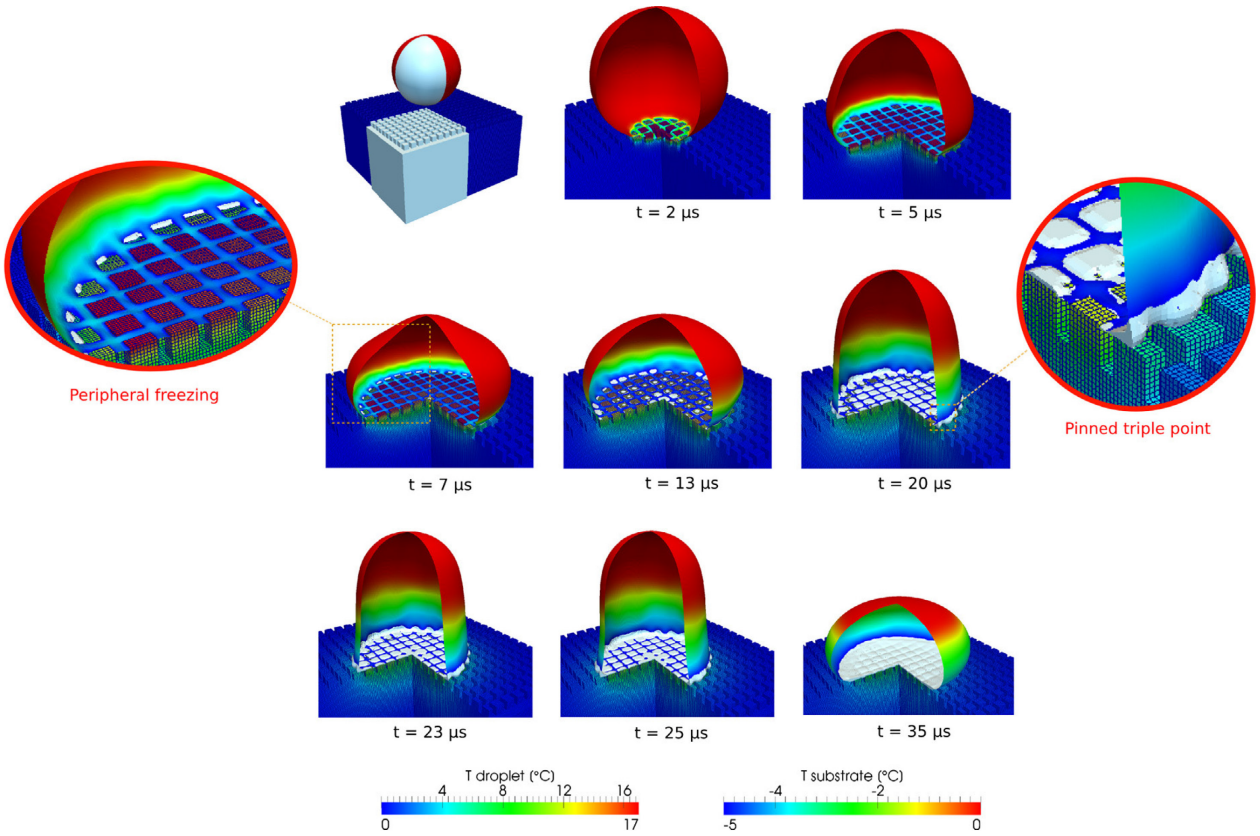

Figure 3-13: Time Lapse Sequence of the Freezing Front Dynamics Inside the Micro-Droplet (V = 1.6 m/s; T = 17 °C) onto a Cold (T = -5°C) Aluminum Substrate [97].

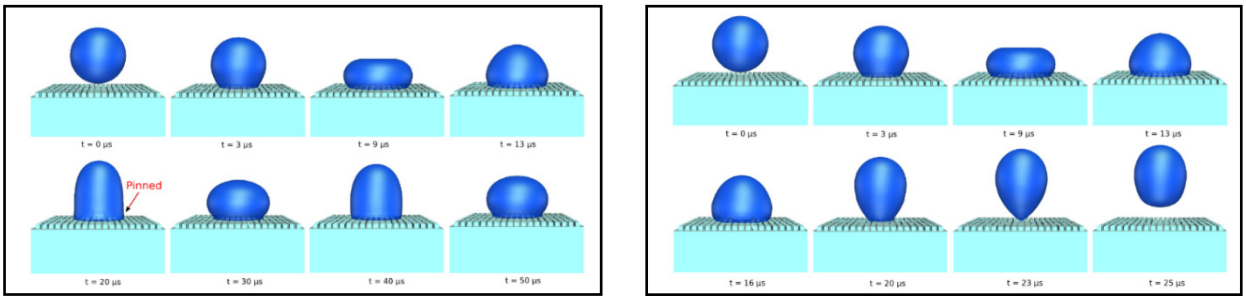

(a) Aluminum Surface. (b) TiO_2 Surface.

Figure 3-14: Simulations of Droplet Impact on Cold Coated Micro-Structured Superhydrophobic Surfaces with Different Substrate Materials [97].

3.3.3.4 Hybrid Approach

Zhang et al. [99] proposed a hybrid approach based on a variant of the Heterogeneous Multi-Scale Method (HMM), using a continuum solver (VOF method) sequentially coupled with a MD solver to study the dynamic wetting of nanodroplets on surfaces. In a certain sense, the idea is to see how far one can apply the VOF method since it is less computationally expensive than a fully MD method. Thus, the VOF model is applied everywhere while the MD is only used along the wetted interface to provide the crucial boundary information for both the three-phase contact-line dynamics (Type I sub-domain) and the solid/liquid interfacial slip (Type II sub-domain) to the VOF model (Figure 3-15). By comparing full and hybrid VOF/MD simulations (Figure 3-16), the authors demonstrate that one needs to account for slip across the entire solid/liquid interface to model molecular effects, in particular the large slip behavior at the contact-line. All of these results also demonstrate that the VOF method can be adapted to simulate the dynamic wetting of a nano-droplet at a reduced computational time up to one order of magnitude compared to MD simulation.

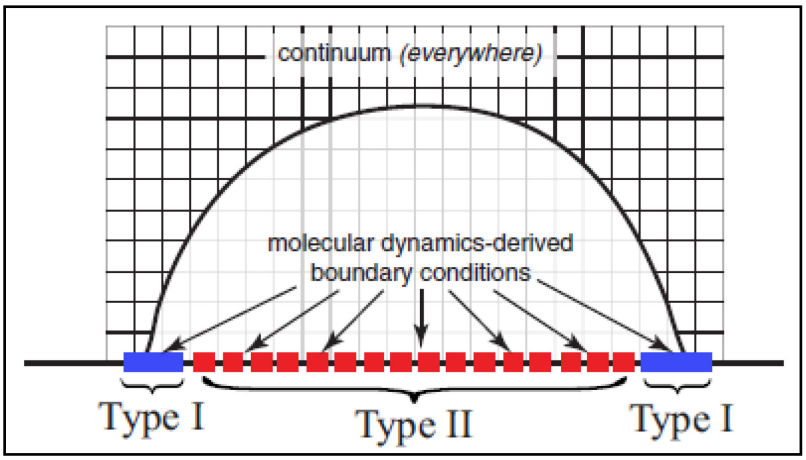

Figure 3-15: Multi-Scale Approach and MD Sub-Domain Locations [99].

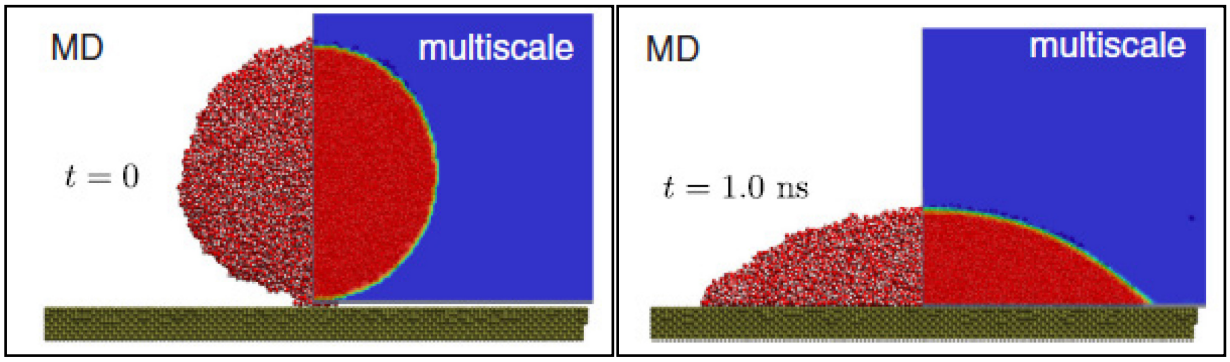

Figure 3-16: Comparisons of the MD and VOF Solutions of a Spreading Nano-Droplet at the Initial and Final Times [99].

3.3.4 Hybrid IPS

There are very few studies available in the literature dealing with the modelling and simulation of hybrid systems (active IPS plus icephobic coating). A study was performed by Strobl et al. [100] concerning a thermal/mechanical/coating hybrid system. As shown in Figure 3-17, the system consists of two active components. A carbon fiber cord heater is placed at the leading edge and piezoelectric actuators are placed on the upper and lower inner surfaces of the airfoil aft of the stagnation line. The system also uses an ultrasmooth, nanostructured hydrophobic surface in the critical area of the airfoil for droplet impingement and freezing to enhance the de-icing capabilities.

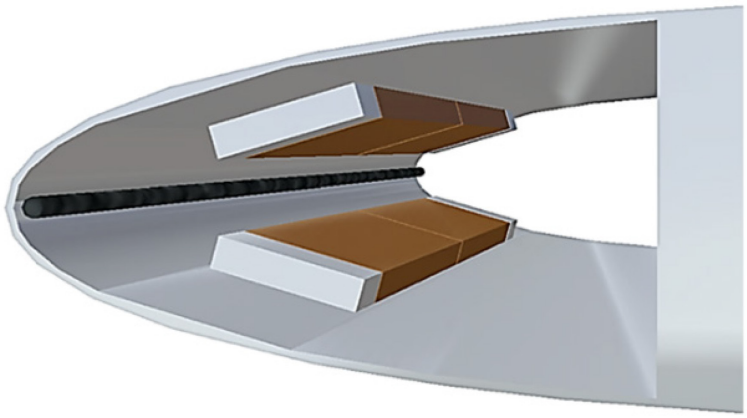

Figure 3-17: Hybrid Ice Protection System Studied by Strob et al. [100].

The electro-thermal aspects of the system were simulated using LEWICE2D [4] whereas the mechanical effect of the piezoelectric actuators was simulated with Abaqus [37]. LEWICE2D is first used to perform transient simulations and generate a time history of the residual ice shapes that build-up aft the thermally protected area. These shapes are then used to perform a finite element analysis with Abaqus. The idea is to determine whether or not the piezoelectric actuators generate enough deformation to lead to ice shedding. Mechanical ice shedding is performed by comparing the shear stress at the ice/airfoil interface with the experimental shear strength.

3.4 VERIFICATION AND VALIDATION DATABASES

All simulation tools require Verification and Validation (V&V) to establish confidence in the simulation results [101]. Verification refers to the process of ensuring that a certain model is implemented correctly. Validation refers to the process of comparing the simulation results with experimental results. Especially the last step is a key process to show the credibility and accuracy of a simulation tool.

A wide range of experimental data is available in the literature that can be used for the validation of icing simulations tools. These experiments are mostly conducted in specialized icing wind tunnels, where results can be obtained under controlled laboratory conditions. An overview of the available experimental datasets in the open literature is given in Appendix 3-1. The database is also available online and will be continuously updated [102]. This database was generated in the scope of the 1st AIAA Ice Prediction Workshop [103], which is an ongoing collaborative effort that aims to assess modern 3D icing simulation tools and practices, identify areas of improvement, and recommend practices and share knowledge. A similar workshop has been conducted in the late 1990s, which was reported in the AGARD 344 Report [104].

3.5 REMAINING GAPS AND CHALLENGES

The capability of current codes to simulate IPS systems has improved significantly in recent years. As shown in previous sections, several numerical tools now allow the study of complex 3D systems. However, some limitations still exist in terms of modelling.

The first difficulties are related to the modelling of ice accretion. Indeed, remaining gaps were identified due to inadequate modelling of several processes important to ice shape development in the AGARD-AR-344 report [104], about 20 years ago. These gaps are still relevant despite the progress that has been made so far. The processes were categorized as follows:

- The surface physics associated with the ice-water-substrate interaction.
- Formation of complex 3D ice shapes (“lobster tail” ice growth).
- Ice roughness development and interaction with the boundary layer.
- Convective heat transfer rates and evaporative cooling rates over such rough surfaces.

For aircraft icing, the evolution of certification requirements leads to the study of an increasingly wide range of icing conditions (SLD, ice crystals, and snow conditions). For example, simulation of SLD requires special attention to the droplet physics. Due to the large size of the droplets, typically with a diameter greater than 50 μm, special mechanisms are at work, which need to be captured for an accurate SLD simulation modelling. Modelling ice accretion for these conditions is currently an important and active area of research.

When considering the simulation of an IPS system, new physical phenomena, which potentially interact with the ice accretion process, must be modelled. This can lead to several challenges, including:

- **Transient de-icing mode:** State-of-the-art icing codes are mainly based on the classical Messinger approach to compute the ice growth rate on an unprotected surface (see Section 3.2). However, a major assumption of the model is that the temperature does not vary within the ice block in the direction normal to the surface. As a consequence, the model is not able to capture the melting dynamics of an ice block when a thermal IPS is activated during each cycle in transient de-icing mode. In addition, one must take into account the unsteady heat and mass transfer phenomena. Different solutions have been proposed in the literature to extend the Messinger’s model by using a multi-layered approach [105]-[111]. However, improvements to the models are still needed to better describe the unsteady coupled physics and improve the robustness of numerical procedures. Also, the lack of experimental data, and its high scatter, does not at the time of writing allow for a full validation of all these approaches.

- **Ice accretion with higher order turbulence models:** Ice accretion typically generates large flow separation effects and leads to a significant increase in turbulence. Accurately modelling this turbulence is essential for predicting aerodynamic performance losses, and also for ice accretion modelling. Most icing tools today solve the RANS equations with low-order turbulence modelling. Higher order turbulence models such as large-eddy simulation or direct numerical simulation offer a better resolution of turbulent processes. However, this comes at the cost of significantly increased computational requirements, which is the main reason these methods have not been implemented in icing models. The development of CFD turbulence modelling in the future should be closely monitored and adapted to icing simulations when feasible.
- **Icing simulation at low Reynolds numbers:** Most existing research on icing has been conducted at high Reynolds numbers (in the order of 10^7) and aimed at manned aviation. Unmanned Aerial Vehicles (UAVs) are an emerging technology that is also challenged with atmospheric in-flight icing. UAVs are smaller and fly at lower speeds than most manned aircraft, and therefore operate at Reynolds numbers typically an order of magnitude lower. The effects of low Reynolds number should be considered carefully in simulations of icing on UAVs [11]. Furthermore, icing codes typically assume that the flow is fully-turbulent once icing starts and this assumption makes sense for larger ice accretions and high Reynolds numbers. However, at lower Reynolds numbers, e.g., for UAVs, the effect of ice accretions on transition behavior can be important. Experiments at low Reynolds numbers are required for validation of icing tools. In addition, more research is needed to understand how icing and low Reynolds number effects (e.g., laminar separation bubbles) interact with each other and to understand how early stages of ice accretion (ice roughness) affect transitions.
- **Multi-scale bridging:** To be able to fully capture the interactions of any given structure with water or ice, the true surface properties of the structure need to be taken into account. This includes small-scale interactions determined by overall surface chemistry and topography, leading to the observed macroscopic behavior. In this respect, simulating large-scale systems, such as ice accretion/shedding on aircraft or sea vessel components, by using accurate small-scale tools (such as MD) becomes overly expensive computationally, while efficient continuum methods become too inaccurate. One solution, beyond the above-mentioned hybrid approach [99], is methodologies based on multi-scale bridging [112]. Here, important material parameters are accurately calculated in small-scale approaches, such as MD, for establishing databases of small-scale dynamics, in which the parameters are fed into the continuum methods to accurately capture the multi-scale physics with significantly reduced computational costs. In case of physical or chemical changes to the surface properties during the simulated process, the small-scale step (either MD or *ab initio* MD) needs to be repeated during the simulation to feed updated parameters into the continuum approaches. Owing to the complexity and challenges multi-scale bridging represents, there are very few reports in the literature in the field of icing/anti-icing. However, being a promising prospect, small-scale methods are continuously developed to more easily couple with continuum methods – one example being the MD solver mdFoam+ which is optimized for (but not limited to) coupling with CFD applications [113].
- **Artificial Intelligence (AI) and machine learning:** Another interesting emerging approach with great potential is the use of AI to assess whether a proposed IPS is suitable for an application. By machine learning algorithms, an AI program could be trained by searching through the entire literature to identify whether or not a proposed surface or system would be suitable for an IPS. A well-trained AI should also be able to predict important parameters such as water contact angle, ice nucleation rate and ice adhesion strength, without the need to do any actual simulations of such processes. As a future prospect, this methodology would be revolutionary and outperforming in terms of computational efficiency compared with conventional methods (also including multi-scale bridging). Although becoming more widespread, the use of machine learning is still at its infancy and has not in the time of writing resulted in any known reports in the field of anti-icing. A few studies have started to explore this approach for icing prediction [114], [115].

- **Uncertainty Quantification (UQ):** Currently, a few studies have implemented UQ for icing applications. For example, DeGebbaro et al. [116] used polynomial-chaos-expansion-based UQ to study several airfoil-icing scenarios. This enables linking the uncertainty in the evaluation of the aerodynamics of the iced airfoil, directly to the uncertainty inherent in the calculation of the ice shape. In particular, the modelling of ice accretion and IPS is a process associated with a high degree of uncertainty since it involves complex coupled physical phenomena and many physical parameters that are known in a statistical sense (icing conditions, material properties, etc.). Therefore, UQ should be performed to study the sensitivity of the IPS models to these input parameters. Moreover, it may help to strengthen the certification process by quantifying the effects of physical uncertainties.

3.6 CONCLUSIONS

The current state of modelling and simulation of IPS has been reviewed in this chapter. The modelling of each IPS technology is a challenge that often requires taking into account coupled multi-physical phenomena (solid mechanics, fluid mechanics, thermodynamics, physics and chemistry of materials). A broad field of expertise is therefore necessary for the development and implementation of complete simulation tools.

Nevertheless, significant progress has been made over the last thirty years in the development of models and numerical tools for the simulation of active IPS (mechanical and thermal). This has led to improved simulation capabilities for systems of increasing complexity. The development of commercial simulation software in the field of icing also reflects a certain level of maturity of the numerical methods and the dissemination of these tools. Currently, these tools are increasingly used for the design, calibration and optimization of IPS in the aeronautical industry.

The simulation methods for active IPS presented in the literature are mainly based on CFD tools for the treatment of fluid media (aerothermal coupling, phase change, etc.) and FEM resolution methods for solid media (substrate deformation, crack propagation in icing, etc.). These tools are based on numerical methods that are well known and relatively mature, in which the models are mainly based on a macroscopic continuum description. The physical phenomena are described by systems of equations derived from local conservation laws. However, these models can also involve a certain degree of empiricism through poorly controlled physical parameters (mechanical ice properties, etc.) or experimental correlations. This degree of empiricism often requires the implementation of experimental campaigns, in addition to numerical studies, to confirm and validate the results of the latter. Improving the understanding and characterization of accreted ice properties could help reduce the need for expensive experiments.

As developments in numerical tools have accompanied the choice of technologies, the modelling and simulation of passive IPS have only been studied more recently. In the literature, the simulation of these systems is mainly based on fine descriptions at microscopic scales with approaches such as MD. Studies have shown that these methods yield very promising results for the design of new icephobic surfaces. However, these methods are very computationally expensive and are limited to very small spatial and temporal scales. Thus, these approaches are mainly used to study the properties and behavior of a coating or textured surface in simplified academic configurations. They do not allow the simulation of a complete large-scale system for conditions encountered by, e.g., an aircraft in-flight. In addition, the modelling of aging and degradation of passive IPS with such small-scale approaches remains an open area of research.

To reduce the energy consumption of active systems, hybrid IPS (both active and passive) are increasingly studied. These systems represent a new challenge for modelling and numerical simulations as they combine multi-scale physics. Emerging methodologies such as multi-scale bridging and machine learning (see Section 3.5) have great potential and may offer new opportunities. Nevertheless, additional research needs to be conducted in this area to realize the full potential of these promising emerging technologies.

3.7 REFERENCES

[1] Kind, R.J., Potapczuk, M.G., Feo, A., Golia, C. and Shah, A.D., "Experimental and computational simulation of in-flight icing phenomena", Progress in Aerospace Sciences, 34, pp. 257-345, 1998.

[2] Habashi, W.G., Aubé, M., Baruzzi, G., Morency, F., Tran, P. and Narramore, J.C., "FENSAP-ICE: A fully-3D in-flight icing simulation system for aircraft, rotorcraft and UAVs", in 24th International Congress of Aeronautical Sciences (ICAS 2004), Yokohama, Japan, 29 August – 3 September 2004.

[3] Trontin, P., Blanchard, G., Kontogiannis, A. and Villedieu, P., "Description and assessment of the new ONERA 2D icing suite IGLOO2D," 9th AIAA Atmospheric and Space Environments Conference, AIAA 2017-3417, Denver, CO, USA, 5 – 9 June 2017.

[4] Wright, W., "User's manual for LEWICE version 3.2", NASA Contract Report NASA-CR-2008-214255, 2008.

[5] Messinger, B.L., "Equilibrium temperature of an unheated icing surface as a function of air speed", Journal of the Aeronautical Sciences, 20, pp. 29-42, 1953.

[6] Beaugendre, H., Morency, F. and Habashi, W.G., "FENSAP-ICE's three-dimensional in-flight ice accretion module: ICE3D", Journal of Aircraft, 40, pp. 239-247, 2003.

[7] Gent, R.W., "TRAJICE2-A combined water droplet trajectory and ice accretion prediction program for aerofoils", RAE TR, 90054, 1990.

[8] Dillingh, J.E. and Hoeijmakers, H.W.M., "Simulation of ice accretion on airfoils during flight", in FAA In-Flight Icing / Ground De-Icing International Conference & Exhibition, Chicago, IL, USA, 16 – 20 June 2003.

[9] Hedde, T. and Guffond, D., "ONERA three-dimensional icing model", AIAA Journal, 33, pp. 1038-1045, 1995.

[10] Paraschivoiu, I. and Saeed, F., "Ice Accretion simulation code CANICE", in Proceedings of the International Aerospace Symposium, "Carafoli 2001", Bucharest, Romania, 19 – 20 October 2001.

[11] Hann, R. and Johansen, T.A., "Unsettled topics in unmanned aerial vehicle icing", SAE International, SAE EDGE Research Report EPR2020008, 2020.

[12] Kulyakhtin, A. and Tsarau, A., "A time-dependent model of marine icing with application of computational fluid dynamics", Cold Regions Science and Technology, 104-105, pp. 33-44, 2014.

[13] Horjen, I., "Numerical modeling of two-dimensional sea spray icing on vessel-mounted cylinders", Cold Regions Science and Technology, 93, pp. 20-35, 9 2013.

[14] Forest, T.W., Lozowski, E.P. and Gagnon, R., "Estimating marine icing on offshore structures using RIGICE04", International Workshop on Atmospheric Icing Structures (IWAIS 2005), Montreal, QC, Canada, 12 – 16 June 2005.

[15] Lozowski, E.P., Forest, T.W., Chung, V. and Szilder, K., "Study of marine icing: final report", NRC Contract Report CR-2002-03, Institute for Ocean Technology, National Research Council of Canada 2002.

[16] Dehghani-Sanij, A.R., Dehghani, S.R., Naterer G.F. and Muzychka, Y.S., "Sea spray icing phenomena on marine vessels and offshore structures: review and formulation", Ocean Engineering, 132, pp. 25-39, 2017.

[17] Lozowski, E.P., Szilder, K. and Makkonen, L., "Computer simulation of marine ice accretion", Philosophical Transactions of the Royal Society of London. Series A: Mathematical, Physical and Engineering Sciences, 358, pp. 2811-2845, 11 2000.

[18] Dehghani, S.R., Naterer, G.F. and Muzychka, Y.S., "Droplet size and velocity distributions of wave-impact sea spray over a marine vessel", Cold Regions Science and Technology, 132, pp. 60-67, 2016.

[19] Zumwalt, G.W., Schrag, R.L., Bernhart, W.D. and Friedberg, R.A., "Analyses and tests for design of an electro-impulse de-icing system", NASA Contract Report NASA-CR-174929,1985.

[20] Zumwalt, G. and Friedberg, R., "Designing an electro-impulse de-icing system", 24th AIAA Aerospace Sciences Meeting and Exhibit, Reno, NV, USA, 6 – 9 January 1986.

[21] Zumwalt, G.W., Schrag, R.L., Bernhart, W.D. and Friedberg, R.A., "Electro-impulse de-icing testing analysis and design", NASA Contract Report NASA-CR-4175, 1988.

[22] Bernhart, W. and Gien, P., "A structural dynamics investigation related to EIDI applications", AIAA 24th AIAA Aerospace Sciences Meeting and Exhibit, Reno, NV, USA, 6 – 9 January 1986.

[23] Bernhart, W.D. and Schrag, R.L., "Electroimpulse deicing-electrodynamic solution by discrete elements", Journal of Aircraft, 26, pp. 547-553, 1989.

[24] El-Markabi, M.H.S. and Freeman, F.M., "Electromagnetic properties of a circular cylindrical coil in a set of planar ferromagnetic regions", IEE Proceedings A (Physical Science, Measurement and Instrumentation, Management and Education, Reviews), 129, pp. 582-589, 1982.

[25] Henderson, R.A. and Schrag, R.L., "Theoretical analysis of the electrical aspects of the basic electro-impulse problem in aircraft de-icing applications", NASA Contractor Report NASA-CR-176808, 1986.

[26] Henderson, R.A. and Schrag, R.L., "Theoretical analysis of the electrical aspects of the basic electro-impulse problem in aircraft de-icing applications", NASA Contractor Report NASA-CR-180845, 1987.

[27] Khatkhate, A., Scavuzzo, R. and Chu, M., "A finite element study of the EIDI system", 26th AIAA Aerospace Sciences Meeting and Exhibit, Reno, NV, USA, 11 – 14 January 1988.

[28] Scavuzzo, R.J., Chu, M.L., Woods, E.J., Raju, R. and Khatkhate, A.A., "Finite element studies of the electro impulse de-icing system", Journal of Aircraft, 27, pp. 757-763, 1990.

[29] Labeas, G.N., Diamantakos, I.D. and Sunaric, M.M., "Simulation of the electroimpulse de-icing process of aircraft wings", Journal of Aircraft, 43, pp. 1876-1885, 2006.

[30] Möhle, E., Haupt, M.C. and Horst, P., "Coupled numerical simulation and experimental validation of the electroimpulse de-icing process", Journal of Aircraft, 50, pp. 96-102, 2013.

[31] Sommerwerk, H., Luplow, T. and Horst, P., "Numerical simulation and validation of electro-impulse de-icing on a leading edge structure", Theoretical and Applied Fracture Mechanics, 105, p. 102392, 2020.

[32] Lemont, H.E. and Upton, H., "Vibratory ice protection for helicopter rotor blades", Ft. Belvoir Defense Technical Information Center, June 1978.

[33] Ramanathan, S., Varadan, V.V. and Varadan, V.K., "Deicing of helicopter blades using piezoelectric actuators", in Smart Structures and Materials 2000: Smart Electronics and MEMS, SPIE's 7th International Symposium on Smart Structures and Materials, Newport Beach, CA, USA, 6 – 9 March 2000.

[34] Palacios, J., Smith, E., Rose, J. and Royer, R., "Instantaneous de-icing of freezer ice via ultrasonic actuation", AIAA Journal, 49, pp. 1158-1167, 2011.

[35] Pommier-Budinger, V., Budinger, M., Rouset, P., Dezitter, F., Huet, F., Wetterwald, M. and Bonaccurso, E., "Electromechanical resonant ice protection systems: initiation of fractures with piezoelectric actuators", AIAA Journal, 56, pp. 4400-4411, 2018.

[36] Palacios, J.L., Smith, E.C., Gao, H. and Rose, J.L., "Ultrasonic shear wave anti-icing system for helicopter rotor blades", Annual Forum Proceedings, 62nd American Helicopter Society International Annual Forum, Phoenix, AZ, USA, 9 – 11 May 2006.

[37] "Abaqus", https://www.3ds.com/products-services/simulia/products/abaqus/ Retrieved December 18, 2020.

[38] Venna, S.V., Lin, Y.-J. and Botura, G., "Piezoelectric transducer actuated leading edge de-icing with simultaneous shear and impulse forces", Journal of Aircraft, 44, pp. 509-515, 2007.

[39] Yin, C., Zhang, Z., Wang, Z. and Guo, H. "Numerical simulation and experimental validation of ultrasonic de-icing system for wind turbine blade", Applied Acoustics, 114, pp. 19-26, 2016.

[40] Overmeyer, A., Palacios, J. and Smith, E., "Ultrasonic de-icing bondline design and rotor ice testing", AIAA journal, 51, pp. 2965-2976, 2013.

[41] Ameduri, S., Brindisi, A. and Guida, D., "Investigations on the use of Lamb waves for de-icing purposes", ICAST 2014 – 25th International Conference on Adaptive Structures and Technologies, The Hague, The Netherlands, 6 – 8 October 2014.

[42] Maio, L., Ameduri, S., Concilio, A., Monaco, E., Memmolo, V. and Ricci, F., "Development of a de-icing system for aerodynamic surfaces based on ultrasonic waves", Health Monitoring of Structural and Bioligical Systems XII, Denver, Colorado, USA, 5 – 8 March 2018.

[43] Budinger, M., Pommier-Budinger, V., Bennani, L., Rouset, P., Bonaccurso, E. and Dezitter, F., "Electromechanical resonant ice protection systems: analysis of fracture propagation mechanisms", AIAA Journal, 56, pp. 4412-4422, 2018.

[44] Marbœuf, A., Bennani, L., Budinger, M. and Pommier-Budinger, V., "Electromechanical resonant ice protection systems: numerical investigation through a phase-field mixed adhesive/brittle fracture model", Engineering Fracture Mechanics, 230, p. 106926, 2020.

[45] Wright, W.B., "Users manual for the improved NASA Lewis ice accretion code LEWICE 1.6", NASA Contractor Report NASA-CR-189355, 1995.

[46] Donatti, C.N., Silveira, R.A., Bridi, G., Maliska, C.R. and Da Silva, A.F.C., "Ice accretion simulation in presence of a hot air anti-icing system", 19th International Congress of Mechanical Engineering, Brasilia, Brazil, 5 – 9 November 2007.

[47] Yaslik, A.D., De Witt, K.J., Keith Jr, T.G. and Boronow, W., "Three-dimensional simulation of electrothermal deicing systems", Journal of Aircraft, 29, pp. 1035-1042, 1992.

[48] Henry, R., "Development of an electrothermal de-icing/anti-icing model", 30th AIAA Aerospace Sciences Meeting and Exhibit, Reno, NV, USA, 6 – 9 January 1992.

[49] Wright, W., "LEWICE 2.2 capabilities and thermal validation", 40th AIAA Aerospace Sciences Meeting and Exhibit, Reno, NV, USA, 14 – 17 January 2002.

[50] Reid, T., Baruzzi, G., Aliaga, C., Aubé, M. and Habashi, W., "FENSAP-ICE: application of unsteady CHT to de-icing simulations on a wing with inter-cycle ice formation", AIAA Atmospheric and Space Environments Conference, Toronto, ON, Canada, 2 – 5 August 2010.

[51] Bennani, L., Villedieu, P. and Salaun, M., "Two dimensional model of an electro-thermal ice protection system", 5th AIAA Atmospheric and Space Environments Conference, San Diego, CA, USA, 24 – 27 January 2013.

[52] Martin, H., "Heat and mass transfer between impinging gas jets and solid surfaces", Advances in Heat Transfer, Elsevier, 13, pp. 1-60, 1977.

[53] Jambunathan, K., Lai, E., Moss, M.A. and Button, B.L., "A review of heat transfer data for single circular jet impingement", International Journal of Heat and Fluid Flow, 13, pp. 106-115, 1992.

[54] Wright, W., "An evaluation of jet impingement heat transfer correlations for piccolo tube application", 42nd AIAA Aerospace Sciences Meeting and Exhibit, Reno, NV, USA, 5 – 8 January 2004.

[55] Brown, J.M., Raghunathan, S., Watterson, J.K., Linton, A.J. and Riordon, D., "Heat transfer correlation for anti-icing systems", Journal of Aircraft, 39, pp. 65-70, 2002.

[56] Croce, G., Habashi, W., Guevremont, G. and Tezok, F., "3D thermal analysis of an anti-icing device using FENSAP-ICE", 36th AIAA Aerospace Sciences Meeting and Exhibit, Reno, NV, USA, 12 – 15 January 1998.

[57] Saeed, F., Morency, F. and Paraschivoiu, I., "Numerical simulation of a hot-air anti-icing system", 38th AIAA Aerospace Sciences Meeting and Exhibit, Reno, NV, USA, 10 – 13 January 2000.

[58] Saeed, F., "Numerical simulation of surface heat transfer from an array of hot-air jets", Journal of Aircraft, 45, pp. 700-714, 2008.

[59] Fregeau, M., Gabr, M., Paraschivoiu, I. and Saeed, F., "Simulation of heat transfer from hot-air jets impinging a three-dimensional concave surface", Journal of Aircraft, 46, pp. 721-726, 2009.

[60] Hannat, R. and Morency, F., "Numerical validation of conjugate heat transfer method for anti-/de-icing piccolo system", Journal of Aircraft, 51, pp. 104-116, 2014.

[61] Huang, X., Tepylo, N., Pommier-Budinger, V., Budinger, M., Bonaccurso, E., Villedieu, P. and Bennani, L., "A survey of icephobic coatings and their potential use in a hybrid coating/active ice protection system for aerospace applications", Progress in Aerospace Sciences, 105, pp. 74-97, 2019.

[62] Wright, W., Al-Khalil, K. and Miller, D., "Validation of NASA thermal ice protection computer codes. II-LEWICE/Thermal", 35th AIAA Aerospace Sciences Meeting and Exhibit, Reno, NV, USA, 6 – 9 January 1997.

[63] Reid, T., Baruzzi, G.S. and Habashi, W.G., "FENSAP-ICE: unsteady conjugate heat transfer simulation of electrothermal de-icing", Journal of Aircraft, 49, pp. 1101-1109, 2012

[64] Pourbagian, M. and Habashi, W., "CFD-based optimization of electro-thermal wing ice protection systems in de-icing mode", 51st AIAA Aerospace Sciences Meeting Including the New Horizons Forum and Aerospace Exposition, Grapevine, TX, USA, 7 – 10 January 2013.

[65] Pourbagian, M. and Habashi, W.G., "Surrogate-based optimization of electrothermal wing anti-icing systems", Journal of Aircraft, 50, pp. 1555-1563, 2013.

[66] Pourbagian, M. and Habashi, W.G., "Aero-thermal optimization of in-flight electro-thermal ice protection systems in transient de-icing mode", International Journal of Heat and Fluid Flow, 54, pp. 167-182, 2015.

[67] Chauvin, R., Villedieu, P., Trontin, P. and Bennani, L., "A robust coupling algorithm applied to thermal ice protection system unsteady modeling", 6th AIAA Atmospheric and Space Environments Conference, Atlanta, GA, USA, 16 – 20 June 2014.

[68] Scavuzzo, R.J., Chu, M.L. and Ananthaswamy, V., "Influence of aerodynamic forces in ice shedding", Journal of Aircraft, 31, pp. 526-530, 1994.

[69] Zhang, S., El Kerdi, O., Khurram, R.A. and Habashi, W.G., "FEM analysis of in-flight ice break-up", Finite Elements in Analysis and Design, 57, pp. 55-66, 2012.

[70] Bennani, L., Villedieu, P., Salaun, M. and Trontin, P., "Numerical simulation and modeling of ice shedding: Process initiation", Computers & Structures, 142, pp. 15-27, 2014.

[71] Bennani, L., Villedieu, P. and Salaun, M., "A mixed adhesion–brittle fracture model and its application to the numerical study of ice shedding mechanisms", Engineering Fracture Mechanics, 158, pp. 59-80, 2016.

[72] Chen, Y., Fu, L. and Dong, W., "Novel cohesive/adhesive ice shedding model for spinner cone", Journal of Propulsion and Power, 34, pp. 647-659, 2018.

[73] Thomas, S.K., Cassoni, R.P. and MacArthur, C.D., "Aircraft anti-icing and de-icing techniques and modeling", Journal of Aircraft, 33, pp. 841-854, 1996.

[74] Yeoh, G., Beaugendre, H., Morency, F., Gallizio, F. and Laurens, S., "Computation of ice shedding trajectories using Cartesian grids, penalization, and level sets", Modelling and Simulation in Engineering, 2011, p. 274947, 2011.

[75] Baruzzi, G.S., Lagacé, P., Aubé, M.S. and Habashi, W.G., "Development of a shed-ice trajectory simulation in FENSAP-ICE", SAE Aircraft and Engine Icing International Conference, Seville, Spain, 24 – 27 September 2007.

[76] "LAMMPS", https://lammps.sandia.gov Retrieved December 18, 2020.

[77] "GROMACS", http://www.gromacs.org Retrieved December 18, 2020.

[78] Xiao, S., He, J. and Zhang, Z., "Nanoscale deicing by molecular dynamics simulation", Nanoscale, 8(30), pp. 14625-14632, 2016.

[79] Xiao, S., Skallerud, B.H., Wang, F., Zhang, Z. and He, J., "Enabling sequential rupture for lowering atomistic ice adhesion", Nanoscale, 11(35), pp. 16262-16269, 2019.

[80] Xiao, S., Zhang, Z. and He, J., "Atomistic dewetting mechanics of Wenzel and monostable Cassie-Baxter states", Physical Chemistry Chemical Physics, 20(38), pp. 24759-24767, 2018.

[81] Wang, F., Xiao, S., Zhuo, Y., Ding, W., He, J. and Zhang, Z., "Liquid layer generators for excellent icephobicity at extremely low temperatures", Materials Horizons 6(10), pp. 2063-2072, 2019.

[82] Singh, J.K. and Müller-Plathe, F., "On the characterization of crystallization and ice adhesion on smooth and rough surfaces using molecular dynamics," Applied Physics Letters, 104, p. 021603, 2014.

[83] Metya, A.K., Singh, J.K. and Müller-Plathe, F., "Ice nucleation on nanotextured surfaces: the influence of surface fraction, pillar height and wetting states", Physical Chemistry Chemical Physics, 18(38), pp. 26796-26806, 2016.

[84] Liu, J., Zhu, C., Liu, K., Jiang, Y., Song, Y., Francisco, J.S., Zeng, X.C. and Wang, J., "Distinct ice patterns on solid surfaces with various wettabilities", Proceedings of the National Academy of Sciences, 114, pp. 11285-11290, 2017.

[85] Zhuo, Y., Xiao, S., Håkonsen, V., He, J. and Zhang, Z., "Anti-icing ionogel surfaces: inhibiting ice nucleation, growth, and adhesion", ACS Materials Letters, 2, pp. 616-623, 2020.

[86] Leroy, F. and Müller-Plathe, F., "Rationalization of the behavior of solid-liquid surface free energy of water in Cassie and Wenzel wetting states on rugged solid surfaces at the nanometer scale", Langmuir, 27, pp. 637-645, 2011.

[87] Leroy, F. and Müller-Plathe, F., "Can continuum thermodynamics characterize Wenzel wetting states of water at the nanometer scale?", Journal of Chemical Theory and Computation, 8, pp. 3724-3732, 2012.

[88] Leroy, F. and Müller-Plathe, F., "Dry-surface simulation method for the determination of the work of adhesion of solid–liquid interfaces", Langmuir, 31, pp. 8335-8345, 2015.

[89] Khalkhali, M., Kazemi, N., Zhang, H. and Liu, Q., "Wetting at the nanoscale: a molecular dynamics study", The Journal of Chemical Physics, 146, p. 114704, 2017.

[90] Rønneberg, S., Xiao, S., He, J. and Zhang, Z., "Nanoscale correlations of ice adhesion strength and water contact angle," Coatings, 10, 2020.

[91] Ambrosetti, A., "van der Waals-corrected ab initio study of water ice–graphite interaction", The Journal of Physical Chemistry C, 117, pp. 321-325, 2013.

[92] Anick, D.J., "Static density functional study of graphene–hexagonal bilayer ice interaction", The Journal of Physical Chemistry A, 118, pp. 7498-7506, 2014.

[93] "Quantum Expresso", https://www.quantum-espresso.org Retrieved December 18, 2020.

[94] "CP2K", https://www.cp2k.org Retrieved December 18, 2020.

[95] "VASP", https://www.vasp.at Retrieved December 18, 2020.

[96] "CRYSTAL", https://www.crystal.unito.it/index.php Retrieved December 18, 2020.

[97] Attarzadeh, R. and Dolatabadi, A., "Icephobic performance of superhydrophobic coatings: A numerical analysis", International Journal of Heat and Mass Transfer, 136, pp. 1327-1337, 2019.

[98] Tembely, M., Attarzadeh, R. and Dolatabadi, A., "On the numerical modeling of supercooled micro-droplet impact and freezing on superhydrophobic surfaces," International Journal of Heat and Mass Transfer, 127, pp. 193-202, 2018.

[99] Zhang, J., Borg, M.K. and Reese, J.M., "Multiscale simulation of dynamic wetting", International Journal of Heat and Mass Transfer, 115, pp. 886-896, 2017.

[100] Strobl, T., Storm, S., Thompson, D., Hornung, M. and Thielecke, F., "Feasibility study of a hybrid ice protection system", Journal of Aircraft, 52, pp. 2064-2076, 2015.

[101] Guide: Guide for the Verification and Validation of Computational Fluid Dynamics Simulations, AIAA G-077-1998, 2002

[102] Hann, R., and Müller, N. Icing Validation Database. DataverseNO, Version 1, 2020. doi: 10.18710/5XYALW

[103] 1st AIAA Ice Prediction Workshop (IPW), www.icepredictionworkshop.com Retrieved December 18, 2020.

[104] AGARD, Advisory Group for Aerospace Research and Development, "Ice accretion simulation", AGARD Advisory Report AGARD-AR-344, Neuilly-Sur-Seine, France, December 1997.

[105] Myers, T.G. and Hammond, D.W., "Ice and water film growth from incoming supercooled droplets", International Journal of Heat and Mass Transfer, 42, pp. 2233-2242, 1999.

[106] Myers, T.G., "Extension to the Messinger model for aircraft icing", AIAA Journal, 39, pp. 211-218, 2001.

[107] Verdin, P., Charpin, J.P.F. and Thompson, C.P., "Multistep results in ICECREMO2", Journal of Aircraft, 46, pp. 1607-1613, 2009.

[108] Yanxia, D., Yewei, G., Chunhua, X. and Xian, Y., "Investigation on heat transfer characteristics of aircraft icing including runback water", International Journal of Heat and Mass Transfer, 53, pp. 3702-3707, 2010.

[109] Gori, G., Zocca, M., Garabelli, M., Guardone, A. and Quaranta, G., "PoliMIce: A simulation framework for three-dimensional ice accretion", Applied Mathematics and Computation, 267, pp. 96-107, 2015.

[110] Myers, T.G., Mitchell, S.L., Muchatibaya, G. and Myers, M.Y., "A cubic heat balance integral method for one-dimensional melting of a finite thickness layer", International Journal of Heat and Mass Transfer, 50, pp. 5305-5317, 2007.

[111] Chauvin, R., Bennani, L., Trontin, P. and Villedieu, P., "An implicit time marching Galerkin method for the simulation of icing phenomena with a triple-layer model", Finite Elements in Analysis and Design, 150, pp. 20-33, 2018.

[112] Xiao, J. and Chaudhuri S., "Design of anti-icing coatings using supercooled droplets as nano-to-microscale probes", Langmuir, 28, pp. 4434-4446, 2012.

[113] Longshaw, S.M., Borg, M.K., Ramisetti, S.B., Zhang, J., Lockerby, D.A., Emerson, D.R. and Reese, J.M., "mdFoam+: advanced molecular dynamics in OpenFOAM," Computer Physics Communications, 224, pp. 1-21, 2018.

[114] Kreutz, M., Ait-Alla, A., Varasteh, K., Oelker, S., Greulich, A., Freitag, M., Thoben, K.-D., "Machine learning-based icing prediction on wind turbines", Procedia CIRP, 81, pp. 423-428, 2019.

[115] Li, S., Qin, J., He, M. and Paoli, R., "Fast evaluation of aircraft icing severity using machine learning based on XGBoost", Aerospace, 7(4), p. 36, 2020.

[116] DeGennaro, A.M., Rowley, C.W. and Martinelli, L., "Uncertainty quantification for airfoil icing using polynomial chaos expansions", Journal of Aircraft, 52, pp. 1404-1411, 2015.

Appendix 3-1: NTNU ICING DATABASE

NTNU Icing Database Version: 1.0 (22.07.2020) / Authors: Nicolas Carlo Müller, Richard Hann / Contact: richard.hann@ntnu.no

ID	Title	Application	Test facilities	Year	Data Type	Geometry	2D/3D	Reynold s ×10^6	Mach	Icing Conditions	Results	Source/Reference	Authors, Title
1	NTNU low-speed IWT tests	UAV	VTT Finland, Cranfield UK	2019	Ice shapes	RG-15	2D	1	0.1	App. C (CM)	Manual tracings, photos, multiple experiments at identical setting	Unpublished data	
2	Ice accretions and icing effects for modern airfoils	Fixed-wing airfoil	IRT	2000	Ice shapes	Business jet, commercial transport, general avaition	2D	3-10	0.1-0.45	App. C, SLD	Tracings, black/white photos	NASA/TP--2000-210031	Addy, Harold E. Ice accretions and icing effects for modern airfoils. National Aeronautics Administration, Glenn Research Center, 2000.
3	Technical Report 38,"Ice Accretion Simulation Evaluation Test,	Fixed-wing airfoil, rotorcraft airfoil	Artington, IRT, CEPr, BRAIT	2001	Ice shapes	NACA0012, GLC305, NLF0414, 3-element airfoil, SuperPuma blade, cylinder, NACA23014,	2D	3-6	0.3-0.5	App. C	Tracings	RTO-TR-038	NATO, RTO. Technical Report 38,"Ice Accretion Simulation Evaluation Test,". RTO-TR-038 AC/323 (AVT-006) TP/26, 2001.
4	Experimental investigation of water droplet impingement on airfoils, finite wings, and an S-Duct engine inlet	Airfoils, Finite Wings and a S-Duct Engine Inlet	NASA IRT, USA	2002	Impingement	2D airfoils single element and multi-element, swept Tail, S-duct engine inlet	2D/3D	1.6	0.22-0.4	MVD 11 to 94 microns	Blotter paper/measurements. Contains uncertainty analysis in Ref. 30.	NASA/TM—2002-211700	Experimental investigation of water droplet impingement on airfoils, finite wings, and an S-Duct engine inlet; Papadakis, Michael(Wichita State Univ., Wichita, KS United States) Hung, Kuohsing E.(Wichita State Univ., Wichita, KS United States)
5	An Experimental Correlation between Rotor Test and Wind Tunnel Ice Shapes on NACA 0012 Airfoils	Helicopter	AERTS	2011	Ice shapes	NACA 0012 helicopter test blades	3D	1	0.1	App. C	3D scans	DOI: 10.4271/2011-38-0092	Han, Yiqiang, Palacios, Jose, Luis Smith, Edward C.;An Experimental Correlation between Rotor Test and Wind Tunnel Ice Shapes on NACA 0012 Airfoils;SAE Technical Papers;2011
6	Ice-Accretion Test Results for Three Large-Scale Swept-Wing Models in the NASA Icing Research Tunnel	Aircraft	IRT	2016	Ice shapes	CRM	3D	0.34-0.41		App. C	3D Scans	DOI: 10.2514/6.2016-3733	Ice-Accretion Test Results for Three Large-Scale Swept-Wing Models in the NASA Icing Research TunnelBroeren, Andy P.(NASA Glenn Research Center, Cleveland, OH United States) Potapczuk, Mark G.(NASA Glenn Research Center, Cleveland, OH United States)
7	Effects of thermal conductivity of airframe substrate on the dynamic ice accretion process pertinent to UAS	UAV	ISU-IRT	2018	Ice shapes	NACA0012	2D	0.4	0.1	LWC 1-2 MVD 20	Photos/Temperature Profiles	DOI: 10.1016/2018.11.132	Linkai Li, Yang Liu, Zichen Zhang, Hui Hu, Effects of thermal conductivity of airframe substrate on the dynamic ice accretion process pertinent to UAS inflight icing phenomena, International Journal of Heat and Mass Transfer, Volume 131, 2019, Pages 1184-1195, ISSN 0017-9310,
8	An experimental study on the aerodynamic performance degradation of a UAS propeller model	UAV	ISU-IRT	2018	Ice shapes, Aero impact	UAV Propeller Modell	3D	0.03	0.1	LWC 1-2 MVD 20	Ice Shapes/PIV Measurements	DOI: 10.1016/2018.11.008	Yang Liu, Linkai Li, Wenli Chen, Wei Tian, Hui Hu, An experimental study on the aerodynamic performance degradation of a UAS propeller model induced by ice accretion process, Experimental Thermal and Fluid Science, Volume 102, 2019, Pages 101-112, ISSN 0894-1777,
9	Effect of Variable LWC on Ice Shape in the NASA-GRC IRT	UAV	NASA - GRC IRT	2003	Ice shapes	NACA 0012	2D	?		LWC 0.35-2.4/ MVD 20	Manual tracings, photos	DOI: 10.2514/6.2003-904	George G. Koenig, Charles C. Ryerson, J. Larsson, Andrew Reehorst;EFFECT OF VARIABLE LWC ON ICE SHAPE IN THE NASA-GRC IRT,NASA Glenn Research Center,2003
10	The Icing of an Unheated, Nonrotating Cylinder. Part II. Icing Wind Tunnel Experimentsm Low Temperature	General	NRC	1983	Ice shapes	Zylinder	2D	0.06-0.2	0.1-0.5	LWC = 0.13-1.25	Manual tracings, photos	doi.org/10.1175/1520-0450(1983)022<2063:TIOAUN>2.0.CO;2	E. P. Lozowski, J. R. Stallabrass, and P. F. Hearty, The Icing of an Unheated, Nonrotating Cylinder. Part II. Icing Wind Tunnel Experimentsm Low Temperature Laboratory, Division of Mechanical Engineering, National Research Council of Canada, Ottawa, Ontario, Canada KIA OR6
11	An experimental study on the dynamic ice accretion processes on bridge cables with different surface	General	ISU-IRT	2019	Ice shapes, Aero impact	Cables	2D	0.125-0.15	0.1	LWC 1-3	Pictures/Transient Icing Data	https://doi.org/10.1016/j.jweia.2019.05.007	Yang Liu, Wenli Chen, Yihua Peng, Hui Hu, An experimental study on the dynamic ice accretion processes on bridge cables with different surface modifications, Journal of Wind Engineering and Industrial Aerodynamics, Volume 190, 2019, Pages 218-229, ISSN 0167-6105,
12	An experimental study on the aerodynamic performance degradation of a wind turbine blade	Wind turbine	ISU-IRT	2018	Ice shapes, Aero impact	DU91-W2-250 Airfoil	2D	0.42	0.1	MVD 20; LWC 1.1	Pictures/Transient Icing Data/Transient Performance Data/PIV Measurements	https://doi.org/10.1016/j.renene.2018.10.032	Linyue Gao, Yang Liu, Wenwu Zhou, Hui Hu, An experimental study on the aerodynamic performance degradation of a wind turbine blade model induced by ice accretion process, Renewable Energy, Volume 133, 2019, Pages 663-675, ISSN 0960-1481
13	An Experimental Study to Evaluate Hydro-/Ice-Phobic Coatings for Icing Mitigation over Rotating Aero-engine	Engine	ISU-IRT	2019	Ice shapes, Aero impact						Pictures/Transient Icing Data/Transient Performance Data	https://doi.org/10.4271/2019-01-1980	Tian, Linchuan and Liu, Yang and Li, Linkai and Hu, Hui;An Experimental Study to Evaluate Hydro-/Ice-Phobic Coatings for Icing Mitigation over Rotating Aero-engine Fan Blades;International Conference on Icing of Aircraft, Engines, and Structures;2019
14	An Experimental Study of the Dynamic Ice Accreting Process over a Rotating Aero-engine Fan Model	Engine	ISU-IRT	2018	Ice shapes, Aero impact	Engine Inlet Model	3D	0.1	0.05	MVD ~ 20; LWC 0.5-2	Pictures/Transient Icing Data/Transient Performance Data	doi: 10.2514/6.2018-3013	Linkai Li, Yang Liu, Hui Hu; An Experimental Study of the Dynamic Ice Accreting Process over a Rotating Aero-engine Fan Model; Department of Aerospace Engineering, Iowa State University; 2018
15	An experimental study on the anti-icing performance of superhydrophobic surface on a	UAV	ISU-IRT	2017	Ice shapes, Aero impact	UAV Propeller Modell	3D	0.05	0.1	Wet Glaze ice	Pictures/Transient Icing Data/Transient Performance Data	DOI: 10.2514/6.2017-4474	Liu, Y., Li, L., & Hu, H. (2017). An experimental study on the anti-icing performance of superhydrophobic surface on a rotating UAS propeller. In 9th AIAA Atmospheric and Space Environments Conference, 2017. American Institute of Aeronautics and Astronautics Inc, AIAA.
16	Wind Turbine Performance under Icing Conditions	Wind Turbine	Anti-icing Materials International	2008	Ice Shapes	NACA 63 415 blade profile	2D	0.26-0.733	0.1	MVD 27.6; LWC 0.37-0.48	Pictures/Manual Tracings/Ice Mass/Aerodynamic Performance Data	DOI: 10.1002/we.258	Clement Hochart, Guy Fortin and Jean Perron,Wind Turbine Performance under Icing Conditions, Université du Québec à Chicoutimi, 2008
17	An Experimental Study on the Dynamic Ice Accretion Processes on Bridge Cables with Different Surface	General	ISU-IRT	2019	Ice shapes, Aero impact	Bridge Cables	2D	n/a	n/a	MVD 20; LWC ~3	Pictures/Transient Icing Data/Transient Performance Data	https://doi.org/10.4271/2019-01-2018	Liu, Yang and Peng, Yihua and Chen, Wenli and Hu, Hui;An Experimental Study on the Dynamic Ice Accretion Processes on Bridge Cables with Different Surface Modifications;International Conference on Icing of Aircraft, Engines, and Structures;SAE International;2019
18	An experimental investigation of dynamic ice accretion process on a wind turbine airfoil model considering	Wind Turbine	ISU-IRT	2018	Ice shapes, Aero impact	DU96-W-180	2D	0.4	0.1	MVD 20; LWC 0.3-3	Pictures/Transient Icing Data/Transient Performance Data/Temperature	https://doi.org/10.1016/j.ijheatmasstransfer.2018.12.181	Linyue Gao, Yang Liu, Hui Hu, An experimental investigation of dynamic ice accretion process on a wind turbine airfoil model considering various icing conditions, International Journal of Heat and Mass Transfer, Volume 133, 2019, Pages 930-939, ISSN 0017-9310,
19	An experimental investigation on the dynamic glaze ice accretion process over a wind turbine airfoil surface	Wind Turbine	ISU-IRT	2019	Ice shapes, Aero impact	DU91-W2-250	2D	0.3	0.1	MVD 20; LWC = 3.3-6.7	Pictures/Transient Icing Data/Transient Performance Data/3D Scans	https://doi.org/10.1016/j.ijheatmasstransfer.2019.119120	Linyue Gao, Yang Liu, Hui Hu, An experimental investigation on the dynamic glaze ice accretion process over a wind turbine airfoil surface, International Journal of Heat and Mass Transfer, Volume 149, 2020, 119120, ISSN 0017-9310,
20	An Experimental Study of Dynamic Ice Accretion Process on Aero-engine Spinners	Engine	ISU-IRT	2017	Ice shapes	Boeing 18-inch fan rig/Spinner	3D	0.3	0.05	MVD 10-50	Pictures/Transient Icing Data	https://arc.aiaa.org/doi/abs/10.2514/6.2017-0551	Linkai Li and Hui Hu; An Experimental Study of Dynamic Ice Accretion Process on Aero-engine Spinners; 55th AIAA Aerospace Sciences Meeting;2017
21	An experimental study on a hot-air-based anti-/de-icing system for aero-engine inlet guide vanes	Engine	ISU-IRT	2019	De-Icing/Runback Icing	Naca 0012 Airfoil (Inlet Guide Vane)	2D	0.3	0.1	MVD = 20	Pictures/Transient Icing Data	https://doi.org/10.1016/j.applthermaleng.2019.114778	Linkai Li, Yang Liu, Linchuan Tian, Haiyang Hu, Hui Hu, Xuejun Liu, Isaac Hogate, Atul Kohli, An experimental study on a hot-air-based anti-/de-icing system for aero-engine inlet guide vanes, Applied Thermal Engineering, Volume 167, 2020, 114778, ISSN 1359-4311,
22	An Experimental Study on the Effects of the Layout of DBD Plasma Actuators on Its Anti-/De-Icing Performance for	Engine	ISU-IRT	2019	De-Icing	Naca 0012 Airfoil	2D	n/a	n/a		Pictures/Transient Icing Data/Transient Performance Data/Temperature	DOI: 10.4271/2019-01-2033	Kolbakir, Cem and Liu, Yang and Hu, Haiyang and Hu, Hui; An Experimental Study on the Effects of the Layout of DBD Plasma Actuators on Its Anti-/De-Icing Performance for Aircraft Icing Mitigation; 2019
23	Dynamic ice accretion process and its effects on the aerodynamic drag characteristics of a power transmission	General	ISU-IRT	2020	Ice shapes, Aero impact	Power Cable	2D	0.5	0.1	LWC = 1-2	Pictures/Transient Icing Data/Transient Performance Data/3D Scans	https://doi.org/10.1016/j.coldregions.2019.102908	Ramsankar Veerakumar, Linyue Gao, Yang Liu, Hui Hu, Dynamic ice accretion process and its effects on the aerodynamic drag characteristics of a power transmission cable model, Cold Regions Science and Technology, Volume 169, 2020, 102908, ISSN 0165-232X,
24	Quantification of the 3D shapes of the ice structures accreted on a wind turbine airfoil mode	Wind Turbine	ISU-IRT	2019	Ice shapes, Aero impact	DU91-W2-250	2D	0.3	0.1	MVD = 20; LWC = 1.2	Pictures/Transient Icing Data/Transient Performance Data/3D Scans	https://doi.org/10.1007/s12650-019-00567-4	Linyue Gao, Ramsankar Veerakumar, Yang Liu, Hui Hu; Quantification of the 3D shapes of the ice structures accreted on a wind turbine airfoil mode; 2019
25	An Experimental Study on the Transient Ice Accretion Process over the Blade Surfaces of a Rotating UAS	UAV	ISU-IRT	2017	Ice shapes, Aero impact	UAV Propeller Modell	3D	0.05	0.1	Appendix C	Pictures/Transient Icing Data/Transient Performance Data	DOI: 10.2514/6.2017-0727	Yang Liu, Linkai Li, Zhe Ning, Wei Tian and Hui Hu;An Experimental Study on the Transient Ice Accretion Process over the Blade Surfaces of a Rotating UAS Propeller; Department of Aerospace Engineering, Iowa State University; 2017

26	Experimental and Computational Ice Shapes and Resulting Drag Increase for a NACA 0012 Airfoil	Aircraft	IRT	1992	Ice shapes	Naca 0012 Airfoil	2D	2-3	0.3	MVD = 10-40 ; LWC 0.3 -3	Tracings	NASA Technical Memorandum 105743	Jaiwon Shin and Thomas H. Bond; Experimental and Computational Ice Shapes and Resulting Drag Increase for a NACA 0012 Airfoil; 1992
27	30th Aerospace Sciences Meeting and Exhibit	Aircraft	IRT	1992	Ice shapes	Naca 0012 Airfoil	2D	2-3	0.3	MVD = 20-30; LWC = 0.55-1.8	Tracings	NASA Technical Memorandum 105374	Jaiwon Shin and Thomas H. Bond ; Results of an Icing Test on a NACA 0012 Airfoil in the NASA Lewis Icing Research Tunnel; 1992
28	Scaled ice accretion experiments on a rotating wind turbine blade	Wind Turbine	AERTS	2011	Ice Shapes	S809	3D	0.9-1.2	0.2	MVD = 20-30; LWC = 0.08-1.2	Tracings, Shaft Torque	http://dx.doi.org/10.1016/j.jweia.2012.06.001	Yiqiang Han, JosePalacios,SvenSchmitz; Scaled ice accretion experiments on a rotating wind turbine blade; Journal of Wind Engineering and Industrial Aerodynamics; 2012
29	Icing Wind Tunnel Test of a Full Scale Heated Tail Rotor Model	Helicopter	NRC	2014	Ice shapes	Helicopter Tailplane	3D	n/a	n/a		n/a		Wright, J., and Aubert, R., "Icing Wind Tunnel Test of a Full Scale Heated Tail Rotor Model," presented at the AHS 70th Annual Forum, Montreal, Canada, 20-22 May, 2014.
30	The Influence of SLD Drop Size Distributions on Ice Accretion in the NASA Icing Research Tunnel	Airfoil	IRT	2019	Ice shapes	NACA 23012 airfoil	2D	6-15	0.3	Appendix O	Tracings/Photos/Scans	GRC-E-DAA-TN68067	Potapczuk, Mark G,Tsao, Jen-Ching; The Influence of SLD Drop Size Distributions on Ice Accretion in the NASA Icing Research Tunnel; 2019
31	An overview of a model rotor icing test in the NASA Lewis Icing Research Tunnel	Helicopter	IRT	1994	Ice shapes	PFM/UH60 1/5.727	3D	1.5	0.6	App C	Tracings/Molds	doi:10.2514/6.1994-716	Britton, R., Bond, T., & Flemming, R. (1994). An overview of a model rotor icing test in the NASA Lewis Icing Research Tunnel. 32nd Aerospace Sciences Meeting and Exhibit.
32	Spring Rotor Blade Tests in Icing Wind Tunnel	Helicopter	AMIL IWT	2009	Ice shapes	SRB/NACA0012	3D	0.77-5.9	0.4-0.7		Pictures/Force and Power Readings	AIAA-2009-4260	Fortin, G. and Perron, J., "Spring Rotor Blade Tests in Icing Wind Tunnel," AIAA-2009-4260, 1st AIAA Atmosphere and Space Environments Conference, June 2009
33	Large and Small Droplet Impingement data on Airfoils and Two Simulated Ice Shapes	Airfoils	Goodrich IWT, NASA IRT	2000	Impingement	2D Airfoils	2D	1.6	0.2	MVD 11 to 270 microns/App C	Blotter paper/measurements.		
34	Experimental ice shape and performance characteristics for a multi-element airfoil in the NASA lewis icing	Airfoils	NASA IRT, USA	1991	Ice shapes, Aero impact	2D Multi-element (737 section 18%)	2D	1.25	0.15	App C	traces, data tables, lift, drag and pitching moment,	NASA TM 105380	Experimental ice shape and performance characteristics for a multi- element airfoil in the NASA lewis icing research tunnel Berkowitz, Brian M.(Sverdrup Technology, Inc., Brook Park, OH., United States) Potapczuk, Mark G.(Boeing Computer Services Co., Sea le, WA., United States)
35	Improvement of the ONERA 3D Icing Code, Comparison with 3D Experimental Shapes												
36	Icing Analysis and Test of's Business Jet Engine Inlet Duct	Inlet	Cox Icing Wind Tunnel	2000	Ice Shapes (Impingement though Lewice)	S-duct engine inlet	3D	n/a	n/a	MVD 15-60	Pictures	AIAA 2000-1040	K. Al-Khalil, R. Hitzigrath,0. Philippi,C. Bidwell,,Icing Analysis and Test of's Business Jet Engine Inlet Duct, 2000
37	Project „SOPHIA-2" – Final Report	UAV Propeller	CWT	2019	Ice Shapes /Aero results	UAVs	3D	n/a	0.05	MVD 20-40; LWC 0.48-2.5	Pictures Force Measurements	Project „SOPHIA-2" – Final Report	Dr. Martin Fengler CEO;Project „SOPHIA-2" – Final Report; Meteomatics AG Lerchenfeldstrasse; 2019
38	THE EXPERIMENTAL INVESTIGATION OF A ROTOR ICING MODEL WITH SHEDDING	Helicopter	AERTS	2010	Ice Shapes	Helicopter Rotor model	3D	0.6-0.9	0.3	MVD 15-40; LWC 3-6	Pictures /Traces	https://etda.libraries.psu.edu/files/final_submissions/1875	Edward W. Brouwers; THE EXPERIMENTAL INVESTIGATION OF A ROTOR ICING MODEL WITH SHEDDING; The Pennsylvania State University ; 2010
39	Validation Ice Crystal Icing Engine Test in the Propulsion Systems Laboratory at NASA Glenn Research Center	Engine	PSL 3	2015	Performance/Ice Shapes	ALF502-RS	3D	n/a	n/a	App C	Pictures/Perfomrance Readings	https://ntrs.nasa.gov/search.jsp?R=20150002330	Michael J. Oliver; Validation Ice Crystal Icing Engine Test in the Propulsion Systems Laboratory at NASA Glenn Research Center; NASA Glenn Research Center, Cleveland, OH, 44135; 2015
40	Experimental Study on Icing and Anti-Icing Characteristics of Engine Inlet Guide Vanes	Engine	YBF-02	2015	Ice Shapes/Deicing	Inlet Guide Vanes	3D	n/a	0.3	MVD = 20; LWC = 0.5-2	Pictures/Temperature	DOI: 10.2514/1.B35679	W. Dong,* J. Zhu,† M. Zheng,‡ and G. L. Lei, Z. X. Zhou; Experimental Study on Icing and An- Icing Characteris cs of Engine Inlet Guide Vanes; JOURNAL OF PROPULSION AND POWER, 2015
41	Experiment Investigation of Hot-air Anti-icing Structure of Engine Inlet Vane	Engine	Small open-circuit icing wind tunnel	2016	Deicing	Inlet Vane	2D	?	0.1	MVD 20; LWC = 1-2	Pictures	978-1-5090-1087-5/16	Ma Hui, Zhang Dalin; Experiment Investigation of Hot-air Anti-icing Structure of Engine Inlet Vane; 2016 IEEE/CSAA International Conference on Aircraft Utility Systems (AUS); 2016
42	Collection Efficiency and Ice Accretion Characteristics of Two Full Scale and One 1/4 Scale Business Jet Horizontal	Aircraft	IRT	2005	Ice Shapes	Jet Horizontal Tail	3D	5	0.2	MVD = 21	Collection Efficiency Plots	NASA/TM—2005-213653	Colin S. Bidwell, Michael Papadakis; Collection Efficiency and Ice Accretion Characteristics of Two Full Scale and One 1/4 Scale Business Jet Horizontal Tails; SAE General Aviation Technology Conference and Exposition; 2000
43	Ice Accretions and Full-Scale Iced Aerodynamic Performance Data for a Two-Dimensional NACA 23012 Airfoil	Aircraft	IRT	2016	IceShapes/Aero Data	NACA 23012 Airfoil	2D	########	0.1-0.29	App C	Tracings/Pressure Plots/ Photos	NASA/TP-2016-218348	Ice Accretions and Full-Scale Iced Aerodynamic Performance Data for a Two-Dimensional NACA 23012 Airfoil Addy, Harold E., Jr.(NASA Glenn Research Center, Cleveland, OH, United States) Broeren, Andy P.(NASA Glenn Research Center, Cleveland, OH, United States)
44	Validation of 3-D Ice Accretion Measurement Methodology for Experimental Aerodynamic Simulation		IRT/University of Illinois low-speed wind	2015	Aerodynamic Performance/Ice shapes	NACA23012	2D	1.8	0.18	MVD 15-30 LWC 0.3-0.75	Scan/Photos/Aerodynamic Dat	NASA/TM-2015-218724	Validation of 3-D Ice Accretion Measurement Methodology for Experimental Aerodynamic Simulation Broeren, Andy P.(NASA Glenn Research Center, Cleveland, OH United States) Addy, Harold E., Jr.(NASA Glenn Research Center, Cleveland, OH United States)
45	Ice Accretions on a Swept GLC-305 Airfoil	Aircraft	IRT	2002	Ice Shapes		3D	2	0.2	App C	Photos/Molds	NASA/TM-2002-211557	Ice Accretions on a Swept GLC-305 Airfoil Vargas, Mario(NASA Glenn Research Center, Cleveland, OH United States)
46	Modern Airfoil Ice Accretions	Aircraft	IRT	1997	ICE Shapes		2D	3.5	0.4	App C	Pictures/Tracings/Aerodynamic Results		Modern Airfoil Ice Accretions Addy, Harold E., Jr.(NASA Lewis Research Center, Cleveland, OH United States) Potapczuk, Mark G.(NASA Lewis Research Center, Cleveland, OH United States)
47	A Database of Supercooled Large Droplet Ice Accretions		IRT	2007	Ice Shapes	Jet Aircraft airfoils	2D	2.5-13	0.1-0.3	App C	Pictures/Scans	NASA/CR—2007-215020	Van Zante, J.F., "A Database of Supercooled Large Droplet Ice Accretions," NASA/CR—2007-215020, Sept., 2007.
48	Experimental Investigation of Ice Accretion Effects on a Swept Wing	Aircraft	IRT/WSU	2005	Ice Shapes/Aerodynamics	Swept Wing	3D	1-4	0.1-0.3	App C	Tracings/Pictures/Molds/Aerodynamic Performance	DOT/FAA/AR-05/39	Experimental Investigation of Ice Accretion Effects on a Swept Wing Papadakis, M. Yeong, H. W.
49	An Integrated Approach to Swept Wing Icing Simulation		IRT/Wichita State University Walter H.		Aerodynamic Performance/Ice shapes	CRM65	3D	1.8-15.9	0.1-0.28	App C	Tracing/Scans/Photos/Aerodynamic Performance	GRC-E-DAA-TN44244	An Integrated Approach to Swept Wing Icing Simulation Potapczuk, Mark G.(NASA Glenn Research Center, Cleveland, OH United States) Broeren, Andy P.(NASA Glenn Research Center, Cleveland, OH United States)
50	Summary of Ice Shape Geometric Fidelity Studies on an Iced Swept Wing		IRT/Wichita State University Walter H.	2018	Aerodynamic Performance/Ice shapes	CRM65	3D	1.8-15.9	0.1-0.28	App C	Tracing/Scans/Photos/Aerodynamic Performance	GRC-E-DAA-TN56726	Summary of Ice Shape Geometric Fidelity Studies on an Iced Swept Wing Woodard, Brian S.(Illinois Univ., Urbana-Champaign, IL, United States) Broeren, Andy P.(NASA Glenn Research Center, Cleveland, OH, United States)
51	Water droplet impingement on airfoils and aircraft engine inlets for icing analysis	Aircraft	IRT	1991	Impingement	Airfoils/Engine inlet	2D/3D	-	-	-	Impingement measurement	19910053920	Water droplet impingement on airfoils and aircraft engine inlets for icing analysis Papadakis, Michael(Wichita State University, KS, United States) Elangovan, R.(Wichita State Univ., Wichita, KS, United States)

52	Experimental Water Droplet Impingement Data on Airfoils, Simulated Ice Shapes, an Engine Inlet		IRT	1994	Impingement	Airfoils/Engine inlet	2D/3D	4.5	0.2	App C	Impingement measurement	19950065794	Experimental Water Droplet Impingement Data on Airfoils, Simulated Ice Shapes, an Engine Inlet and a Finite Wing Papadakis, M.(Wichita State Univ., Wichita, KS, United States) Breer, M.(Boeing Military Airplane Development, Wichita, KS., United States)
53	Experimental Study of Supercooled Large Droplet Impingement Effects		?	2003	Impingement	?	?	?	?	App C	?	20040006403	Experimental Study of Supercooled Large Droplet Impingement Effects Papadakis, M. Rachman, A.
54	Large and Small Droplet Impingement Data on Airfoils and Two Simulated Ice Shapes	Aircraft	IRT	2007	Impingement	Airfoil/Simulated Ice Shapes	2D	1.6	0.2	App C	Impingement measurement	NASA/TM-2007-213959, E-15275	Large and Small Droplet Impingement Data on Airfoils and Two Simulated Ice Shapes Papadakis, Michael(Wichita State Univ., Wichita, KS, United States) Wong, See-Cheuk(Wichita State Univ., Wichita, KS, United States)
55	Water Droplet Impingement on Simulated Glaze, Mixed, and Rime Ice Accretions	Aircraft	IRT	2007	Impingement	MS(1)–317 Airfoil, NACA 23012 Airfoil	2D	1.6	0.2	App C	Impingement measurement	NASA/TM-2007-213961, E-15277	Water Droplet Impingement on Simulated Glaze, Mixed, and Rime Ice Accretions Papadakis, Michael(Wichita State Univ., Wichita, KS, United States) Rachman, Arief(Wichita State Univ., Wichita, KS, United States)
56	Validation Results for LEWICE 3.0	Aircraft	IRT	2005	Impingement	Airfoils	2D	1.6	0.2	App C	Impingement measurement	NASA/CR-2005-213561, E-15007, AIAA Paper 2005-1243	Validation Results for LEWICE 3.0 Wright, William B.(QSS Group, Inc., Cleveland, OH, United States) NASA/CR-2005-213561, E-15007, AIAA Paper 2005-1243
57	An Experimental and Numerical Study of Icing Effects on the Performance and Controllability of a Twin Engine	Aircraft	IRT	1998	Ice Shape	Aircraft Wing Section	2D	10	0.2	MVD 20-270; LWC 0.52-0.85	Pictures/Tracings/Aerodynamic Results	NASA/TM-1999-208896, E-11495, NAS 1.15:208896, ICOMP-99-	An Experimental and Numerical Study of Icing Effects on the Performance and Controllability of a Twin Engine Aircraft; Reehorst, A.(NASA Lewis Research Center, Cleveland, OH United States) Chung, J.(NASA Lewis Research Center, Cleveland, OH United States)
58	Ice Protection System	Aircraft	IRT	2001	Ice Protection	Airfoil	2D	2.5-5.0	0.1-0.2	App C	Tracings	NASA/TM—2001-210907	Validation of NASA Thermal Ice Protection Computer Codes Part 3: The Validation of Antice; Al-Khalil, Kamel M.(Cox and Co., Inc., New York, NY United States) Horvath, Charles(Cox and Co., Inc., New York, NY United States)
59	Ice Roughness and Thickness Evolution on a Swept NACA 0012 Airfoil	Aircraft	IRT	2017	Ice Shape	NACA0012	2D	4	0.2	App C/App O	Ice Scan/Ice Roughness	GRC-E-DAA-TN42660	Ice Roughness and Thickness Evolu on on a Swept NACA 0012 Airfoil;McClain, Stephen T.(Baylor Univ., Waco, TX, United States) Vargas, Mario(NASA Glenn Research Center, Cleveland, OH United States)
60	Improvement of the ONERA 3D Icing Code, Comparison with 3D Experimental Shapes	Helicopter	CEPr	1993	Ice Shape	Rotor Blade Tip	3D	1-6.5	0.3	MVD = 14-20	Tracings	AIAA 93-0169	T.Hedde, D.Guffond; Improvement of the ONERA 3D Icing Code, Comparison with 3D Experimental Shapes; 31st Aerospace Science Meeting Exhibit, Reno, NV 1993
61	Independent Effects of Reynolds and Mach Numbers on the Aerodynamics of an Iced Swept Wing	Wing	ONERA F1	2018	Aerodynamic Performance	CRM	3D	1.6-11.9	0.09-0.34	Appendix C	Aerodynamic Performance	doi:10.2514/6.2018-3492	Broeren, A. P., Lee, S., Woodard, B., Lum, C. W., & Smith, T. G. (2018). Independent Effects of Reynolds and Mach Numbers on the Aerodynamics of an Iced Swept Wing. 2018 Atmospheric and Space Environments Conference.
62	A Wind Tunnel Study of Icing Effects on a Business Jet Airfoil	Aircraft	LTPT	2003	Aerodynamic Performance	GLC-3059 airfoil	2D	3.5-10.5	0.12-0.28	Appendix C	Aerodynamic Performance	AIAA–2003–0727	H. Addy, A. Broeren, J. Zoeckler, S. Lee; A Wind Tunnel Study of Icing Effects on a Business Jet Airfoil; 41st Aerospace Sciences Meeting and Exhibit;2003
63	Comparison of Iced Aerodynamic Measurements on Swept Wing from Two Wind Tunnels	Aircraft	ONERA F1/WSU	2018	Aerodynamic Performance	CRM	3D	1.6-2.7	0.09-0.18	Appendix C	Aerodynamic Performance	doi:10.2514/6.2018-3493	Lee, S., Broeren, A. P., Woodard, B., Lum, C. W., & Smith, T. G. (2018). Comparison of Iced Aerodynamic Measurements on Swept Wing from Two Wind Tunnels. 2018 Atmospheric and Space Environments Conference. doi:10.2514/6.2018-3493
64	Super Cooled Large Droplet Analysis of Several Geometries Using LEWICE3D Version 3	Aircraft	IRT	2011	Aerodynamic Performance/ Collection	Sweept 64A008 wing/ Multi Element model	3D	5	0.25	SLD	Aerodynamic Performance/Impingement	NASA/TM—2011-216945	Colin S. Bidwell; Super Cooled Large Droplet Analysis of Several Geometries Using LEWICE3D Version 3; Glenn Research Center, Cleveland, Ohio; 2011
65	Icing Simulation Research Supporting the Ice-Accretion Testing of Large-Scale Swept-Wing Models	Aircraft	IRT	2018	Aerodynamic Performance/Ice Shapes	65% CRM Hybrid Test Model	3D	2.5-6.5	0.2-0.41	LWC = 0.3-1; MVD 20-28	Ice Shape Scan/Aerodynamic Performance Data	NASA/CR—2018-219781	Yoram Yadlin,Jaime T. Monnig, Adam M. Malone, and Bernard P. Paul; Icing Simulation Research Supporting the Ice-Accretion Testing of Large-Scale Swept-Wing Models; 2018
66	Lewice Modelling of Swept Wing Ice Accretions	Aircraft	IRT/Wichita State University Subsonic Wind	2003	Ice Shapes/Aerodynamic	Sweept GLC-305	3D	2.5-4.3	0.18-0.3	App. C	Molds	AIAA 2003-730	Mark G. Potapczuk,Michael J. Papadakis,Mario Vargas; LEWICE MODELING OF SWEPT WING ICE ACCRETIONS; 41st Aerospace Sciences Meeting and Exhibit; 2003
67	Implementation and Validation of 3-D Ice Accretion Measurement Methodology	Aircraft	IRT	2014	Ice Shapes	NACA 23012, Sweept NACA0012	2D/3D	2.6-6.0	0.3	MVD 0.15-0.32; LWC 0.45-0.6	Photographs/Scans/Castings	AIAA 2014-2613	Sam Lee,Andy P. Broeren, Richard E. Kreeger, Mark Potapczuk,Lloyd Utt; Implementation and Validation of 3-D Ice Accretion Measurement Methodology; 6th AIAA Atmospheric and Space Environments Conference; 2014
68	Ice Shapes on a Tail Rotor	Aircraft	IRT	2014	Ice Shapes	Tail Rotor	3D	0.26-0.65	0.1-0.22	LWC = 0.5; MVD = 15-110	Photographs/Scans/Tracings	AIAA 2014-2612	Richard E. Kreeger, Jen-Ching Tsao; Ice Shapes on a Tail Rotor; 6th AIAA Atmospheric and Space Environments Conference; 2014
69	Icing Analysis of a Swept NACA 0012 Wing Using LEWICE3D Version 3. 48	Aircraft	IRT	2014	Ice Shapes	Sweept Naca 0012	3D	2.6-6.0	0.15-0.3	MVD 0.15-0.32; LWC 0.45-1.5	Wax Moldings/Ice density/Ice Volume	AIAA 2014-2200	Colin S. Bidwell; Icing Analysis of a Swept NACA 0012 Wing Using LEWICE3D Version 3. 48; 6th AIAA Atmospheric and Space Environments Conference; 2014
70	Collection Efficiency and Ice Accretion Calculations for a Sphere, a Swept MS(1)-317 Wing, a Swept NACA-0012 Wing Tip, an Axisymmetric Inlet, and a Boeing 737-300 Inlet	Aircraft	IRT	1995	Aerodynamic Performance/Impingement	Sphere, Swept MS(1)-317 Wing, Swept NACA-0012 Wing Tip, Axisymmetric Inlet, Boeing 737-300 Inlet	3D	0.75-5	0.2	MVD 11.5-20.4	Impingement / Aerodynamic Measurement	AIAA-95-0755	Colin S. Bidwell, S.R. Mohler, Jr.; Collection Efficiency and Ice Accretion Calculations for a Sphere, a Swept MS(1)-317 Wing, a Swept NACA-0012 Wing Tip, an Axisymmetric Inlet, and a Boeing 737-300 Inlet; 33rd Aerospace Sciences Meeting and Exhibit; 1995
71	An Experimental Method for Measuring Water Droplet Impingement Efficiency on Two- and Three-Dimensional Bodies	Engine	IRT	1989	Impingement	2D Flow Models, Engine Inlets	2D/3D	0.4-5	0.2-0.25	MVD: 16.45-20.36	Impingement	DOT/FAA/CT–87/22	M. Papadakis, R. Elangonan, G.A. Freund, Jr., M. Breer, G.W. Zumwalt, and L. Whitmer; An Experimental Method for Measuring Water Droplet Impingement Efficiency on Two- and Three-Dimensional Bodies; 1989

Chapter 4 – EXPERIMENTAL ICING FACILITIES

Giuseppe Mingione and Biagio Esposito
Centro Italiano Ricerche Aerospaziale (CIRA)
ITALY

Julio Mora and Paloma García
Instituto Nacional de Técnica Aeroespacial (INTA)
SPAIN

Ki-Han Kim
Office of Naval Research
UNITED STATES

Francisco Redondo
Airbus Military
SPAIN

4.1 INTRODUCTION

There are numerous icing research laboratories and facilities worldwide, ranging from small-scale laboratories typically doing basic research in academia and R&D organizations to large Icing Wind Tunnels (IWT) that can simulate more realistic icing environments and test large-scale structures such as airplane wings and other aircraft components, including full-scale engines. Since the nature of icing and operational environments for aircraft and marine vessels are very different, there are no large-scale testing facility for icing on marine vessels operating in the high-latitude regions.

Several previous studies on worldwide icing tunnels are available. In 1999, the US Society of Automotive Engineers (SAE) AC-9C Committee published a report (Aerospace Information Report, AIR5320) [1] based on the multi-year survey of 27 icing tunnels as well as other ground testing facilities around the world, including the USA, Canada, and Europe. The data in this report [1] represented the state of the facilities in 1996. This report was updated in 2015 and published as AIR5320A.

In 2001, the US Federal Aviation Administration (FAA) published a collection of papers as a report contributed by two groups [2]: 1) Industry users of icing simulation tools (facilities and computer codes) describing how they are used in design and certification processes; and 2) Developers and providers summarizing the numerical and experimental simulation capabilities and limitations of ice simulation tools available at that time in their respective areas. The industry users also presented a table summarizing gaps noted by different industry users and recommendations for improvement.

In this chapter, we reviewed these two documents focusing on regulations related to IWTs in an effort to identify areas of improvement in view of increased aircraft operations in the cold environment since these documents were published two decades ago. In particular, operations of Unmanned Aerial Vehicles (UAVs) in cold environment by the NATO nations have drastically increased. We also reviewed major worldwide IWTs to identify any upgrades made since the FAA and SAE studies have been published, and to identify any capability gaps to meet the emerging requirements by the rapidly increasing number of operations of air vehicles in cold environment.

In Section 4.2, we briefly reviewed general icing test facility and capabilities, including IWTs and flying test facilities, and identified advantages and disadvantages of testing in idealized and real icing environments. Section 4.3 focused on issues related to aircraft icing certification from FAA and European Aviation Safety Agency (EASA). We reviewed the so-called FAA Certification Specifications (CS-25) Appendix C, where they defined safe operating envelopes, and Appendix O, where they included more stringent requirements for safe operating envelopes. Sections 4.4 and 4.5 presented challenges for both IWTs and flying test facilities, respectively, to meet the emerging requirements. We then reviewed major worldwide IWTs in Section 4.6 and flying test facilities in Section 4.7 and identified some upgrades made since the SAE report in 1999, followed by a summary and some discussions (Section 4.8) and a list of references used for Chapter 4.

4.2 OVERVIEW OF ICING TEST FACILITIES AND CAPABILITIES

Icing test facilities can be grouped in two categories: icing wind tunnels and flying facilities. The IWTs can simulate a variety of idealized icing conditions and are primarily used for evaluation of performance of ice detection and protection systems, whereas flying test facilities provide more realistic icing environments than those created in IWTs. Despite high cost, there are occasions that would require flying tests, for example, for aircraft development and certification purposes. In this section, a brief overview is presented for the basic capabilities of IWTs and calibration issues, followed by an overview of flying facilities and representative flying test in artificial and natural icing conditions.

IWTs can also be classified depending on various factors, including the testing envelope with respect to certification requirements, the test article size, the speed and testing objectives. Major testing applications include airfoil/airframe, ice protection system, icing physics, ice accretion code validation, propulsion system, icing instrumentation and aircraft sensors (pitot probes, total temperature probes, etc.).

4.2.1 Icing Wind Tunnel (IWT)

An IWT is similar to a classic aerodynamic wind tunnel with two major additional features and functions (see Figure 4-1): a spray bar to inject water droplets in the flow circuit and a cooling chamber with a refrigeration system to control the temperature below freezing.

As in a classical wind tunnel the fan will provide the required air speed. The cooling chamber includes a heat exchanger that will control the air temperature to the desired values. Once the test speed and temperature are reached, the spray bar is activated. The spray bar consists of a large number of nozzles that will spray water droplets with a controlled diameter and concentration to simulate an actual cloud.

The IWTs are used to evaluate the effectiveness of ice detection and ice protection systems and to evaluate the shape and amount of ice accreted onto the test article. The amount of ice and profile accreted on the surfaces are required to evaluate the aerodynamic performance degradation, and in some cases to manufacture simulated ice shapes to be used on test aircraft to evaluate aircraft performance degradation in icing conditions.

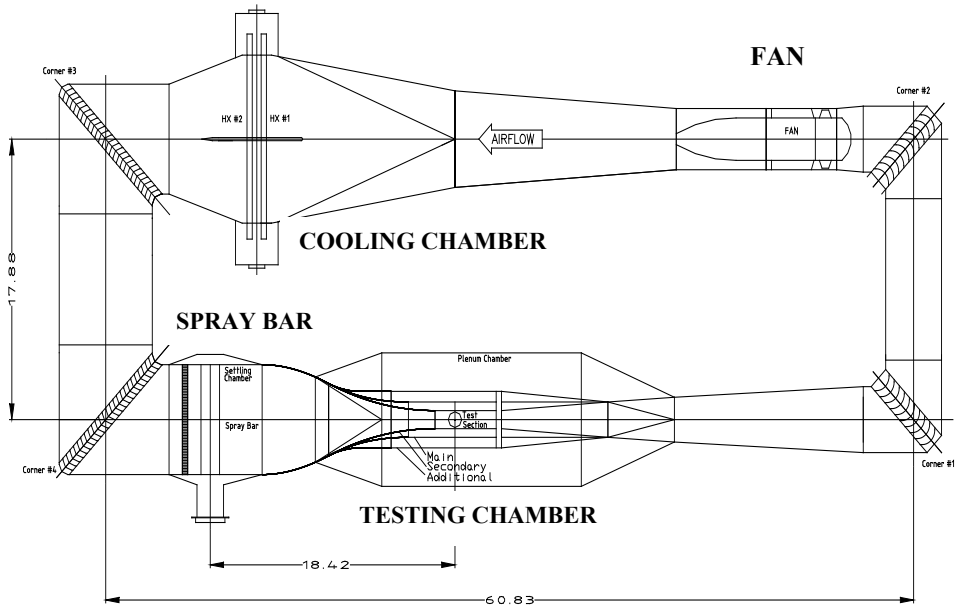

Figure 4-1: Typical Icing Wind Tunnel Layout.

In general, icing tests take longer than aerodynamics tests and are therefore more expensive. There are several factors that contribute to longer testing time. First, each test requires time for air temperature stabilization. The lower the target temperature, the longer the waiting time. Actual testing time varies from 5 minutes for icing encounter to 45 minutes for simulation of a holding condition. In addition, it is necessary to stop the tunnel after each test to measure the ice shape. Although an automatic ice shape scanning system is available, which could in principle reduce the tunnel time significantly, the accuracy is not sufficient to measure irregular ice shapes. Therefore, it is not currently used as a routine IWT procedure.

After ice shape tracing is completed, the test article will be deiced completely before performing a new test. In addition, some tunnels have the capability to simulate altitude pressure. In this case, the testing time will be even longer since before each test the operator has to wait until the tunnel reaches the target altitude pressure, and after the test ambient pressure has to be restored to allow the operator to enter the test chamber to measure the icing profile.

4.2.1.1 Range of Capabilities for Icing Wind Tunnels

At present many icing facilities are available worldwide. These facilities can be classified depending upon their size and functions:

- ***Large industrial icing wind tunnel:*** Large IWTs can host large test articles, including full-scale aircraft components during the developmental phase and the certification phase. These are very complex facilities and therefore their use is quite expensive. Only a limited number of such large facilities are available worldwide.
- ***Engine test cell:*** These facilities are dedicated to test engine performance in icing conditions. Since they test operating engines, they are designed with stringent safety requirements. Sometimes engine test cells are also used as IWTs, but the flow quality is not as good as the classical IWTs. Only a limited number of such facilities are available worldwide.
- ***Small facilities:*** Small facilities are usually characterized by small test sections. Because of the small size, test conditions can be easily controlled, and cost is low. Therefore, these facilities are typically used for research activities or for development of probes and sensors.

Table 4-1 shows a summary of ranges of test chamber sizes and test parameters of the currently available IWTs worldwide.

Table 4-1: Ranges of Test Chamber Size and Test Parameters of Worldwide IWTs.

Test Chamber Size	0.25 m (H) × 0.25 m (W) to 3.5 m (H) × 4.6 m (W).
Air Speed	A few m/s to Mach 0.6
Altitude	Most facilities are atmospheric, but a few facilities have altitude simulation capabilities up to 7,000 m.
Ice Crystals	Only small facilities or engine test cells.
Median Volume Diameter (MVD)	Most facilities cover the CS-25 Appendix C conditions (MVD up to 50 µm). Recently some facilities have been upgraded for larger diameters to satisfy the new CS-25 Appendix O requirements. However, usually only a portion of CS-25 Appendix O is achieved (freezing drizzle) and usually only very small facilities can simulate freezing rain conditions, which requires more validation work.
Liquid Water Content (LWC)	The full LWC range (up to 2.9 g/m^3) is usually covered. Sometimes it is difficult to obtain the required droplet spectrum (LWC-droplet diameter distribution) and to obtain low LWC when high droplet diameters are tested.
Temperature	0 to -40°C

4.2.1.2 Tunnel Calibration

A major issue of IWT testing is the wind tunnel calibration. Even if a standard calibration procedure has been issued by SAE [3], some criticalities are present especially concerning cloud uniformity and measurements of LWC and droplet diameter.

Usually cloud uniformity is assessed by accreting ice on a 2-inch diameter cylinder. As an alternative a rectangular grid can be used. Ice thickness is measured at various locations within the tunnel and these values are then compared to the value obtained at the center of the test section. For most facilities cloud uniformity is considered acceptable if the LWC will not vary more than ± 20% from the value at the center of IWT. This means that due to the contraction of the flow and droplet trajectories, for most tunnels only the central area of the test section is used for tests because it provides a uniform cloud condition.

For LWC measurements a standard icing blade is used with typical dimensions of 6-inch span, ¾-inch chord and 1/8-inch thickness. It is installed in the middle of the tunnel at a low temperature (e.g., -32°C) where rime is expected. In these conditions since temperature is very low the ice thickness is proportional to LWC. The measurement of droplet diameter is more complicated and is done with optical instruments.

Uncertainties of measurement depend on instrument calibration, the skills of personnel involved in measurements and on the facilities themselves. NASA Icing Research Tunnel (IRT) has provided guidance [3] for acceptable uncertainties for typical IWT testing parameters as follows: temperature (± 1.5°F), air speed (± 4%), MVD (± 12%), and LWC (± 12%). Among these parameters, the uncertainty related to MVD measurements could be higher than the NASA guideline. This is because MVD measurements require the use of optical instrumentation and therefore specialized skilled personnel are required. Furthermore, in order to cover the full range of MVD diameters, a different set of instruments (with different measurement and calibration errors) is used.

LWC measurement uncertainties come from two different sources. One source of error is related to the ice thickness measurement on the icing blade. Usually, LWC measurement is performed in the empty test chamber with only a calibration cylinder installed. In actual testing conditions, a blockage effect by the test article could cause changes in LWC. In addition to the measurement uncertainties, uncertainties of 20% due to cloud non-uniformity have to be added [3].

Repeatability is also an important experimental issue that needs to be evaluated. As in all experimental testing, tests in assumed same conditions at different times could present different results, because, for example, some modifications may have been made to the tunnel, or to a nozzle, etc. Furthermore, apart from actual changes to the tunnel and equipment, there is always some degree of uncertainty in operating conditions. The effect of factors such as these is evident in the repeatability tests on ice shape at the leading edge of NACA 0012 airfoil at 0° angle of attack presented by NASA IRT [2], as shown in Figure 4-2.

4.2.2 Flying Facilities and Flight Test

Although ground testing facilities, including IWTs, ground spray rigs and small laboratories, are very useful for ice protection research, they cannot fully reproduce real icing conditions, which comprise a variety of conditions and combinations of LWC, droplet size, flow field, pressure, and random shedding patterns that occur in real conditions [4]. It is, therefore, necessary to carry out in-situ tests in real icing conditions.

There are currently three types of in-flight icing tests:

- **Artificial icing tests:** performed in artificial plumes produced by an icing tanker which generates a controlled spray-water plume in front of the tested aircraft.

- **Natural icing tests:** performed in natural icing clouds, where icing processes take place. Natural icing tests are used to verify aircraft ice protection systems and aircraft behavior or for research purposes to better characterize icing clouds.
- **Flight tests with simulated ice shapes:** artificial ice shapes are applied on critical aircraft surfaces. The main objective of these tests is to verify aerodynamic performance of the aircraft in icing conditions.

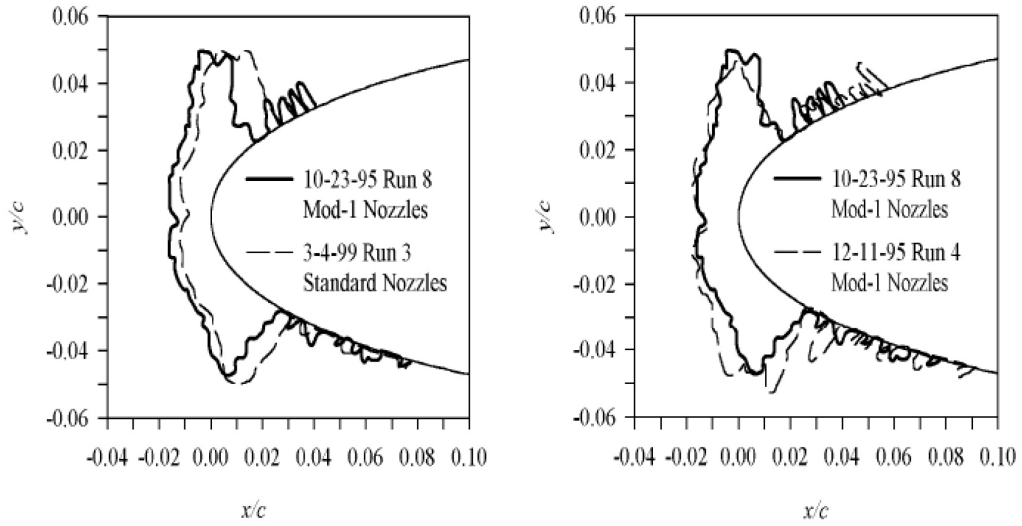

(a) Tests made in 1995 and 1999. **(b) Test Results for two Entries in 1995.**

Figure 4-2: Repeatability Tests from NASA IRT [2].

4.2.2.1 Artificial Icing Tests

Since natural icing conditions are difficult to find when it is needed, tests are conducted in icing conditions generated by the icing tanker (see Figure 4-3). Both national and artificial conditions have been extensively used in the anti-icing research field, but artificial icing shows some advantages related to the success of the mission.

Figure 4-3: Image of Artificial Icing Tests [5].

According to Schumacher [6], the frequency of finding clouds ranges from 10 to 30 percent in natural icing tests, during which approximately 10 flight hours are used for each hour of icing data. In artificial icing conditions, however, every hour of flight is estimated to produce approximately 45 minutes of test data. Furthermore, the test plane can travel very close to the tanker, even a few feet laterally or downward, still in perfectly safe Visual Flight Rules (VFR), and the duration of tests can range from just a few seconds to over an hour in icing conditions.

However, the effects of other parameters such as relative humidity and solar radiation must also be considered when correlating artificial icing tests with natural icing tests. In addition, the icing tanker (i.e., water spray tanker) spray plume must be able to completely encompass the relevant portions of the target aircraft (see Figure 4-3) and must have uniformity and repeatability when the conditions of the generated plumes are changed. Spray-plume conditions change when the distance between the two aircraft changes and are also affected by droplet evaporation due to a nonrealistic relative humidity. Tankers cannot generate the entire spectrum of drops necessary to meet the certification requirements, and two aircraft are needed for every flight, which complicates logistics and increases the cost.

In some cases, testing in both artificial and natural icing conditions have been used to correlate results or just to complete a certification process, e.g., testing conducted for UH-60A helicopter configured with the XM-139 Multiple Mine Dispensing System (VOLCANO) [7].

During the certification program of the Piaggio P.180 “Avanti” aircraft, apart from IWT tests, natural and artificial (behind US Air Force air tanker NKC-135) flight tests were also accomplished [8]. Slight discrepancies between data in artificial and natural tests were reported.

In summary the main benefits of artificial icing tests using spray tankers are:

- Year-round availability of icing conditions.
- Depending on the capacity of the water spray tanker, tests at continuous ice accretion rates are feasible.
- Selected critical areas on new aircraft can be evaluated without the safety risks associated with exposure of the entire vehicle.
- Most tankers can cover a large part of Appendix C and a portion of SLD in Appendix O envelopes (see Section 4.3 for Appendices C and O).
- Models not required.
- Testing can be accomplished in any weather.
- Full-scale testing provides more accurate results than model scale.
- Significant time saved by not having to look for natural icing conditions.

Due to the high cost of full-scale testing, however, a very few tankers are operational today.

4.2.2.2 Natural Icing Tests for Atmospheric Characterization

Most reported work in flight testing in natural icing conditions is for meteorological research focused on:

- Evaluation/confirmation of the validity of forecast models.
- Better knowledge of determined icing conditions from the different CS-25 Appendices (C, O, P) to improve and advance certification processes.

Isaac et al. [9] presented in-situ collected cloud microphysics data to characterize aircraft icing environments associated with Supercooled Large Drops (SLD) during the first and third Canadian Freezing Drizzle Experiments. 38 flights were conducted with a Convair-580 aircraft equipped with FSSP 3 – 45 mm,

FSSP 5 – 95 mm, 2D-C, 2D-P, Nezorov LWC-TWC probes, and a Rosemount icing detector (Figure 4-4). This study obtained the information to characterize the SLD and learned the mechanisms of SLD formation, but the forecasting of icing conditions remains a challenge. More physically realistic in-flight icing forecast schemes were developed. Verification of these forecasts using the in-situ aircraft data showed that considerable improvement can still be made.

Figure 4-4: Image of Canadian NRC Convair-580 Aircraft Equipped with Meteorological Probes [9].

The EURICE project (1996 – 1998) [10] had three objectives:

1) Find SLD conditions and determine the characteristics of the cloud;
2) Understand the growth processes for liquid drops from 20 to 50 μm; and
3) Understand the limiting and favorable atmospheric conditions for SLD formation.

Three aircraft were used: Do-228-212: (from DLR, Germany), Fairchild Metro II: (from NLR, Netherlands), and a C-212-200 Aviocar (from INTA, Spain). All aircraft were equipped with systems to measure temperature, LWC and cloud droplets size. 16 flights were carried out during March and April 1997, characterizing CS-25 Appendix C and Appendix O conditions and obtaining relevant information on SLD formation.

The Canadian NRC's Convair-580 instrumented research aircraft was also used in the Buffalo Area Icing and Radar Study of 2013 [11]. The goal of the 3 missions (14 hours) was to target specific winter weather scenarios, known to exhibit an aviation icing hazard for the purpose of quantifying the microphysical properties of the target zones and verifying the presence of supercooled liquid water to support validation of hydrometeor classification algorithms. These were the first missions to execute in-situ measurements within the Next Generation Weather Radar's (NEXRAD) surveillance range running with the fielded, operational NEXRAD hydrometeor classifier.

A DLR Do-328 aircraft equipped with cloud microphysical and icing documentation instrumentation, supported by specified weather forecasts helped to find atmospheric regions that were characterized by at least moderate icing conditions and temporarily by the occurrence of SLD [12]. Those results were compared with artificial icing generated by a Do-228 icing tanker turboprop aircraft, which artificially generated SLD with 180 μm mean volume diameter (MVD). These activities aim for the physical understanding of SLD generating processes and evaluation of forecast procedures.

From November 2003 to February 2004, the flight test campaign of the Alliance Icing Research Study II (AIRS II) project took place [13]. The operational objectives were to:

a) Develop techniques/systems to remotely detect, diagnose and forecast hazardous winter conditions at airports;

b) Improve weather forecasts of aircraft icing conditions;

c) Better characterize the aircraft icing environment; and

d) Improve our understanding of the icing process and its effect on aircraft.

Five research aircraft were involved in the field project: the NRC Convair-580 and the NASA Glenn Research Center Twin Otter operated out of Ottawa, Ontario, the National Science Foundation C-130 from the National Center for Atmospheric Research (NCAR) operated out of Cleveland, Ohio, and the NASA ER-2 and the University of North Dakota Citation operated out of Bangor, Maine. These aircraft flew special flight operations over a network of ground in-situ and remote-sensing meteorological measurement systems, located at Mirabel, Quebec. This project, which involved approximately 26 government and university groups from Canada, USA and Europe, was born with the aim to assist in providing the aviation community with better tools to avoid aircraft icing, and to improve the efficiency of airport operations and forecasting procedures.

More recently, within the European ICE GENESIS project, the Russian aircraft-laboratory Yak-42D "Roshydromet" and the French ATR 42 research aircraft from SAFIRE will perform 2 flight test campaigns (75 flight hours) out of France and Russia [14]. The primary objective is to best characterize snow particle microphysical properties to complement existing partial databases with a set of data for detailed microphysical closure studies of snow crystal populations (Figure 4-5).

These experiments will provide the first modern extensive data set of snow conditions to be considered for icing studies and as such will be a unique resource for fundamental research, development of snow capabilities and for airworthiness authorities.

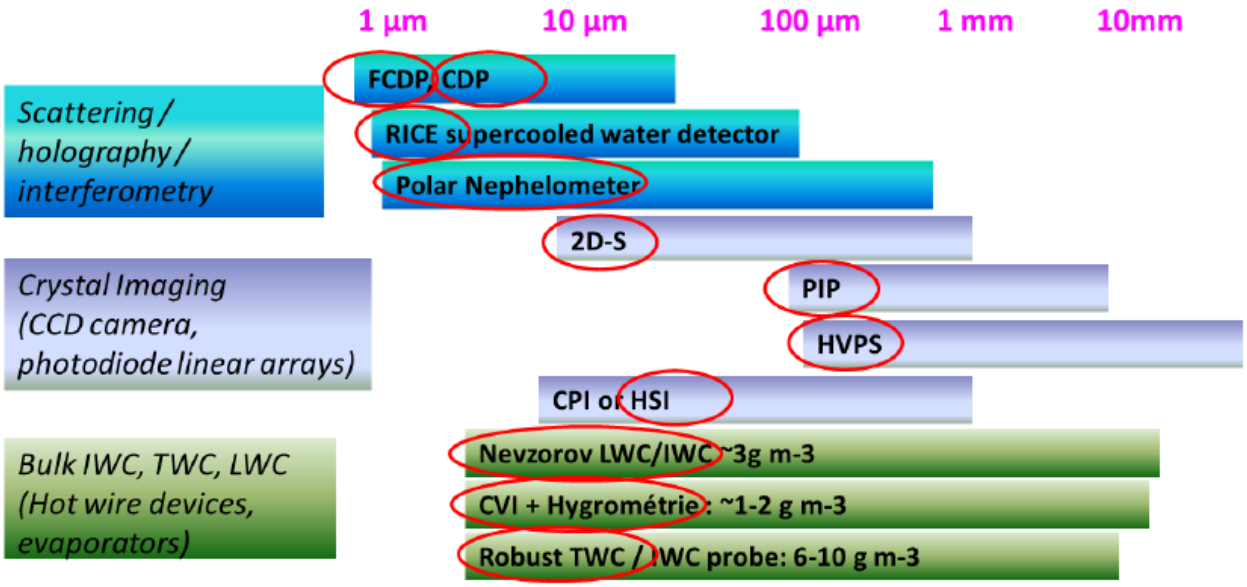

Figure 4-5: ATR-42 Instruments to Cover Complete Range of Droplet Diameters from 1 µm to 10 mm and Beyond. Red circles were for the selected ATR-42 cloud instruments in the ICE GENESIS project [14].

4.2.2.3 Natural Icing Tests for Aircraft Development

Natural icing tests are often used for ice detection and ice protection system development and verification.

4.2.2.3.1 Ice Detection Systems Flight Tests

Ice detection principles and technologies are described in detail in Chapter 1. Cloud phase discrimination, coupled with measurements of LWC and Ice Water Content (IWC) as well as the detection and discrimination of SLD, are of primary importance in aviation safety due to several high-profile incidents over the past two decades. Ice detection on aircraft components is an important field that is continuously improving. There are two main categories of ice detection systems:

- Direct methods: methods to detect the ice accretion over surfaces and methods to detect meteorological conditions prone to icing.
- Indirect methods: indirect techniques to detect ice accretion on airframe and change of aircraft performance characteristics, e.g., using simulated shapes.

The previously mentioned 2013 Buffalo Area Icing and Radar Study [11] contributed to the development of a new method to determine Supercooled Liquid Water (SLW) by radar. The on-board X-band radar on the Convair-580 provided an opportunity to quantify the radar reflectivity and improve the supercooled water detection.

Other ice detection flight test results are presented in the UTC Aerospace Systems Optical Ice Detector (OID) testing report [15]. This is a prototype laser sensor intended to discriminate cloud phase, to quantify LWC and IWC, and to detect SLD and differentiate SLD conditions from those of Appendix C. The OID has flown on the University of North Dakota Cessna Citation II research aircraft in a wide variety of atmospheric conditions which cloud probes on the aircraft have verified to corroborate the OID data.

In 1955, a NACA heated wire LWC instrument was flight tested using a Convair model 340 from United Air Lines [16]. Data obtained simultaneously with rotating multi-cylinders indicated that reliable flight measurements of LWC could be made with the heated-wire instrument.

Under the SENS4ICE project framework [17] 125 hours of flight test campaigns are planned in the first quarter of 2022 using three aerial platforms: Safire ATR-42 (France), Embraer Phenom 300 (Canada) and CAO Yak-42D Roshydromet (Russia). The tests will be used for the evaluation of direct, indirect and hybrid methods (combination of different methods).

4.2.2.3.2 Ice Protection Systems Flight Tests

Ice Protection Systems (IPS) are described in detail in Chapter 2 and can be categorized into two systems:

- **Active systems:** those that need an energy supply for its anti-icing or de-icing activity.
- **Passive systems:** based on different chemical or physical principles, the surfaces of these systems show low ice accretion or ice accretion rates, but energy supply is not necessary.

Currently, only active systems have been shown to be effective, while passive systems require further development to be practically used for flight testing as a certification tool. Thus, most open literature information on IPS is related to active systems, which was typically government-sponsored research activities. Commercial activities are rarely reported in the open domain because of their proprietary nature.

In 1984, the NASA Lewis Research Center reported the results of IWT and flight tests to evaluate the Electro-Impulse De-Icing (EIDI) system [18]. The objectives of this flight test campaign were to make direct comparisons between the EIDI performance in the icing tunnel and in natural icing conditions, and to

explore possible electro-magnetic interference problems. 21 flights were made over the Lake Erie area, using a DHC-6 Twin Otter aircraft and a Cessna TU206 model.

In 1996, Innovative Dynamics, Inc. developed a low-cost icing flight testbed, Piper Malibu (PA46-310P) to use in the development, testing and certification of IPS [19]. Over 30 hours of successful ice flight testing were conducted. An additional 50 hours of in-flight system evaluation and procedural development were performed. These activities proved the testbed as a promising low-cost option for icing flight tests to support the certification process.

During the 2003 – 2004 winter season, Goodrich Corporation tested a Low Power Electrothermal De-icing (LPED) in an IWT and in a flight test campaign [20]. This included flight behind an icing tanker and in-flight in natural icing conditions. Six flight test results were reported, and the LPED showed high efficiency and good correlation with IWT and flight test results, but further the details of the aerial platform have not been disclosed.

There is one example of passive systems flight tests. In the framework of the European project entitled, Super-IcePhobic Surfaces to Prevent Ice Formation on Aircraft (PHOBIC2ICE: 2016-2019) [21], [22], 14 most promising anti-icing coating candidates, screened from IWT and durability tests, were selected for a flight test campaign. A new testing configuration using airfoil-shape made of aluminum alloy (AA6061-T6) will allow qualitative evaluation of seven different coated profiles simultaneously (see Figure 4-6). The flight test campaign was delayed to 2021 – 2022 winter season. The ice accretion over the different specimens will be video-recorded from two different GoPro cameras, and results will be correlated with the data obtained from the meteorological probes (LWC, MVD, temperature, pressure) attached on the wing of the C-212 testing aircraft from INTA (Spain).

This methodology attracted interests from different icing research groups worldwide, and a new NATO Applied Vehicle Technology (AVT) RTG activity (AVT-332: In-Flight Demonstration of Icephobic Coating and Ice Detection Sensor Technologies) [22] was developed and approved by the NATO AVT management as an RTG activity during 2020 – 2021. Under this project, 22 icephobic coatings that will be flight tested were provided by 9 organizations from 6 participating countries. The tests will be distributed over 4 additional flights, piggybacking the PHOBIC2ICE project sometime in the fall of 2021 or winter of 2022. In all flights, the results obtained from a new fiber optic ice detection sensor, embedded in the airfoil-shape aluminum substrate, will be compared with IWT results for the same conditions.

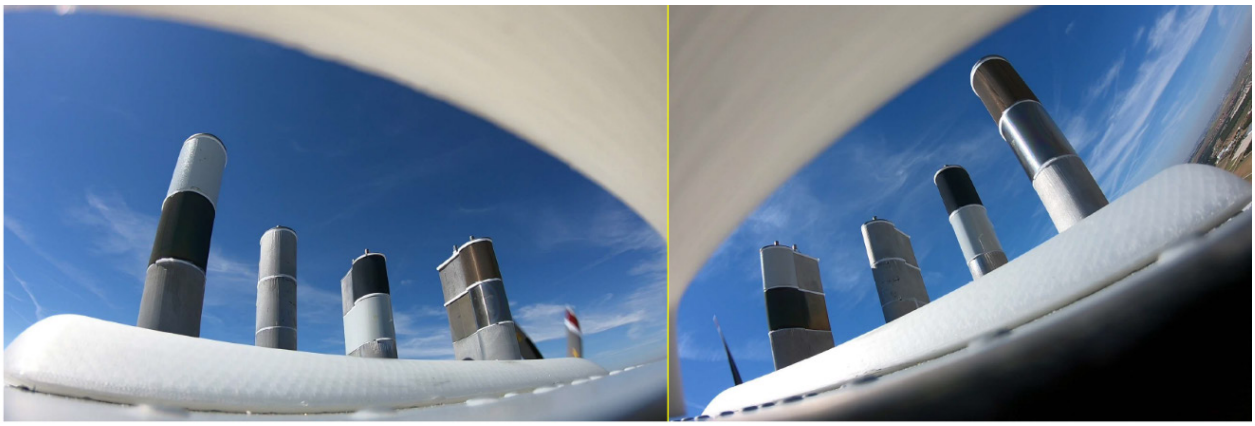

Figure 4-6: Images of Test Specimens Coated on Airfoil-Shape Substrates from Two (Left and Right) GoPro Cameras During a Certification Flight [21].

4.2.2.4 Flight Tests with Simulated Ice Shapes

These types of tests use simulated ice shape molds on aerodynamic surfaces to study the degradation of aerodynamic performance in icing conditions and to support the aircraft certification process. In 2007, a low-wing, T-tail twin pod-mounted turbofan light business jet, which was modified for Cessna's development testing, was used to simulate three types of ice accretions: preactivation roughness, runback shapes that form downstream of the thermal wing ice protection system, and a wing ice protection system failure shape [24].

Figure 4-7: Flight Test with Simulated Ice Shaper: (Left) Runback Shape and (Right) Wing Ice Protection System Failure Case [25].

The test results were used for simulation models that were implemented in the NASA Ice Contamination Effects Flight Training Device (ICEFTD) to enable company pilots to evaluate flight characteristics of the simulation models.

In 2012, DLR and Embraer established a 4-year joint research cooperation to obtain a better understanding of the distinct influences of SLD-ice shapes on aircraft performance and handling, and to evaluate strategies for future airplane certification under CS-25 Appendix O [26]. The work methodology was: first, clean aircraft data were gathered in flight tests to identify a dynamic simulation model as a base for the subsequent evaluations. Second, data from test flights with artificial CS-25 Appendix C ice configurations were analyzed and used for the development of distinct modifications of the base aircraft simulation model. Third, after the generation of SLD-ice shapes, wind tunnel testing, and flight clearance, a second flight test campaign with these artificial SLD-ice shapes provided the data for an additional model modification and identification. The results of the final data analysis and model evaluation showed an observable degradation of aircraft performance and handling due to SLD-ice, which is comparable to the results obtained from the CS-25 Appendix C ice configurations.

4.3 ICING CERTIFICATION

Icing on aircraft is directly related to safety and therefore icing tests and facilities are strongly constrained by certification requirements. The goal of the certification process is to obtain confirmation of proper ice protection functioning and demonstration of acceptable flight performance. In Chapter 2, Section 2.4, a summary of the existing regulations on Ice Protection Systems (IPSs) in the USA (FAA) and in Europe (EASA) was presented. In this section, regulations and certification processes will be briefly reviewed that would require flight testing for safe operations of aircraft in various icing environments. The icing envelopes for two atmospheric icing conditions presented in Chapter 2, Section 2.4 will be referred to, without duplications in this section.

4.3.1 Aircraft Icing Certification

Icing regulations for large aircraft were mainly based on the FAA Federal Aviation Regulation Certification Specifications (CS), FAR/CS-25 Appendix C [26], [27], whose icing envelope extends to a maximum Median Volumetric Diameter (MVD) of 50 μm. The FAA Advisory Circular Joint, ACJ 25.1419, also requires a limited assessment of aircraft and system vulnerability to ice crystal conditions. Recently certification requirements have been updated by both FAA and EASA to include droplets with MVD larger than 50 μm and to review requirements for ice crystal conditions.

Certification authorities require that compliance with certification rules be shown with a combination of methods: IWT testing, ice accretion computational analysis, dry air flight testing (with artificial ice shapes) and flight testing in natural icing conditions.

All these methods are still limited in accuracy. Some engineering judgement based on the experience accumulated on previous aircraft is also required, especially for:

a) Estimation of the amount and shape of ice accreted on the aircraft;

b) Demonstration that flight controls are free of ice-jamming;

c) Estimation of the effect of ice on aircraft performance and handling characteristics; and

d) Evaluation of performance of ice detection and protection systems.

The certification flight testing should address all phases of flight, including take-off, holding, descent landing and go-around. Adequate performance and handling should be demonstrated for the most serious ice accretion pertinent to each flight phase and related configuration. The certification requirements do not specify the amount of testing to be carried out. The specific critical atmospheric conditions have to be identified. Service experience has also shown that airplanes may encounter icing conditions that are more severe than EASA CS and FAA FAR/CS-25 Appendix C describe, which may have significant consequences. The number of individual tests could be large in order to cover the most extreme conditions.

Tests in dry air are carried out with simulated ice shapes. For performance tests the ice shapes which have the most adverse effect on lift and drag have to be selected, and for handling-quality tests, the ice shapes which have the most adverse effect on lift and pitching moment have to be selected. A degree of roughness should be approved by the authorities as representative of natural ice accretion. On the protected parts, the effect of rest-time of de-icing cycle or of runback should be evaluated, as well as the effect of ice protection failure. Deterioration of both performance and handling qualities must be included in the Aircraft Flight Manual.

4.3.1.1 CS-25 Appendix C

The Appendix C to the FAR/CS-25 (and hereafter will be referred to just as ‘Appendix C’) presents the atmospheric conditions envelopes (*Design envelopes*), in which an aircraft to be certified for flight in known icing conditions must be able to fly safely. The original icing envelope is the result of the NASA analysis using the statistical processing of a large number of observations and experimental data collected in the 1950s.

In Appendix C, two types of atmospheric icing conditions are presented in terms of Liquid Water Content (LWC) vs Mean Effective Drop diameter (MED) for temperature ranging from 0°C to -30°C. The MED is approximately equivalent to the more modern variable called the mean volume diameter (MVD). Figure 2-2 in Chapter 2 shows a) ‘Continuous maximum icing conditions’, representing stratiform clouds or layer-type clouds; and b) ‘Intermittent maximum icing conditions’, representing cumuliform or convective clouds. Traditionally, continuous maximum icing conditions have been applied to airframe ice protection and intermittent maximum icing conditions have been applied to engine ice protection.

4.3.1.2 CS-25 Appendix O

Some aircraft accidents, such as the American Eagle Flight 4184 accident in Roselawn, Indiana, USA [28] caused by SLDs, resulted in the development of new certification requirements related to flights in SLD conditions [29], [30]. The investigation of Roselawn accident determined that freezing drizzle-sized drops created a ridge of ice on the wing's upper surface aft of the de-icing boots and forward of the ailerons.

It was also found that the presence in the atmosphere of high ice crystal concentration was an issue for flight safety. Ice crystals can be found at high altitude, but they can also be mixed with liquid water droplets, which is defined as the "mixed phase". Mixed phases can be found at aircraft cruise conditions (~10/12 km altitude) and therefore an extension of the icing certification envelope was required to lower temperatures. The accident of A330-203 flight AF447 (Rio de Janeiro – Paris) in June 2009 was caused by the mixed phase [31].

Based on the investigations of these accidents, FAA and EASA concluded that a modification to the existing icing certification envelopes was required. New envelopes were introduced in 2001 for the SLD conditions in CS-25 Appendix O and for the ice crystal and mixed phase conditions in CS-25 Appendix P by the EASA and CS-25 Appendix D by the FAA. These new envelopes will be integrated with the conditions that already existed in CS-25 Appendix C.

The CS-25 Appendix O defines SLD icing conditions in which the drop Median Volume Diameter (MVD) is less than or greater than 40 μm that corresponds to the maximum Mean Effective Drop (MED) diameter of Appendix C to 14 CFR Part 25, continuous maximum (Stratiform Clouds) icing conditions. For Appendix O, SLD icing conditions consist of Freezing Drizzle (FZDZ) (Figure 2-4 (Left) in Chapter 2) and Freezing Rain (FZRA) (Figure 2-4 (Right) in Chapter 2) environments. Both curves represent the cumulative water mass spectra as a function of droplet size for MVD < 40 μm and for MVD > 40 μm. Therefore, the main difference between Appendix O and Appendix C is that in Appendix O the actual droplet distribution expressed as LWC as a function of droplet diameter must be reproduced, and it is not sufficient to use a single median droplet diameter to reproduce the icing conditions. The droplet must be between the two curves: MVD < 40 μm and MVD > 40 μm. The main difference between FZDZ and FZRA is that while FZDZ includes droplets up to a 500 μm diameter, FZRA droplet diameter can reach 2000 μm.

4.3.1.3 Ice Crystal Icing

Ice accumulation on aircraft surfaces is normally caused by the freezing of liquid droplets upon impact on a surface; however, in recent decades an additional risk has been identified when flying in clouds with high concentrations of ice crystals with the size ranging from 50 μm to 1 mm, or with mixed phase conditions, i.e., ice crystals combined with water droplets. Under such conditions, ice accretion may occur on warm parts of the engine core, resulting in sudden loss of engine thrust, engine flame-out, and even irreversible engine damage leading to a strong risk of permanent power loss and of being unable to restart the engine.

A study [32] has identified 140 engine power loss events due to engine core icing since the early 1980s. Newer aircraft are also affected by the ice crystals, as identified in the warning issued by Boeing in November 2013 regarding their 747-8 and 787 Dreamliner planes, after six incidents occurred in the previous six months [33]. Pitot probes are also likely to be affected, as the exposed tube acts as a particle collector, which may lead to probe blockage if heating is not sufficient to completely melt the ice, or if the water cannot be fully eliminated.

Safety concerns and their potential operational consequences for aircraft fleets and engine maintenance were critical enough to motivate new certification rules for aircraft. In the USA, airframe and engine manufacturers created the Ice Crystals Consortium (ICC) and the FAA proposed new certification requirements for flying in ice crystals and icing conditions in 2014 [34]. In Europe, work on ice crystal icing

conditions was included in the European Aviation Safety plan and this resulted in the issuing of new certification specifications in March 2015 [35]. In Appendix P: Mixed phase and Ice Crystal Icing (ICI) envelope (Deep convective clouds) of [36], the ICI envelope was introduced (see left figure in Figure 4-8). The right figure in Figure 4-8 displays TWC for the standard cloud length of 32.2 km (17.4 nautical miles) over a range of ambient temperature within this ice crystal envelope.

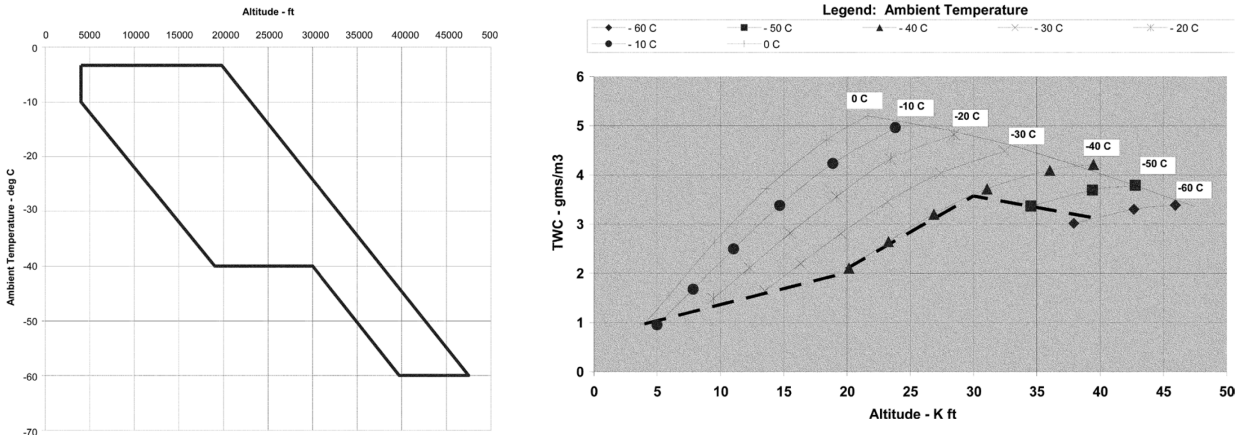

Figure 4-8: Appendix P: (Left) Convective Cloud Ice Crystal Envelope, (Right) Total Water Content (TWC) [36].

4.3.2 Ice Protection System Certification

At the start of the design and development of an airplane, a certification plan is submitted for different Ice Protection Systems (IPS) in the aircraft. In this plan Acceptable Means of Compliance (AMC) such as analysis, similarity, or tests must be included for each of the different paragraphs of the certification basis.

In the major aircraft certification rules in the Western world (FAA and EASA), the most relevant paragraphs for certification of IPS are the CS-25.1419 (Ice Protection).

CS-25.1419, paragraph (b) states:

> "*To verify the ice protection analysis, to check for icing anomalies, and to demonstrate that the ice protection system and its components are effective, the airplane or its components must be flight tested in the various operational configurations, in measured natural atmospheric icing conditions and as found necessary, by one or more of the following means:*
>
> *1) Laboratory dry air or simulated icing tests, or a combination of both, of the components or models of the components.*
>
> *2) Flight dry air tests of the ice protection system as a whole, or of its individual components.*
>
> *3) Flight tests of the airplane or its components in measured simulated icing conditions.*

It is clear that a flight test in natural icing conditions is to be included as AMC. However, the extent of the flight testing is an open discussion given the basis of the design of the IPS (new development or based on a previously certified platform) and other development means like IWT testing, flight test in dry air or flight tests in simulated icing conditions. Then, previous flight test data may be used provided it can be shown that the data is applicable to the airplane to be certified. If there is uncertainty about the similarity, then flight tests in natural icing conditions must be conducted.

The design of IPS is a complex task due to many parameters to be considered; aircraft flight conditions and flight phase, geometry and location of the surface to be protected, icing conditions (fog, drizzle, rain, snow, glaciated, mix of liquid and crystals, etc.), and engine operation for each aircraft flight condition.

There are already powerful tools for the analysis of IPS performance and credited IWTs that can perform acceptable simulations of icing conditions. However, there are important limitations: 1) Tools and tunnels are validated for SLD but not for freezing drizzle/rain, snow or mixed conditions; 2) Tunnels are limited in simulating flight, water conditions and size of test specimen. In addition, there is the interaction between the IPSs of different aircraft components and systems, which can only be encountered in the actual aircraft.

When performing flight tests for certification of IPS, there are two steps: 1) Dry air flight tests with ice protection system operating; and 2) Natural ice flight tests. The initial dry air tests are conducted to verify that the IPSs do not affect the operation of the aircraft and to assess their function, basic performance and compatibility of all system components installed in the aircraft.

Typical dry air flight tests for IPS certification are described below.

4.3.2.1 Thermal Hot Air

The system components are instrumented to measure anti-icing mass flow rate, supply temperature and protected surface temperatures. The flight test plan includes airplane operating modes of climb, holding and descent. The measurement of anti-icing mass flow rate and supply air temperature allows the determination of energy available to the system. The adequacy of the ice protection then can be compared with the theoretical analysis over the icing envelope. The surface temperatures measured in dry air can be useful in extrapolating the maximum surface temperature in-flight, the heat transfer characteristics, and the thermal energy available. The supply air temperatures also may be used to verify the adequacy of IPS materials. When a de-icing system is being certified, the rise of surface temperatures and the cycle definition may also be assessed. The effects of bleed extraction on engine and airplane performances can also be performed in dry air.

4.3.2.2 Pneumatic De-Icing Boots

The tests should demonstrate the increase and decrease in pressures inside the boots which will results in effective removal of ice. The demonstration should be done throughout the altitude band defined for certification. Boots should be operated in-flight at the minimum icing temperature to demonstrate adequate performance and that no damage occurs during inflation and deflation.

4.3.2.3 Electrical Ice Protection

The measurement of current and voltage supplied to the system would indicate power consumed by the system. Then, measurement of the surface temperatures would facilitate determining the efficiency of the system and possible losses. In a de-icing system, the temperature rise/fall and cycle would provide a good indication of the appropriateness of the power during heating and the ice accretion between cycles. In the case of propeller systems, operation of the system should be tested throughout the expected range of propeller rotational speed. In the case of windshield systems measurement of inner and outer windshield temperatures would be of use to validate thermal analysis. Visibility through the heated area for possible distortions should be evaluated for both day and night operations. Evaluation of the size and location of the protected area for adequate visibility during approach and landing should also be done.

The flight testing in natural ice conditions is the most comprehensive certification process for the IPS designs. Typical certification practices are as follows:

- The natural ice flight testing should be aiming at the critical design point conditions identified during the compliance analysis. Icing tests should also investigate the effects of runback ice aft of the protected surfaces to determine if they are hazards to continued safe flight. When de-icing systems are to be certified, inter-cycle ice shapes should also be investigated.
- The data collected during the natural icing conditions should serve for validation of the analysis performed for certification.
- During the natural icing flight tests, the systems must be activated according to the Airplane Flight Manual including delayed activation to simulate events when the pilot may unintentionally delay activation of the systems. Ice-build resulting from delay intervals may produce damages when impacting structures or engines.
- The effects of preactivation ice accretion should also be determined. Preactivation ice includes ice buildup that occurs from the time the detectors indicate icing or icing conditions (if present) and the time before thermal systems achieve their operating temperature or fluid system clear ice accretion.
- For thermal systems where the runback ice could occur, flight testing recording means shall be provided to characterize them thoroughly when occurring.
- Tests should be performed to determine if moisture can be trapped and prevent normal operation on pneumatic sensing lines, inside small cavities in equipment.
- Experience indicates that flight testing in natural intermittent maximum icing may be a risk not justified. When design analyses show that the critical ice protection design points are adequate under these conditions, and sufficient ground or previous flight data exist to validate the analysis, a flight test in intermittent maximum icing conditions may not be necessary.
- Determine if ice accretes on areas where accretion was not predicted or considered not a risk due to accumulation or when shedding.

4.4 CHALLENGES IN ICING WIND TUNNEL TESTING

4.4.1 Measurements

In recent years, several efforts have been made to improve IWT calibration and measurement issues. New instrumentation and new techniques based on optical instruments have been developed and tested, but even with these new developments there are several open issues remaining to be resolved:

a) *Calibration and measurement standard*. Usually each facility has its own calibration procedure and measurement standard, therefore it is often not straightforward to compare the performance and capability of different facilities.

b) *Large MVD.* Even if significant progress has been made in recent years, a technology gap still exists for LWC and droplet measurements. Therefore, Appendix O test conditions are not yet fully feasible to produce in IWTs even if these conditions have already been included in certification requirements.

c) *Droplet temperature measurement.* One of the emerging critical issues is related to droplet temperature measurements. As the new certification includes requirements for testing larger-size droplets, it can be difficult to achieve temperature equilibrium between the water and air due to the short residence time. Therefore, a reliable system for water droplet temperature measurements needs to be developed and made available.

d) *Ice shape measurement.* Most IWTs rely on manual profile tracing for ice shape characterization. This technique is time-consuming and requires a long tunnel stop time after each test, which implies higher cost. Some remote ice shape scanning systems are available, but their robustness and accuracy must be evaluated further when scanning complicated ice shapes such as feathered ice shapes or complicated glaze ice shapes.

e) *Remote measurements.* The usual IWT procedure is to perform a periodic tunnel calibration and to set specific parameters such as nozzle water mass flow rate and nozzle air pressure to obtain the required conditions for each test. It would be useful to have a system that is able to make non-intrusive remote measurements of the actual icing conditions (LWC and MVD). This would reduce the calibration time and facilitate monitoring the actual icing conditions during the tests.

f) *Other effects.* There is a lack of understanding of how other parameters affect the droplets in an IWT, such as: walls affecting streamlines and droplet parameters that cause break up, speed effects on breakup and bouncing, etc.

4.4.2 Scaling Laws

Currently the aerodynamic performance scaling procedure is quite well established, and a good scaling is achieved by maintaining the same Reynolds number and Mach number between the model and full-scale objects.

Scaling in icing conditions is completely different. Usually for a theoretically perfect scaling of the icing phenomena the number of equations to be solved is larger than the number of available critical parameters. It means that from an analytical point of view it is impossible to obtain a solution that satisfies all physical requirements. Therefore, several empirical scaling rules have been developed, each one with different assumptions. The scaling, which is already difficult when only ice accretion has to be evaluated, becomes even more difficult when the objective of a test is IPS evaluation.

For this reason, icing tests are usually performed at full scale, typically on a portion of the aircraft since most IWTs are not large enough to accommodate full-scale aircraft. Even if most of the tests are done at full scale, scaling rules are still required. For example, that would be the case if the facility is not able to reach the required testing speed, or LWC values.

4.4.3 Certification Requirements

Only large industrial facilities are used in the certification process. Testing in large icing facilities, however, has always been accompanied by a certain number of flight tests to complete the certification process, which represents a further investment of time and resources. Minimizing that additional investment implies the need to improve the confidence and reliability of icing test facilities.

Even if most facilities can simulate Appendix C conditions, very few facilities are able to simulate the Appendix O conditions. In addition, Appendix O conditions require freezing drizzle and freezing rain conditions. Though some IWT facilities can simulate a portion of the freezing rain/drizzle envelopes, no single facility is able to simulate the full envelopes. This is prohibitively challenging at the present time. The main reasons for these difficulties are:

Liquid Water Content (LWC): Currently most IWTs can generate LWC close to the maximum values for freezing drizzle with MVD < 40 μm (FZDZ_In). The maximum LWC reported for freezing drizzle with MVD > 40 μm (FZDZ_Out) represents icing conditions in an IWT that are challenging to generate. This is due to the difficulties in achieving the very low LWC values required.

Droplet Temperature: To avoid water freezing in the nozzles, water is usually injected at a temperature higher than 0 ºC. Once sprayed the droplets reach an equilibrium temperature with the air before

impacting on the test article. While for small droplets (Appendix C) the required resident time to obtain a supercooled temperature is compatible with the distance between the spray bar and the test article, for larger droplets this distance is not enough, especially at high test temperatures where the temperature gradient between the droplet and the air is low. As a result of the larger thermal inertia, it is difficult for the droplet to reach thermal equilibrium in FRDZ conditions and nearly impossible in FZRA conditions.

Drop Diameter Distribution: For each subset of Appendix O, all droplet spectra concentrations were averaged to derive a single droplet spectrum considered representative of the Appendix O subset [36]. Appendix O droplet spectra are reported for FZDZ and FZRA (Figure 2-4 in Chapter 2). The plots show the average cumulative mass spectrum for cases with MVD < 40 µm and with MVD > 40 µm. In consideration of the thresholds defined by the average cumulative mass spectrum for the two FZDZ subsets, the droplet spectra shapes produced by an IWT may change within the boundary indicated by these threshold curves (FZDZ_In and FZDZ_Out), as presented in Figure 4-9.

Cloud Uniformity: Due to droplet mass, droplet trajectories do not follow the air streamline (that is curved by the wind tunnel contraction) and tend to follow a straight line, impacting on the convergent wall or causing water concentration in the tunnel's central area. In addition, especially for larger droplets, they are affected by gravity. These effects are larger for FRDZ and FZRA conditions. Within Appendix C the uniform icing cloud is defined as the "area of the test section over where the LWC does not vary by more than ± 20 percent from the test section centerline LWC value for a given airspeed and water droplet size". A similar definition should be applicable for Appendix O conditions.

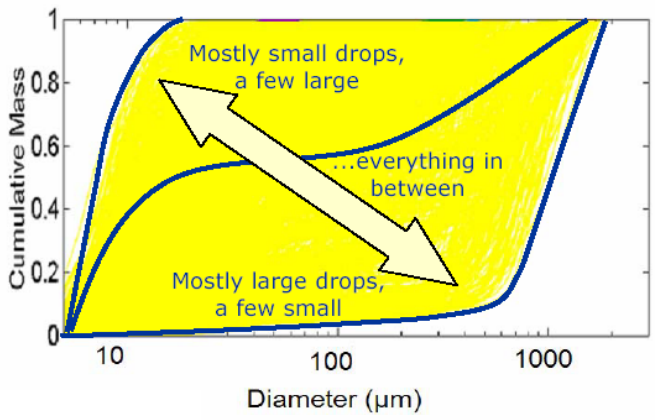

Figure 4-9: Requirement on SLD Droplet Spectrum.

4.5 CHALLENGES IN FLYING FACILITIES AND FLIGHT TESTS

Flight tests can be divided into four categories:

1) Certification tests in natural icing conditions,
2) Research tests in natural icing conditions,
3) Certification tests with simulated ice shapes, and
4) Certification tests with an ice tanker.

There are unique challenges in each flight testing category.

4.5.1 Certification Tests in Natural Icing Conditions

Flight tests in natural icing conditions are necessary to evaluate effectiveness of IPS and to evaluate the aircraft behavior in actual icing conditions. These tests are mandatory for new aircraft certification.

There are several challenges in flight tests in natural icing conditions: Finding icing conditions for flight testing may be difficult, especially when aircraft require testing during seasons with weather that is not conducive to in-flight icing conditions. Even when the weather is conducive to in-flight icing, the prevailing icing intensity may not be enough to achieve test objectives. This may lead to a longer than planned flight testing campaign and/or a delay in testing. Unexpected failures in the aircraft having an effect on IPSs or the demonstrations planned may lead to stopping the campaign. Performing the campaign at a later stage in the certification project may lead to some delays if unexpected results are encountered and aircraft design modifications are needed. Flight testing is the biggest cost item compared to the other means of compliance such as analysis, IWT testing and ground testing.

4.5.2 Research Tests in Natural Icing Conditions

Flight tests in natural icing conditions are also often performed for research activities with the objective to better identify critical icing conditions. These tests are used to improve or update icing certification requirement and for better understanding of icing physics.

4.5.3 Certification Tests with Simulated Ice Shapes

During aircraft certification to evaluate aerodynamic performance in icing conditions it is mandatory to perform flight tests with artificially simulated ice shapes. The limitation of these tests is that, for cost reasons, a limited number of ice shapes can be tested while actual icing accumulations can have a greater variety of shapes. Therefore, the most critical part of these tests is the definition and the identification of the most critical ice shapes.

4.5.4 Certification Tests with Ice Tanker

Ice spray tankers have been extensively used in the past to simulate ice shapes. However, this approach is increasingly less popular because maintaining a spray tanker is very expensive and the demand is not high. Requirement for spray-plume calibration during some tests could further increase cost.

In addition, even if the use of spray tanker is a powerful method to evaluate aircraft and aircraft system's behavior in icing conditions, several drawbacks exist, including:

- **Small spray-plume cloud diameter –** The tanker may produce relatively small-diameter clouds so that in some cases the spray-plume cloud extent is not sufficient to cover the intended testing items.
- **Spray-plume cloud uniformity –** Fairly homogenous clouds can be obtained, however, LWC decreases towards the outer edges and is affected by gravity (see Figure 4-10).
- **Effect of humidity –** Evaporation of small droplets occurs in the low relative humidity. This problem increases in magnitude with increase in test vehicle separation distance.
- **Temperature control –** With outside air temperature data available from both special instrumentation and the tanker production gage, the aircraft could be flown to within 2 or 3 degrees of the desired temperature at altitude. However, for special applications such as duplicating the ATR-72 scenario, the desired range of ±1 degree, or less, is difficult to maintain.
- **Effect of droplet velocity –** Droplets may have a higher horizontal velocity component than natural droplets.

- **Effect of turbulence –** Turbulence in the tanker airstream wake can affect the accretion pattern on test aircraft.
- **Effect of droplet temperature –** The droplet temperature is affected by the separation distance, and therefore it is difficult to evaluate the distance required to assure that the droplets are supercooled.

LWC is strongly affected by the separation distance between the tanker and the test aircraft and therefore must be accurately monitored and controlled during the tests (Figure 4-11).

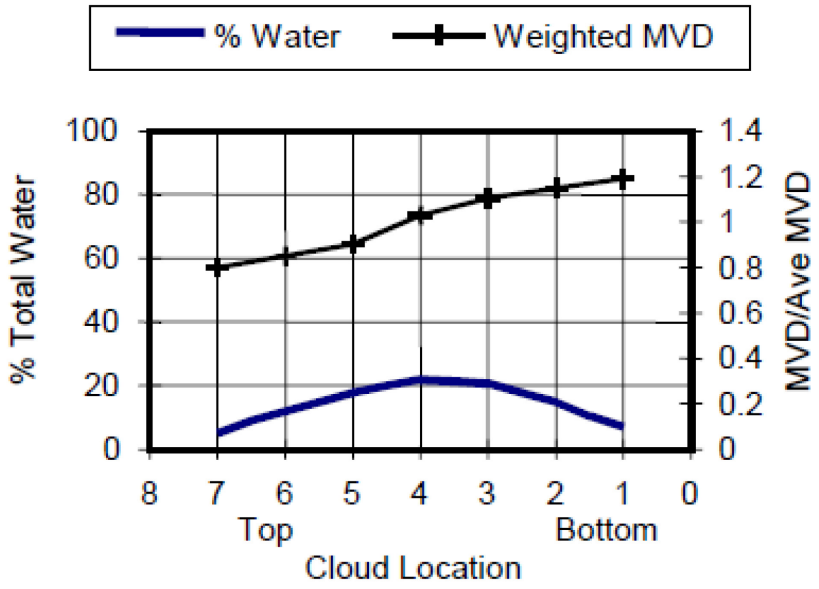

Figure 4-10: Water Concentration and Droplet Diameter Variation in a Tanker Cloud [37].

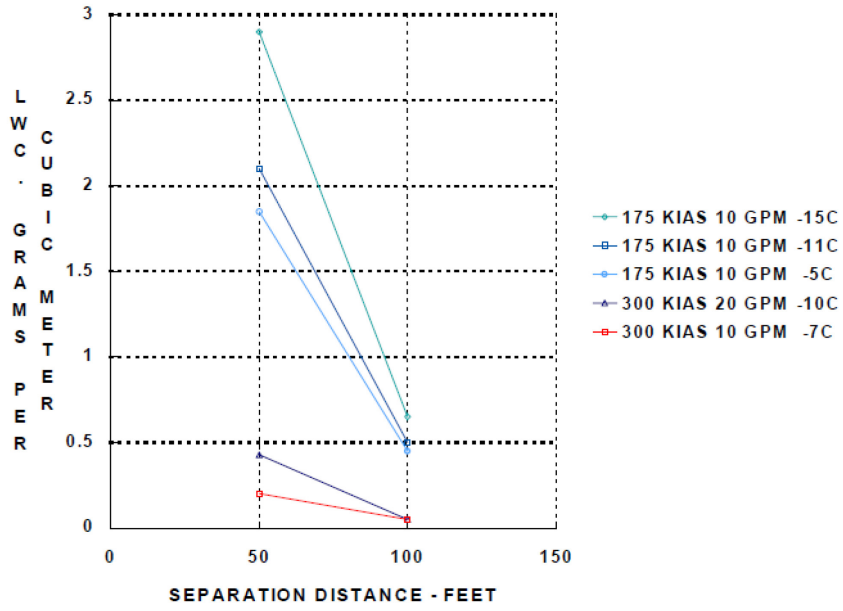

Figure 4-11: Spray Cloud LWC Variation with Separation Distance from the Tanker [37].

4.6 MAJOR ICING WIND TUNNELS

In this Section, a short description of major worldwide icing facilities is provided. These facilities are classified depending upon their size and functions (see Section 4.2.1.1): a) Large industrial IWTs; b) Engine test cells; and c) Small facilities.

The information on the flight test facilities presented in this Section was obtained from various sources, including papers published in journals and presented to conferences, technical reports and internet websites available in open domain. One of the biggest challenges was limited information open to the general public. Results of flight tests for commercial companies or for military research used for certification or other purposes are not available in public domain in many cases. Most reported work in flight testing is related to meteorological research, and just a few in ice detection, ice protection or effects of ice on the aerodynamic surfaces.

4.6.1 Large Industrial Facilities

4.6.1.1 CIRA-IWT

The CIRA-IWT facility [38] in Capua, Italy is a closed loop circuit, refrigerated wind tunnel, with three closed interchangeable test sections and one Open Jet configuration (Figure 4-12). The facility settling chamber is fitted with a honeycomb module to reduce large-scale eddies thus ensuring flow straightening. Downstream of the honeycomb, an interchangeable section provides the possibility to replace the spray bar module generating the cloud for icing tests, with screen module when lower turbulence airflow is required for aerodynamic tests.

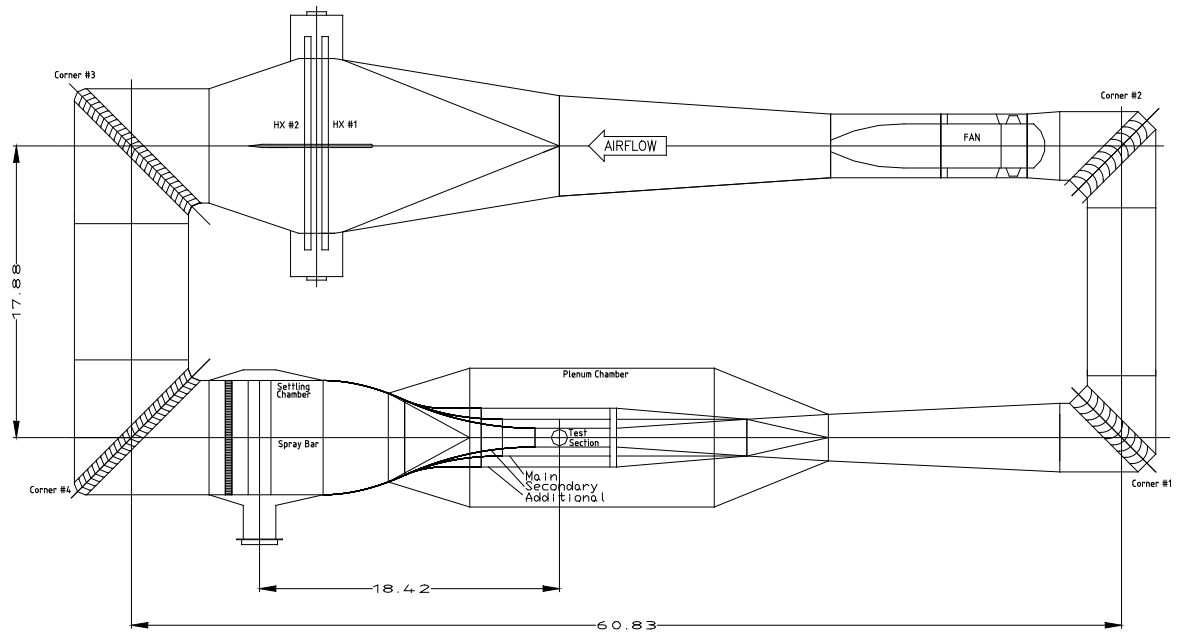

Figure 4-12: CIRA Icing Wind Tunnel Aerodynamic Layout [38].

CIRA-IWT can be configured with four different test sections. In all of them, synchronized turntables are installed to be able to set the desired model orientation with respect to the flow. Table 4-2 shows the size and airflow conditions achievable for each test section configuration. The Spray Bar System (SBS) has 20 bars having a low drag aerodynamic shaped section whose main feature is a low sensitivity to flow separation.

Each bar is equipped with 50 spraying nozzle positions for a maximum total of 1000 possible spraying positions over 20 bars. To optimize the losses, the system is equipped with 500 active spraying nozzles only. The remaining 500 nozzle positions are plugged or can be used for different spray nozzles set-up. The number of operating nozzles may be changed during a run using the Facility Management System Software.

Table 4-2: CIRA-IWT – Size and Airflow Conditions Achievable for Each Test Section Configuration.

Test Section	Size H (m) × W (m) × L (m)	Airspeed (m/s)	SAT (°C)	Altitude (m)
Main (MTS)	2.35 × 2.25 × 7	30 to 135	to -32	to 7000
Secondary (STS)	2.35 × 1.15 × 5	40 to 225	to -40	to 7000
Additional (ATS)	2.35 × 3.6 × 8	20 to 90	to -32	to 7000
Open Jet (OJ)	2.35 × 2.25 × 8	30 to 135	to -32	to 7000

4.6.1.2 NASA IRT

The NASA Icing Research Tunnel (IRT) [39] in Cleveland, Ohio, USA is the longest running, icing facility in the world and has been in operation since 1944 (see Figure 4-13). Most ice protection technologies in use today were largely developed at this facility. In this facility, natural icing conditions are produced to test the effects of icing conditions on aircraft components such as wings, tails and engine inlets.

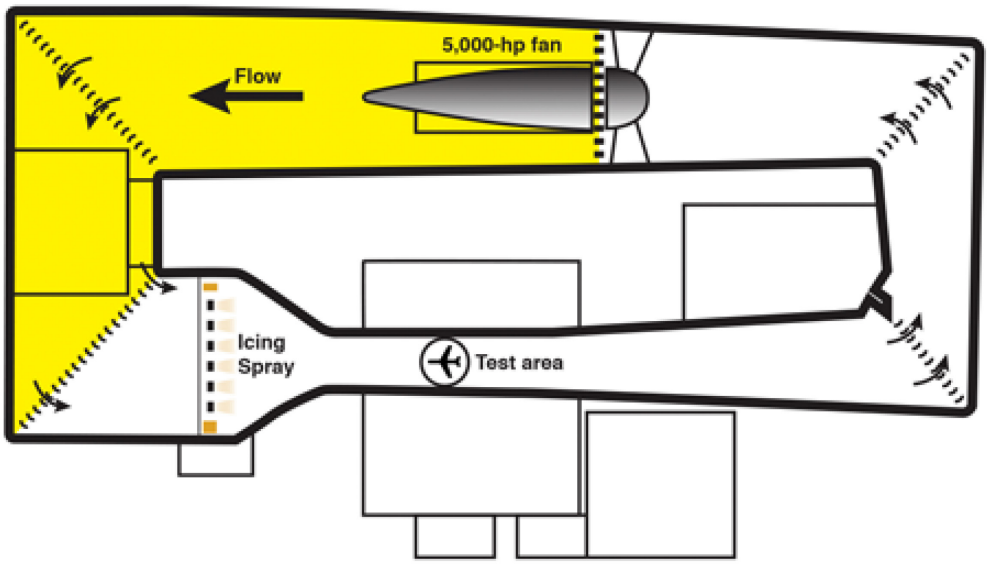

Figure 4-13: NASA IRT Icing Wind Tunnel Aerodynamic Layout [39].

A variety of tests are performed in the IRT including fundamental studies of icing physics, icing prediction validation, and ice protection system development and certification. These tests have been used successfully to reduce flight test hours for ice detection instrumentation and ice protection systems certification.

The IRT can produce airspeed from 50 to 325 knots and temperature as low as -35°C year-round, controllable to within 0.5°C. SLDs between 15 and 275 µm with LWC between 0.15 and 4.0 g/m^3 can be produced to form an icing cloud. The 6’ (H) × 9’ (W) × 20’ (L) main test section can accommodate many

full-sized aircraft components as well as large-scale models and an 8.6 ft diameter turntable in the test section can rotate horizontally ±20 degrees for various angles of attack.

4.6.1.3 CARDC IWT

The Cranfield University Icing Wind Tunnel, CARDC IWT is located in Cranfield, U.K. [40]. It is a high subsonic speed single closed circuit wind tunnel with 3 test sections which are switchable. It is one of the IWTs with large test sections, including the main test section (3 m(H) × 2 m(W) × 6.5 m(L)) FL-16, which was put into service in 2013 and is mainly used in aircraft icing experiments and evaluation experiments of de-icing system. It can also be used in high altitude, low Reynolds number experiments (Table 4-3).

Major capabilities include:

- Icing and ice shedding experiments of aircraft and components.
- Evaluation of wind turbine, cables of bridge and other facility performance in icing conditions.
- Evaluation of aircraft de-icing systems.
- Evaluation of helicopter rotor wing performance in icing conditions.
- Aircraft inlet de-icing.
- Normal aerodynamics tests.
- High altitude, low Reynolds number tests.

Table 4-3: CARDC IWT – Size and Airflow Conditions Achievable for Each Test Section Configuration.

Test Section	Size H (m) × W (m) × L (m)	Airspeed (m/s)	SAT (°C)	Altitude (ft)
Main	3.0 × 2.0 × 6.5	21 to 210	to -40	to 20000
Second	4.8 × 3.2 × 9.0	8 to 78	to -40	to 20000
High-Speed	2.0 × 1.5 × 4.5	26 to 256	to -40	to 20000

4.6.1.4 Boeing – BRAIT

The Boeing Research Aerodynamic & Icing Tunnel (BRAIT) [41] in Seattle, WA, USA is a closed loop circuit refrigerated wind tunnel (see Figure 4-14). It was built in the late 1960s as a low-speed research facility and was upgraded in 1992 to include the refrigeration system and spray bars to be capable of icing tests (Table 4-4).

Icing conditions in BRAIT are accomplished by an R-22 refrigeration system and the water spray system to simulate cloud conditions encountered in flight. The refrigeration system includes a 19 ft 8 in by 34 ft 8 in heat exchanger located in the tunnel circuit between the 3rd and 4th corners. The R-22 refrigerant system uses 1,250 hp and 900 hp screw compressors to feed the heat exchanger coils with -52°F liquid Freon to provide uniform temperature across the face of the coils.

The water spray system is composed of a water spray bar assembly, a water heater, and an air heater that provides conditioned air to the individual spray bars. The water spray bar assembly consists of eight individually controlled spray bars, each containing 27 nozzles. The nozzles are modified designs of the NASA Lewis Icing Tunnel nozzle. Air and water control to each nozzle and activation and deactivation are accomplished electronically. A spray air heater provides 75°F to 300°F conditioned air to the spray bars. The spray water heater provides 35°F to 200°F conditioned water to the spray bars. This system

provides stabilized spray conditions in less than 20 seconds after initiating spray. The refrigeration and water spray systems, along with the thermal anti-ice air system allows BRAIT to conduct the following types of testing:

- Ice accretion testing;
- Evaluation and certification of anti-ice and deice systems;
- Typical aerodynamic testing; and
- Ice shape development.

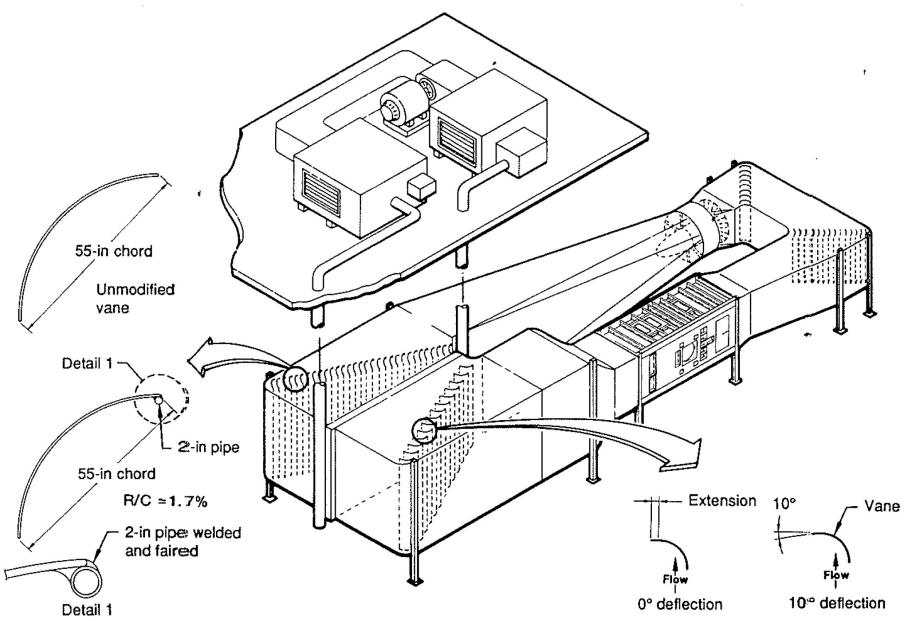

Figure 4-14: Boeing Research Aerodynamic and Icing Tunnel (BRAIT) Layout [41].

Table 4-4: Boeing – BRAIT – Size and Airflow Conditions Achievable for Each Test Section Configuration.

Test Section	Size H (ft) × W (ft) × L (ft)	Max Velocity (ft/s)	SAT (°R)	Altitude
Main	4’ × 6’ × 14’	422	430 to 520	atmospheric

4.6.1.5 RTA IWT

The RTA IWT [42] in Vienna, Austria is a climatic facility with a very long test section (100 m) for non-icing rotorcraft climatic tests (see Figure 4-15, Figure 4-16, Figure 4-17). In 2013 RTA completed and commissioned an icing spray bar system and calibration equipment for use in the large climatic wind tunnel. In 2019 the IWT was expanded with the capability of freezing drizzle and freezing rain simulation according EASA CS-25/29 Appendix O. The facility can be used for engineering and certification tests on full-scale tail rotors installed on a helicopter and components of a rotorcraft fuselage in icing conditions, as well as rotorcraft and aircraft full-scale and scaled components (Table 4-5).

Table 4-5: RTA IWT – Size and Airflow Conditions Achievable for Each Test Section Configuration.

Test Section	Size (H × W)	Airspeed (m/s)	SAT (°C)	Altitude (m)	Cloud Conditions
Test set-up 1	3.5 m × 4.6 m	10 – 20	-2 to -30	0	EASA CS-25 Appendix C
Test set-up 2	3.5 m × 2.5 m	20 – 80	-2 to -30	0	EASA CS-25 Appendix C EASA CS-25 Appendix O Freezing Drizzle MVD < 40 µm Freezing Drizzle MVD > 40 µm Freezing Rain MVD > 40 µm

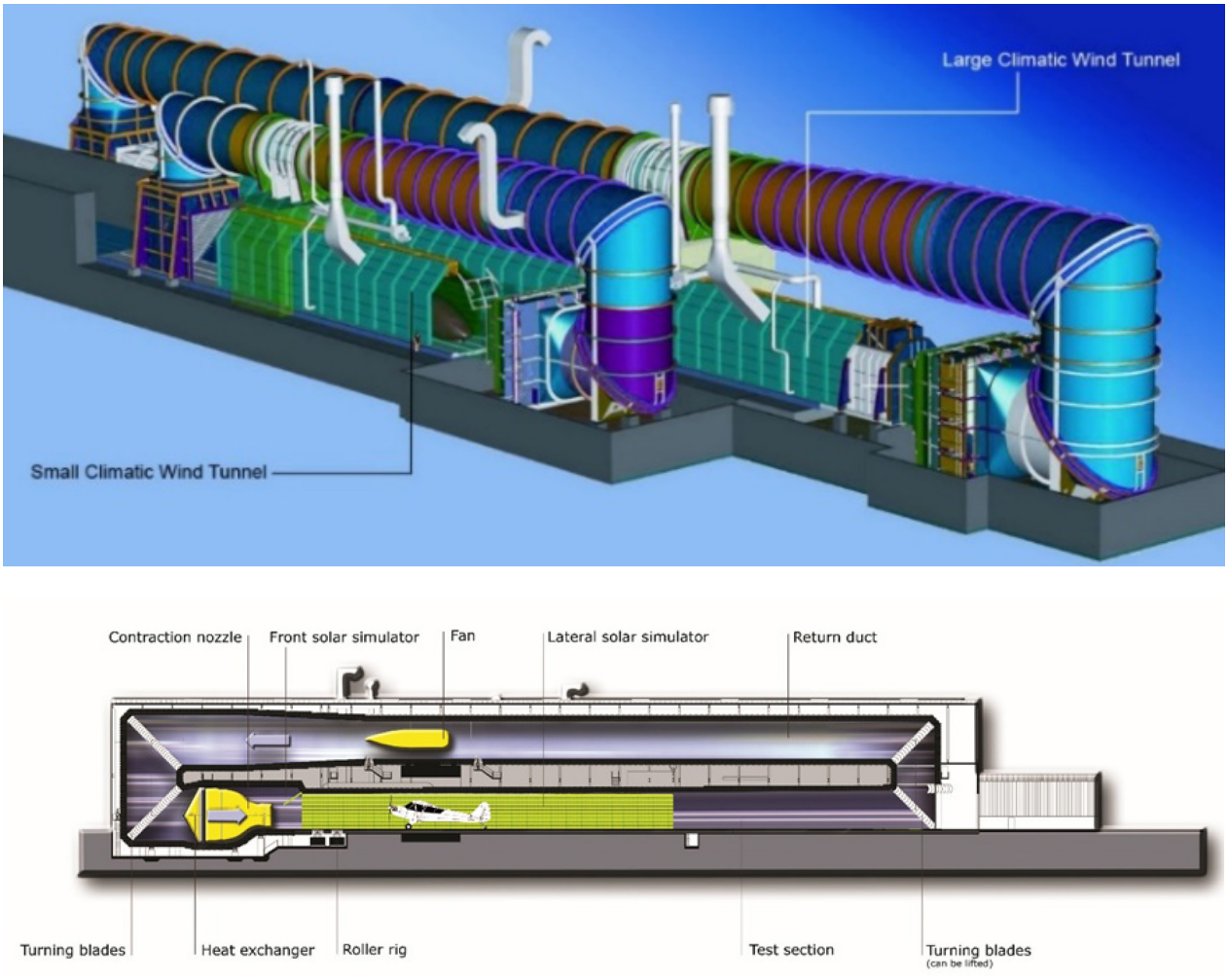

Figure 4-15: RTA Icing Wind Tunnel Aerodynamic Layout (Vienna, Austria) [42].

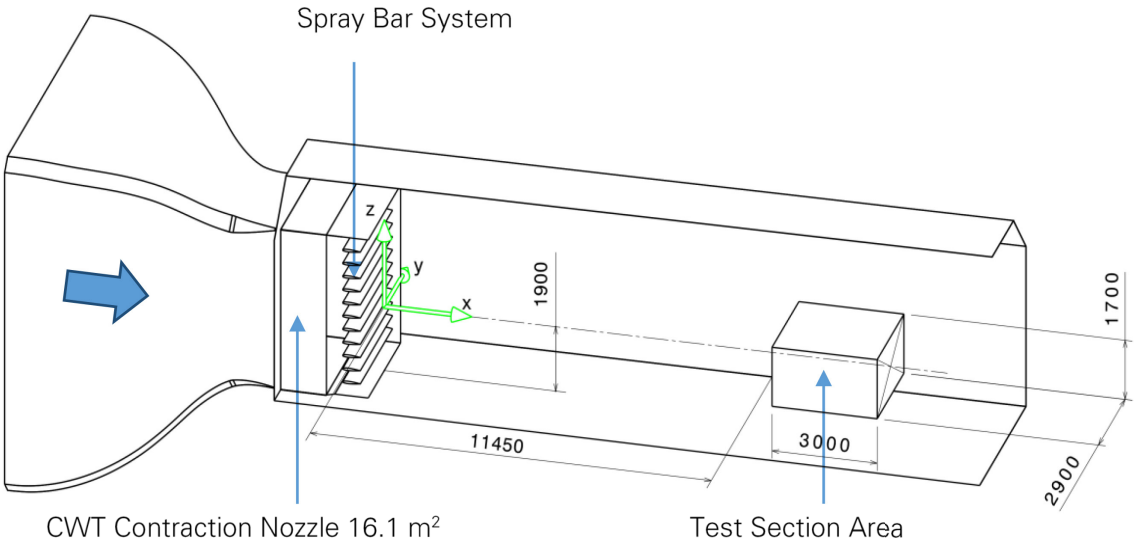

Figure 4-16: RTA Icing Wind Tunnel Test Set-Up 1.

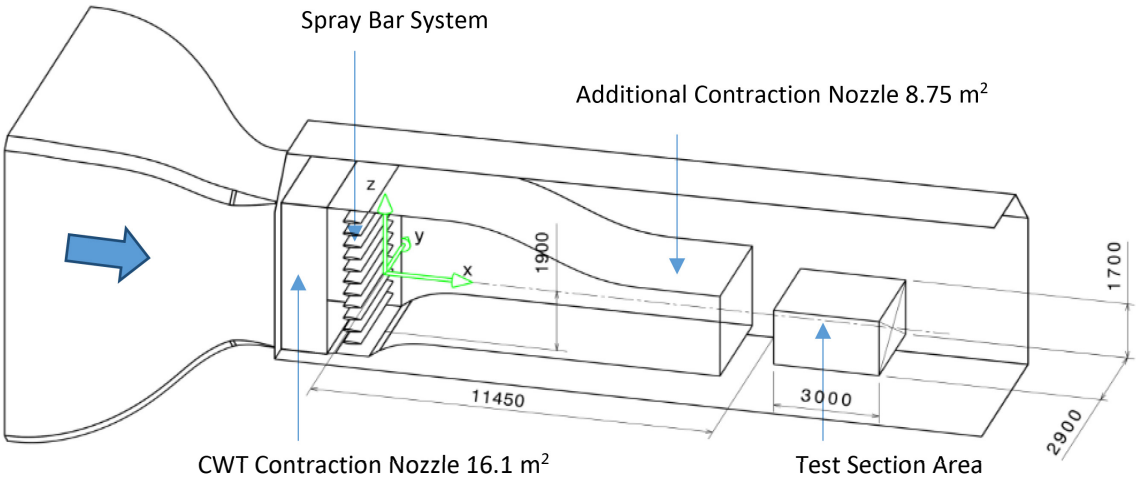

Figure 4-17: RTA Icing Wind Tunnel Test Set-Up 2.

4.6.2 Engine Test Cells

4.6.2.1 NASA Propulsion Systems Laboratory (PSL-3)

NASA Propulsion Systems Laboratory (PSL) [43], in Cleveland, Ohio, USA is a direct-connect facility that can accommodate engine and rig diameters of 24 to 72 inches (see Figure 4-18). The engine test cell, PLS-3 can simulate altitudes up to 70,000 ft and speeds up to Mach 3 for most engine applications; altitudes up to 90,000 ft are capable at lower airflows. The facility inlet air is provided by the NASA Central Process System (CPS) combustion air which delivers pressurized clean, dry, and ambient temperature air. The air passes through up to three parallel configured turbo-expanders which can cool the air to -50ºF, at a pressure of 25 psia, and flowrate of 110 lbm/s each for a total maximum mass flowrate of 330 lbm/s. The air can be injected with steam. This fully-mixed steam-infused air enters the plenum and passes through the icing spray

bar grid where it is then injected with an icing cloud. The tunnel can also produce ice crystals. The ice particles are formed by the rapid freeze-out of the water droplet cloud generated from the spray bar system.

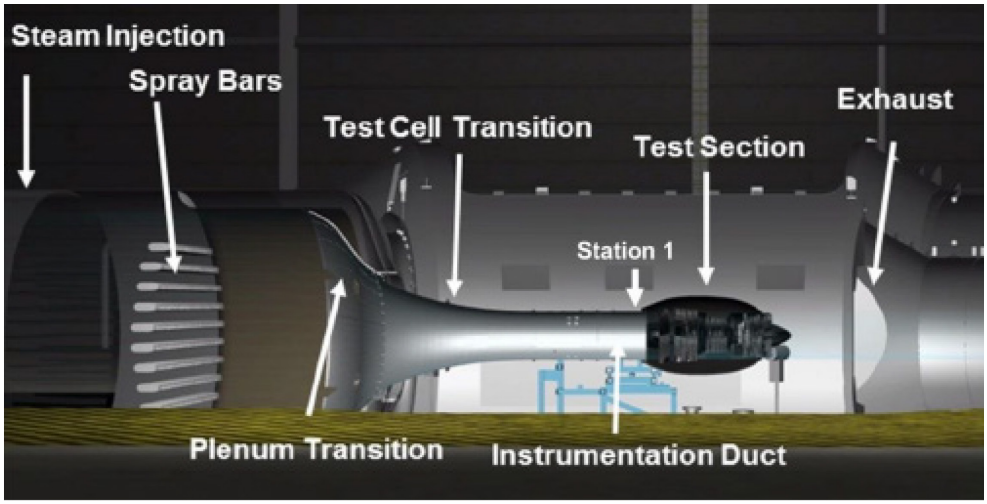

Figure 4-18: Layout of NASA PSL-3 [43].

The tunnel walls are grounded in order to prevent the static cling of ice crystals on the wall. Once the air passes through the engine, the air is then exhausted into the chamber which is being pulled to 2.5 psia by the CPS altitude exhaust system. The facility conditions are set by adjusting the tunnel inlet pressure to achieve the desired Mach number and the exhaust pressure to maintain the altitude. When PSL-3 is configured for ICI tests, the separate bypass airflow is closed off to prevent any potential ice buildup in the bypass duct. Therefore, under icing configurations the facility has limited ability to simulate rapid throttle movements. The icing systems consist of ten spray bars which are installed in the PSL-3 inlet plenum, just downstream of the inlet screens and flow straighteners. The spray bars utilize two types of flow nozzles. They are both internally mixed nozzles using the differential between water and atomizing air pressure to set droplet size.

The major characteristics of PSL-3 are as follows:

- Inlet duct size from 24 to 84 inches.
- Altitude pressure from 12.7 to 2.78 psia, corresponding altitudes from 4 to 40 kft.
- Mach up to 0.8 or Air Mass Flow Rate from 50 to 330 lbm/s.
- Inlet total temperature from -60 to +50°F.
- Plenum relative humidity from ambient (0.3 to 3%) to 50%.
- Total temperature from -50°C to 10°C.
- Total LWC from 0.15 to 8 g/m^3.
- MVD from 15 to 100 µm.

4.6.2.2 DGA S1

The DGA Aero-Engine Testing has built several facilities to test and certify parts and equipment of aircraft and rotor craft in icing conditions since 1960s (see Figure 4-19). Engine tests in ice conditions are performed at the DGA S1 facility that is located in Saclay, France. The S1 test bench is an open-loop altitude test facility including an icing capability [44], [45]. The DGA EP air supply network, connected upstream and downstream of the test cell, allows icing tests in simulated flight conditions:

- Flight conditions adjustment (air speed, temperature, altitude, humidity).
- Icing conditions adjustment by automaton (liquid water content, droplets diameter).

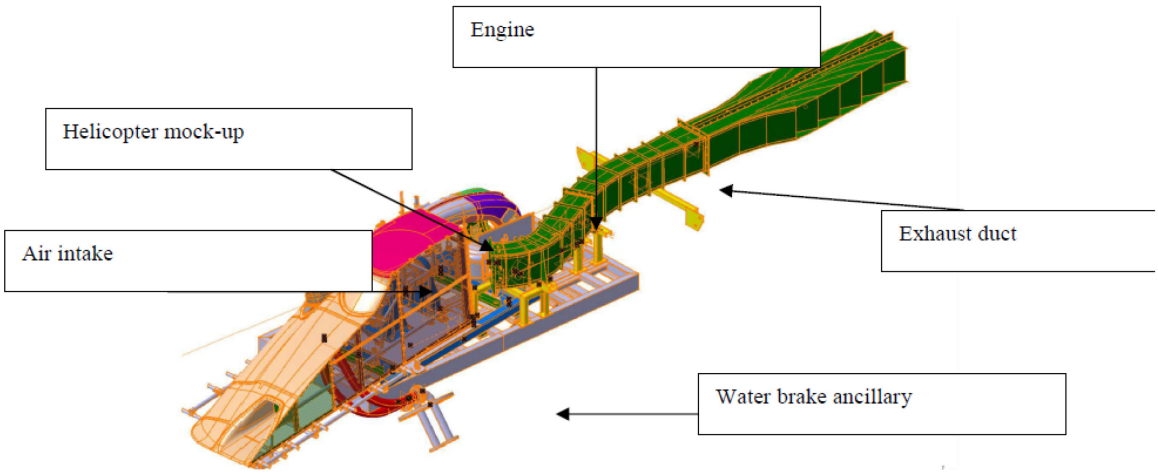

Figure 4-19: Helicopter Mock-Up with Turbo Engine Set-Up for Icing Certification Testing in DGA-S1 [47].

These capabilities comply with the icing specification of the FAR/CS 21, 23, 25, 27 and 29 standards Appendix C. The FZDZ capability has been demonstrated during EXTICE project [46]. The FZRA capability will be available soon.

S1 test capabilities are subsonic free-jet testing in icing conditions for:

- Airfoils (helicopter rotor blades, wing part);
- Helicopter air intakes with or without the engine running; and
- All types of probes (pressure, temperature, drop size distribution, liquid water content).

S1 dimensions are:

- Inside diameter of the cell: 3.50 m.
- Total length: 9.6 m.
- Deck/vein axis: 0.882 m.
- A universal deck to set-up specimens under testing.
- Designed with three tracks parallel to the axis vein.

S1 flight envelope is:

- Inlet temperature: from -65°C to 110°C [-85°F to 212°F].
- Inlet pressure: from 5kPa to 150kPa [0.7 psi to 22 psi].
- Air flow: 110 kg/s [241 lb/s].
- Minimum air speed: 10 m/s.
- Maximum flight air speed: Mach 0.8 in icing conditions.
- LWC: above 0.1 g/m^3 for Mach number above 0.2.

Icing tests are carried out in a free-jet mode. Several nozzle diameters varying from 0.7 to 1.3 m are available in order to comply with the specified air speed. A specific nozzle diameter is chosen depending on the specimen size (blade chord, engines sizes). For tests on an airfoil or a rotor blade, a specific nozzle with a 0.8 m by 0.82 m exit section was designed.

The spray bars are composed of 61 nozzles with a uniform hexagonal distribution. To generate the Appendix O conditions, standard and SLD atomizers are mixed on the spray bars.

- Max MVD up to 500 µm for Mach number (M) ≤ 0.4 and up to 800 µm for M > 0.4.
- Max LWC above 0.1 g/m^3 for M>0.2.

4.6.2.3 NRC TC4 – TC5

The Canadian NRC's (National Research Council) TC4 and TC5 in Ottawa, Canada are engine test cells research facilities [48], equipped with the state-of-the-art instrumentation to perform multiple testing environments (see Figure 4-20, Figure 4-21). There are multiple gas turbine engine test cells with unique specifications to support performance, operability and certification testing. The facilities are capable of testing under a variety of conditions, including icing, bird-ingestion, blade-off, alternative fuel certification and endurance trials. NRC has extensive experience working with gas turbine engines of all sizes and configurations.

Figure 4-20: NRC-TC4 Turbofan on Thrust Stand.

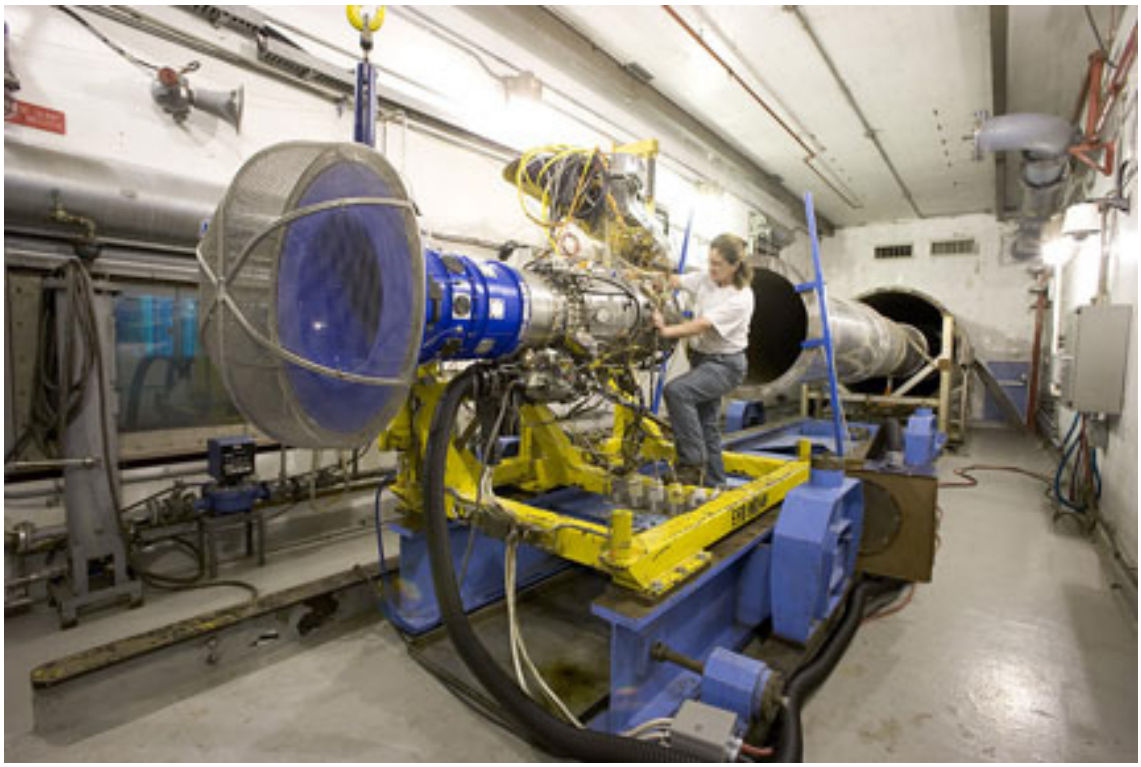

Figure 4-21: NRC-TC5 Turbojet on Thrust Stand.

The NRC maintains two operational gas turbine engine icing test facilities (TC 4 and TC 5) (Table 4-6).

Table 4-6: Specifications of NRC TC4 – TC5 Gas Turbine Engine Icing Test Facilities.

	TC 4	TC 5 – Engine	TC 5 – Tunnel
Engine Type	Turbofan/jet	Turbofan/jet	Icing Tunnel
Dimensions	7.6 m × 7.6 m × 22.9 m (25’ × 25’ × 75’)	4.6 m × 4.6 m × 22.9 m (15’ × 15’ × 75’)	0.9 m (35” dia.) × 3.1 m (10 ft long)
Thrust/Power	222 kN (50K lbs)	222 kN (50K lbs)	222 kN (50,000 lbs)
Air Flow	454 kg/s (1000 lb/s)	227 kg/s (500 lb/s)	Vmax = 150 m/s (292 kts)
Ice Crystal Icing (g/m^3)	0.1 to 5 (local max up to 15)		
Ice Crystal Icing, Median Mass Diameter (MMD) (µm)	35 to 700+		
Supercooled LWC (g/m^3)	0.2 to 3		
Supercooled LWC, MMD (µm)	15 to 40		
Temperature (ºC)	Ambient (-20 to +30)		
Design and Correlation	SAE AIR 4869, SAE ARP 741		

4.6.3 Small-Scale Facilities

4.6.3.1 DGA PAG IWT

The DGA PAG IWT [49] is located in Saclay, France. The PAG test bench (derived from the French Petit Anneau Givrant meaning Small Icing Ring) is a closed loop and ground test facility with the aim of providing flexibility in service, being rapidly operational and independent of all the air conditioning facilities of DGA (see Figure 4-22). For aerofoil or blade testing, a 2D test set-up has been developed. This makes a privileged test bench to perform icing tests for the development or certification of small-sized specimens like probes, airfoil sections, compressor blades, etc.

Until recently, the standard conditions for icing were associated with the presence of clouds composed of supercooled small droplets. Nevertheless, recent accidents and incidents have highlighted the danger of other icing conditions such as Supercooled Large Drops (SLD), ice crystals and mixed phase which is composed of ice crystals and small droplets. So, current and future challenges include the ability to simulate these conditions. To generate droplets larger than 100 micrometers, a new atomizer has been developed and calibration methods have been modified in consequence. The next planned step will be the generation of ice crystals and mixed phase.

The list of test possibilities also includes special setups such as the air intake of a gas turbine engine (Table 4-7). The conventional test cells of the PAG might be replaced by a special geometry test cell in such cases. The PAG test bench is calibrated for Appendix C. Even if the nozzles can generate SLD in the whole range of Appendix O, only a partial calibration has been done for Appendix O.

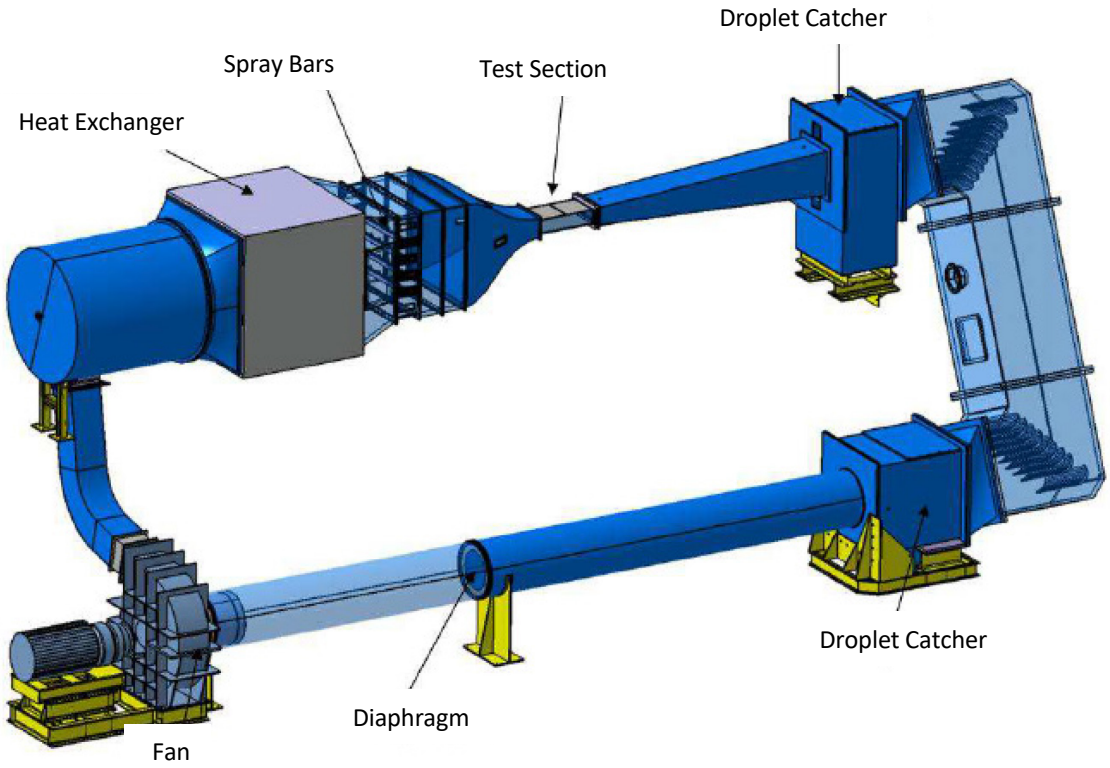

Figure 4-22: Layout of DGA (Direction Générale de l'Armement) PAG Icing Wind Tunnel [49].

Table 4-7: DGA PAG IWT – Size and Airflow Conditions Achievable for Each Test Section Configuration.

Test Section	H (m) × W (m) × L (m)	Airspeed (m/s)	SAT (°C)	Altitude (m)
Section 1	0.2 × 0.2 × 1.0	50 to 200	-40 to +15	Ground
Section 2	0.2 × 0.5 × 1.0	30 to 120	-40 to +15	Ground

4.6.3.2 Cranfield IWT

Cranfield University IWT has two facilities [49], [50]: a main IWT and a vertical droplet tunnel with air speed up to 100 m/s (see Figure 4-23). In the main IWT (0.76 m × 0.76 m), they are able to create realistic icing conditions with temperature variation (-30°C to +30°C) at a component level, providing information on how well ice protection equipment is working and on the adhesion of ice to a given material. In the vertical droplet tunnel (0.21 m × 0.21 m), they can examine how a single water droplet behaves as it strikes a surface at speed. The temperature varies from -20°C to +30°C. This is a microscopic view on the icing process. It allows to see the change in shape of droplets in an air flow as they move close to a solid surface and how they splash and spread when they strike the surface. It is possible to see how the water which does not freeze immediately flows and gathers as rivulets, attached droplets or forms a film of water. These capabilities help us understand the icing process and find better ways to model it. Since the droplet tunnel is a vertical tunnel, it is well-suited to study SLD behavior.

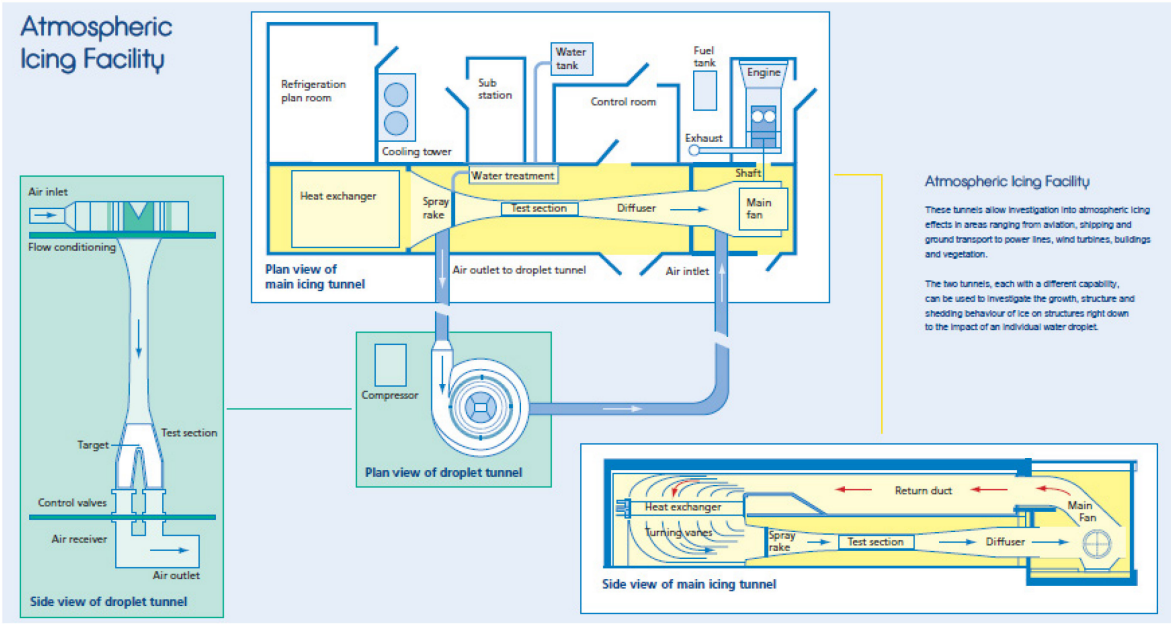

Figure 4-23: Cranfield Icing Wind Tunnel Aerodynamic Layout [51], [40].

4.6.3.3 NRC Altitude IWT

The NRC's altitude IWT is capable of meeting icing certification and research needs, with a proven track record of providing high quality repeatable results to clients [51]. The tunnel's comparatively small test section, combined with its relatively high-speed capabilities, make it particularly suitable and efficient for the testing of instrumentation and viewing of the microphysical processes of ice accretion (see Figure 4-24 and Table 4-8). Its ability to simulate flight at altitudes as high as 40,000 ft (12,000 m) makes this facility unique.

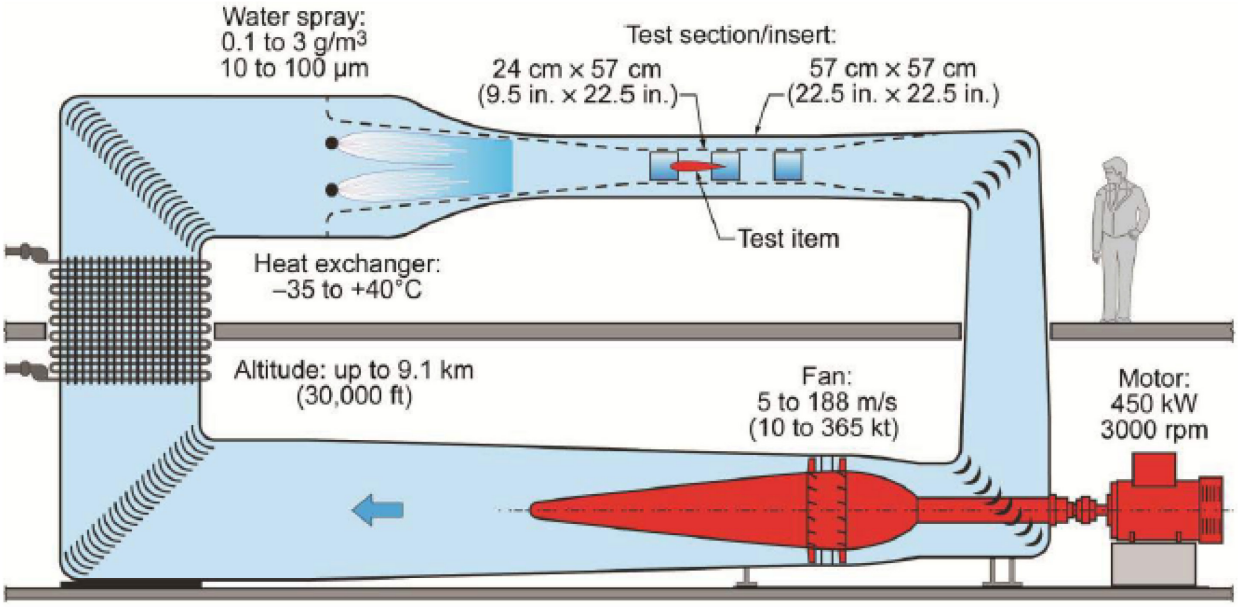

Figure 4-24: NRC Altitude Icing Wind Tunnel Aerodynamic Layout [51].

Icing conditions:

- LWC (at max. velocity): 0.1 to 2.5 g/m^3 (0.1 to 3.5 g/m^3 with insert).
- Droplet Mean Volume Diameter (MVD): 8 to 200 µm.
- Bi-modal spray distribution for freezing drizzle SLD conditions.
- Ice crystal conditions up to MVD of 100 µm (liquid nitrogen injection system).

Aerodynamic and thermal conditions:

- Velocity spatial uniformity variation ±1%.
- Static air temperature (at max. velocity): -40°C to +30°C (-40°F to 86°F).
- Static air temperature spatial uniformity variation: 0.5°C.
- Flow angularity: 0.25° in pitch and yaw.
- Turbulence intensity: 0.9%.
- Altitude simulation: ground to 12.2 km (40,000 ft).

Standard working section:

- Test section size in m (H × W × L): 0.57 × 0.57 × 1.83 (22.5 in × 22.5 in × 72 in).
- Air velocity: 5 to 100 m/s (Mach 0.015 to 0.3).

Reduced working section:

- Size: 33 cm high × 52 cm wide × 60 cm long (13 in × 20.5 in × 24 in) (with insert).
- Air velocity: 8 to 180 m/s (Mach 0.025 to 0.53).

Table 4-8: NRC Altitude IWT – Size and Airflow Conditions Achievable for Each Test Section Configuration.

Test Section	Size H (m) × W (m)	Airspeed (m/s)	SAT (°C)	Altitude (m)
Standard	0.57 × 0.57	100	-40 to +30	12,200
Reduced	0.33 × 0.52	180	-40 to +30	12,200

4.6.3.4 Cox IWT

The LeClerc Icing Research Laboratory (LIRL) [52] in Plainview, NY, USA was designed and constructed by Cox & Company in 1996 (see Figure 4-25 and Table 4-9). The facility was engineered to meet a number of design criteria in addition to being environmentally non-intrusive to the surroundings. It consists of a closed loop refrigerated wind tunnel with the capability to simulate a cloud of SLDs as specified in the FAR's Part 25-C. Two test sections are provided with an airspeed up to 100 m/s in the Primary Test Section (No. 1) and 56 m/s in the Secondary Test Section (No. 2). They also provide a capability of testing engine inlet nacelles with a scavenge flow system that is capable of simulating engine core inlet air flows of up to 15 lb/sec. The tunnel air temperature can be controlled down to -22°F at the maximum heat load conditions.

Recently the facility has been upgraded to test glaciated and mixed phase conditions. The facility has also been updated to simulate SLD conditions.

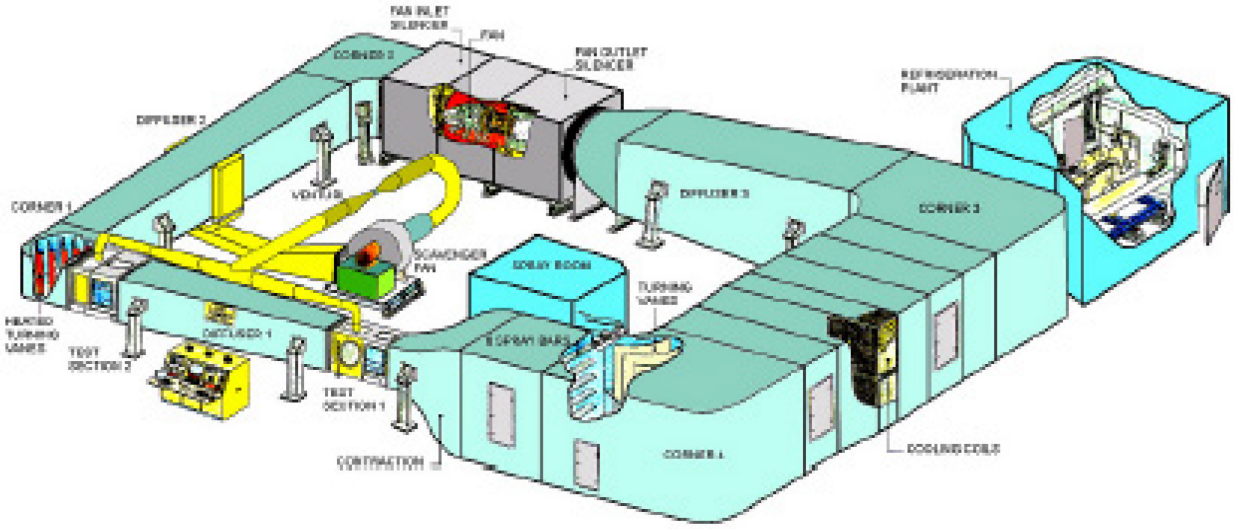

Figure 4-25: Cox LeClerc Icing Research Laboratory (LIRL) Altitude Icing Wind Tunnel [52].

Table 4-9: Cox LIRL IWT – Size and Airflow Conditions Achievable for Each Test Section Configuration.

Test Section	Size H (m) × W (m)	Airspeed (m/s)	SAT (°C)	Altitude (m)
Section 1	0.5 × 1.1	100	-30 to 0	N/A
Section 2	1.2 × 1.2	50	-30 to 0	N/A

4.6.3.5 Braunschweig IWT

The Technical University of Braunschweig, Germany designed and built an IWT in 2013 [53]. It is used for fundamental research on the physics of ice accretion and serves as a test bed for benchmark studies on measurement techniques for droplet sizing and ice shape determination and offers industrial clients an affordable facility for their preliminary design studies.

The test section size is 0.5 m × 0.5 m with maximum velocity of up to 40 m/s (see Figure 4-26). The static air temperature ranges from -25°C to +30°C. Supercooled droplet icing with LWC up to 3 g/m^3 can be reproduced. The unique aspect of this facility is the combination of an icing tunnel with a cloud chamber system for making ice particles. These ice particles are more realistic in shape and density than those usually used for mixed phase and ICI experiments. Ice water contents up to 20 g/m^3 can be generated.

Ice crystal icing and mixed phase icing (i.e., both ice crystals and liquid droplets are involved in the process of ice accretion) can be simulated with the Ice crystal Generation and conveyance System (IGS). The IGS is unique in that it can create natural, low-density and irregular shaped ice crystals. One main component of the IGS is the cooling chamber (dimensions 4 m × 7 m × 3 m), which provides a cold environment to allow ice crystal growth. Inside the cooling chamber, natural ice crystals (hexagonal plates and needles) are generated in two cloud chambers and stored at very low temperatures in two chest freezers to prevent them from sintering. Once a sufficient mass of ice crystals is produced, the particles are conveyed into the icing tunnel. Particle dosing is realized by a custom-made sieving machine. The sieving machine selects the stored ice particles of desired size range and directly supplies them to the conveying system. Fluidization of the particles is realized by an injector technology. Being fluidized, the particles are conveyed with one pipe inside the IWT, providing a moderate uniform concentration of ice crystals across the tunnel test cross section. The conveying airflow is extracted from the IWT using a bypass construction driven by a radial fan. Due to the energy input of the fan, the air is heated by about 11°C. To prevent the particles from melting and to compensate heat exchange with the environment, an aftercooler is implemented into the conveyance system. The aftercooler and the evaporator of the cooling chamber are connected to a common state-of-the-art CO_2 refrigeration system.

4.6.3.6 Goodrich IWT

The Goodrich IWT [54] in Uniontown, OH, USA, was inaugurated in 2013 and has a closed loop design (see Figure 4-27). An axial fan, driven by a 36 kW electrical engine, circulates the air. Featuring a contraction ratio of 10:1, the wind tunnel nozzle accelerates the air to more than 40 m/s inside the test section, which has dimensions of 0.5 m × 0.5 m. The air is cooled with a heat exchanger, which is connected to an external refrigeration system. A continuous cooling capacity of 30 kW is achieved. Over short periods, even higher capacities of up to 80 kW are possible. Consequently, the air inside the tunnel can be cooled down to -20°C. To simulate SLD icing (EASA CS-25 Appendix C & O), a removable spray system consisting of 6 × 5 modular nozzles is positioned in the settling chamber of the tunnel.

4.6.3.7 ONERA Vertical Research IWT

The ONERA Vertical Research IWT in Toulouse, France is a vertical closed loop wind tunnel dedicated to the SLD studies (Figure 4-28). It is equipped with a long convergent section that allows large droplets to accelerate without breakup It was designed to obtain a dynamic equilibrium for 300 µm droplets diameter. The test section size is 0.1 m (H) × 0.2 m (W). The maximum air speed is 150 m/s. The lowest temperature is -40°C with the maximum altitude of 11,000 m.

The facility was completed in 2020. At the time of writing calibration is still in progress and therefore a limited amount of information is available. The facility will be capable of producing monodispersed spray up to 100 – 300 µm. The test section will be equipped with large windows in order to do detailed visualizations of the impact phenomena.

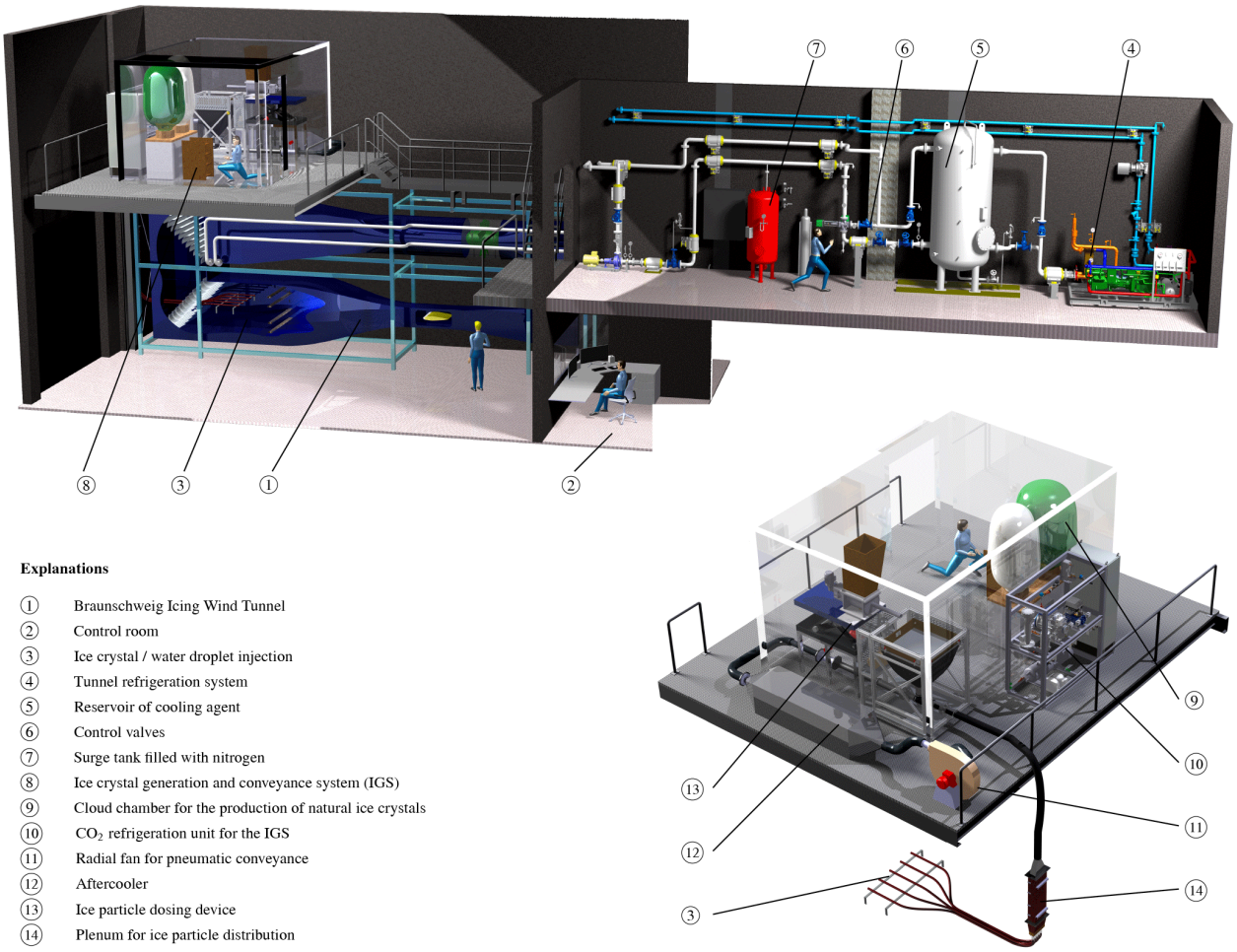

Explanations

1. Braunschweig Icing Wind Tunnel
2. Control room
3. Ice crystal / water droplet injection
4. Tunnel refrigeration system
5. Reservoir of cooling agent
6. Control valves
7. Surge tank filled with nitrogen
8. Ice crystal generation and conveyance system (IGS)
9. Cloud chamber for the production of natural ice crystals
10. CO_2 refrigeration unit for the IGS
11. Radial fan for pneumatic conveyance
12. Aftercooler
13. Ice particle dosing device
14. Plenum for ice particle distribution

Figure 4-26: Braunschweig Icing Wind Tunnel Aerodynamic Layout [53].

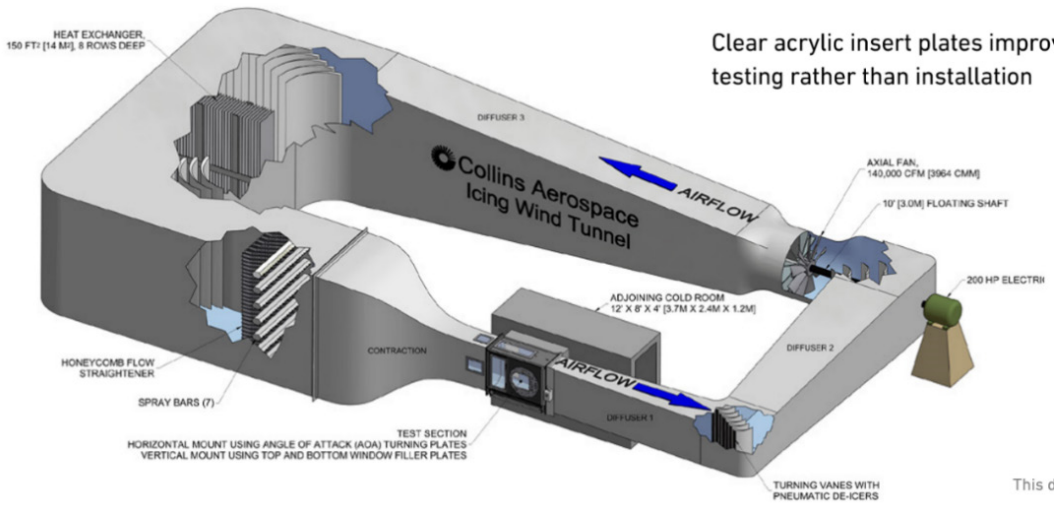

Figure 4-27: Goodrich Icing Wind Tunnel Aerodynamic Layout [54].

Figure 4-28: ONERA Icing Wind Tunnel.

4.6.3.8 NRC Research Altitude Test Facility (RATFac)

Canadian NRC's RATFac [48] consists of an altitude chamber that is approximately 32 ft (L) × 8.5ft (W) × 8.5 ft (H) (see Figure 4-29 and Figure 4-30). Upstream is a refrigeration cooling system to cool and dry the air down to approximately -45°C Total Air Temperature (TAT) but can cool down further to approximately -70°C using LN2 with a heat exchanger or direct injection system. Compressors downstream of this chamber are used to draw airflow through it and valves upstream of the chamber are closed off to reduce the pressure (and therefore increase the altitude) inside the chamber providing an approximate altitude range of 500 to 51,000 ft.

The ICI rig test system and the ice particle generating system are installed in separate parts of the RATFac chamber so that their temperatures can be independently controlled (Figure 4-30). This allows the generating system to produce ice particles consistently, independent of the environment seen by the rig. The rig side of the facility can therefore simulate both the ICI environment seen in an engine (warm, small particles, lower speeds, higher pressures) or the one seen in the atmosphere by an aircraft (cold, large particles, higher speeds, lower pressures).

To create ice crystals for the facility, ice is fed into a grinder, which produces particles of the desired sizes which are then injected into the rig inlet by the ice injection pipe. The ice flow rate, particle size reduction and injection speeds are independently controlled. Another key aspect is that it has a flow-through facility, which means there is no recirculation of air or particles and the inlet humidity can be controlled down to very low dewpoints, typically dewpoint<-40°C.

For mixed phase conditions, the ice particles will naturally melt by controlling the rig side TAT and humidity to set the wetbulb temperatures above zero. The ability to control humidity allows the wetbulb temperature (and therefore melt) to change independent of TAT. If additional water is desired for higher LWC or LWC where wetbulb is below 0°C (and therefore not allowing melting), there is also the ability to add supplemental water using the spray mast at the ice gun outlet.

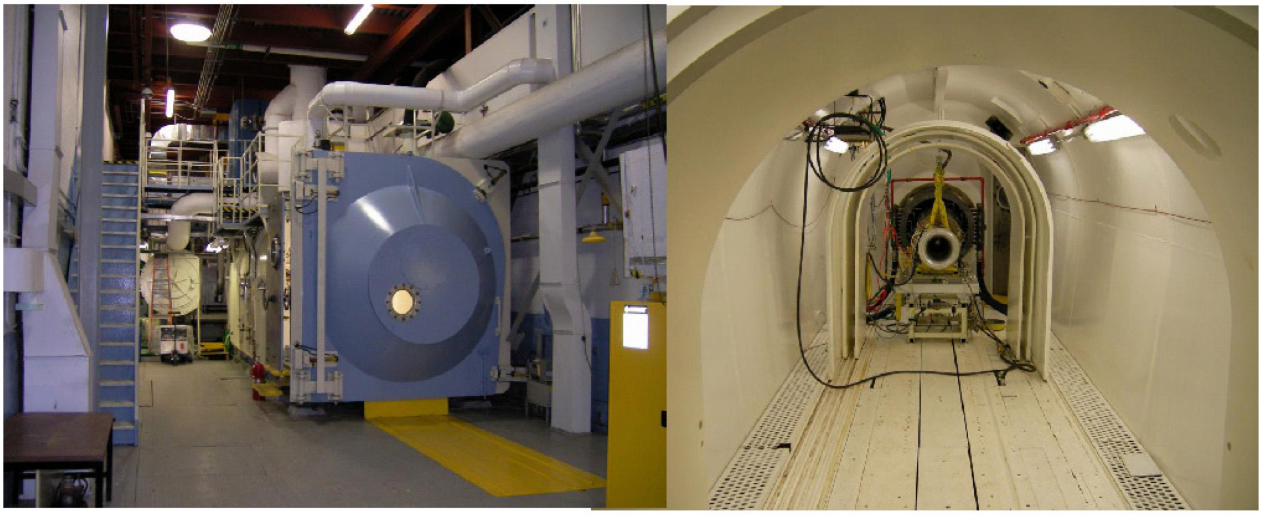

Figure 4-29: RATFac Chamber, Left: Overall Exterior View Looking at Large Front Door, Right: Inside View with Large Door Open, Looking Towards Chamber Outlet [48].

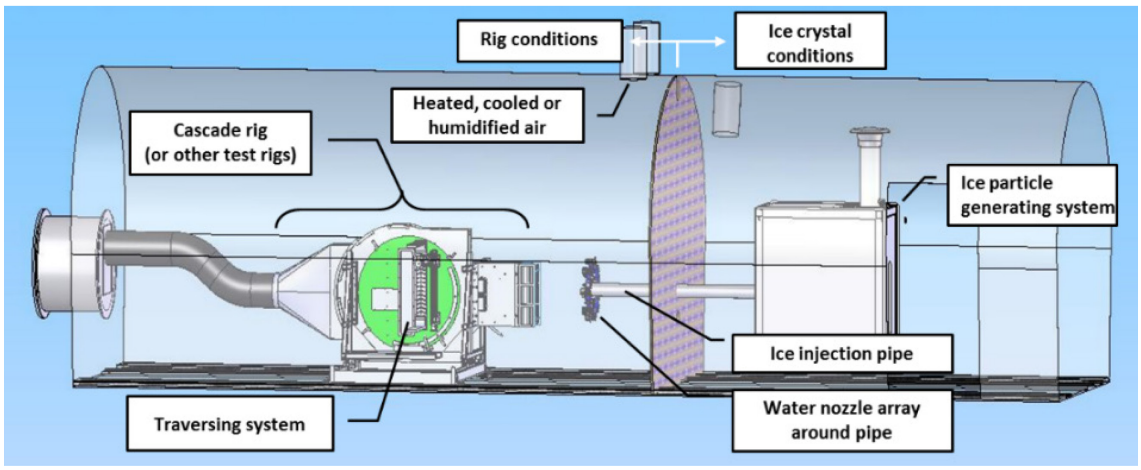

Figure 4-30: Ice Crystal Icing System Installed in the Research Altitude Test Facility (RATFac), Ichamber Outlet on Left Side.

4.6.3.9 von Karman Institute (VKI) IWT (CWT-1)

The VKI icing wind tunnel, CWT-1 [55] is an atmospheric pressure, closed loop wind tunnel capable of operating in subfreezing temperatures (see Figure 4-31). The flow is generated by a centrifugal fan driven by a PC-controlled variable-speed motor to achieve any specific speed-time history. The settling chamber, fitted with a honeycomb to straighten the flow, is followed by a 12.4 to 1 contraction and a 1.6 m long test section with 0.1 m by 0.3 m cross section. Three sides of the test section are made of double glazing windows to provide optical access. Due to interchangeable top walls, a water injection spray nozzle can be mounted right at the beginning of the test section. Cooling of the facility is obtained by injection of pressurized liquid nitrogen through spray nozzles located in the return circuit. In 2018, the return circuit was modified, adding a bypass section equipped with a chiller which allows a pre-cooling of the facility down to -5°C, reducing the liquid nitrogen consumption during tests.

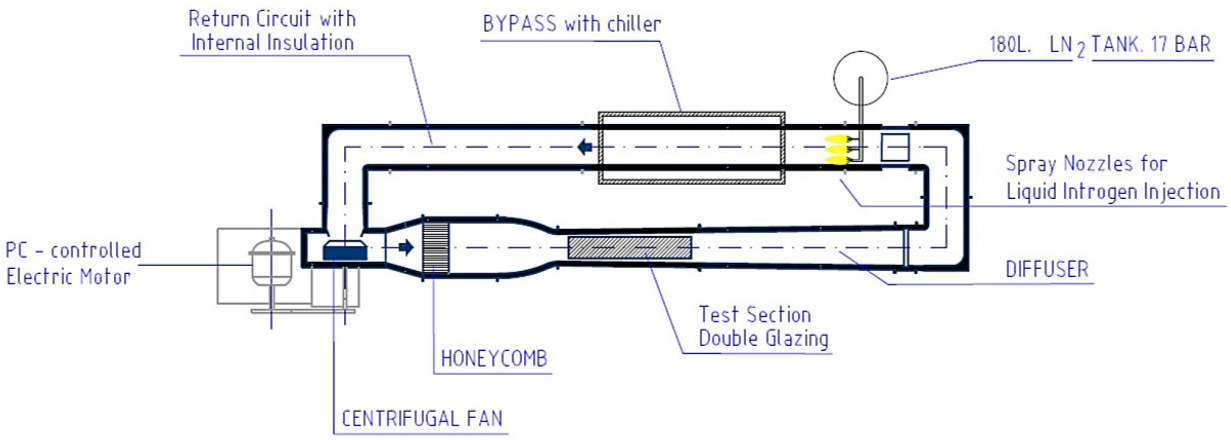

Figure 4-31: von Karman Institute Icing Wind Tunnel (CWT-1) Aerodynamic Layout [55].

The facility can run between 30°C to -40°C, with a wind speed ranging from 1 to 65 m/s. The Liquid Water Content (LWC) can be varied between 0.1 to 1 g/m^3, with supercooled water droplets between 20 to 50 µm. The facility is also equipped with an ice crystal generator.

The CWT-1 was specially designed to study the motion of films of anti-icing fluids applied to aircraft wings during a simulated take-off. It was used to define the international standards for certification of aerodynamic acceptance of aircraft de-icing/anti-icing fluids. It is also suitable for optical measurements of surface wave motion and general flow studies. Presently, it is used for fundamental research of de-icing physics, development of anti-icing and de-icing solutions, characterization of small items (coatings, sensors) and instrument calibration at temperatures as low as -40ºC.

4.7 FLYING FACILITIES AND FLIGHT TEST

Aerial platforms are used for icing research in natural and artificial icing conditions. They are also able to characterize the cloud conditions that produce the desired icing conditions. In this section, major icing instrumentations and equipment for flight tests and icing aerial platforms are described.

4.7.1 Instrumentations and Equipment for Icing Flight Tests

The on-board instrumentation is essential for in-flight icing tests, which would enable monitoring the weather conditions and thermodynamic characteristics of the surrounding atmosphere at the time of icing as well as microphysics of clouds. NASA Airborne Science Program Instrument Database [56] and EUFAR (EUropean Facility for Airborne Research) Aircraft & Instruments database [57] provide detailed description of equipment and instrumentation in all types of cloud microphysics parameters. Major instrumentations that are used for most natural and artificial in-flight icing testing are briefly described below. Ice detection systems are also essential but will not be mentioned here since they have already been extensively described in Chapter 1 of this report.

4.7.1.1 Cloud Microphysics

Cloud microphysics is a branch of the atmospheric science concerned with the many particles that form a cloud. The characterization of the cloud microstructure will allow us to study in detail the behavior of the icing process. This includes knowledge of the size, shape, phase and concentration of the particles that make up the cloud.

Most of the equipment is able to measure more than one parameter at the same time, i.e., Cloud Aerosol and Precipitation Spectrometer (CAPS) include three instruments: Cloud Imaging Probe (CIP), the Cloud and Aerosol Spectrometer (CAS), and the Hotwire Liquid Water Content (LWC) Sensor.

4.7.1.2 Particle Size Distribution and Particle Concentration

An accurate characterization of the hydrometeor size distribution is very important in icing research. The droplet size combined with the LWC can lead to different types of ice. Hydrometeor size instrumentation frequently offers complementary information, such as detailed morphology or particle mass calculation. Instruments for measuring hydrometeor diameters within icing clouds are generally measured by different optical techniques.

Optical array probes (OAPs) are used to derive shape, size, and number concentration of cloud and precipitation particles from 1 or 2-D images. OAPs are based on the principle of a linear array of photodetectors illuminated by a laser to image cloud particles crossing the laser beam. 1D only measures the size and 2D also provides shapes.

Particle imagers use a cross section image produced from a laser source by particles to obtain size distributions. Spectrometers use diffusion of lights produced by a particle to determine size distribution. Other techniques can be used, such as vaporization of droplets based on the balance of the exchange of energy between heated wires and two-phase flow, and mechanical systems based on the mechanical collection of droplets (for example, by multi-cylinders, grids, or blade) or systems based on the impact of droplets on a reference soot-coated slide such as the cloud gun.

4.7.1.3 Cloud Water Content

Total water content and discrimination of liquid cloud particles from the ice phase are other essential parameters in icing research. Liquid Water Content (LWC) is the more commonly measured parameter, but in the case of a campaign that includes solid particles (e.g., snow or ice crystals) a total water content (TWC = LWC + IWC) measurement is necessary. Other parameters such as particle extinction or terminal fall speed can also be measured.

4.7.1.4 Temperature

Outside air temperature is an essential parameter in icing tests. Calibrated temperature probes are used to measure the Static Air Temperature (SAT). The SAT can be measured by using the total temperature measurement device in conjunction with the measurement of the air speed under the hypothesis of adiabatic transformations. Icing is most frequent when the SAT is between +2°C and -20°C, although ice can accrete outside this range.

4.7.1.5 Humidity

Humidity is related to air pressure. It is basic for the dew point in relation to the temperature, which gives us information about the humidity. If the dew point is close to the temperature, humidity is high, which can cause hazy conditions, fog or even frost. A high dew point means a higher density altitude, which reduces aircraft performance. Temperature, humidity and dew/frost point have influence on the type and shape of ice accreted on aircraft surfaces.

4.7.2 Icing Aerial Platforms

The platforms mentioned in this section are not for exclusive use in icing tests, but their configuration (on-board equipment) may vary depending on the objective of the campaign. A short description of major worldwide flight icing facilities, which can be used in natural or artificial flight tests, is provided in this

section. Flight performance and basic aircraft characteristics that are important for icing flight tests are also included in a tabular format.

4.7.2.1 CNRS SAFIRE ATR-42

The ATR-42 is a large tropospheric research aircraft equipped with basic meteorological measurements and some cloud instrumentation, operated by SAFIRE (Service des Avions Francais Instrumentés pour la Recherche en Environnement) [58]. The ATR-42 is a twin-turboprop, short-haul regional airliner, designed to have better performance especially in hot and high conditions (see Figure 4-32). This aircraft is part of the EUFAR TA fleet.

SAFIRE has its own pilots, mechanics, and technical staff for instrument installation and certification services. Safire has performed many ice microphysics campaigns along with Laboratoire de Météorologie Physique, a leading cloud microphysics laboratory, which means that many state-of-the-art instruments are certified in these campaigns.

Figure 4-32: CNRS SAFIRE ATR-42 Aircraft [58].

This aircraft is currently participating in SENS4ICE project. SENS4ICE will address the development, testing, validation, and maturation of the different detection principles, the hybridization and the airborne demonstration of technology capabilities in relevant natural icing conditions. This is one of the three aircraft chosen with the objective of validating the hybrid ice detection system approach on different types of airplanes and under different flight conditions.

ATR-42 is, with 25 flight hours campaign programmed for winter 2020/2021, also part of the ICE GENESIS project as one of the two experimental aircraft used for flight tests. The top-level objective of the ICE GENESIS project is to provide the European aeronautical industry with a validated new generation of 3D icing engineering tools (numerical simulation and test capabilities) addressing Appendix C, Appendix O and snow conditions, for safe, efficient and cost-effective design and certification of future aircraft and rotorcraft. Data acquisition is centralized, and each scientist can display all parameters on his/her screen. Time series of all data can be provided within 2 hours after each flight.

Flying performance envelopes and aircraft characteristics are described in Table 4-10.

Table 4-10: CNRS SAFIRE ATR-42 Flying Performance Envelopes and Aircraft Characteristics.

Speed Range:	From 70 to 134 m/s
Max Flight Level:	25,000 ft
Flight Distance:	2,200 km (at min scientific payload and max fuel)
Max Take-Off Weight:	16,900 kg
Take-off Distance:	1,200 m
Wingspan:	24.57 m
Fuselage Length:	22.67 m

4.7.2.2 Yak-42D Roshydromet

Yak-42 Roshydromet is a new-generation research aircraft developed in 2013 by the Central Aerological Observatory of Russian Federal Service for Hydrometeorology and Environmental Monitoring as an aircraft-laboratory with a measurement system capable of monitoring flight parameters and atmospheric thermodynamic characteristics [59]. It is intended to measure different parameters of the atmosphere and the underlying surface.

The measuring system of aircraft-laboratory Yak-42D "Atmosphere" includes three levels:

- The first level is different kinds of sensors and instruments: temperature and pressure sensors, navigation systems, spectrometers, radars, radiometers, particles counters and others.
- The second level is hardware-software complexes which combine sensors and measuring systems through a special software. These provide measurements of navigation parameters, thermodynamic characteristics, solar radiation and radiation balance in the atmosphere, microphysical parameters of clouds, location of clouds and surfaces, radioactive pollutants and gas and aerosol concentrations.
- The third level is the integration of the hardware-software complexes to the common on-board measuring system of the aircraft. This system contains the Data Acquisition System (DAS), facilities for cloud modification, satellite connection for fast transmission of data from the aircraft to ground-based centers and means for providing control of local experiments from the special ground center.

Flying performance envelopes and aircraft characteristics are described in Table 4-11.

Table 4-11: Yak-42 Roshydromet Flying Performance Envelopes and Aircraft Characteristics.

Speed Range	From 350 up to 700 km/h
Max Flight Level	10200 m
Flight Distance	3500 km
Max Take-Off Weight	58 tons
Crew	3 members
Scientific Crew	Up to 14 members

4.7.2.3 NRC Convair 580

The Canadian NRC Convair 580 (see Figure 4-4 in Section 4.2.2.2) is a twin-engine, pressurized aircraft capable of long-distance operation carrying several racks of instrumentation and up to a dozen research crew members, as well as a multi-purpose flying laboratory for atmospheric studies, gradient aeromagnetics, advanced navigation, spotlight synthetic aperture radar and precision aircraft positioning using a differential global positioning system [11].

The aircraft has standard research support capabilities that include high-speed data acquisition systems, multi-camera video recording systems, free-stream chemistry sampling inlets, multiple navigation sensors, high bandwidth data-link communications, electro-optic and infrared sensors, wing-mounted pylons, and wingtip-mounted pods.

The NRC Convair 580 team has an international reputation for high quality research work on winter storms and aircraft icing issues. The aircraft has supported atmospheric studies about cloud physics and aircraft icing and has been part of many Canadian in-flight icing research campaigns:

***Canadian Atlantic Storms Program (CASP)*:** This project was conducted from 15 January to 15 March 1986 over Atlantic Canada in conjunction with the American Genesis of Atlantic Lows Experiment (GALE). The goals of CASP were to begin the process of understanding and eventually better predicting the mesoscale structure of East Coast storms as well as the storms themselves.

***First International Satellite Cloud Climatology Project (ISCCP)*:** The first project of the World Climate Research Program (https://en.wikipedia.org/wiki/World_Climate_Research_Program). Since its inception in 1982, there have been two phases; 1983 – 1995 and 1995 – 2009. The project is responsible for collection and analysis of weather satellite (https://en.wikipedia.org/wiki/Satellite) radiance measurements. The results were studied to understand clouds in climate, including their effects on radiative energy exchanges (https://en.wikipedia.org/wiki/Radiative_forcing).

***Regional Experiment Arctic Cloud Experiment (FIRE.ACE)*:** The First ISCCP Regional Experiment (FIRE) Arctic Clouds Experiment (ACE) was conducted during April-July 1998 to study Arctic cloud systems under spring and summer conditions. The main goal of the experiment was to examine the effects of clouds on radiation exchange between the surface, atmosphere and space, and to study how the surface influences the evolution of boundary layer clouds.

***Supercooled Liquid Drop Flight Research Study*:**

- Canadian Freezing Drizzle experiment and Canadian Freezing Drizzle Experiment III.
- Alliance Icing Research Study.
- Buffalo Icing research Study I.
- HAIC/HIWC Cayenne 2015 Flight Test Campaign.

4.7.2.4 University of North Dakota Cessna Citation II

Cessna Citation II twin-engine fanjet is an atmospheric research aircraft manufactured by Cessna and modified and operated by University of North Dakota [60], [61]. This aircraft has several design and performance characteristics that make it an ideal platform for a wide range of atmospheric studies, including both high performance and the ability to fly at slower speeds necessary for many types of measurements. The basic instrument package includes measurements of aircraft speed and position, along with atmospheric state parameters, such as temperature, relative humidity and winds.

A series of structural modifications have been made to the basic airplane, including pylons under the wing tips for a variety of probes in the undisturbed air flow away from the fuselage; a gust probe for wind measurement; and air inlet ports for air sampling inside the pressurized cabin. Fuselage mounting locations are available for a

6-angle electric field mill configuration and other instruments. A dropsonde capability is also included. A variety of instruments are available in-house for observing atmospheric conditions. The installation of instruments provided by other investigators can be accommodated, subject to space, weight and electrical requirements. Also, a variety of 19-inch racks are available to accommodate instruments and support systems. They also have their own hangar lab, a calibration lab and a penthouse lab for supporting Citation II research aircraft.

However, research projects typically involve deployment of very advanced instruments to conduct specific scientific measurements, such as hydrometeor concentration, size and mass. Most projects performed by Citation II aircraft are in the field of cloud physics, but the platform has also done projects to study electric fields, atmospheric chemistry and weather modification.

The data acquisition system always records basic parameters such as position, altitude and speed. The meteorological package includes measurements of temperature, dew point temperature, pressure and wind. The three-dimensional wind field algorithms use measurements of acceleration, pitch, roll and yaw combined with angle of attack, angle of sideslip and airspeed measurements. An Applanix POS-AV strap-down gyro system, with integrated Global Positioning System (GPS), provides the ground relative parameters, while the gust probe provides the air relative parameters. Software calculates the turbulence intensity from differential pressure transducer measurements.

Flying performance envelopes and aircraft characteristics are described in Table 4-12.

Table 4-12: Cessna Citation II Flying Performance Envelopes and Aircraft Characteristics.

Speed Range	Sampling speed: 160 knots (82.3 m/s) Cruise speed: 340 knots (175 m/s)
Max Flight Level	43,000 ft (13.1 km)
Flight Distance	1,998 Nmi
Max Take-Off Weight	14,500 lbs
Crew (pilots + Operators)	3 (minimum)
Seats Available for Scientists	2

4.7.2.5 NASA Twin Otter

The NASA Icing Research Aircraft – N607NA is a modified DeHavilland DHC-6 Twin Otter powered by two 550 shaft horse power Pratt and Whitney PT6A-2 turbine engines driving three-bladed Hartzell constant speed propellers [62], [63], [64].

It is a versatile aircraft capable of flying various mission profiles with an array of instruments. The aircraft has instrument mounts on both wings as well as numerous fuselage mounting points. It is an economical aircraft for missions flown below 20,000 ft at speeds of around 90 to 140 knots.

The flight controls are mechanically operated through a system of cables and pulleys. Control surfaces consist of elevator, ailerons, rudder, and wing flaps. The horizontal tailplane has a fixed stabilizer with an elevator and trim tab. Twin Otter aircraft has participated in numerous projects [63], [64], such as the Iced Aircraft Flight Data for Flight Simulator Validation and AIRS.

The research data acquisition systems enabled measurement and recording of the aircraft dynamics, wing and tailplane surface pressure and video documentation of wing & tailplane flow visualization and pilot actions.

Flying performance envelopes and aircraft characteristics are described in Table 4-13.

Table 4-13: NASA Twin Otter Flying Performance Envelopes and Aircraft Characteristics.

Speed Range	120 – 140 KIAS (Knots Indicated Airspeed)
Max Flight Level	25,000 ft
Flight Distance	420 Nautical miles
Max Take-Off Weight	11,000 lb
Wingspan	65 ft
Fuselage Length	59ft-9 in
Crew (Pilots + Operators)	1 – 2
Seats Available for Scientists	1 – 3

4.7.2.6 DLR Dornier 228-212

This aircraft is a twin-engine turboprop primarily used for remote-sensing missions by the German Aerospace Center's (Deutsches Zentrum für Luft- und Raumfahrt; DLR) Oberpfaffenhofen flight facility. It has a large box-shaped cabin and large cabin floor openings. This makes it especially well-suited for setting up special camera systems such as the High Resolution Stereo Camera (HRSC), which is also used for space observation [11], [13], [16], [65].

Digital sensors are installed as required. These sensors deliver optical remote-sensing data in the infrared spectrum in high resolution. The so-called multi- and hyperspectral sensors were developed by the German Aerospace Center in cooperation with its partners.

The airborne digital sensors measure data in a range of between several kilometers and a few decimeters. Repeat measurements are performed at the same location, using different digital sensors such as the Digital Airborne Imaging Spectrometer (DAIS), the Reflective Optics System Imaging Spectrometer (ROSIS), the Hyperspectral Scanner (HYMAP), and the Airborne Reflective Emissive Spectrometer (ARES). This yields much more precise information about the Earth's surface and its vegetation than could previously be obtained using camera systems.

The DLR Microwaves and Radar Institute (DLR-Institut für Hochfrequenztechnik und Radarsysteme) operates DLR's Experimental Synthetic Aperture Radar (E-SAR) system and its successor F-SAR, to gather data for atmospheric research. Because of their modifications, only this longer 212 variant of the Dornier 228 can fly with these radar systems. Amongst other uses, the E-SAR and F-SAR systems are deployed in preliminary studies for future satellite missions, such as the German TerraSAR-X radar satellite.

The Do 228-212 research aircraft is deployed for the following fields of research:

***Geophysics, glaciology and climate studies*:** Using the E-SAR radar system developed by DLR, geophysical radar measurements of the internal structure of the Antarctic and Greenland ice sheets are performed on board the Do 228-212. The research contributes to the determination of ice dynamics and makes it possible to predict changes in the large ice sheets as a result of climate change.

***En route with E-SAR for ICE-SAR*:** The DLR participated in a large-scale measurement campaign in connection with the International Polar Year (IPY) 2007/2008. DLR was hoping to gain new insights into

the formation and properties of land and sea ice. Between March and April 2007, scientists and technicians of the DLR Microwaves and Radar Institute used the E-SAR airborne radar system to conduct research in Spitsbergen, Norway, within the framework of the ICE-SAR campaign (Iceland Association for Search and Rescue). The aim is to find characteristic parameters of land and sea ice, which are required in order to be able to establish the mutual influence between ice and atmosphere. The IPY is a global scientific research campaign covering both the Arctic and the Antarctic. It receives substantial support from ESA. Scientists from over 60 countries participate in this two-year research program.

***EURICE*:** The EURICE project was fundamentally aimed at carrying out a coordinated effort in Europe to examine current aircraft icing problems and the related certification process, operation procedures and flight standards. Flight campaign objectives were to find SLD conditions and determine the characteristics of the cloud, understand the growth process for liquid drops and understand the limiting and favorable atmospheric conditions for SLD formation.

Flying performance envelopes and aircraft characteristics are described in Table 4-14.

Table 4-14: DLR Dornier 228-212 Flying Performance Envelopes and Aircraft Characteristics.

Speed Range	From 40 to 100 m/s
Max Flight Level	25,000 ft
Flight Distance	2,700 km (at min. scientific payload and max. fuel)
Wingspan	16.97 m
Fuselage Length	16.86 m (18.7 m including nose boom)
Crew (Pilots + Operators)	VFR 1 Pilot, IFR 2 Pilots
Seats Available for Scientists	19 (Pax Configuration)

4.7.2.7 INTA Aviocar C-212

The C212-200 aircraft (Figure 4-33), owned and operated by Spanish INTA (National Institute for Aerospace Technology), is a high wing, turboprop aircraft, with highly versatile Short Take-Off and Landing (STOL) capabilities, with the ability to take off and land on unprepared runways. Its service ceiling is 25,000 ft (7,620 m) Mean Sea Level (MSL). Considering that the cabin is not pressurized, a mandatory supply of oxygen is available to operate at altitudes above 10,000 ft (3,000 m). The rear loading ramp allows easy loading and unloading of scientific instrumentation. The high wing design facilitates safe maneuvering around the aircraft during ground operations. Four rails along the fuselage, two of them on the floor and two on both sides, provide a safe and fast means of attaching racks and equipment to the aircraft structure.

Two C-212 aircraft are available in INTA: C-212 S/N (serial number) 270 and C-212 S/N 301. C-212 S/N 270 aircraft carries out remote sensing and Earth observation campaigns, with high performance imaging sensors, in particular an Airborne Hyperspectral Scanner (AHS) sensor and a CASI-1500i spectrometer. The AHS is an 80-band whiskbroom radiometer, manufactured by Sensytech Inc. (now Argon ST, and previously Daedalus Inc.) under INTA specifications in 2003. It is based on previous hyperspectral scanners such as the Multispectral Infrared and Visible Imaging Spectrometer (MIVIS) and the MAS prototype (MODIS Airborne Simulator). The AHS has been integrated with a GPS / INS POS-AV 410 module provided by Trimble-Applanix that offers precise positioning to geolocate the center of each pixel in the scene using direct call technique. For its part, the CASI 1500i sensor is an aerial spectrometer that allows obtaining images with a resolution of less than one meter, with a field of view of 40°.

The C-212 S/N 301 aircraft has the necessary instrumentation to carry out campaigns to study the atmosphere, develop airborne instrumentation and validate sensors. Two pods were installed under the wing to install different types of probes: CAPS, PCASP-100X, FSSP-100er, OAP-2D2-C and OAP-2D-GB2, among others. A Flight Test Instrumentation (FTI) module records and monitors in real time the performance parameters of the aircraft during flight operations.

Instruments are also available on board to measure temperature, pressure, and relative humidity and GPS position. In addition, there are different registers that provide the electrical power necessary for the scientific instrumentation installed outside the aircraft. In addition, standard 19-inch wide certified racks are available for the installation of scientific equipment, computers and data display screens.

Figure 4-33: INTA In-Flight C-212.

These aircraft are in the EUFAR platform and have been used in the following flight test campaigns related to icing:

- EURICE project (1997 – 1999): Aircraft icing SLDs.
- EXTICE project (2009 – 2013): Aircraft icing shape determination.
- TECOAGUA (2014 – 2015): Precipitation enhancement.
- METEORISK (2015 – 2017): Improve weather forecast.
- PHOBIC2ICE (2016 – 2019): Icing on passive systems. Flights will take place on 2020-2021 winter.
- NATO AVT-332 (2019 – 2022): Icing on icephobic coatings. Flights will take place sometime in fall 2021 or winter 2022.

The data acquisition system can record basic parameters such as position, altitude, angle of attack, angle of slip, and speed. The meteorological package includes measurements of temperature, dew point temperature, pressure and wind. It is possible to register aircraft performance related to the engines (power, torque, RPM, fuel flow) or with the attitude (angles, velocities and angular accelerations). Trajectories by GPS and D-GPS are always recorded and can be synchronized with the obtained data in the thermodynamic characterization of the atmosphere.

Flying performance envelopes and aircraft characteristics are described in Table 4-15.

Table 4-15: INTA Aviocar C-212 Flying Performance Envelopes and Aircraft Characteristics.

Speed range	From 46 to 102 m/s
Max flight level	25,000 ft
Flight distance	1,760 Km
Max take-off weight	7,700 Kg
Take-off distance	630 m
Wingspan	19.0 m
Fuselage length	15.2 m

4.7.3 Spray Tankers

The early use of icing tankers was done by the US military, with the US Army Corps of Engineers modifying a Boeing CH-47D Chinook to test how ice would form on various helicopters. The Chinook was equipped with a spray bar system to create droplets to show how they reacted on a helicopter's rotors. The Chinook was equipped with a 1,200-gallon tank that allows roughly 30 minutes of spray time. The tanker's sprayer system is hung below the aircraft and allows even distribution across the helicopter under testing. The spray system had holes at the leading edge of the tube to allow for wind to flow and create a water-air blend and distribute the water into the correct droplet sizes.

The aircraft under testing (Figure 4-34) was monitored by a Beechcraft King Air that had been modified with icing sensors to see how severe the icing conditions get on the testing airframe. The tests would stop if the aircraft in question was exhibiting degraded flight capability to an extent that the safety risk for the crew and aircraft had reached the maximum acceptable level.

Both the government and private companies have used water spray tankers to produce an artificial icing cloud for simulation of natural icing conditions. The most extensively used tanker was a modified Boeing NKC-135A aircraft, US Air Force (USAF) S/N 55-3128. This tanker was used to evaluate anti-icing/de-icing systems and other critical areas such as engine inlets of all new military aircraft over several decades. The KC-135 saw massive usage after the crash of American Eagle Flight 4184 with numerous aerospace companies testing their jets alongside the FAA in the mid to late 1990s. The ATR's crash and the new discovery of supercooled droplets reducing performance on light commercial and business jets forced the KC-135R to test a large portion of the business and regional jet aircraft to certify their airworthiness during severe icing conditions.

The tanker program was overhauled through the late 1990s with one aircraft being retired and the other being modified to attempt to increase the spray into newer icing envelopes. Since then, the KC-135R has gone on to providing icing tests for various other large and small aircraft, as it is the required testing aircraft for large transport planes. Some aircraft that have been tested using the KC-135R include the Boeing 777-200 and Saab 2000, which both passed their respective tests. Further enhancements have also been studied. Edwards Air Force Base (EAFB) released a study in 2013 highlighting attempted improvements in structural flow around the icing boom.

Other water spray systems used for icing cloud generation include a modified T-47 owned by Cessna Aircraft, a Cessna Citation II aircraft which was modified for Lockheed-Martin by Cessna Aircraft Company, a Raytheon (King Air) tanker, and the US Army helicopter icing spray system (HISS). Although most of these aircraft have been removed in recent years as their limited icing creation hurts their validation for certification, Cessna has gone ahead and created its own icing tanker to run tests in-house. The company

modified a used Cessna Citation XLS+ with registration N563XP to allow for the aircraft to operate as an aircraft icing tanker.

Figure 4-34: Example of Spray Tanker Test with Three Different Aircraft Involved [66].

In the following sections, a brief description of capabilities of these spray tankers is presented based on the information in the paper by Ford [38].

4.7.3.1 US Air Force Icing Tanker

The NKC-135A S/N 55-3128, was an aerial refueling tanker modified to perform water spray missions for both in-flight icing and in-flight rain evaluations of new and modified USAF aircraft. This aircraft was first modified in the late 1950s to perform these missions. Beginning in 1987, it was upgraded to correct spray tanker deficiencies and to improve cloud physics. This upgrade also provided for dual use of the tanker for uninstrumented air refueling of local test sorties at EAFB.

In the water spray configuration, the forward body fuel tanks were capped and separated from the remainder of the fuel system and were filled with 2000 gallons of demineralized water. This was enough water for about 2 1/2 hours of testing, depending on the flow rate selected. Bleed air from the number 2 and 3 engines was used to prevent the water in the array and around the nozzles from freezing, and for atomization of water from the nozzles to obtain the desired cloud physics characteristics.

The airspeed and altitude ranges for in-flight icing testing using the circular array were 150 to 300 Knots Indicated Airspeed (KIAS) and 5,000 feet Above Ground Level (AGL) to 30,000 feet Pressure Altitude (PA). A Laser Distance Measuring System (LDMS) and video camera were mounted in a pod in the aft fuselage area. The LDMS was used to maintain the desired separation distance between the tanker and the system under test.

4.7.3.2 USAF KC-135R Multi-Use Tanker

The KC-135R program has been established to replace the old tanker water spray system with a newer and more capable system. Called the "Airborne Icing Tanker", this new capability provided a larger cloud and droplet MVD within the 14 CFR Part 25, Appendix C envelope up to 1.0 g/m^3. The KC-135R tanker contained multi-use provisions to reduce operating costs.

A main feature of KC-135R is the laser distance measuring system that allows an accurate positioning of the aircraft behind the tanker. The laser system is also equipped with a video camera that allows very good documentation of ice accretion when sea marker dye is used in the spray water. An additional feature of the system is measurement of the SLD icing conditions. During ATR-72 tests, the maximum calculated MVDs were in the range of 120 µm. One of the limitations is a small cloud diameter. Small cloud diameter of 4 to 8 feet does not allow complete coverage of large areas such as the Boeing 777 type turbofan engines.

4.7.3.3 Cessna Icing Tanker

The Cessna icing tanker is a modified T-47, with enough water for about 40 minutes of "water on" air work. The aircraft runs a water pressure of 120 psi inside the cabin. The spray boom is a "V" shape extension off the top of the aircraft vertical fin and generates a spray plume about 4 to 6 feet in diameter, depending on separation distance. The array contains four hydraulic atomization type nozzles, which produce small droplet sizes by injecting the water at opposing angles into the airstream. The USAF tanker used nozzles that injected air parallel to and surrounding the water jet, which were both injected directly aft into the airstream. The Cessna nozzles have been calibrated twice, and both calibration reports are available by request of Cessna.

Through data collected during many years of use, it has been determined that the Cessna system provides a droplet diameter of 30 µm. The spray boom is partially heated but will ice up if the nozzles are dirty (i.e., the water doesn't leave the spray nozzle in a clean manner). Also, all conditions that are not optimum result in droplets that are larger than 30 µm. LWC for the test conditions is measured using instrumentation aboard the test aircraft and can be varied by changing the distance from the tanker.

4.7.3.4 Raytheon Icing Tanker

The Raytheon icing tanker is a type-B200 King Air twin-engine turboprop, high T-tail aircraft. The normal tanker speed and altitudes for testing are 160 kts and 5,000 to 18,000 ft, respectively. The aircraft is operated by single pilot but normally flown with two pilots and requires a water tank operator. The water tank is locally manufactured, removable, and holds approximately 300 gallons. It feeds bleed air aspirated icing nozzles. There are four nozzles in the top of the vertical tail to provide the icing pattern. The plume is approximately 4 feet in diameter at approximately 100 feet behind the tanker. The previous Air Force tanker had 100 nozzle positions, 49 of which were actually used for spraying water and the rest used for bleed air heating to help keep the nozzles from icing up. The new Air Force tanker icing array will have 216 nozzles. The US Army HISS contains eight nozzles, the Cessna tanker contains three nozzles, and the Dornier spray array will accommodate up to 61 nozzles.

4.7.3.5 US Army Icing Spray System

The US Army HISS consists of a horizontal spray boom arrangement mounted on the rear of a CH-47 Chinook helicopter. The cloud size is 8 feet high by 36 feet wide, which is designed to expose the entire length of the rotor blades of a helicopter under test to the plume. Spray nozzles are hydraulically aspirated. Water is contained in a tank within the fuselage. The test airspeed range is from 80 to 130 KIAS and the test altitude range is from 1,500 ft AGL to 12,000 ft MSL. Test temperature range is down to -23.5°C. Below that temperature the nozzles begin freezing up. Tests are conducted during the winter months each year at Duluth, Minnesota.

4.7.3.6 Dornier Icing Tanker

The Dornier icing tanker used for certification flights is a DO228-200, D-ICDO. It is equipped with two water tanks of 500 liters each. The system provides a spray time of about 37 minutes with 43 nozzles and about 26 minutes with 61 nozzles in the spraybar.

The pressure of the water pump is 70 bar (adjusted). To avoid freezing of the nozzles, it is necessary to have noninterrupted water flow in the nozzles. This works until -25°C. For cloud calibration and certification flights, L212.205 nozzles (from Lechler GmbH, Metzingen, Germany) are used in the spraybar. The outlet diameter of the nozzles is 0.6 mm and the narrowest cross section is 0.3 mm. The calculated mass flow for 70 bar with 61 nozzles is 38.4 l/min and for 70 bar with 43 nozzles is 27.1 l/min. During the calibration, the relative humidity in percent and the rate of water flow in liters per minute is measured and recorded. A digital GPS is used for accurate position between the tanker aircraft and the test aircraft (in three dimensions). A reference GPS is installed in the tanker aircraft. With this configuration an accuracy of measurement of 30 cm is possible. The tanker aircraft is also equipped with two video cameras above and below the spraying rig in order to position the test aircraft accurately in the water spray plume. During a recent certification test, a LWC between 0.3 g/m^3 and 1.6 g/m^3 (depending on distance between tanker and test aircraft, number of nozzles and outside air temperature) with an MVD of about 40 microns was achieved.

4.8 SUMMARY

In this chapter, we first reviewed intrinsic functions of icing test facilities, primarily icing wind tunnels, and flying facilities and their capabilities. IWTs are categorized into large industrial IWTs, engine test cells and small facilities. Flying tests consist of three types: artificial icing tests in clouds produced by an icing tanker, natural icing tests in natural icing clouds and testing with simulated ice shapes.

We then reviewed icing certification process and protocols for IPS and aircraft development, which have a strong influence on the requirements for icing tests and facilities. The certification processes and protocols are described in FAA and EASA Certification Specifications (CS-25) Appendix C, where they defined safe operating envelopes. Appendix O was developed to include more stringent requirements for safe operating envelopes as part of the certification process, including Supercooled Liquid Drops (SLDs), Ice Crystal Icing (ICI) and mixed phases. Consequently, the testing facilities must improve their capabilities to properly simulate new testing environment.

Although the testing capabilities of IWTs and flight testing continue to improve, there are still challenges remaining in accurate measurements of droplets and ice shapes in IWTs and in finding desired icing conditions for flight testing in natural icing conditions. Generation of artificial icing conditions is not easy due to many technical challenges such as accurately prescribing the small cloud/plume diameter and uniformity, and humidity, to name a few.

We then reviewed major worldwide IWTs (in the Western world) in three categories: large industrial facilities, engine test cells and small-scale facilities. We described unique capabilities of each facility and testing parameter ranges. For flying test facilities, we briefly reviewed major icing aerial platforms (i.e., fixed-wing spray tankers and a helicopter spray tanker), together with instrumentations and equipment used by these platforms.

4.9 ACKNOWLEDGMENTS

Special thanks go to several icing specialists who have contributed to the preparation of this chapter:

- Meredith Fleming, Cris Bosetti, Adam Malone: NW Aerodynamic Testing Manager, Boeing Aero/Noise/Propulsion Laboratories.

- Stephan Bansmer: Braunschweig Icing Wind Tunnel.
- Hugo Pervier: Research Fellow, School of Aerospace, Transport and Manufacturing, Cranfield University.
- Claire Freudenreich (mailto:claire.freudenreich@intradef.gouv.fr): DGA aero-engine testing.
- Dan Fuleki: Gas Turbine Laboratory / Aerospace Research Centre, National Research Council / Government of Canada.
- Pierre Berthoumieu (mailto:Pierre.Berthoumieu@onera.fr): The French aerospace lab ONERA.
- Hermann Ferschitz, Wolfgang Breitfuss, Michael Wannemacher: RTA Climatic Wind Tunnel and Icing Wind Tunnel Vienna.
- Antonio Carozza: CIRA Centro Italiano Ricerche aeronautiche.

4.10 REFERENCES

[1] SAE, "Summary of icing simulation test facilities", SAE AIR5320 – REV. A 2015) [Original SAE AIR5320 published in 1999].

[2] FAA, "Capabilities and prospects for improvement in aircraft icing simulation methods: contributions to the 11C working group", DOT/FAA/AR-01/28 May 2001.

[3] "Calibration and acceptance of icing wind tunnels", SAE Aerospace Recommended Practice, ARP 5905 2003.

[4] Federal Aviation Administration, US Department of Transportation, Advisory Circular, AC-29-2B.

[5] global Security.org. Image of Artificial Icing Tests. Credit: US DoD / Roger-Viollet). https://www.globalsecurity.org/jhtml/jframe.html#https://www.globalsecurity.org/military/systems/aircraft/images/hu-25-dvic243.jpg||| (accessed 12 Dec 2025).

[6] Schumacher, P.W.J., "Reckoning with ice ….", Aerospace Safety, AFRP 62-1. 25(10), pp. 4-5, October 1969.

[7] Downey, D.A., Murrell, R.C. and Young, C.J., "Artificial and natural icing tests of the UH-60A helicopter configured with the XM-139 multiple mine dispensing system (VOLCANO)", U.S. Army's Aviation Engineering Flight Activity (AEFA) at Edwards Air Force Base (CA), Technical Report, AD-A205 031, March 1988.

[8] Cinquetti, P. and Martini, S., "Artificial and natural icing conditions flight tests on the Piaggio P.180 Avanti Aircraft", SAE Technical Paper 911004, 1991.

[9] Isaac, G.A., Cober, S.G., Strapp, J.W., Korolev, A.V., Tremblay, A. and Marcotte, D.L., "Recent Canadian research on aircraft in-flight icing", Canadian Aeronautics and Space Journal, 47(3), pp. 213-221, 2001.

[10] Amendola, A., Mingione, G., Caihol, D. and Hauf, T. "EURICE – A European effort for the improvement of in-flight aircraft icing safety", 36th AIAA Aerospace Sciences Meeting and Exhibit, Reno, NV, 12 – 15 January 1998.

[11] Williams, E.R., Donovan, M.F., Smalley, D.J., Hallowell, R.G., Griffin, E., Hood, K.T. and Bennett, B.J., "The 2013 Buffalo Area Icing and Radar Study (BAIRS)", MIT Lincoln Laboratory Report for FAA, 2015.

[12] Schröder, F., Welte, D. and Hauf, T., "Airborne observations of ice accretion and aircraft performance in artificial and natural supercooled ice clouds on Dornier 228 and 328 aircraft", 22nd International Congress of Aeronautical Sciences (ICAS 2000), Harrogate, UK, 27 August – 1 September 2000.

[13] Isaac, G.A. et al., "First results from the Alliance Icing Research Study II", 43rd AIAA Aerospace Sciences Meeting and Exhibit, Reno, NV, 10 – 13 January 2005.

[14] Schwarzenboeck, A. and Dezitter, F., "ICE GENESIS – creating the next generation of 3D simulation means for icing: Deliverables D5.1", 2019.

[15] Ray, M. and Anderson, K., "Analysis of flight test results of the optical ice detector", SAE Int. J. Aerosp. 8(1), 2015. doi: 10.4271/2015-01-2106

[16] Neel, C.B., "A heated-wire liquid-water-content instrument and results of initial flight tests in icing conditions", Research Memorandum of the National Advisory Committee for Aeronautics, NACA RM A54123, 1955.

[17] SENS4ICE, "Flight test platforms". https://www.sens4ice-project.eu/flight-test-platforms (accessed 11 Dec 2025).

[18] Zumwalt, G. and Mueller, A., "Flight and wind tunnel tests of an electro-impulse de-icing system", General Aviation Technology Conference, Hampton, VA, 10 – 12 July 1984.

[19] Catarella, R., Parkins, D. and Rogowicz, J., "Icing flight tests in Piper Malibu N77DE", SAE Technical Paper 965506, 1996.

[20] Botura, G., Sweet, D. and Flosdorf, D., "Development and demonstration of low power electrothermal de-icing system", 43rd AIAA Aerospace Sciences Meeting and Exhibit, Reno, NV, 10 – 13 January 2005.

[21] European Commission, Cordis Research Results, "Super-icephobic surfaces to prevent ice formation on aircraft", 1 February – 30 April 2019. https://cordis.europa.eu/project/id/690819/es

[22] Mora, J., García, P. and Agüero, A. "Deliverable 5.10" PHOBIC2ICE- 690819, 2019.

[23] NATO STO, "NATO AVT-332: In-flight demonstration (CDT) of icephobic coating and ice detection sensor technologies", 2019. *Cancelled activity.*

[24] Ratvasky, T., Barnhart, B., Lee, S. and Cooper, J., "Flight testing an iced business jet for flight simulation model validation", 45th AIAA Aerospace Sciences Meeting and Exhibit, Reno, NV, 8 – 11 January 2007.

[25] Deiler, C., Ohme, P., Raab, C. and Mendonca, C., "Facing the challenges of supercooled large droplet icing: results of a flight test based joint DLR-Embraer research project", SAE Technical Paper 2019-01-1988, 2019. doi:10.4271/2019-01-1988

[26] FAA of the USA, Final rule dated 04 November 2014 (Federal register 79, No. 213: Docket No. FAA-2010-0636; Amendment 25-140.

[27] EASA, CS-25 – Amendment 16, 12 March 2015 (Related documents: EASA Notice of Proposed Amendment (NPA), Comment-Respond Document (CRD), No. 2011-03 (NPA/CRD 2011-03 and 2012-22.

[28] National Transportation Safety Board, "Aircraft accident report – in-flight icing encounter and loss of control, American Eagle Flight 4184, Roselawn, Indiana, October 31, 1994", NTSB/AAR-96/01, 1996.

[29] FAA, Notice of Proposed Rulemaking (NPRM), "Airplane and engine certification requirements in supercooled large drop, mixed phase, and ice crystal icing conditions", Docket No. FAA-2010-0636; Notice No. 10-10, 29 June 2010.

[30] EASA, Notice of Proposed Amendment (NPA), "Large aeroplane certification specifications in supercooled large drop, mixed phase, and ice crystal conditions", NPA No. 2011-03, 21 March 2011.

[31] Ministère de l' Écologie, du Développement durable, des Transports et du Logement, "Final report on the accident on 1st June 2009 to the Airbus A320-203 registered F-GZCP operated by Air France flight AF 447 Rio de Janeiro – Paris", Bureau d'Enquêtes et d'Analyses (BEA), 2009. https://www.bea.aero/docspa/2009/f-cp090601.en/pdf/f-cp090601.en.pdf

[32] FAA, "Technical compendium from meetings of the engine harmonization working group", FAA Report No. DOT/FAA/AR-09/13, April 2009.

[33] Scott, A., and Sano, H., "Boeing warns of engine icing risk on 747-8s, Dreamliners", Reuters, 23 November 2013. http://www.reuters.com/article/us-airlines-boeing-idUSBRE9AM03G20131123

[34] FAA, CFR – Title 14 – Part 33.68 (Induction System Icing) and AC 20-147A, Oct 2014.

[35] EASA – European Union Aviation Safety Agency, "Certification Specifications and Acceptable Means of Compliance for Engines – CS-E", Amendment 4 and CS-25 – Appendix P, March 2015.

[36] Cober, S.G., Isaac, G.A. and Strapp, J.W., "Characterizations of aircraft icing environments that include supercooled large drops", Journal of Applied Meteorology, 40(11), 2001.

[37] Ford, J., "Capabilities and limitations of icing simulators in the simulation of icing conditions for the design and certification of aircraft and engines: Tankers", in DOT/FAA/AR-01/28, 2001.

[38] Vecchione, L, de Matteis, P. and Leone, G., "An overview of the CIRA icing wind tunnel", 41st Aerospace Sciences Meeting and Exhibit, Reno, NV, 6 – 9 January 2003. doi: 10.2514/6.2003-900

[39] NASA Glenn Icing Research Tunnel, Cleveland, OH. https://www.nasa.gov/centers-and-facilities/glenn/icing-research-tunnel/ (accessed 11 Dec 2025).

[40] Cranfield University Icing Tunnel, Cranfield, U.K. https://www.cranfield.ac.uk/facilities/icing-tunnel (accessed 11 Dec 2025).

[41] Chintamani, S.H, and Belter, D.L., "Design features and flow qualities of the Boeing research aerodynamic icing tunnel", 32nd Aerospace Sciences Meeting and Exhibit, Reno, NV, (AIAA 94-0540), 10 – 13 January 1994.

[42] RTA Icing Wind Tunnel, Vienna Austria. https://www.rta.eu/en/facility/customer-area/icing-wind-tunnel-iwt (accessed 11 Dec 2025).

[43] NASA Glenn Research Center, Propulsion Systems Laboratory. NASA PSL-3 https://www.nasa.gov/centers-and-facilities/glenn/propulsion-systems-laboratory/ (accessed 11 Dec 2025).

[44] Hervy, F., "New SLD icing capabilities at DGA aero-engine testing (2011-38-0086)", SAE International Conference on Aircraft and Engine Icing and Ground Deicing, Chicago, USA, 2011.

[45] Jérôme, E, Hervy, F. and Maguis, D., "Icing test capabilities at DGA aero-engine testing", International Journal of Engineering Systems Modelling and Simulation, 8(2), pp.77-85, 2016 doi: 10.1504/IJESMS.2016.075562

[46] Mingione, G., Iuliano, E., Guffond, D. and Tropea, C., "EXTICE: EXtreme Icing Environment", SAE International Conference on Aircraft and Engine Icing and Ground Deicing, Chicago, ICE-0052/2011-38-0063, 2011.

[47] Le Mézo, F. S1, Saclay, France, DGA Aero-Engine Testing. Air Transport Net, April 2013. https://airtn.eu/wp-content/uploads/airtn-dga-s1.pdf

[48] National Research Council Canada, NRC Altitude Icing Wind Tunnel Research Facility, 12 January 2022. https://nrc.canada.ca/en/research-development/nrc-facilities/altitude-icing-wind-tunnel-research-facility

[49] Le Mézo, F. PAG Icing Wind Tunnel, Saclay, France, DGA Aero-Engine Testing, Air Transport Net, April 2013. https://www.airtn.eu/downloads/airtn---dga---pag.pdf

[50] Hammond, D., "The Cranfield University Icing Tunnel", 41st Aerospace Sciences Meeting and Exhibit, Aerospace Sciences Meeting, Reno, Nevada, USA, 2003. http://dx.doi.org/10.2514/6.2003-901

[51] Oleskiw, M., Hyde, F. and Penna, P., "In-flight icing simulation capabilities of NRC's altitude icing wind tunnel", 39th AIAA Aerospace Sciences Meeting & Exhibit, Reno, NV, USA 8 – 11 January 2001.

[52] Cox and Company, LeClerc Icing Research Laboratory (LIRL) https://www.coxandco.com/assets/files/LeClerc_Specsheet.pdf (accessed 11 Dec 2025).

[53] Bansmer, S.E., Baumert, A., Sattler, S., Knop, I., Leroy, D., Schwarzenboeck, A., Jurkat-Witschas, T., Voigt, C., Pervier, H. and Esposito, B., "Design, construction and commissioning of the Braunschweig icing wind tunnel", Atmos. Meas. Tech. 11, 2018. https://doi.org/10.5194/amt-11-3221-2018

[54] Collins Aerospace, Icing Wind Tunnel. http://www.goodrichdeicing.com/services/icing-wind-tunnel/ (accessed 11 Dec 2025).

[55] von Karman Institute, Icing Wind Tunnel CWT-1. https://www.vki.ac.be/index.php/facilities-other-menu-148/low-speed-wind-tunnels/48-research-and-consulting/facilities/low-speed-wind-tunnels/63-cold-wind-tunnel-cwt-1 (accessed 11 Dec 2025).

[56] NASA Airborne Science Program Instrument Database. https://airbornescience.nasa.gov/instrument/all (accessed 11 Dec 2025).

[57] European Facility for Airborne Research (EUFAR), Aircraft and Instruments. https://www.eufar.net/instruments/ (accessed 11 Dec 2025).

[58] CEDA Archive. ATR42-SAFIRE Aircraft documents, 2010 – 2012. https://catalogue.ceda.ac.uk/uuid/8291c6659fb04c0ead2af01941a79c0e

[59] Borisov, Y. et al., “New Russian aircraft – laboratory Yak-42D atmosphere for environmental research and cloud modification”, 16th International Conference on Clouds and Precipitation, 2012.

[60] University of North Dakota, Citation Research Aircraft. https://aero.und.edu/atmos/citation-research-aircraft/index.html (accessed 11 Dec 2025).

[61] Ray, M. and Anderson, K., “Analysis of flight test results of the optical ice detector”, SAE International Journal of Aerospace, 8(1), 2015. doi: 10.4271/2015-01-2106

[62] NASA Glenn Research Center, Flight Research Building, Twin Otter Capabilities. https://airbornescience.nasa.gov/nsrc/aircraft/Twin_Otter_-_GRC (accessed 11 Dec 2025).

[63] Ratvasky, T., Blankenship, K., Rieke, W., and Brinker, D., “Iced aircraft flight data for flight simulator validation”, Technical Paper 2002-01-1528, SAE Transactions 111, pp. 100-112, 2002. https://www.sae.org/papers/iced-aircraft-flight-data-flight-simulator-validation-2002-01-1528

[64] Isaac, G. et al., “First results from the Alliance Icing Research Study II”, 43rd Aerospace and Science Meeting and Exhibit, Reno, NV, 2005. doi: 10.2514/6.2005-252

[65] German Aerospace Center, DLR Dornier Do 228-212. https://www.dlr.de/en/research-and-transfer/research-infrastructure/research-aircraft-fleet/dornier-do-228-212 (accessed 11 Dec 2025).

[66] McMurtry, I., “The lost art of airborne ice accretion testing”, Airline Geeks, 21 February 2019. https://airlinegeeks.com/2019/02/21/the-lost-art-of-airborne-ice-accretion-testing/

NATO OTAN
Science & Technology Organization (STO)

REPORT DOCUMENTATION PAGE

1. Recipient's Reference	2. Originator's References	3. Further Reference	4. Security Classification of Document
	STO-TR-AVT-299 AC/323(AVT-299)TP/1159	ISBN 978-92-837-2471-1	PUBLIC RELEASE

5. Originator

Science and Technology Organization
North Atlantic Treaty Organization
BP 25, F-92201 Neuilly-sur-Seine Cedex, France

6. Title

Assessment of Anti-Icing and De-Icing Technologies for Air and Sea Vehicles

7. Presented at/Sponsored by

This report documents the findings and recommendations of the Research Task Group AVT-299.

8. Author(s)/Editor(s)	9. Date
Multiple	January 2026
10. Author's/Editor's Address	**11. Pages**
Multiple	192

12. Distribution Statement

There are no restrictions on the distribution of this document. Information about the availability of this and other STO unclassified publications is given on the back cover.

13. Keywords/Descriptors

Ice detection systems; Ice protection systems; Ice-phobic coatings; Ice-phobic surfaces; Icing computational modelling and simulation; Icing flight testing; Icing numerical simulation; Icing wind tunnels

14. Abstract

This report summarizes the findings and recommendations of the RTG AVT-299 activity on "Assessment of Anti-Icing and De-Icing Technologies for Air and Sea Vehicles". During this RTG activity, the technical team members conducted a critical review and assessment of a number of current and emerging technologies related to icing and ice risk mitigation with application to military air and sea vehicles in mind. Four focus technology areas (topics) were covered in this activity and state-of-the-art and recommendations are provided for each of the four focus areas. The four topics are; Ice Detection Technologies, Ice Protection Technologies, Computational Modelling and Simulation Methods, and Experimental Icing Facilities.

NORTH ATLANTIC TREATY ORGANIZATION

SCIENCE AND TECHNOLOGY ORGANIZATION
BP 25
F-92201 NEUILLY-SUR-SEINE CEDEX
FRANCE
Télécopie 0(1)55.61.22.99

E-mail mailbox@cso.nato.int

DIFFUSION DES PUBLICATIONS STO NON CLASSIFIEES

Les publications de l'AGARD, de la RTO et de la STO peuvent parfois être obtenues auprès des centres nationaux de distribution indiqués ci-dessous. Si vous souhaitez recevoir toutes les publications de la STO, ou simplement celles qui concernent certains Panels, vous pouvez demander d'être inclus soit à titre personnel, soit au nom de votre organisation, sur la liste d'envoi.

Les publications de la STO, de la RTO et de l'AGARD sont également en vente auprès des agences de vente indiquées ci-dessous.

Les demandes de documents STO, RTO ou AGARD doivent comporter la dénomination « STO », « RTO » ou « AGARD » selon le cas, suivi du numéro de série. Des informations analogues, telles que le titre est la date de publication sont souhaitables.

Si vous souhaitez recevoir une notification électronique de la disponibilité des rapports de la STO au fur et à mesure de leur publication, vous pouvez consulter notre site Web (http://www.sto.nato.int/) et vous abonner à ce service.

CENTRES DE DIFFUSION NATIONAUX

ALLEMAGNE
BAIUDBw FA IV
Fachinformationszentrum der Bundeswehr
Ausleihservice Hardthöhe, Haus 208
Fontainengraben 150, 53123 Bonn

BELGIQUE
Royal High Institute for Defence – KHID/IRSD/RHID
Management of Scientific & Technological Research for Defence, National STO Coordinator
Royal Military Academy – Campus Renaissance
Renaissancelaan 30, 1000 Bruxelles

BULGARIE
Ministry of Defence
Defence Institute "Prof. Tsvetan Lazarov"
"Tsvetan Lazarov" bul no.2, 1592 Sofia

CANADA
DGSIST 2
Recherche et développement pour la défense Canada
60 Moodie Drive (7N-1-F20), Ottawa, Ontario K1A

DANEMARK
Danish Acquisition and Logistics Organization
Lautrupbjerg 1-5, 2750 Ballerup

ESPAGNE
Área de Cooperación Internacional en I+D
SDGPLATIN (DGAM), C/ Arturo Soria 289
28033 Madrid

ESTONIE
Estonian National Defence College
Centre for Applied Research
Riia str 12, Tartu 51013

ETATS-UNIS
Defense Technical Information Center
8725 John J. Kingman Road
Fort Belvoir, VA 22060-6218

FINLAND
Ministry for Foreign Affairs
Telecommunications Centre (24/7)
P.O Box 176, FI-00023 Government

FRANCE
O.N.E.R.A. (ISP)
29, Avenue de la Division Leclerc
BP 72, 92322 Châtillon Cedex
O.N.E.R.A. (ISP)

GRECE (Correspondant)
Defence Industry & Research General Directorate, Research Directorate
Fakinos Base Camp, S.T.G. 1020
Holargos, Athens

HONGRIE
Hungarian Ministry of Defence
Development and Logistics Agency
P.O.B. 25, H-1885 Budapest

ITALIE
Ten Col Renato NARO
Capo servizio Gestione della Conoscenza
F. Baracca Military Airport "Comparto A"

LUXEMBOURG
Voir Belgique

NORVEGE
Norwegian Defence Research Establishment, Attn: Biblioteket
P.O. Box 25, NO-2007 Kjeller

PAYS-BAS
Royal Netherlands Military Academy Library
P.O. Box 90.002, 4800 PA Breda

POLOGNE
Centralna Biblioteka Wojskowa
ul. Ostrobramska 109,
04-041 Warszawa

PORTUGAL
Estado Maior da Força Aérea
SDFA – Centro de Documentação
Alfragide, P-2720 Amadora

ROUMANIE
Romanian National Distribution Centre
Armaments Department
9-11, Drumul Taberei Street
Sector 6
061353 Bucharest

ROYAUME-UNI
Dstl Records Centre
Rm G02, ISAT F, Building 5
Dstl Porton Down
Salisbury SP4 0JQ

SLOVAQUIE
Akadémia ozbrojených síl gen.
M.R. Štefánika, Distribučné a informačné stredisko STO
Demänová 393
031 01 Liptovský Mikuláš 1

SLOVENIE
Ministry of Defence
Central Registry for EU & NATO
Vojkova 55
1000 Ljubljana

SUEDE
Regeringskansliet,
Attn: Adam Hidestå
RK IF AR 5
S-103 33 Stockholm

TCHEQUIE
Vojenský technický ústav s.p.
CZ Distribution Information
Mladoboleslavská 944
PO Box 18, 197 06 Praha 9

TURQUIE
Milli Savunma Bakanlığı (MSB)
ARGE ve Teknoloji Dairesi Başkanlığı
06650 Bakanliklar – Ankara

AGENCES DE VENTE

The British Library Document Supply Centre
Boston Spa, Wetherby
West Yorkshire LS23 7BQ
ROYAUME-UNI

Canada Institute for Scientific and Technical Information (CISTI)
National Research Council Acquisitions
Montreal Road, Building M-55
Ottawa, Ontario K1A 0S2, CANADA

Les demandes de documents STO, RTO ou AGARD doivent comporter la dénomination « STO », « RTO » ou « AGARD » selon le cas, suivie du numéro de série (par exemple AGARD-AG-315). Des informations analogues, telles que le titre et la date de publication sont souhaitables. Des références bibliographiques complètes ainsi que des résumés des publications STO, RTO et AGARD figurent dans le « NTIS Publications Database » (http://www.ntis.gov).

NORTH ATLANTIC TREATY ORGANIZATION

SCIENCE & TECHNOLOGY ORGANIZATION
BP 25
F-92201 NEUILLY-SUR-SEINE CEDEX
FRANCE
Télécopie 0(1)55.61.22.99

E-mail mailbox@cso.nato.int

DISTRIBUTION OF UNCLASSIFIED STO PUBLICATIONS

AGARD, RTO & STO publications are sometimes available from the National Distribution Centres listed below. If you wish to receive all STO reports, or just those relating to one or more specific STO Panels, they may be willing to include you (or your Organisation) in their distribution.

STO, RTO and AGARD reports may also be purchased from the Sales Agencies listed below.

Requests for STO, RTO or AGARD documents should include the word 'STO', 'RTO' or 'AGARD', as appropriate, followed by the serial number. Collateral information such as title and publication date is desirable.

If you wish to receive electronic notification of STO reports as they are published, please visit our website (http://www.sto.nato.int/) from where you can register for this service.

NATIONAL DISTRIBUTION CENTRES

BELGIUM
Royal High Institute for Defence – KHID/IRSD/RHID
Management of Scientific & Technological Research for Defence, National STO Coordinator
Royal Military Academy – Campus Renaissance
Renaissancelaan 30, 1000 Brussels

BULGARIA
Ministry of Defence
Defence Institute "Prof. Tsvetan Lazarov"
"Tsvetan Lazarov" bul no.2, 1592 Sofia

CANADA
DSTKIM 2
Defence Research and Development Canada
60 Moodie Drive (7N-1-F20)
Ottawa, Ontario K1A 0K2

CZECHIA
Vojenský technický ústav s.p.
CZ Distribution Information Centre
Mladoboleslavská 944
PO Box 18, 197 06 Praha 9

DENMARK
Danish Acquisition and Logistics Organization (DALO)
Lautrupbjerg 1-5, 2750 Ballerup

ESTONIA
Estonian National Defence College
Centre for Applied Research
Riia str 12, Tartu 51013

FINLAND
Ministry for Foreign Affairs
Telecommunications Centre (24/7)
P.O Box 176, FI-00023 Government

FRANCE
O.N.E.R.A. (ISP)
29, Avenue de la Division Leclerc – BP 72
92322 Châtillon Cedex

GERMANY
BAIUDBw FA IV
Fachinformationszentrum der Bundeswehr
Ausleihservice Hardthöhe, Haus 208
Fontainengraben 150, 53123 Bonn

GREECE (Point of Contact)
Defence Industry & Research General Directorate, Research Directorate
Fakinos Base Camp, S.T.G. 1020
Holargos, Athens

HUNGARY
Hungarian Ministry of Defence
Development and Logistics Agency
P.O.B. 25, H-1885 Budapest

ITALY
Ten Col Renato NARO
Capo servizio Gestione della Conoscenza
F. Baracca Military Airport "Comparto A"
Via di Centocelle, 301, 00175, Rome

LUXEMBOURG
See Belgium

NETHERLANDS
Royal Netherlands Military Academy Library
P.O. Box 90.002, 4800 PA Breda

NORWAY
Norwegian Defence Research Establishment, Attn: Biblioteket
P.O. Box 25, NO-2007 Kjeller

POLAND
Centralna Biblioteka Wojskowa
ul. Ostrobramska 109
04-041 Warszawa

PORTUGAL
Estado Maior da Força Aérea
SDFA – Centro de Documentação
Alfragide, P-2720 Amadora

ROMANIA
Romanian National Distribution Centre
Armaments Department
9-11, Drumul Taberei Street, Sector 6
061353 Bucharest

SLOVAKIA
Akadémia ozbrojených síl gen. M.R. Štefánika, Distribučné a informačné stredisko STO
Demänová 393
031 01 Liptovský Mikuláš 1

SLOVENIA
Ministry of Defence
Central Registry for EU & NATO
Vojkova 55, 1000 Ljubljana

SPAIN
Área de Cooperación Internacional en SDGPLATIN (DGAM)
C/ Arturo Soria 289
28033 Madrid

SWEDEN
Regeringskansliet, Attn: Adam Hidestål
RK IF AR 5
S-103 33 Stockholm

TÜRKIYE
Milli Savunma Bakanlığı (MSB)
ARGE ve Teknoloji Dairesi Başkanlığı
06650 Bakanliklar – Ankara

UNITED KINGDOM
Dstl Records Centre
Rm G02, ISAT F, Building 5
Dstl Porton Down,
Salisbury SP4 0JQ

UNITED STATES
Defense Technical Information Center
8725 John J. Kingman Road
Fort Belvoir,
VA 22060-6218

SALES AGENCIES

The British Library Document Supply Centre
Boston Spa, Wetherby
West Yorkshire LS23 7BQ
UNITED KINGDOM

Canada Institute for Scientific and Technical Information (CISTI)
National Research Council Acquisitions
Montreal Road, Building M-55
Ottawa, Ontario K1A 0S2, CANADA

Requests for STO, RTO or AGARD documents should include the word 'STO', 'RTO' or 'AGARD', as appropriate, followed by the serial number (for example, AGARD-AG-315). Collateral information such as title and publication date is desirable. Full bibliographical references and abstracts of STO, RTO and AGARD publications are given in "NTIS Publications Database" (http://www.ntis.gov).

ISBN 978-92-837-2471-1